GHENT UNIVERSITY

FACULTY OF PHARMACEUTICAL SCIENCES

Massively parallel sequencing in preimplantation and prenatal genetic diagnosis

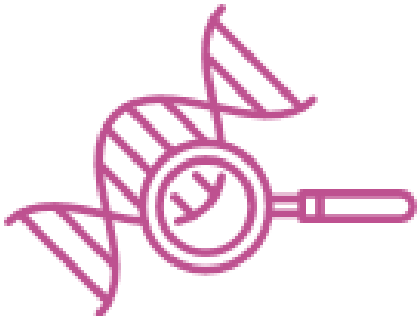

Lieselot DELEYE

Master in Biomedical Sciences

Promotor: Prof. Dr. Apr. Filip Van Nieuwerburgh

Promotor: Prof. Dr. Apr. Dieter Deforce

Lab of pharmaceutical biotechnology

2017

GHENT UNIVERSITY

FACULTY OF PHARMACEUTICAL SCIENCES

Massively parallel sequencing in preimplantation and prenatal genetic diagnosis

Lieselot DELEYE

Master in Biomedical Sciences

Promotor: Prof. Dr. Apr. Filip Van Nieuwerburgh

Promotor: Prof. Dr. Apr. Dieter Deforce

Lab of pharmaceutical biotechnology

2017

Dissertation submitted in fulfillment of the requirements for the degree of Doctor in Pharmaceutical Sciences

Members of the examination committee

Faculty members:

- Prof. Dr. Apr. Sarah De Saeger – Sarah.DeSaeger@ugent.be
- Prof. Dr. Apr. Katrien Remaut – Katrien.Remaut@ugent.be

Members from outside Ghent University:

- Dr. Arjan Tibbe – arjan.tibbe@Vycap.com
- Prof. Dr. Mieke Geens - Mieke.Geens@uzbrussel.be

Members from outside the faculty:

- Prof. Dr. Björn Heindryckx – Bjorn.Heindryckx@ugent.be
- Dr. Bart Broeckx – Bart.Broeckx@ugent.be

Table of Contents

List of abbreviations

A	Adenine
aCGH	Array Comparative Genomic Hybridization
ADO	Allelic dropout
AFA	Adaptive focused acoustics
ART	Assisted reproductive technology
BAC	Bacterial artificial chromosomes
BWA	Burrow-Wheeler-Aligner
C	Cytosine
CBS	Circular binary segmentation
cffDNA	Cell-free fetal DNA
cfDNA	Cell-free DNA
CFTC	Circulating fetal cell
CN	Copy number
CNA	Copy number alteration
CNV	Copy number variant
CTC	Circulating tumor cell
CVS	Chorionic villus sampling
ddNTPs	dideoxynucleotides
DOP	Depth of coverage
DOP-PCR	Degenerate oligonucleotide primed-PCR
EB buffer	Elution buffer
EDTA	Ethylenediaminetetraacetic acid
EPG	electropherogram
ESHRE	European Society of Human Reproduction and Embryology
FDR	False discovery rate
FER	Frozen embryo replacement
FISH	Fluorescence in situ hybridization

FLTR	From left to right
FSH	Follicle stimulating hormone
FWHM	Full width at half maximum
G	Guanine
ICM	Inner cell mass
ICSI	Intracytoplasmic sperm injection
IGV	Integrative Genomics Viewer
IVF	In vitro fertilization
MALBAC	Multiple annealing and looping based amplification cycles
MDA	Multiple displacement amplification
MPS	Massively parallel sequencing
ng	nanogram
NIPD	Non-invasive prenatal diagnosis
NIPT	Non-invasive prenatal testing
NPB	Nucleolus precursor body
PB	Polar body
PBS	Phosphate buffered saline
PEP	Primer extension preamplification
PGD	Preimplantation genetic diagnosis
PGS	Preimplantation genetic screening
pg	picogram
Picoseq	PicoPLEX DNA-Seq
PN	pronuclei
PPV	Positive predictive value
RCT	Randomized controlled trial
RPMI	Roswell park memorial institute
SGD	Single gene disorder
SNP	Single nucleotide polymorphism
SNV	Single nucleotide variation

STR	Short tandem repeat
T	Thymine
T21	Trisomy 21
TE	Trophectoderm
TE-buffer	Tris-EDTA buffer
VOUS	Variance Of Unknown Significance
WGA	Whole genome amplification
WGS	Whole genome sequencing
ZP	Zona pellucida

Dankwoord

Poging nummer 10^6 om een eerste gepaste zin te schrijven in mijn dankwoord. Het dankwoord moet zo wat de meest onderschatte tekst in een doctoraatsthesis zijn. Ik moet erin slagen om iedereen die het verdient (en ook verwacht) op een gepaste en gevatte wijze te bedanken voor zijn of haar bijdrage tijdens mijn doctoraat. Want, een doctoraat dat haal je niet op je eentje, dat haal je door je te omringen met de juiste mensen. Mensen die je helpen, kansen geven en aanmoedigen gedurende ongeveer 4 jaar.

Voor mij is het allemaal begonnen op 30 juli 2013. Ik kwam hier aan als 'vreemdeling' uit de biomedische wetenschappen vanuit de KULeuven. Vandaag, iets meer dan 4 jaar later, stel ik met trots voor waaraan ik de afgelopen jaren zoal heb gewerkt. Maar eerst zal ik dus enkele mensen van harte bedanken.

Ik begin mijn bedanking bij mijn promotoren, Prof. Van Nieuwerburgh en Prof. Deforce, want zonder hen was ik nu zelfs geen dankwoord aan het schrijven.

Filip, zonder jouw hulp was dit doctoraat nooit geworden wat het nu is. Je hebt me gedurende 4 jaar voortreffelijk begeleid bij het bedenken, uitvoeren en schrijven en daarbij heb je me vooral geleerd om zelfstandig te denken en te werken. Je liet me vrij tijdens de uitvoering van mijn projecten, maar stond me bij waar nodig. Vooral wanneer een meer kritische en nuchtere kijk op de resultaten nodig was. De boog moest natuurlijk niet altijd gespannen staan en zo leerde je me, als brouwmeester, ook de skills van het bierbrouwen.

Dieter, zonder jou was ik hoogstwaarschijnlijk nooit aan de farmacie in Gent terecht gekomen. Onze eerste ontmoeting gaat terug naar het tropische Miami in de zomer van 2012, toen ik als enige Belg in jouw 'forensic genetics class' zat. Jouw enthousiasme en gedrevenheid heeft me toen overtuigd om me een aantal maanden later tot jou te wenden voor een doctoraatsplaats in jouw labo. Ik wil je bedanken om me de kans te geven deel uit te maken van lab FBT. Bedankt ook voor jouw opbouwende inbreng en frisse ideeën tijdens onze meetings. Daarnaast maakte je ook voldoende ruimte om te werken aan de groepssfeer binnen het labo door de vele uitstapjes en etentjes die je voor het labo organiseerde. Bedankt!

Ik wil ook mijn dank betuigen aan de andere leden van de examencommissie. Hartelijk dank om mijn thesis zo uitvoerig te evalueren en een constructieve bijdrage te leveren.

Merci ook al alle mensen van het CMGG en het departement Reproductive Medicine aan het UZ Gent voor de productieve samenwerkingen.

Nu, als er één ding is waar ik ongelofelijk veel geluk mee gehad heb tijdens mijn doctoraat, dan zijn het wel mijn collega's. Zonder jullie was mijn tijd op het FFW bijlange niet zo aangenaam geweest.

Om te beginnen, **Elisabeth**, wij zijn hier samen aan ons doctoraat begonnen en hebben dus bijna het ganse PhD parcours samen doorlopen. Reeds vóór mijn aankomst op het FFW stuurde je me, als volstrekt wildvreemde, al een berichtje op facebook om te laten weten dat jij er ook zou zijn bij mijn start aan lab FBT. Ondertussen is er een geweldige vriendschap gegroeid tussen ons. Het schept natuurlijk ook een band als je allebei moet leven met, niet alleen een Dieter als baas, maar ook thuis nog eens met nen Dieter samenwoont. Je was er altijd voor mij als ik nood had om te babbelen, klagen, pauzeren, kalmeren… zowel tijdens als na het werk. Als looppartner was je iets minder geschikt, aangezien je elke uitvlucht goed vond om het lopen toch maar weer eens uit te stellen. Ik zou je

niet willen gemist hebben tijdens de afgelopen 4 jaar en ik ben er vrijwel zeker van dat onze vriendschap niet zal stoppen na dit doctoraat.

Vervolgens wil ik de collega's van het 'foetale team' bedanken voor de leuke, interessante en productieve samenwerking. **Liesbeth**, ik vond het super om met jou samen te werken, onze expertises uit te wisselen en tot tweemaal toe Boston onveilig te maken. De laatste maal moest ik jou spijtig genoeg achterlaten in het verre Amerika. **Ann-Sophie**, je bent een ideale metgezel in het foetale team. Als West-Vlamingen kunnen we namelijk discussiëren in onze eigen taal en zo komen we dus telkens vlotjes tot geniale hersenspinsels. Jammer dat je er pas vorig jaar bij kwam, want ik vond het echt leuk om samen te werken. Zelfs na een maandje rondtoeren tussen Enschede en Lissabon, waren we nog net niet op elkaar uitgekeken. **Jana**, met andere woorden, de lat ligt hoog als opvolging, maar jij doet dat nu al uitstekend! Samen kunnen jullie nu Senne wat onder controle houden daar op jullie bureau. **Senne**, ja, ook jij hoort een beetje bij het foetale team (Al was het maar omdat jij geen team hebt). Je hebt ons uiteraard uitstekend geholpen met alle STR gerelateerde werk. Merci voor alle hulp, vooral bij de vele technische mankementen van niet nader te noemen toestellen. In elk geval, alle drie een dikke negen voor sfeer en leutigheid daar op jullie bureau op het derde!

Uiteraard gaat de dikke tien voor sfeer en leutigheid naar het bureau van Sarah, Ellen, Sylvie, Karolien en mezelf. **Sarah**, merci om je praktische expertise met mij te delen en altijd mee te helpen redeneren bij minder straight forward problemen. **Ellen**, door jou heeft de UGent al vele euro's aan energiekosten bespaard. Daardoor zaten we soms wel eens in een donker en koud bureau, maar even goede vrienden, hé. Ook jouw praktische expertise heeft me enorm vooruit geholpen, merci! **Karolien**, merci voor de ontspannende babbels en de leuke momenten op het bureau en na het werk. Gelukkig kwam er na jouw vertrek opnieuw een leuke bureaupartner. **Sylvie**, ik kende jou al van in het begin maar heb je eigenlijk pas echt leren kennen wanneer je naar boven verhuisde en ondertussen is het super naast jou aan het bureau.

De overige derde verdiepers, **An, Anna, Johan en Hendrik**, merci voor de geweldige sfeer op het derde. Hendrik, jammer dat jij je doctoraat nooit moet afleggen, anders waren er in ieder geval wel enkele hilarische filmpjes te tonen van je skiprestaties.

Het interessantste onderzoek op lab FBT speelt zich af op het derde verdiep, maar op het tweede verdiep vind je het hart van de proteomics van lab FBT. **Maarten**, jouw enthousiasme voor histonen en massaspectrometrie kent werkelijk geen grenzen. Ongelofelijk voor een toestel waarvan de herstellingskosten al meer zouden gekost hebben dan het toestel zelf, ware het niet van jullie servicecontract. Uiteraard verrichten jij, **Simon, Bart, Sander en Laura** fantastisch werk samen met ProGenTomics. Chapeau! **Laura**, jij bent iets minder dromerig over al dat massa gedoe, maar pakt de zaken altijd heel efficiënt en praktisch aan. Jouw praktische ingesteldheid heeft ook al tot vele leuke etentjes en reünies met oud-collega's geleid, waarvoor merci! **Simon**, ook jij zorgt dat er geen gebrek is aan toffe feestjes na het werk, al zijn die natuurlijk iets minder praktisch georganiseerd (zolang er drank is…).

Uiteraard geen genomics en proteomics zonder bio-informatica. **Dieter**, merci om me te introduceren in de wondere wereld van de bio-informatica. Zonder jou was ik waarschijnlijk nog bezig met mijn data analyse. **Laurentijn en Yannick**, ook merci voor alle hulp bij alle bio-informatica gerelateerde problemen. Jullie staan altijd klaar om iedereen te helpen met eender welk computerprobleem, waarvoor dank.

Merci ook aan alle ex-FBT'ers voor de leuke momenten, hulp en ontspannende babbels over de middag en na het werk. **Trees**, bedankt voor alle hulp aan de microscoop. **Pieter**, bedankt om te helpen bij het isoleren van DNA uit

gist. **Veerle,** ik was blij dat je in mijn team zat toen we kub-kampioen van het FFW werden. Jij en **Paulien** waren de eerste collega's die ik zag toen ik op lab FBT aankwam en meteen wist ik dat ik me hier zou amuseren. Paulien, jij bent, geloof ik, de laatste die je doctoraat aflegde alvorens het mijn toer was en een beter voorbeeld kon ik natuurlijk niet hebben. **Kathleen,** je was een super, immer vrolijke postdoc/kwaliteitsverantwoordelijke/collega. **Ellen**, jij hebt me de kneepjes van de celkweek geleerd en ik kan me geen enthousiastere leermeesteres voorstellen. **Bart**, jij hebt me in het begin geholpen bij de voorbereidingen voor het IWT en later ook als er ingewikkelde statistische problemen waren. Je zit dan ook letterlijk op de eerste rij vandaag bij het afronden van mijn doctoraat, waarvoor merci!

Sinds vorige zomer moeten we aankijken op een compleet leeg routine labo. **David,** je bent samen met je groene boekjes naar Brugge verhuisd en dat is goed zo. Versta me niet verkeerd, jou zag ik altijd graag toekomen op mijn bureau, je groene boekjes minder. Merci ook voor de eindeloze hulp bij de stervende '310' en later bij de 3130. Ook bedankt aan **Saskia, Petra, Sabine, Eveline, Evelien, Leen, Astrid en Nadine** voor alle hulp bij STR-analyse, de groene mapjes en de leuke babbels in de wandelgangen.

Evelyne, Jolien en Lotte, merci voor de hulp bij mijn experimenten tijdens jullie thesis.

Merci ook aan **Severine Vanslambrouck en Wim Steelant** voor de kans die jullie me gaven om stage te doen bij jullie aan de St.-Thomas University. Onrechtreeks hebben jullie ervoor gezorgd dat ik hier aan lab FBT ben terecht gekomen.

Merci ook aan de vrienden van het thuisfront om er altijd voor me te zijn. Ook al begrepen sommigen onder jullie niet zo goed waar ik nu precies mee bezig was, toch geloofden jullie in mij en kon ik rekenen op een goede portie ontspanning na het werk.

Elise en Stéphanie, mijn buddy's uit Leuven, jullie begrepen maar al te goed waar ik mee bezig was. Er werd af en toe eens stevig geventileerd over de geneugten, kwellingen en onzekerheden van het leven als PhD student. Waar jullie ook wonen (Kessel-lo of (s)Trondheim), één ding is zeker, als we afspreken is het altijd slecht weer en heb ik hoofdpijn de dag erna.

Ik heb misschien wel de belangrijkste mensen voor op het einde gehouden, want zonder hen was deze avond er al helemaal niet geweest. **Mam en pap**, jullie hebben altijd in mijn 'kunnen' geloofd en hebben me altijd gesteund. Ook al woon ik niet meer thuis, jullie staan nog altijd onmiddellijk paraat als ik jullie nodig heb. Het doet enorm deugd te zien hoe jullie altijd apetrots zijn en hier dan ook vandaag als trouwste supporters zitten te blinken. Ik zeg het misschien te weinig, maar merci, merci, merci voor alles.

Mijn andere twee trouwe supporters zijn uiteraard, mijn zus en mijn vriend. **Hanne**, alias Sceet, ik ken maar weinig mensen die zo een goede band hebben met hun zus. Zelfs drie jaar samenwonen in Heverlee heeft daar niets aan veranderd, integendeel. Nu wonen we wat verder uit elkaar, maar toch kan ik nog altijd op jou rekenen. Jij bent de meest praktische van ons twee en soms is dat echt wel eens nodig. **Dieter,** schatie, uiteraard ben jij degene die tijdens mijn doctoraat het meest gezaag en geklaag heeft moeten aanhoren, zeker in de laatste eindspurt. Ik kan mezelf soms nogal verliezen als ik een bepaald doel wil bereiken, maar jij brengt daar begrip voor op en blijft mij steunen. Merci voor al jouw steun, begrip en ook technische hulp. Ik kijk al uit naar het volgende avontuur dat we samen zullen beleven!

Chapter I: The story behind embryonal and fetal genome analysis

1. In vitro fertilization: a fairy tale or not?

According to the European Society of Human Reproduction and Embryology (ESHRE), one in six couples worldwide are affected by fertility problems (ESHRE, 2014). Assisted reproductive technologies (ARTs) might offer a solution for some of these couples, depending on their reason for infertility (Table 1). An estimated 1.5 million ART cycles are performed worldwide per year, with in vitro fertilization (IVF) and intracytoplasmic sperm injection (ICSI) among the most common forms of ART (1). Fifty-five percent of these cycles are performed in Europe (2) and Belgium belongs to the top 10 most performing countries that report their ART data to the ESHRE (1) (Table 2). The overall number of ART cycles registered by the ESHRE continues to grow each year.

Male infertility	Female infertility
Decreased sperm count	Ovulation disorders
Decreased sperm motility	Blocked/damaged fallopian tubes
Genetic disorders	Endometriosis
	Premature ovarian failure
	Genetic disorders

Table 1: Well-known causes of infertility that might benefit from IVF/ICSI

TREATMENT CYCLES	IVF	ICSI	FER	TOTAL ART
FRANCE	20 995	39 079	23 841	85 594
GERMANY	12 047	39 079	23 841	7 1251
SPAIN	3 759	3 1671	11 736	69 699
ITALY	8 431	47 064	6 513	64 197
RUSSIA	21 967	25 751	10 321	62 620
UK	21 278	24 375	11 069	6 0151
BELGIUM	3 996	13 611	9 277	28 578
EUROPE	139 978	312 600	139 558	640 144

Table 2: Treatment frequencies of ART in European Countries in 2012

Reports from ART clinics to the ESHRE in 2012 (top-7 countries with the highest number of ART cycles performed). FER: frozen embryo replacement, this refers to the thawing of embryos created during an earlier cycle that were subsequently frozen and stored for later use (1). The number of total ART also include less frequent forms of treatments such as egg donation, in vitro maturation and frozen oocyte replacement.

1.1. From follicle-stimulation to embryo transfer

IVF is a process of fertilization by combining an egg and sperm *in vitro*, in a laboratory dish. Infertile couples might turn to IVF for several reasons: blocked/damaged fallopian tubes, decreased sperm count or motility, premature ovarian failure, ovulation disorders, genetic disorders or unexplained infertility etc. (Table 1).

The IVF process consists of five basic steps. First, the oocyte production is stimulated by follicle stimulating hormone (FSH), to increase the number of mature eggs released at ovulation. Without stimulation, only one mature egg is released per menstrual cycle. Until enough follicles are mature, the ovulation is antagonized by either gonadotropin releasing hormone agonists or antagonists. Finale maturation is stimulated by human chorionic gonadotropin and within 34-36 hours after this stimulation, the ovulation takes place. The eggs are removed by a minor surgical procedure. Subsequently, each egg is co-incubated *in vitro* with a large amount of sperm. However, when the sperm quality is low (low sperm count or low mobility), the fertilization is performed by ICSI. Instead of co-incubation, a single sperm is injected directly into the egg (Figure 1). Before ICSI, the surrounding cumulus cells are removed from the oocyte. As male infertility is a very important reason for infertility, ICSI is performed more than conventional IVF (Table 1&2). After fertilization, the embryos are grown *in vitro* until day 3 or day 5 after fertilization, before one good quality embryo is transferred to the mother.

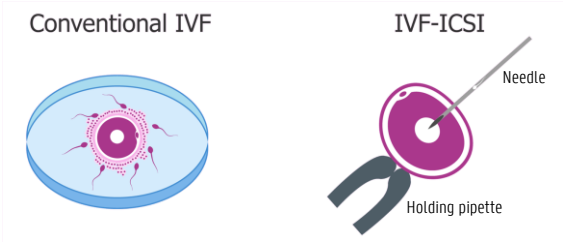

Figure 1: Conventional IVF vs ICSI

1.2. Embryo morphology as a selection criterion

During *in vitro* embryonal development, the quality of the embryo is determined by its morphology at different stages of development. A correlation has been shown between the embryonal morphology and the ability to grow to the blastocyst stage (3). A good embryo selection method is important to maximize the success of the transfer and thereby avoid the need to transfer more than one embryo (4). Transferring more than one embryo risks the occurrence of multiple pregnancies with its complications.

The morphology of the embryo can be scored at the pro-nuclear, cleavage and blastocyst stage. An embryo is in the pronuclear stage before the genetic material of the egg and the sperm have fused. The pronuclei are the nuclei

of the sperm and egg cell during the process of fertilization. They should appear together, centrally in the oocyte and have approximately the same size. Within these pronuclei, nucleoli are visible at the pronuclear junction. A Z-score (Z1-Z4) is appointed to the embryo depending on the size, number and distribution of these nucleoli. Each nucleus should have a similar number (between 3 and 7) and size of nucleoli (3). Embryos with a low Z-score will result in better quality cleavage stage embryos and blastocysts (5).

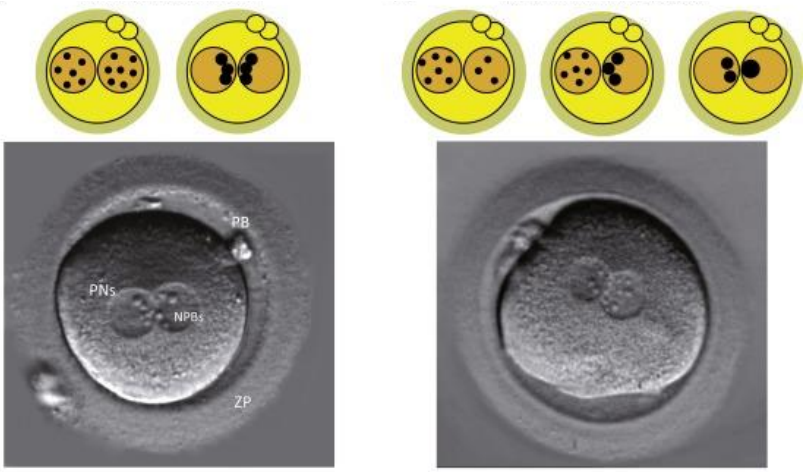

Figure 2: Morphology of the pronuclei stage embryo

Left: a normal distribution of nucleoli (nucleolus precursor bodies (NPBs)); Right: abnormal distribution of NPBs. PN: pronuclei; PB: polar body; ZP: Zona pellucida.

At day 3 after fertilization, the embryo is at the cleavage stage and consists of 6 to 8 cells. Scoring at this stage is most commonly used. This scoring is based on the number and size of the blastomeres and the grade of cytoplasmic fragmentation (6-9) (Figure 3). Nevertheless, the specific grading system differs between centers. However, the number of blastomeres has the highest predictive value (7, 9), because embryos dividing either too fast or too slow may have metabolic or chromosomal defects (8-14).

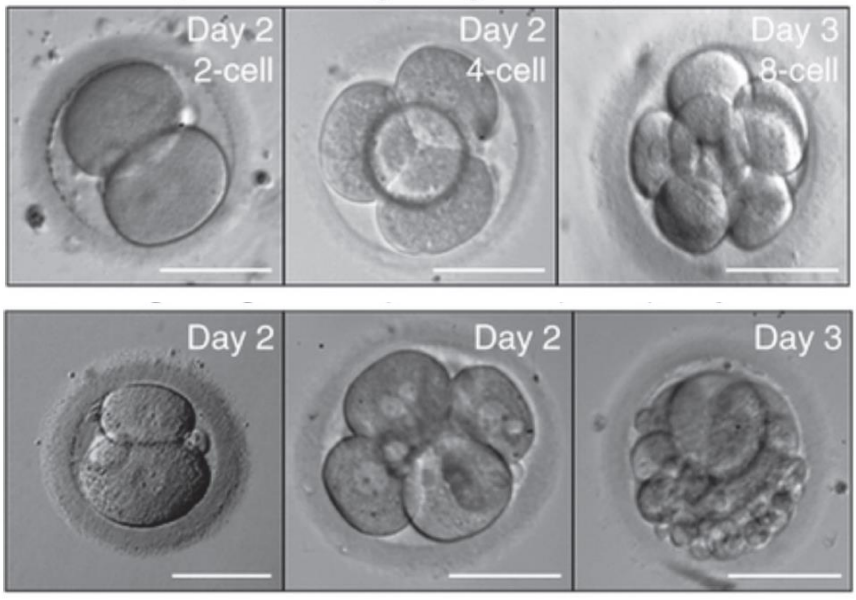

Figure 3: Morphology of the cleavage stage embryo (15)

Top: optimal cleavage stage development; Bottom FLTR: Uneven cleavage, multinucleated blastomeres, high fragmentation.

Towards day 5 or 6 the embryo develops into a blastocyst. A blastocyst consists of an inner cell mass (ICM), which subsequently forms the fetus, a blastocoel, and the trophectoderm (TE), which will form the placental interface (Figure 4a). The Gardner grading system is frequently used to grade blastocysts based on the developmental stage, the ICM and the trophoblast (16). The developmental stage is graded from one to six, with six being the stage were the blastocyst is released from the zona pellucida. This process is called hatching (Figure 4b). The ICM and the TE get each a score from A to C, based on how compact the cells are (17) (Figure 4b). The blastocyst stage is the final stage before implantation takes place. During implantation the embryo adheres to the uterus wall.

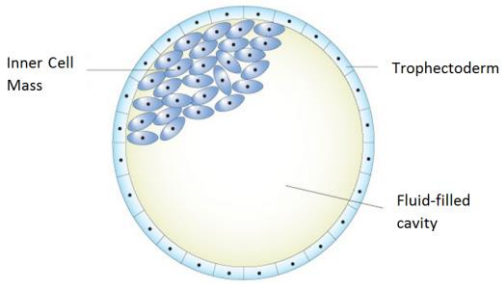

Figure 4a: Schematic representation of a blastocyst
The fluid-filled cavity represents the blastocoel

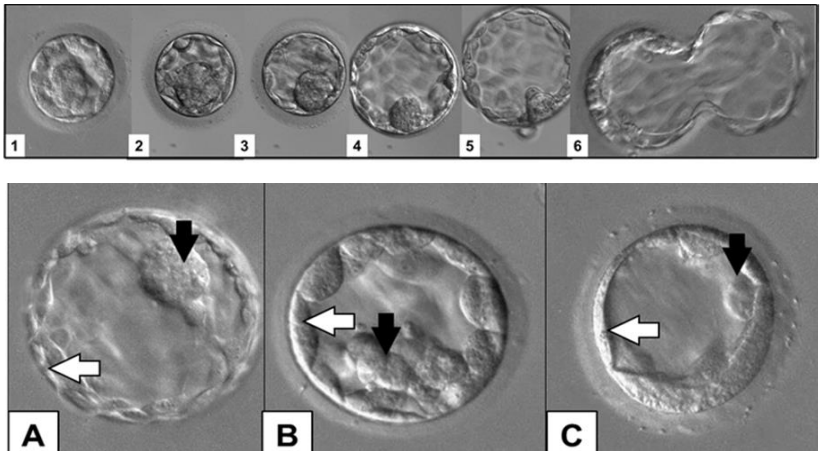

Figure 4b: Grading blastocyst morphology

Top: Developmental stages of the blastocyst: first the blastocoel grows (grade 1-3), than blastocyst expansion occurs (grade 4) until the zona pellucida ruptures and hatching begins (grade 5)
Down: The black arrows indicate the ICM, the white arrow show the TE. Grade A is a good quality embryo, Grade B is also good quality but ICM and/or TE cells are less compact, while grade C is a bad quality embryo (17)

Although IVF is a widespread treatment, with the current state-of-the-art technology, the clinical pregnancy rate per transfer is only 33.8%, and 32.3% for ICSI (1). Obviously, embryo selection based on morphology alone does not predict the developmental potential of the embryo (18-20).

1.3. Preimplantation genetic diagnosis and screening

A lot of embryos suffer from genetic abnormalities during development that might impede with further development or result in birth defects (13, 21, 22). The prevalence of malformation in a pregnancy is approximately

2.5-3.2% of births and thereby, an estimated 8 million infants worldwide are born each year with a major birth defect (23). If diagnosis is performed before implantation, a non-affected embryo could be selected before embryo transfer. For couples with a known balanced or unbalanced chromosomal rearrangement, preimplantation genetic diagnosis (PGD) can be offered during ART to select against unbalanced rearrangements in the embryo (24). Early-stage embryos also suffer from a high rate of spontaneous (mosaic) chromosomal aberrations and aneuploidy, reducing the embryo survival, implantation potential and hence the success rate of ART (25). Couples producing such embryos might benefit from preimplantation genetic screening (PGS). Both PGD and PGS analyze the genetic makeup of the embryo to select an embryo without genetic abnormalities for transfer to the woman. The big difference between PGD and PGS is the targeted patient population. PGD was originally developed to avoid the repeated choice for pregnancy termination in couples whose potential offspring is at risk for a specific severe Mendelian disorder, structural chromosomal aberration or mitochondrial disorder. PGS is often used for women suffering from recurrent implantation failure or repeated miscarriage. Those patients do not carry a specific genetic abnormality, but produce embryos with a general low quality genetic makeup.

PGD/PGS is performed by the isolation of cells at day 3 or day 5 after fertilization or the isolation of a non-functioning haploid polar body after meiosis I, before fertilization. At day 3, cleavage stage biopsy is performed by the isolation of one or two blastomeres through a hole in the zona pellucida (Figure 5). Cells isolated at day 5, the blastocyst stage, are isolated from the TE after hatching. During this blastocyst biopsy, 4 to 6 trophoblasts are isolated for diagnosis.

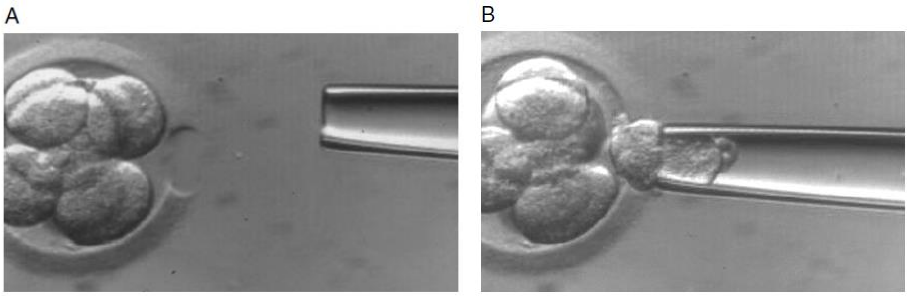

Figure 5: Cleavage stage biopsy. A) Hole in zona pellucida B) Isolation through micromanipulation (26).

1.3.1. PGD/PGS for chromosomal aberrations

Embryos can suffer from structural or numerical abnormalities or even both. Structural abnormalities are mutations such as: translocations, inversions, deletions, duplications or insertions. They occur when a part of the chromosome is missing, multiplied or has switched places with another part. The latter is otherwise known as a chromosomal rearrangement arising by the simultaneous breakage of two chromosomal segments that rejoin within the same or a different chromosome (Figure 6). If no chromosomal parts are lost, this is a balanced rearrangement. A carrier of such balanced chromosomal rearrangement is phenotypically normal and the problem

will only arise during gametogenesis. A couple of which one of the partners is a carrier, might experience difficulties to conceive or give birth to a child with birth defects. Such a parental rearrangement might cause the gain or loss of certain chromosomal parts in some of the gametes, as illustrated in figure 6. Such insertions or deletions of chromosomal parts are referred to as copy number variants (CNVs). A numerical abnormality is the loss or gain of a complete chromosome that might arise during meiotic or mitotic divisions of the gametes or the embryo. The loss or gain of a chromosome, known as an aneuploidy, is the most frequent form and is the most common cause of miscarriages and implantation failure during IVF treatment. Numerical abnormalities are often only discovered by screening, except for Klinefelter syndrome which is a known indication for PGD.

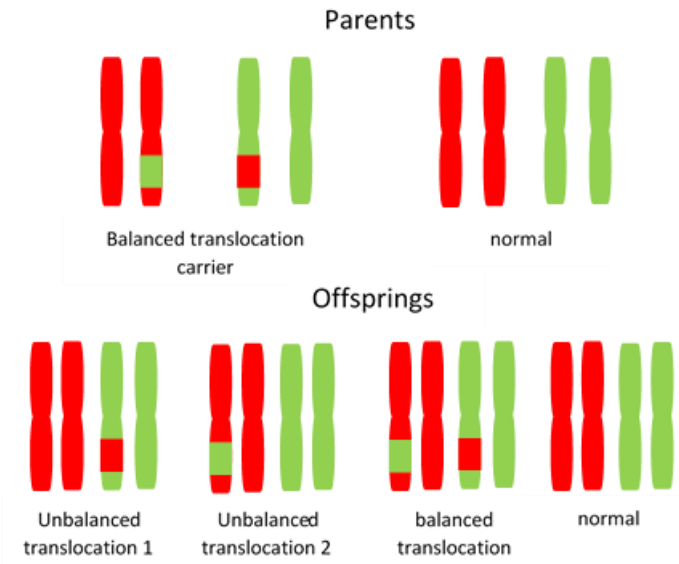

Figure 6: Chromosomal rearrangements

A couple carrying a chromosomal rearrangement and their possible offsprings. They have a 50% chance for an affected child, 25% chance the child is normal and 25% the child is a carrier.

The way a genetic analysis for chromosomal abnormalities in PGD was performed, changed over the years. Fluorescence in situ hybridization (FISH) was one of the first methods used for PGD (27). FISH is a technology that visualizes metaphase chromosomes by hybridization of fluorescent probes. However, it evaluates only a small part of the chromosomes in an embryo, at a relatively low resolution and it is rather labor intensive. Later, array Comparative Genomic Hybridization (aCGH) replaced FISH, enabling simultaneous screening for aneuploidies of all chromosomes, as well as large insertions, deletions and unbalanced translocations (28). In aCGH, the fetal DNA and a reference DNA sample are first labeled with each a different fluorescent dye (for instance Cy3/green color for fetal DNA and Cy5/red color for the reference). Both are then hybridized simultaneously to a microarray coated with single-stranded DNA probes (29). These probes can vary in size, but for PGD the bacterial artificial chromosomes (80000-200000bp) or BAC-arrays are most commonly used. After hybridization, the fluorescent pattern on the microarray will indicate the regions with either a deletion or insertion. A red signal would indicate

the presence of a deletion in that part of the fetal DNA and a green signal would indicate a duplication. ACGH has long been the state-of-the-art method in PGD for chromosomal abnormalities. However, massively parallel sequencing (MPS) is now claiming that position, showing a better resolution, lower cost and better signal-to-noise ratio compared to aCGH (30-32). The resolution of an aCGH is limited by the distance between the probes, which is fixed for a certain type of microarray. During MPS, the reads are distributed randomly across the whole genome and the number of reads will readily change the resolution. MPS allows sequencing different samples on a single run, which is referred to as multiplexing. In this respect, MPS is more flexible and presumably cheaper than aCGH.

As only a small number of cells can be isolated from an embryo, the DNA of the cells will need to be amplified before performing genetic testing. One cell only contains 6 picogram (pg) of DNA and genetic testing, such as aCGH and MPS, will require nanograms (ng) of DNA. However, amplification of the DNA might introduce bias in the DNA sequence during amplification (33). More details about this amplification will be discussed below. However, some methods for genetic testing have been developed, circumventing the need for amplification. For instance, the 4-hour quantitative real-time PCR-based chromosome screening technology uses a more targeted approach. The cells undergo a targeted multiplex PCR for 96 loci and these loci are subsequently interrogated on qPCR. Although, an amplification is still performed, this targeted approach will improve the success of amplification at each loci compared to a whole genome amplification (WGA) (34). Nevertheless, this remains a targeted approach that will probably never obtain the resolution possible by MPS.

1.3.2. PGD for single gene disorders

Single gene disorders (SGDs) or Mendelian disorders can also be analyzed through PGD. SGDs are, in contrast to multifactorial disorders, caused by a mutation in a single gene. They are inherited according to the Mendelian model. Five main modes of inheritance exist: autosomal recessive, autosomal dominant, X-linked recessive, X-linked dominant and mitochondrial. In recessive disorders, two abnormal copies of the gene are essential to manifest the disease. A person with only one abnormal copy is known as a carrier or heterozygote. Two heterozygotes trying to have a child will have a 1 in 4 chance of having an affected offspring. The most common recessive SGD among Caucasians in Europe is cystic fibrosis and it was also the first SGD to be diagnosed by PGD (35). In dominant disorders, one abnormal copy of the gene is sufficient to manifest the disease. An affected individual has a 50% chance to transfer the defective gene to his offspring. Recessive X-linked disorders will mainly affect male offsprings if carried by the mother, as they will not have a normal copy to compensate for the defective one. In contrast, dominant X-linked disorders will mainly affect females, if the male partner was affected. Mitochondrial disorders are only passed on by females, as the male mitochondrial DNA will not enter the fetus.

Some individuals do not know they carry a mutation for a SGD and only discover that after having an affected child or an affected family member. Those couples could rely on PGD to select a non-affected embryo for transfer. However, some mutations occur spontaneously (de novo), during gamete formation or during embryogenesis and those mutations will only be discovered through screening by PGS.

In most SGDs, the disease-causing gene can be mutated in various ways, which makes it harder to develop a universal diagnostic method for each SGD. For instance, more than 1000 different mutations can cause cystic fibrosis. Previously, the specific mutation was first determined in the parents or an affected family member and an individual targeted PCR was developed for each case. However, a PCR reaction can suffer from allelic dropouts (ADOs), especially when amplifying a low lumber of cells. ADO can seriously compromise the reliability of PGD, as a heterozygous embryo could be diagnosed as affected or unaffected depending on which allele would fail to amplify. The introduction of multiplex marker PCR led to some advances in the diagnosis of SGDs (36-38). Markers are determined by identifying family-specific polymorphisms that are linked to the mutation in that family. Changing the focus from one locus to multiple loci diminishes the problems occurring by contamination or ADO (37, 38). A large multicenter study showed a higher validity and diagnostic value for multiplex PCR-based PGD than the singleplex (39). More recently, researchers began to develop SNP-array-based technologies, allowing the simultaneous analysis of (more than) one SGD and chromosome abnormality screening (40-45). However, these technologies are time consuming, costly, extremely complex and did not demonstrate the ability to detect all types of aneuploidies. Another recent advance in SGD diagnosis is the introduction of MPS. The cost and timescale might be reduced by multiplexing amplicons from different PCR reactions on a single sequencing run (46). Still, this approach also requires a specific test per couple.

1.3.3. Cleavage stage versus blastocyst biopsy

Genetic analysis in PGD/PGS is performed on a small number of cells, isolated from the embryo. As mentioned above, three types of biopsy exist. Cleavage stage biopsy has long been the preferred isolation method (47), but in most fertilization centers a shift towards blastocyst biopsy was recently observed (48, 49). Although, the isolated TE cells during blastocyst biopsy are destined for the placenta, it was shown that the TE is an excellent predictor for the genetic makeup of the ICM (50). It was shown that the isolation of cells from a cleavage stage embryo, has an impact on the viability of the embryo and embryo implantation (48, 51, 52). Blastocyst biopsy will not have such an impact, as the fetal-determined cells remain untouched during isolation (53).

The amount of cells available for diagnosis is important to overcome PCR failure, ADOs, non-uniform amplification of the DNA and cell cycle discrepancies (49, 54). Therefore, as only one or two blastomeres are isolated at cleavage

stage, this might result in a diagnostic failure (49). The isolation of more cells during TE biopsy will lead to better amplification and hence, a more confident genetic diagnosis (54).

Furthermore, it has been shown that cleavage stage embryos show a higher rate of mosaicism for numerical and structural chromosomal aberrations (55). Mosaicisms arise when some cells from the same embryo have a different genetic make-up. Since only one or two cells can be biopsied on day 3, the mosaicism might be missed and this might influence the accuracy of PGD (56). Mosaicisms might also occur in blastocysts, but more cells are isolated during blastocyst biopsy, increasing the detection potential. In terms of mosaicisms, the TE is shown to be representative for the embryo, as the mosaic level is not higher for the TE compared to the ICM (18, 57). However, more research needs to be performed to understand the full extent of mosaicisms.

Embryos selected for biopsy on day 5 carry a lower risk of being aneuploid (18, 19). Genomic activation of the embryo sets in at day 3 and thereby DNA-damage and -response pathways will be activated. This will lead to the loss or repair of some or even most of the abnormal embryos (58-60). Due to this natural selection against genomic abnormal embryos, genetic testing is needed for fewer, high quality embryos at the blastocyst stage. This makes genome-wide chromosome analysis on day 5 embryos more appropriate.

However, a TE biopsy can only occur at day 5 and embryos should be transferred by day 6 the latest. TE biopsy, combined with PGD, hampers a fresh embryo transfer and implies vitrification of the embryos. Nevertheless, the cryopreservation methods have improved a lot over the recent years (61-63) and it was recently shown that embryo transfer after freezing and in a natural menstrual cycle leads to better IVF outcomes than fresh transfer in a stimulated cycle (63, 64). All of these issues make TE biopsies the preferred approach for PGD.

2. Prenatal diagnosis: invasive or non-invasive?

The concept of prenatal diagnosis is older than the concept of PGD, and dates back to the sixties. Prenatal diagnosis is performed to obtain information about the genome of the fetus during pregnancy and thereby discover possible genetic abnormalities. A prenatal ultrasound without genetic testing might lead to differential diagnosis (65). The fetal phenotype does not always reflect the fetal genotype, as a genetically abnormal fetus might not always show abnormalities on ultrasound. Sex determination and trisomy 21 detection were among the first indications for prenatal genetic testing. Today, we are able to diagnose big and small chromosomal abnormalities and SGDs at high resolutions. Efficient prenatal genomic-based diagnosis will be important to make an advised reproductive decision (66) or to prepare the future parents for the disability of their future child. Similar to PGD, a couple can perform a genetic analysis based on familial history or screen for *de novo* abnormalities. Based on the DNA material collected for diagnosis, three types of prenatal diagnosis exist.

2.1. Invasive cell-based prenatal diagnosis

The state-of-the-art methods for prenatal diagnosis are amniocentesis and chorionic villus sampling (CVS). The first amniocentesis procedures date back to the late 1960s and were only performed on the highest risk patients (67). As ultrasound guidance was non-existing, the procedure was performed essentially blindly and thereby later in pregnancy (68). Nowadays, amniocentesis is performed in the second trimester, after week 13 and collects a small amount of amniotic fluid from the amniotic sac surrounding the fetus. The fluid is collected by inserting a fine needle through the abdomen into the uterus, guided by ultrasound (Figure 7). This fluid contains fetal cells for genetic testing, and other substances to check the overall fetal health. An amniocentesis is performed in women with an abnormal ultrasound, a family history for certain birth defects or a previous affected child. CVS is performed in the first trimester, between week 10 and 12 and collects chorionic villi from the placenta. The villi are the part were the placenta meets the uterus and are derived from the outer layer of the blastocyst (TE). The villi can be retrieved through the cervix (transcervical) or the abdominal wall (transabdominal) (Figure 7). The indications for CVS and amniocentesis are similar, but CVS will detect genetic problems earlier in pregnancy.

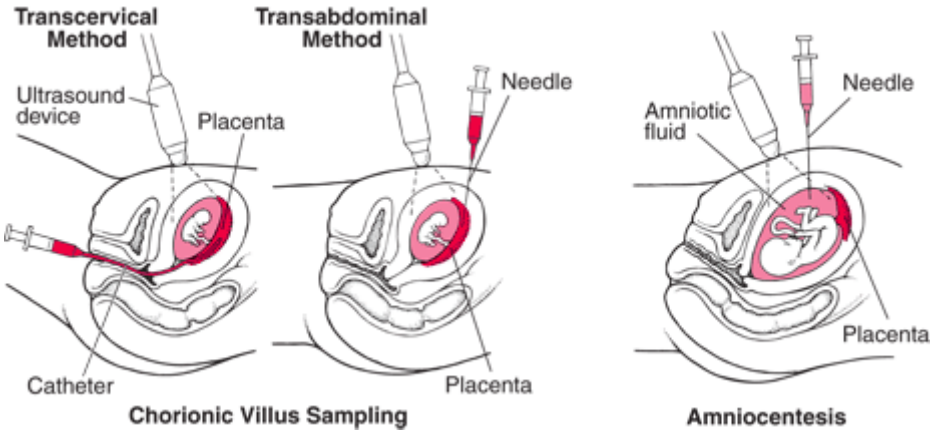

Figure 7: Schematic representation of the two types of CVS vs amniocentesis

During these invasive tests, a large amount of cells is collected. This circumvents the need for WGA and thereby leads to a more accurate diagnosis of small variations. Previously, prenatal diagnosis was performed by generating a karyotype from the isolated DNA. However, the resolution for such analyses is rather limiting (69) and some small CNVs might be missed. The development of array-based techniques has improved the detection of small variants as compared to the standard karyotyping (70, 71). Microarray analysis will provide additional clinically relevant information over karyotyping in 6 % of the cases with an abnormal ultrasound (69). However, balanced chromosomal translocations are not detected by array, as there is no loss or gain of genetic material. Nevertheless, such balanced translocations will have no consequences for the current pregnancy, unless it occurs in an important gene region.

Nevertheless, invasive prenatal testing is not without risks. Amniocentesis and CVS induce, respectively, a 0.81% and 2.2% risk for a miscarriage (72). However, these numbers should be interpreted with caution, as it is likely that pregnancy loss can also originate from other pregnancy-related and maternal factors (72, 73).

2.2. Non-invasive cell-free prenatal diagnosis

A recent evolution in prenatal diagnosis is the introduction of non-invasive prenatal testing (NIPT). In 1997, cell-free fetal DNA (cffDNA) was discovered in the maternal blood circulation (74). CffDNA is fetal DNA circulating freely in the maternal blood stream, derived from the cytotrophoblasts making up the placenta (75). This cell-free DNA can be isolated from the cell fraction of a maternal blood sample. The non-invasive nature of the method makes it an attractive alternative for the invasive methods. However, less than 7% of the cell-free DNA found in the blood is from the fetus (76), which makes it difficult to separate from the maternal DNA. Therefore, most commercially available NIPT tests only offer screening for trisomy 21, 13 and 18 (T21, T13 and T18). As long as not all chromosomal abnormalities are detectable with NIPT (77), the diagnosis by NIPT will not parallel the diagnosis by CVS or amniocentesis.

Since the introduction of NIPT, the amount of invasive prenatal procedures has plummeted (78-80). Giving the limited conditions tested with cell-free NIPT, this decrease might have led to fewer serious genetic conditions detected (81). There is also a small chance for false positive results after cell-free NIPT (82). Therefore, NIPT should only be used as a screening method, as an alternative for ultrasound imaging and maternal serum marker screening (83). Integrating this technique into prenatal screening might have the potential to decrease the amount of invasive procedures due to a false positive ultrasound and serum screening (84).

2.3. Non-invasive cell-based prenatal diagnosis

The presence of fetal cells in maternal blood during pregnancy was already described in the 70s (85-87). Different types of fetal cells are present in the maternal bloodstream and three types have been the subject of research for prenatal diagnosis: fetal leukocytes, fetal nucleated red blood cells and trophoblasts. Over the past years, many attempts have been made to use these fetal cells present in the blood for fetal diagnosis (81). Still, none of them is ready for routine clinical practice.

2.3.1. Leukocytes

Fetal leukocytes were amongst the first fetal cells discovered in the maternal blood of pregnant women (87). They discovered the presence of Y chromosome signals in both the maternal blood and the isolated leukocytes (86-88). However, fetal leukocytes were shown to persist in the maternal bloodstream for many years after giving birth (86, 88-91). Therefore, during a second pregnancy, leukocytes from the previous pregnancy might interfere with a

correct diagnosis of the current pregnancy. This implied the need for a short-lived fetal cell type, with limited replicating capacity, in the maternal bloodstream.

2.3.2. Nucleated red blood cells

The presence of immature erythrocytes in pregnant women was already demonstrated in 1957 by fetal hemoglobin labeling (92). However, it took a longer time to prove the fetal nature of these cells. As these cells were nucleated, Y-chromosome staining was used to show their fetal nature (93). Some research groups showed the possibility to enrich these cells from maternal blood (94-97), and thereby they became the most popular cell types for prenatal diagnosis. However, lacking a specific fetal marker, the majority of the enriched cells were still of maternal origin (98-102). A large multicenter clinical project in 2002 by Bianchi *et al.* failed to show a high sensitivity for detecting fetal aneuploidy and failed to diagnose female fetuses (103). This complicates the use of these cells for prenatal diagnosis. This and their rather fragile nature, tempered the initial popularity of these cells for prenatal diagnosis.

2.3.3. Trophoblasts

Trophoblasts first line the outer layer of the blastocyst and develop into a large part of the placenta. These cells are in close contact with the maternal circulation (104). Extravillus trophoblast cells invade into the maternal tissue during placenta formation and this tumor-like behavior will transform the arteries. During this natural process, uninuclear endovascular trophoblasts might breach through the maternal circulation. It has been demonstrated that trophoblasts are consistently present in the maternal circulation from week 5 of gestation (105) (Figure 8), but are rapidly cleared after pregnancy (105). They can be distinguished from other blood cells by their large cell-size (105) and detected by an epithelial cell marker, cytokeratin, not present on other cells in the blood (106, 107). This makes these cells attractive for use in prenatal diagnosis. One to six trophoblasts are present per milliliter of mother's blood (107, 108). Some promising work has already been done to prove the potential of trophoblasts in prenatal diagnosis (105, 109, 110).

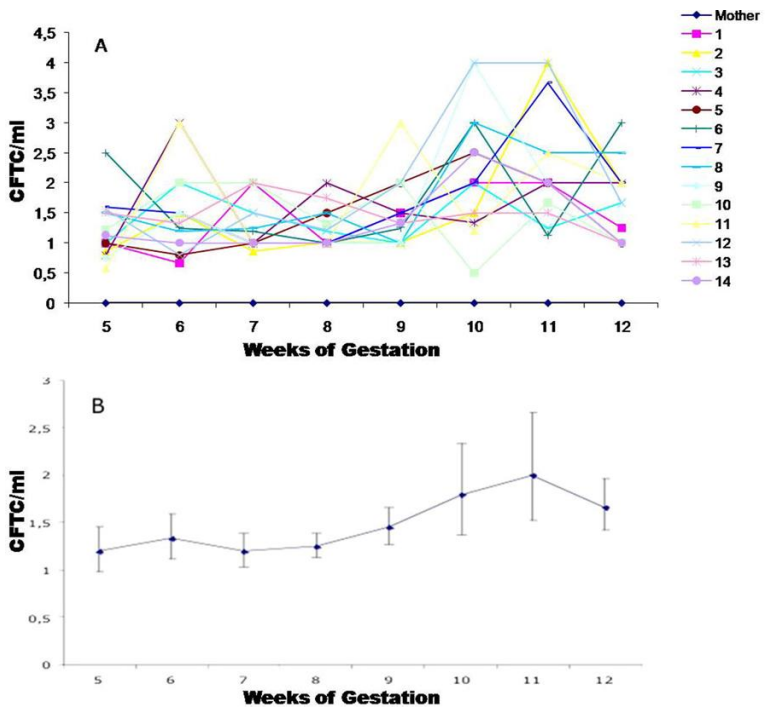

Figure 8: Kinetics of circulating fetal trophoblastic cells (CFTCs)

14 pregnant women during their first trimester from 5 to 12 weeks of gestation. A) Number of CFTCs per ml of blood. B) Mean and 95% confidence interval of CFTC number per ml of blood (105).

3. Whole genome amplification: a necessary evil

For applications, such as PGD and prenatal diagnosis, only limited genetic material is available. One cell contains only six pg of DNA, but analysis technologies such as aCGH and MPS demand nanograms to micrograms of DNA. An amplification of the genome will be essential to obtain reliable information about CNVs, aneuploidies or mutations present in the genome. WGA will amplify the entire genome, resulting in microgram quantities of amplified products. WGA might be compared with making a couple of copies from the genome of the cell. This is a critical component for obtaining genetic information, as the introduction of bias during amplification might influence the downstream results (111-114).

Multiple methods have been developed, each with their specific strength and bias introduction (115-117). Different types of amplification bias exist. Some methods might cause representation bias, by a preferential amplification of certain regions opposed to others, and thereby the representation of the original genome after amplification will be incorrect. Others will introduce ADOs, which occurs when a supposedly heterozygous locus appears as homozygous due to the failure to amplify one of the loci. Nucleotide errors can also be introduced and they might introduce or mask a mutation present in the original genome. Another important contributing factor is the source of input material, as some WGA methods might act differently with degraded, fixed or colored DNA (118). It is important to bear in mind that, to date, no WGA method is perfect. Therefore, the intended application and source material are an important factor to determine the method for amplification.

The existing WGA technologies are divided in 4 categories. They all made modifications to the classical PCR, that will give them their typical strengths and weaknesses.

3.1. Once upon a time

The first attempts to amplify genomic DNA were based on a standard PCR reaction, but with reduced specificity, allowing for a general amplification of the DNA. The two most widely used methods were: primer extension preamplification-PCR (PEP-PCR) and degenerate oligonucleotide primed-PCR (DOP-PCR) (116, 119). PEP-PCR uses a mixture of 15-base random oligonucleotides to perform repeated primer extensions (119) at a low annealing temperature. Although, random bases will increase the amplification yield, it also decreases the fidelity (120). As random primers are used, a high amount of primers is added to be able to cover each part of the genome. This might lead to primer-dimer formation, a well-known problem for PEP-PCR (121). As a consequence, less primers are available for the amplification reaction, thereby reducing the amplification efficiency.

To improve priming, DOP-PCR employs primers with an internal stretch of degenerate bases, flanked with specific sequences and uses an increasing annealing temperature (116). The degenerate part of the primers is a mix of similar sequences where some positions contain bases that can bind to any other base pair. These short base sequences can match easier across the DNA (122), but not completely random because of the presence of the specific region (Figure 9). Nevertheless, the specific bases at 3' can result in over-amplification of regions with a perfect match for this region (123). The annealing temperature starts low, to allow for many aspecific binding sites across the genome. Subsequently the temperature is increased, to prime more specific, only at the fragments previously tagged with the primers (124).
However, both PCR-based methods results in loss of signal and the introduction of nucleotide errors (125).

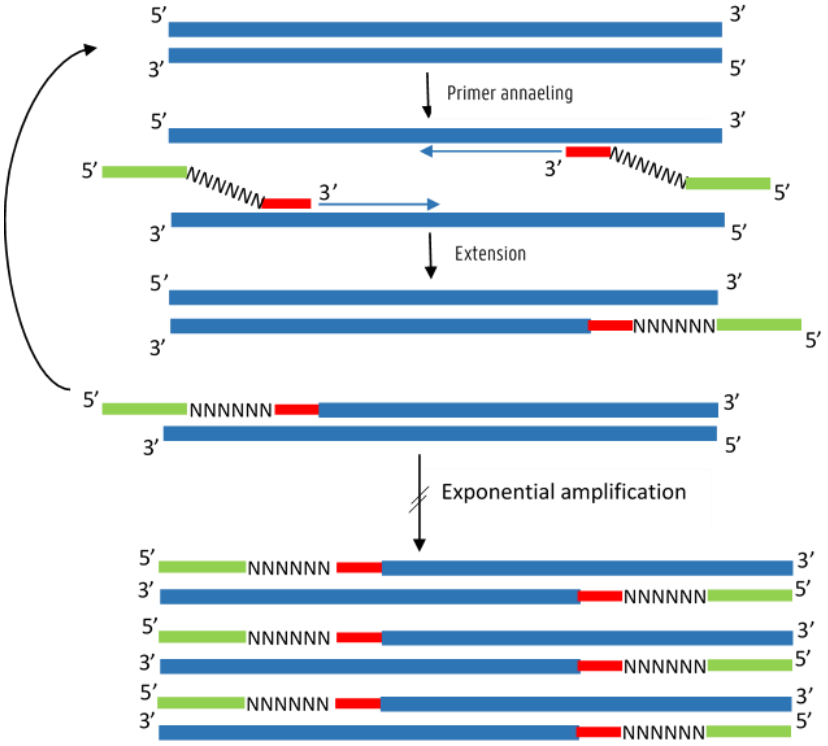

Figure 9: Schematic representation of DOP-PCR

3.2. Multiple displacement amplification

Multiple displacement amplification (MDA) based methods are isothermal, in contrast to the previous thermally cycled WGA (126, 127). These methods use the Phi29 polymerase, which exhibits strand displacement activity (128, 129) and 3'-5' exonuclease activity. Strand displacement occurs when the polymerase encounters other nucleotide sequences on the same strand. The polymerase will displace this sequence and thereby create a new single stranded sequence, which is available again for priming and extension (Figure 10). Due to its 3'-5' exonuclease activity, Phi29 is also a high fidelity and high processivity polymerase, resulting in low error rates, longer reads and higher yields during amplification. In the end, a network of sequences has been created by hyper-branching, covering a bigger part of the genome, with a lower error rate (130).

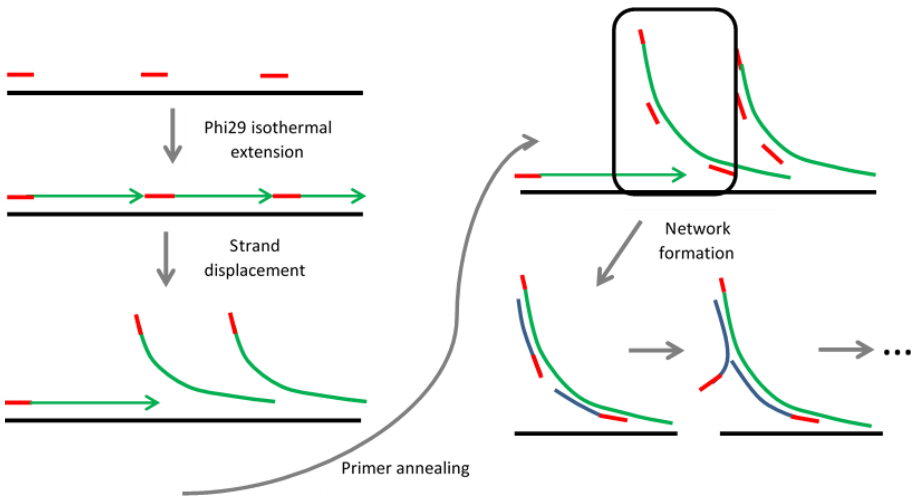

Figure 10: Schematic representation of the multiple displacement amplification (MDA) technology

Comparable to PEP WGA, MDA-based methods use also a random primer, leading to high yields, but low fidelity (126, 131). The most well-known commercially available MDA kits are: GenomiPhi (GE Healthcare Life Sciences) and REPLI-g (Qiagen).

3.3. Hybrid WGA methods

Previous methods were all based on an exponential amplification of the DNA. All errors introduced during amplification will thereby also be amplified exponentially. Hybrid methods perform a semi-linear amplification. First a pre-amplification is performed of only a few cycles, using a MDA-based amplification (Figure 11). The generated amplicons can form loops, as they have complementary parts with a constant sequence, at both ends. As a consequence, they are no longer available as template during this pre-amplification step. Thereby, a more homogeneous template is created for further exponential amplification with universal primers (132, 133). Two recent examples of such hybrid WGA are: PicoPLEX/SurePlex (Rubicon Genomics Inc., MI 48108, USA / BlueGnome Ltd., Mill Court, Great Shelford, Cambridge, UK) and Multiple Annealing and Looping Based Amplification Cycles (MALBAC) (Yikon genomics, Beijing, China). Both methods are similar, but with some discrepancies in the primer-sequence. PicoPLEX will use self-inert degenerative primers, whereas MALBAC uses random primers. However, their primers are both flanked with complementary ends for the looping formation, MALBAC primers are more focused on the formation of these loops (133), whereas PicoPLEX primers are more focused on a good primer distribution across the genome (132).

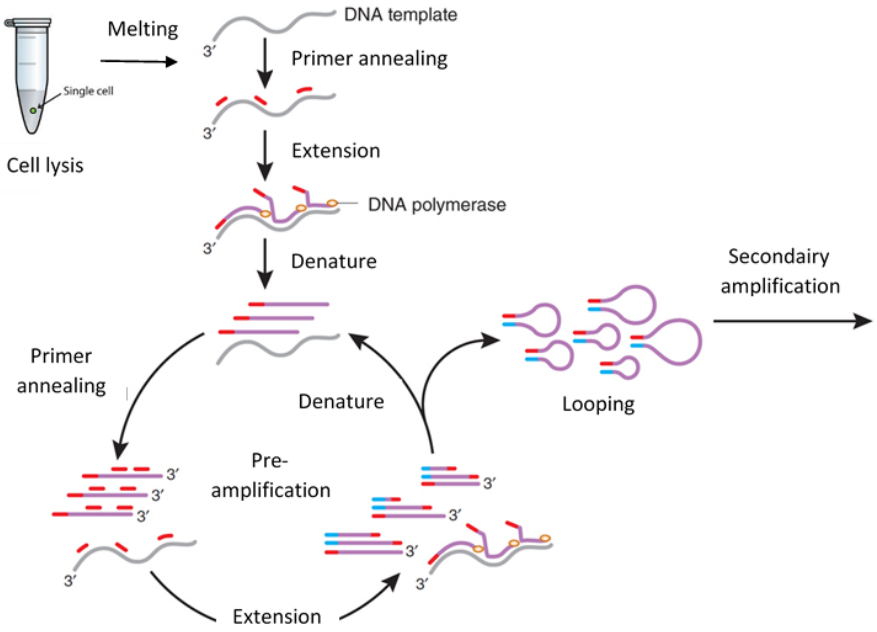

Figure 11: Schematic representation of hybrid WGA technologies

3.4. Ligation-based WGA

The most recent example of ligation-based WGA is Ampli1 (Silicon Biosystems, Castel Maggiore, Italy). The template is fragmented through a restriction enzyme, prior to amplification. This will create sticky ends for the ligation of adaptors. Subsequently, sequence-specific primers (complementary to the adaptor sequence) will bind and thereby start amplification (134). As the primers will bind to only one specific sequence, the binding efficiency is constant for all primers, in contrast to degenerate primers. However, the amplified fragments are shorter, rendering it less useful for applications where linkage information is important. In contrast, Ampli1 will perform better on degraded material (135) than WGA methods creating longer amplicons (118).

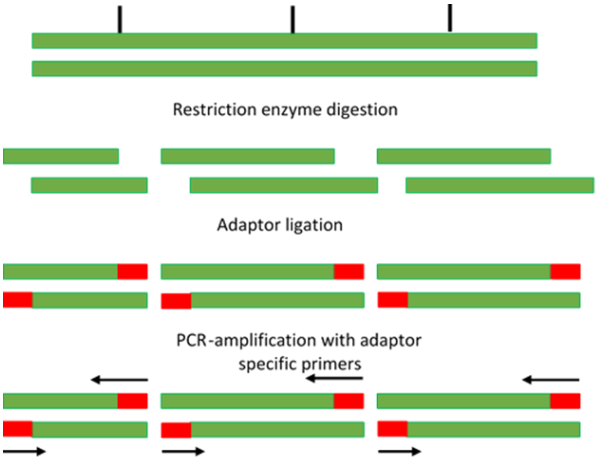

Figure 12: Schematic representation of ligation-based PCR

3.5. The importance of the downstream application

All WGA methods are in some way trying to minimize the introduced bias, but no WGA method, to date, is perfect. However, the impact of the bias on the resulting data could be reduced by selecting the ideal WGA for this application or starting material. For instance, MDA-based methods use a high fidelity polymerase, which makes them more preferable for SNP detection than hybrid methods using Taq polymerase. The high fidelity polymerase, Phi29, has a 3'-5' proofreading activity with an error rate between $1*10^{-6}$ - 10^{-7} (136). Due to the proofreading activity, the polymerase has an exonuclease activity, allowing the removal of erroneously inserted bases. Taq polymerase lacks this proofreading activity and thereby the error rate increases to $2*10^{-4}$ (137, 138). However, the phi29 polymerase will underrepresent regions close to the template termini and tends to over-amplify the first amplified fragments, rendering a non-uniform amplification (130). In contrast, hybrid methods will perform a more balanced amplification than the hyper-branching MDA methods, due to their semi-linear nature. Therefore, hybrid methods will result in a better CNV profile (130).

Some WGA methods have difficulties to amplify degraded material. For instance, due to hyper-branching, MDA will be more sensitive to template fragmentation, as the opportunities for hyper-branching and priming will be

decreased on each short molecule (118). As the polymerase is already sensitive to template termini, the problem of underrepresentation will enlarge with more template termini, as in the case with fragmented DNA (127, 139). Fixative agents are sometimes used to limit biological or chemical degradation of your template. In many non-invasive cell-based prenatal settings, fixation becomes more important (105, 110). However, these fixatives have also shown to damage the DNA (140-143). The most widely used fixative is formaldehyde and it is known to break inter-chain hydrogen bonds in AT-rich regions of a double-stranded template. Formaldehyde will further react with the free bases (144), which could lead to DNA fragmentation (144). This renders formaldehyde fixed samples also less preferable templates for some WGA methods. Therefore, Ampli1 or other WGA methods creating short fragments might be more preferable for fixed templates.

4. Low-pass whole-genome sequencing

4.1. DNA sequencing in general

DNA sequencing is used to determine the precise order of nucleotides within a DNA molecule. DNA consists of four basic types of nucleotides, based on their present nitrogenous base: Adenine (A), Cytosine (C), Guanine (G) or Thymine (T). DNA occurs as a double-stranded molecule in nature. Each base will form a pair through hydrogen bonds with a complementary base (A-T or G-C) on the opposite DNA-strand (Figure 13). All humans carry DNA in their cells and the precise order of these bases in their DNA will be unique for every person, except for homozygous twins.

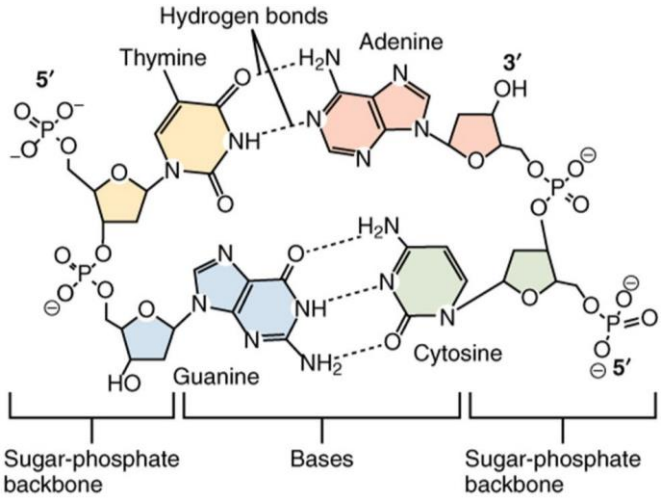

Figure 13: Nucleotide formations in the DNA structure

The human DNA consists of three billion base pairs. To sequence the complete human genome at a single base pair resolution, a very high sequencing coverage is required. The sequencing coverage is the average number of times each nucleotide is sequenced. This will depend on the number of reads created during the sequencing run, the length of these reads and the assumption that reads are distributed randomly across the genome (145). The breadth of coverage is different from the sequencing coverage, as this is the percentage of target bases that are sequenced

a given number of times. For instance, a genome sequenced at a coverage of 30X, with a breadth of coverage of 95% at 30X, will indicate that 5% of the bases failed to reach the 30X coverage. Obviously, a higher coverage inevitably requires a higher cost, as the read number or read length will increase. Therefore, it is important to consider the desired coverage for the downstream application before sequencing.

To detect large CNVs or aneuploidies, a deep sequencing at a single base pair resolution is not required. Low pass or shallow whole-genome sequencing will be more cost effective to detect these large CNVs (Figure 14). In contrast to deep sequencing, the coverage is low in low-pass sequencing. Still, this will be enough to detect the real CNVs, as the absence of big genomic parts will not be the result of the random read distribution.

Figure 14: Shallow sequencing vs deep sequencing

4.2. First generation sequencing

F. Sanger developed the first DNA sequencing method in 1975 (146). Sanger sequencing has been the dominant sequencing technique for several decades. It is based upon the random incorporation of dNTPs and chain-terminating dideoxycucleotides (ddNTPs) during *in vitro* DNA replication. This is an example of sequencing by synthesis (SBS), as the sequence is determined by re-synthesis of that sequence. The ddNTPs lack a 3' OH group, which impedes further incorporation of nucleotides. Thereby, a mixture of complementary DNA strands of variable length are synthesized and they are subsequently size-separated using capillary electrophoresis. The four different ddNTP types were initially labeled, each to a unique fluorochrome. Therefore, every last nucleotide of a fragment can be identified by its label and thereby listing all fragments by size will identify the complete sequence. Sanger sequencing allows for long read sequencing, up to 1000bp and longer, but in terms of large-scale sequencing it will be too expensive (147-149).

4.3. Second-generation sequencing

By the mid-1990s, several second-generation sequencing methods, also called next-generation sequencing or MPS methods, made their appearances. They are able to generate an enormous amount of sequencing data during a single sequencing run and this at an affordable price. Multiple samples can be sequenced in parallel on one run, called multiplex sequencing. Each sample is labeled with a unique index sequence for later identification. Initially,

several competitors entered the market for second generation sequencing, nowadays Illumina and Ion Torrent mainly dominate this market.

4.3.1. Illumina sequencing

The standard workflow for Illumina sequencing consists of three main parts: a library preparation, followed by clonal amplification and sequencing (149-151). During library preparation, the DNA is prepared to be compatible with the sequencing system. In the case of Illumina, the DNA should be able to bind to the probes on the flowcell. These probes are short identical single stranded sequences. Different types of library preparation methods exist, depending on the source material and the desired application (genomic sequencing, targeted sequencing…). However in general, the core steps for library preparation are: *i)* fragmentation/sizing of the DNA to the desired length, *ii)* making all fragments completely double-stranded and *iii)* attach adapters to the end of the fragments.

For CNV detection in PGD or prenatal samples, the source material is WGA material or genomic DNA. In such settings, three well-known library preparation methods are available for genome-wide Illumina sequencing. TruSeq (originally from Illumina) and NEBnext Ultra (generic version from New England Biolabs) are two examples of library preparation methods that rely on a fragmentation step independently from the library preparation protocol. In those settings, physical fragmentation is often performed by acoustic shearing of the DNA with, for instance, a Covaris instrument (Covaris, Woburn, MA). A third library preparation method, Nextera (Illumina), has an integrated enzymatic fragmentation step, called tagmentation. The DNA is fragmented and simultaneously tagged with adaptor sequences using a transposase enzyme. This will decrease preparation and handling time during library preparation, but enzymatic fragmentation is less precise than physical fragmentation (152).

Only the fragments with adaptors attached to the end will bind to the flowcell (Figure 15). Most library prep methods will enrich for these fragments using an enrichment PCR. However, PCR will introduce bias during amplification and therefore the reliability of the library preparation might increase by omitting this step. Illumina has already developed such a PCR-free library preparation method (TruSeq PCR-free library prep).

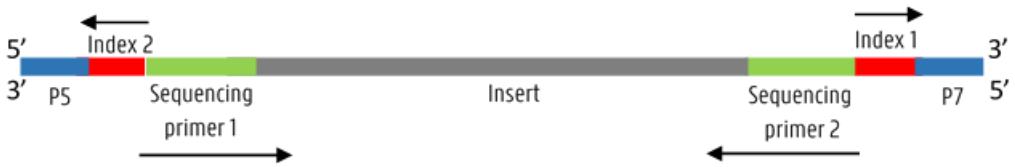

Figure 15: Adaptor-ligated fragment for Illumina sequencing.

An insert is a fragment with an unknown sequence; P5 and P7 are probe binding sites for flowcell binding; the sequencing primers are the primer binding sites used during the actual sequencing-step and index 1 & 2 are barcodes that will identify the individual samples during analysis. All molecules derived from one sample carry the same index sequence. For single-end sequencing only prime-site 1 is introduced, paired-end sequencing will need both sites. Similar for single and dual indexing.

After library preparation, the adaptor-ligated fragments are denatured and immobilized on the flowcell for subsequent clonal amplification by an isothermal bridge PCR (Figure 16). First, the immobilized probe is used as a primer to create the complement of each fragment, whereupon the original strands are washed away. Subsequently, these single stranded fragments will form bridges by binding to a complementary probe using their free end. The probe sequence is again used as a primer for the replication of these fragments, after which the new and old fragments are separated by a denaturation step. This bridge formation will be repeated until clusters are created, consisting each of a 1000 identical copies of a single DNA molecule.

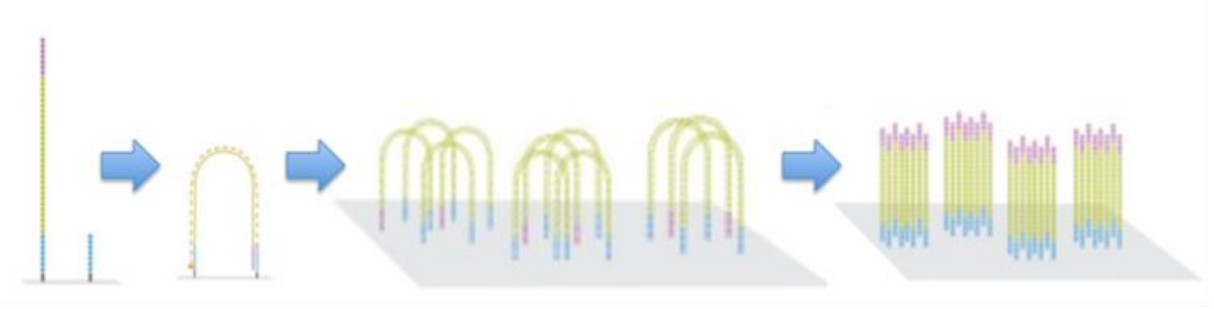

Figure 16: Schematic illustration of bridge amplification during Illumina sequencing

Finally, the sequence of each single molecule is determined during a sequencing-step. The sequencing starts from the sequencing primer binding site at the 3' side of the created fragments. Illumina also uses the SBS technology, as the sequence is determined by a step-by-step incorporation of a fluorescent nucleotide complementary to the single-ended fragment (Figure 17). Similar to Sanger, a chain-termination principle is used and four differentially labelled nucleotides were added simultaneously, competing each cycle for incorporation. Different from Sanger is the reversibility of the chain-termination and the absence of non-fluorescent labelled nucleotides. The incorporation of a fluorescent labelled nucleotide can be detected immediately, as for each molecule a complete cluster of fragments lights-up simultaneously. After detection, the blocking group and fluorescent label are removed and another cycle is initiated. At the end of this sequencing process, a sequencing read is created for each cluster/molecule.

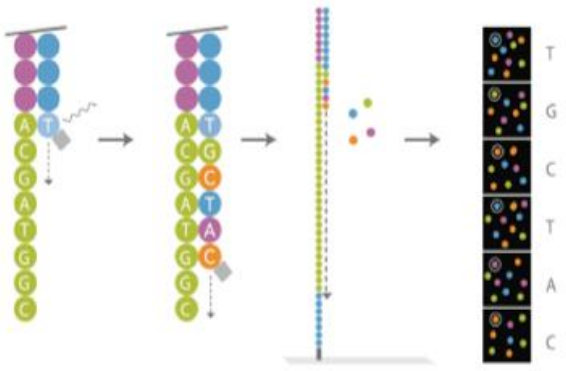

Figure 17: The sequencing by synthesis technology by Illumina

The number of cycles will determine the length of these reads, but at this point the read length is limited to 300bp (153). Different commercial kits are available for sequencing at specific read lengths, performing single or paired-end sequencing. Single-end sequencing is performed as described above, creating one read per molecule starting from the sense strand. For paired-end sequencing, the whole process is repeated starting from the anti-sense strand. In this way, two reads are created per molecule, each starting from another side. This will increase the coverage of the genome and is more preferable when longer fragments are sequenced. Illumina offers different sequencing platforms, ranging from benchtop sequencers (MiniSeq, MiSeq and NextSeq series) to production-scale sequencers (HiSeq and NovaSeq series). The choice for a specific sequencer series depends on the size of sample genome, the aimed sequence depth and the amount of samples to sequence at a certain depth. More samples per run will result in less sequence coverage/depth per sample, but also a lower price per sample.

4.3.2. Ion Torrent sequencing

The Ion Torrent semiconductor technology from Life Technologies translates simple chemical changes to digital information on a semiconductor chip. The standard workflow also consists of a library preparation, clonal amplification and sequencing. The adaptor-ligated fragments are linked to 3-micron diameter beads, known as Ion Sphere particles. The fragments are further clonally amplified by emulsion PCR on the beads and those beads are loaded on a semiconductor chip, each in separate wells. During the sequencing-step, each of the four nucleotides is introduced sequentially, as they do not carry a blocking group. If the correct base is introduced, a hydrogen ion will be released and change the charge. This will, subsequently, change the pH and this pH change will be detected proportional to the number of bases incorporated (Figure 18).

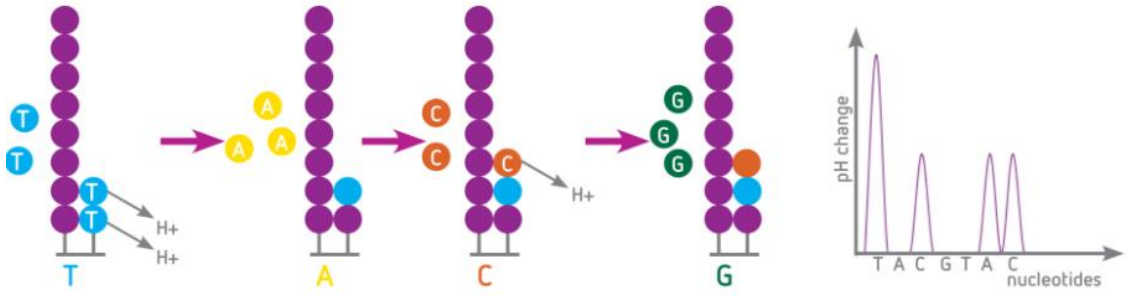

Figure 18: semiconductor sequencing by the Ion Torrent technology

Ion Torrent has four different sequencing platforms: The Ion Proton, the Ion Personal Genome Machine, and the Ion S5 and S5 XL systems. None of them is able to reach the capacity of Illumina, but they can create reads up to 400bp and with the S5 systems even up to 600bp. Ion Torrent's biggest downside is the difficulty to sequence homopolymer DNA stretches. As no blocking group is present, more nucleotides of the same type can be introduced during one cycle. Unfortunately, the signal does not increase proportionally with the number of bases introduced and after eight bases, the signal will no longer represent the correct number of bases.

4.4. Third generation sequencing

Recently, single-molecule technologies have been introduced. They promise to sequence high throughput, without the need for the clonal amplification step. The two most well-known single-molecule instruments are: The MinION from Oxford Nanopore and the PacBio RS from Pacific Biosciences (CA, USA). Pacific Biosciences (CA, USA) developed the Pacbio RS with the single molecule real-time sequencing technology to create true long reads of ±20kb. Zero-Mode Waveguides allow for real-time monitoring of base incorporation without the need for clonal amplification of the single molecule. This approach does not only result in unobstructed views of the sequence, it also reduces the degree of bias introduced. Nevertheless, the Pacbio instrument is very expensive, takes up a lot of space and requires multi-mg sample input. Another company engaged in long read sequencing, called Oxford Nanopore, has developed a low-cost, portable instrument to create true long reads. The MinION, as the instrument is called, consists of 512 pores to each fit a single DNA molecule. Common read lengths during Nanopore sequencing range from 6000 to 48000 bases (154). Similar to the PacBio, the bases are monitored in real-time without clonal amplification, but the identification and detection of the bases is different. An ion current flows through the pore and is partly blocked when a stretch of bases enters the pore. The fraction of the ion current that is blocked depends on the nucleotide within the pore (155-157). Nevertheless, this MinION has some drawbacks, as it is not yet commercially available, has a lower base-calling accuracy than conventional methods and whole-genome sequencing (WGS) is not yet possible.

4.5. Data analysis

Based on the hypothesis that there is a correlation between depth of coverage of a genomic region and the copy number (CN) of that region, the detection of CNVs, after low-pass MPS, might be performed using 'Depth of coverage' (DOP) analysis methods (158). Different types of DOP methods exist, but it would lead us too far to list all of these possibilities in this dissertation. QDNASeq and ReadDepth are examples of DOP methods that are not using a reference to call CNVs and are both correcting for GC content and mappability. They divide the genome in non-overlapping fixed size parts, so called windows/bins (159, 160). The size of these windows will determine the minimum size of the CNVs which can be detected. Generally, CNVs three to five times the size of the windows can be detected. First, the number of reads mapped to each window is determined. As this reads number is influenced by certain factors, such as GC-content and mappability, the number of reads mapped per window is normalized according to these factors. After GC-content and mappability normalization, read counts are also median-normalized by dividing the number of reads in each window by the median number of reads across all windows. As CNVs are assumed to be rare, the median number of reads across all windows is a fair estimate of the expected number of reads per window for a perfectly diploid genome. As such, the median-normalized read counts represent a measure for the deviation from diploidy for each window and a CN estimate is calculated using the following

formula: CN= 2(read count/median read count). Then, a circular binary segmentation (CBS) algorithm (161) is applied which groups windows into larger contiguous regions with an equal CN. The mean of read counts of the windows contained in the segments are used as an estimator of the copy number of the whole segment. After this segmentation, CNVs are called when the segment's $\log_2$(CN/2) surpasses a certain threshold. Based on literature review and own experience a threshold of +/- 0.35 performs well (161). The ideal window size for a specific sample will depend on its variance in read distribution across the genome. Bigger window sizes will smoothen the variance, lowering the chance of detecting false CNVs, but also lowering the resolution for CNV detection. A bigger variation in read distribution across the genome might indicate the presence of bias in the genome. Samples with a bigger variation might benefit from such larger window sizes, as this will avoid the detection of false CNVs. Nevertheless, too much smoothing, in samples with a very low amount of variance, might result in undetected CNVs. Therefore, the window size will be an important factor for a correct CNV determination.

Chapter II: Aims and overview

This dissertation consists of three parts. In the first main part we focus on CNV detection after shallow MPS on a limited amount of cells, as would be performed in a PGD-like setting using MPS. The second part is focused on another aspect of PGD, the SGDs. In the last part, we focus no longer on PGD, but on cell-based non-invasive prenatal diagnosis. More specific, the possibility to determine fetal identity of an isolated cell using short tandem repeat (STR) profiling.

One of the main goals of this dissertation was to show the possibility to apply shallow MPS for CNV detection in PGD and add evidence that MPS is a valuable and efficient substitute for state-of-the-art aCGH technology. As only 4 to 6 trophoblast cells are available to perform PGD, amplifying the DNA of those cells without introducing bias, will be an important first step in our workflow. The WGA method chosen to amplify the DNA must be able to reproduce a reliable representation of the CNVs present in the original cells. Therefore, in **Chapter III**, two prominent WGA methods, PicoPLEX/SurePlex (Rubicon Genomics Inc., MI 48108, USA / BlueGnome Ltd., Mill Court, Great Shelford, Cambridge, UK) and MALBAC (Yikon genomics, Beijing, China), were compared for their ability to amplify a limited number of cells for CNV detection after shallow MPS. SurePlex is the standard WGA method for PGD using aCGH and MALBAC was, at that time, a new WGA method using a similar technology as SurePlex. They are both hybrid PCR methods resulting in a semi-linear amplification. As a standard library preparation method also includes a PCR-step, two different library preparation methods were compared, one with and one without the PCR-step. The study was designed to resemble a possible workflow for CNV detection in PGD using MPS and to thereby discover which WGA method would be most suitable in such setting.

Subsequently, a large clinical study was initiated to evaluate the use of shallow MPS for CNV detection in PGD on trophectoderm cells of blastocysts and compare the results with the state-of-the-art technology in terms of accuracy. ACGH was the state-of-the-art technology in PGD, but in terms of cost, resolution, accuracy and flexibility, shallow MPS could possibly outperform aCGH. This study is described in **Chapter IV**. SurePlex amplified DNA material of 47 embryos was analyzed after shallow MPS for the presence of CNVs and aneuploidies of ≥3Mb and the outcome was compared to previous aCGH results. Sequencing was performed using both Illumina (NextSeq) and Ion Torrent (Ion Proton) sequencing as most clinical genetic labs should have access to one of these benchtop sequencers. After this study, our first main goal, to introduce shallow MPS in PGD, should be accomplished.

CNA analysis starting from a limited amount of DNA has also several other applications. Therefore, the complete workflow used in Chapter IV has been described in detail in **Chapter V**, including some tips and tricks to guarantee the success.

Although SurePlex has been successfully applied for PGD, a resolution of < 3Mb was hampered by WGA representation bias introduced during amplification. In the meantime, we were also approached by several commercial partners to test their new WGA methods for CNV detection after single cell MPS. Therefore, our next goal was to find a WGA method that was able to amplify single cells without representation bias for CNV analysis after shallow MPS. In **Chapter VI**, the TruePrime WGA method (Sygnis, Heidelberg, Germany) was compared in this context to previous SurePlex results. TruePrime uses a new type of amplification technology, as no artificial primers are added to the reaction. A DNA primase, TthPrimPol, will synthesize primers for the Phi29 DNA polymerase. Subsequently, Phi29 polymerase performs polymerization and strand displacement as in a classical MDA. The non-artificial primers, which could lead to a lower representation bias, combined with the high-fidelity of Phi29, could theoretically lead to an ideal WGA method. However, TruePrime WGA seemed unsuitable for CNV detection after MPS on a limited number of cells.

In **Chapter VII**, two new methods, DOPlify (Reproductive Health Science, Thebarton, Australia) and PicoPLEX DNA-Seq (Rubicon Genomics Inc., MI 48108, USA) , were compared to two older WGA methods, Ampli1 (Silicon Biosystems, Castel Maggiore, Italy) and REPLI-g (Rubicon Genomics Inc., MI 48108, USA). Thereby, four of the main types of WGA were tested in one study. DOPlify is an advanced DOP-PCR based WGA method, PicoPLEX DNA-Seq is a hybrid PCR method based on the SurePlex WGA principle, Ampli1 is a ligation-based method and REPLI-g is a MDA method. They were compared in a similar setting as the studies described above, except for the library preparation. In Chapter III we demonstrated that a PCR-free library preparation improved the CNV analysis and therefore all samples in the current study were prepped using a PCR-free library preparation. After this study, we hope to accomplish our goal with at least one WGA method, amplifying single cells without bias influencing CNV analysis at a 3Mb resolution after shallow MPS.

Another goal in this dissertation was to simultaneously analyze several monogenetic disorders in PGD using MPS. Current procedures for monogenetic PGD are time consuming, as for each mutation a specific test is designed. A test, applicable to all patients, simultaneously testing for multiple disorders would be more efficient. The TruSight One sequencing panel might be such a test, as it has been applied to screen for different monogenetic disorders in prenatal diagnosis using CVS. This panel simultaneously captures more than 4800 genomic regions associated with certain monogenic disorders and analyzes them on a single sequencing run. In contrast to PGD samples, CVS samples contain a lot of cells and thereby do not need amplification before analysis. The TruSight panel was

optimized for such bulk DNA samples and might therefore perform differently on WGA samples. In **Chapter VIII**, SurePlex, MALBAC, Ampli1 and REPLI-g were used to amplify the DNA of three-cell samples and the amplification products were prepped with the TruSight panel. DOPlify and PicoPLEX DNA-Seq did not exist yet and were therefore not included. The study should show if a reliable detection of SNVs is possible using the panel after amplification of only three cells.

The final part of this dissertation is focused on the preparation of genetic analysis tools applicable in cell-based prenatal diagnosis. Current state-of-the-art prenatal diagnostic methods are invasive and carry some risks for the fetus. The isolation of fetal cells from maternal blood, cell-based NIPT, would be a non-invasive alternative. Similar to PGD, only a limited number of fetal cells is available in one blood sample. Therefore, our workflow, previously developed for CNV detection in PGD, could also be applied in cell-based NIPT. As no specific marker for fetal cells is available, the fetal origin of the isolated cells should be determined in another way before genetic analysis. In **Chapter IX**, STR-analysis is proposed to identify the genetic origin of a single cell. The DNA of this cell is also needed for the genetic diagnosis, such as CNV analysis. Therefore, WGA is inevitable. Similar to CNV analysis, the used WGA method might influence the STR results. We compared SurePlex, Ampli1, DOPlify and REPLI-g for their suitability to detect STR markers after single cell amplification.

However, genetic analysis in cell-based NIPT cannot always be performed on-site or immediately upon blood retrieval. The widely used EDTA blood tubes demand blood processing within 4 hours, otherwise the cell quality might drop, hampering fetal cell isolation. Cell-free DNA BCT (cfDNA) tubes (Streck, Nebraska, USA) are designed to prevent lysis of nucleated blood cells by fixation of the cells. This fixation step might have an influence on the DNA of the cell and the performance of the WGA method. In **Chapter X**, we demonstrated the use of BCT reagents from Streck as a fixative for STR and CNV analysis of a single cell after amplification. The influence on the performance of SurePlex, Ampli1, DOPlify and REPLI-g was analyzed. A WGA method suitable for cell-based NIPT, should be able to amplify a single cell to determine the genetic identity of a cell and perform a reliable detection of CNVs after amplification of a single cell. After this study, we should have the tools for a possible genetic analysis of single fetal cells isolated in the context of cell-based NIPT.

Chapter XI provides a general conclusion of this dissertation. In **Chapter XII**, the broader international context of this dissertation and possible future perspectives were described.

Chapter III: Whole genome amplification with SurePlex results in better copy number alteration detection using sequencing data compared to the MALBAC method

Lieselot Deleye[1,*], Dieter De Coninck[1,*], Christodoulos Christodoulou[2], Tom Sante[3], Annelies Dheedene[3], Björn Heindryckx[2], Etienne Van den Abbeel[2], Petra De Sutter[2], Björn Menten[3], Dieter Deforce[1,†] & Filip Van Nieuwerburgh[1,†]

[1]Laboratory of Pharmaceutical Biotechnology, Ghent University, Ottergemsesteenweg 460, 9000 Ghent, Belgium.

[2]Department for Reproductive Medicine, Ghent University Hospital, De Pintelaan 185, 9000 Ghent, Belgium.

[3]Center for Medical Genetics, Ghent University, De Pintelaan 185, 9000 Ghent, Belgium.

[*]These authors contributed equally to this work: LD was responsible for the practical part and data acquisition, DDC was responsible for the bio-informatics part of the project.

[†]These authors jointly supervised this work.

Scientific Reports | 5:11711 | DOI: 10.1038/srep11711; Published: 30 June 2015

1. Abstract

Current whole genome amplification (WGA) methods lead to amplification bias resulting in over- and under-represented regions in the genome. Nevertheless, certain WGA methods, such as SurePlex and subsequent aCGH analysis, make it possible to detect copy number alterations (CNAs) at a 10 Mb resolution. A more uniform WGA combined with massively parallel sequencing (MPS), however, could allow detection at higher resolution and lower cost. Recently, MALBAC, a new WGA method, claims unparalleled performance. Here, we compared the well-established SurePlex and MALBAC WGA for their ability to detect CNAs in MPS generated data and, in addition, compared PCR-free MPS library preparation with the standard enrichment PCR library preparation. Results showed that SurePlex amplification led to more uniformity across the genome, allowing for a better CNA detection with less false positives compared to MALBAC amplified samples. An even more uniform coverage was observed in samples following a PCR-free library preparation. In general, the combination of SurePlex and MPS led to the same chromosomal profile compared to a reference aCGH from unamplified genomic DNA, underlining the large potential of MPS techniques in CNA detection from a limited number of DNA material.

2. Introduction

Today, massively parallel sequencing (MPS) techniques undergo a rapid and continuous evolution and improvement in accuracy, speed, and cost efficiency. An important factor determining the success of the sequencing of limited numbers of starting material is the whole genome amplification (WGA) protocol. Bias introduced during this amplification process may lead to misinterpretations of the genomic profile. Especially when very low amounts of DNA have to be amplified, such as DNA from single cells, some WGA methods will lead to a disproportionate amplification of genomic regions. This results in false positive or false negative copy number changes and allelic dropouts and will be of great importance for applications with the purpose of detecting copy number changes in the genome. An example of such application is pre-implantation genetic diagnosis (PGD) to select an embryo fit for implantation based on the DNA analysis of 4-7 trophectoderm cells. State-of-the-art PGD, using array Comparative Genomic Hybridization (aCGH), allows to determine the aneuploidy in the embryo as well as copy number alterations (CNAs), such as deletions, duplications and unbalanced translocations of size larger than 10Mb. Nowadays, MPS techniques are being introduced in this field (32, 162-164) which rises the opportunity to increase the resolution at a reasonable price. Oncogenetics is another field where a faithful analysis of a limited number of DNA is of great interest. Analyzing the genome of individual cells is important to dissect cancer evolution and to provide the potential to considerably change both cancer research and clinical practice (165).

A number of commercially available WGA kits have already been individually tested for single cell sequencing, including degenerate oligonucleotide primed PCR (166) and primer extension PCR (119, 167). However, these resulted in allelic drop out (ADO) or preferential amplification of one of both alleles (125). Another technique, PicoPLEX/SurePlex (Rubicon Genomics Inc., MI 48108, USA / BlueGnome Ltd., Mill Court, Great Shelford, Cambridge, UK) which is the current standard WGA method for PGD aCGH, is based on the use of specific self-inert degenerative primers in the formation of an *in vitro* molecular library that can be amplified by PCR utilizing flanking universal priming sites. Based on the company brochures, an ADO rate limited to 10% can be expected, which is a major improvement over previous PCR-based methods. Recently, a new method, Multiple Annealing and Looping Based Amplification Cycles (MALBAC) (Yikon genomics, Beijing, China) was developed. According to their patent, this method would lead to less amplification bias compared to the SurePlex procedure (WO 2012166425 A2). As the name suggests, loops are formed from the first generated amplicons, which ensures that these amplicons are no longer available as template during this first amplification round. During a second amplification step, these loops will form a more homogeneous template for PCR amplification. In this way, a semi-linear amplification takes place. Ning *et al.* (2014) compared MALBAC with two other WGA methods, Multiple Displacement Amplification (MDA) and a GenomePlex PCR-based method, and concluded that MALBAC had the best genome coverage with excellent reproducibility (168). In general, it has been shown that each WGA method has its own advantages and disadvantages and that the best method should be selected based on its intended application. A recent article, for instance, suggested that MDA would be better for single nucleotide polymorphism (SNP) detection while MALBAC would be better for CNA detection (130).

On top of the representation bias introduced by WGA, MPS library preparation can also introduce additional bias due to the enrichment PCR amplification of adapter-ligated fragments. Extra cycles of amplification could lead to extra representation bias in the results.

The goal of this study was to compare commercial SurePlex and MALBAC WGA protocols for their ability to produce optimal MPS data for aneuploidy screening and copy number analysis from a limited number of cells. Samples consisting of 1, 3 or 5 cells, in triplicate, were collected from the Loucy lymphoblastoid cell line using micromanipulation. The samples were amplified using both WGA methods and Illumina library preparation and sequencing was performed on these WGA products. Subsequent enrichment PCR or PCR-free MPS library preparation was performed in parallel to compare the representation bias. For the different WGA and sequencing library preparation methods, the variability in distribution of the reads across the genome and the ability to correctly detect chromosomal aneuploidies and large CNAs was compared using the bioinformatics tool ReadDepth (159). The final MPS results were compared to a 180K aCGH profile (Agilent technologies) of unamplified genomic

DNA of the Loucy cell line which was determined prior to the experiments to serve as a reference performance standard.

3. Material and methods

3.1. Experimental design

This study was performed on cells derived from the female Loucy cell line (ATCC CRL-2629; (169)). A reference 180K aCGH profile (Agilent Technologies) from unamplified genomic DNA from this cell line was obtained prior to the start of the experiments, i.e. before handling and isolation of the samples (Figure 1). The sequencing results will be compared to this reference aCGH profile for CNAs of 3Mb and larger. The cell line was grown in suspension which allowed isolation of individual cells. The influence of two commercially available WGA kits (MALBAC and SurePlex) on the ability to detect CNAs in a MPS approach was assessed. For each amplification method, a total of 12 samples was used. Triplicates of samples with 1, 3 or 5 cells were prepared with a standard enrichment PCR based Illumina sequencing library preparation (Figure 2a). Secondary, triplicates of samples with 3 cells were prepared with a PCR-free Illumina sequencing library preparation (Figure 2b).

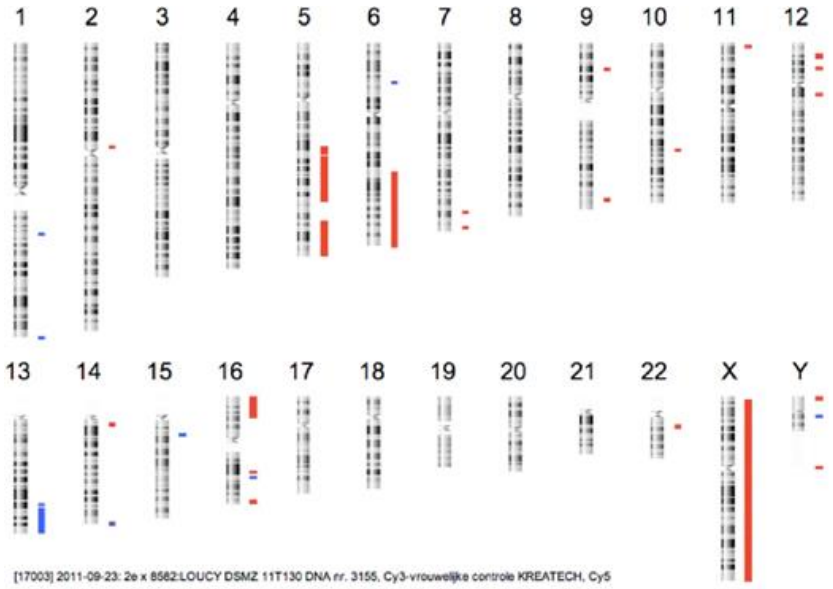

Figure 1: 180K aCGH of genomic DNA from the female Loucy cell line

This profile shows all CNAs detected in the female Loucy cell line up to a resolution of 50 kb. Red bars indicate deletions and blue bars indicate insertions. The deletions in chromosomes X, 5, 6, and 16 and duplication in chromosome 13, all with a size of >3Mb, were the ones expected to be detected by the sequencing results.

3.2. Growth and isolation of cells

The cells were grown in Roswell Park Memorial Institute (RPMI-1640) medium (Life technologies, Carlsbad, USA), supplemented with 10% fetal bovine serum (Life technologies, Carlsbad, USA). For optimal growth they were kept at a temperature of 37°C and a 5% CO_2 level. A known amount of cells was isolated with an ergonomic denuding handle from STRIPPER (Origio, Måløv, Denmark) and MXL3-100 needles with a diameter of 100 µm (Origio, Måløv,

Denmark). A serial dilution with sterile phosphate buffered saline (PBS) (Life technologies, Carlsbad, USA) spots to the desired amount of cells for isolation was performed on a Petri dish (5.5cm) under an Axiovert 25 light microscope (Zeiss, Jena, Germany). All cells were collected in a maximum volume of 1µl for the MALBAC samples and 2.5µl for the SurePlex samples, as this is required for optimal lysis of the cells, according to manufacturer's instructions. Immediately after collection, all samples were snap frozen in liquid N_2.

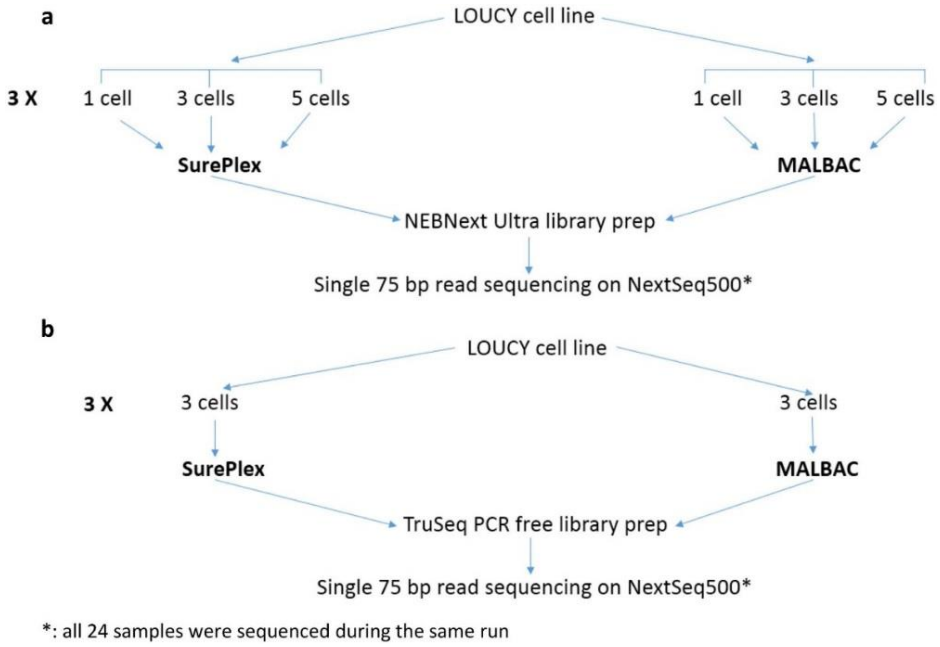

Figure 2: Experimental design

a) Experiment comparing SurePlex and MALBAC WGA methods. B) Experiment to investigate effect of enrichment PCR during library preparation for both SurePlex and MALBAC amplified samples.

3.3. MALBAC WGA

Cell lysis and amplification was performed, using the MALBAC kit (Yikon genomics YK001A/B version 1302.1, Jiangsu, China), following manufacturer's instructions. As a positive control, 1µl of male control DNA (9948; Promega; 10ng/µl) was used at a concentration of 30pg/µl. The blank was 1µl of PBS. All samples were purified according to the manufacturer's protocol of the Genomic DNA Clean & Concentrator kit (version 1.0.0, Zymo Research, Irvine, USA) with 5 X binding buffer. Concentration was measured using Qubit dsDNA High Sensitivity Assay kit (Life technologies, Carlsbad, USA).

3.4. SurePlex WGA

Cell lysis and amplification was performed following manufacturer's instructions using the SurePlex Amplification system (Bluegnome, Cambridge, United Kingdom). As a positive control, 2.5µl of female control DNA (G1521; Promega; 187ng/µl) was used at a concentration of 25pg/µl. The blank was equal to 2.5µl of PBS. Purification and concentration measurements were done in the same way a described above.

3.5. ACGH

One of the three cell samples, amplified by SurePlex, was also analyzed using a 1Mb BAC array (Bluegnome) (Supplementary fig. S1). The CNAs observed on this array should also be observed on the reference array profile. The aCGH was performed according to the 24Sure Protocol (Bluegnome) with a male genomic DNA sample as reference.

3.6. Illumina library preparation

Hundred ng of the WGA products was fragmented to an average size distribution of 200bp with the S2 Focused Ultrasonicator with Adaptive Focused Acoustics (AFA) technology (Covaris, Woburn, USA). All samples were diluted in Tris-EDTA buffer (TE-buffer) to a volume of 130 µl in microTUBES (Covaris, Woburn, USA). The programmed guidelines for fragmentation to 200bp were followed (Duty cycle of 10%, Intensity of 5 and 200 cycles/burst), but the fragmentation time was prolonged to 190sec based on previous experience.

Subsequently, libraries of the fragmented samples were created using NEBNext Ultra DNA Library Prep (Chapter 2B, New England Biolabs, Ipswich, USA), following manufacturer's protocol with modifications as described here. After incubation with the USER enzyme, a DNA purification step (Zymo Genomic DNA Clean & Concentrator) was included before the size selection step. Size selection was performed with the E-Gel iBase Power system (Invitrogen) using an E-gel EX 2% agarose gel and a 1kb Plus DNA ladder (Thermo Fisher Scientific, Waltham, USA). For all samples, fragments with a size of ±300bp were cut from the gel and DNA was recovered using the Zymoclean gel DNA recovery kit (Zymo research). The size selected DNA samples were then subjected to an enrichment PCR using NEBNext Multiplex Oligos for Illumina (Index Primers Set 1 and 2) according to the protocol, with addition of tRNA to minimize the loss of DNA via tube interaction. The quality of the different samples was assessed with the Agilent High-Sensitivity DNA kit (Bioanalyser, Agilent Technologies, California, USA).

The PCR-free libraries were created entirely according to the TruSeq DNA PCR-free HT sample preparation kit (Illumina), which does not require an enrichment PCR. For each sample, the entire amount of WGA product was used as starting material, which was on average 700ng. This is lower than the 1µg input required by the protocol. From here onwards, these samples are called 'PCR-free' samples.

Before sequencing the samples, the amount of sequence-able library fragments was determined by performing a qPCR according to the Sequencing Library qPCR Quantification kit (Illumina, San Diego, USA). Samples were diluted to 10nM with elution buffer (EB buffer) (QIAGEN, Hilden, Germany). The control template used for the standard curve was a PhiX control library (10nM).

Finally, single-end index 75bp sequencing was performed on a high output flowcell on a NextSeq500 (Illumina, California, USA). 24 samples with each a different index were multiplexed on one flowcell. Samples were pooled at 2nM each and diluted to a final concentration of 2.3pM. Sequencing of 24 samples at 75 bp on a NextSeq500 should lead to an average genome coverage of 0.4X per sample (16M reads /sample).

3.7. Data analysis

The FastQ files imported from Basespace (Illumina), were quality controlled using FastQCv0.10.1 (Babraham bioinformatics). This revealed a disproportionate oscillation of the percentage of the bases in the first 30bp of the reads. The disproportionate oscillation in the percentage of bases was more pronounced in the SurePlex amplified samples (Supplementary fig. S2). In addition to trimming these 30 bp, TruSeq adapters and low quality read ends with Phred quality score < 20 were trimmed with Cutadapt v1.4.2.

Reads with minimum length of 30 bp were subsequently aligned to the human genome hg19 using the Burrow-Wheeler-Aligner (BWA) v0.7.5a algorithm and non-uniquely mapping reads were removed with SAMtools v0.1.19 and BEDtools v2.17.0 (170, 171). CNA detection was performed using the bioinformatics tool ReadDepth (159), which performed best in a recent comparison of different CNA detection methods (172). For this, the genome sequence was divided into non-overlapping windows or bins of 1Mb in size and the number of reads per bin was calculated. The number of reads per bin was corrected for bias introduced by the inability to map reads into repetitive regions of the genome by using mappability tracks created via self-alignment of the reference genome. Additionally, the mappability corrected read numbers per bin were normalized for GC-content. For this, the average read depth for bins with GC content was calculated in intervals of 0.1% before using LOESS smoothing to fit a regression line to this data. Finally, bins were median normalized. The number of reads per bin was scaled using a correction value equal to the difference between the median read depth and the average read depth of that bin and in such way that the correction was neutral with respect to the total number of reads. Bins with a similar amount of reads were detected using a circular binary segmentation algorithm (alpha value of 0.01 and min.width value of 2) and considered as one segment. Based on an estimated amount of copy-number gain or loss in the genome (both 5%; standard settings determined by the authors of the ReadDepth tool yielding a good performance (159)) and an overdispersion factor equal to 5 (for which the observed and modeled distributions were most similar), three different negative binomial distributions were modeled for monosomic, diploid or trisomic regions, respectively. The two values at which the three peaks of these distributions were maximally separated were considered as thresholds for monosomic and trisomic regions. Estimated copy numbers for segments that exceeded these thresholds were flagged as CNAs. Copy numbers were estimated under the assumption that for a diploid genome the majority of the genome is copy number two. The copy number of other regions was subsequently estimated based on the segment ratio relative to two.

Comparing the yield after amplification and library preparation between the different groups was performed using t-test statistics. The variance in number of reads per 1Mb bin across the genome was compared between MALBAC, SurePlex and the PCR-free samples by means of a mean-scaled first order estimator. In more detail, GC-content and mappability normalized count data per bin was divided by the average number of reads per bin, thus correcting for possible differences in sequencing depth. We then estimated the variance across bins as the running sum of the squared difference between the mean scaled number of reads of one bin and the previous bin divided by the total number of bins, which is the same for all samples. The variance due to counting statistics in profiles, normalized so that the mean value is 1.0, is equal to 1/N, where N is the average number of reads per bin (neglecting small effects due to copy number aberrations and counting corrections). As such, the difference between the variance of the copy number profile, estimated by the first-order estimator, and the variance due to counting statistics (1/N) for that profile gives a measure of the noise contribution from the entire sample handling, preparation and analytical process, independent of sequencing depth. The difference in percentage of reads mapped in the different groups was analyzed by a one-way ANOVA on the arcsine transformed data, followed by a Bonferroni's multiple comparison post-hoc test. When the prerequisites for valid ANOVA testing could not be met, an ANOVA on ranks followed by post-hoc Dunn's method was performed instead. P-values <0.05 were considered significant. Numbers given after '±' symbol in results indicates standard deviation. The sensitivity was defined as the number of true positive calls divided by all positive results for the cell line (true positive + false negatives). The positive predictive value (PPV) was defined as the number of true positive calls divided by the number of positive calls (false positive + true positive). Raw sequencing data are deposited in the NCBI Sequence Read Archive under project accession number SRP051311.

4. Results

4.1. Evaluation of Loucy cell line stability

As a reference for our DNA samples, a 180K aCGH profile of unamplified genomic DNA of the Loucy cell line was used (Figure 1). The 180K arrays have an average resolution of ±50kb. The resolution aimed by the MPS analysis is to find CNAs of 3Mb in size or larger. This resolution was chosen in view of performing PGD using MPS. Currently the resolution for PGD is 3-10Mb. However, some small CNAs are not well-defined at this resolution. Opting for a higher resolution could include these CNAs as well. 3Mb was considered a minimum because the variation caused by the WGA was a limiting factor at lower bin sizes. BAC aCGH analysis was performed on amplified DNA at a resolution of 10Mb (Supplementary fig. S1). If the 180 aCGH profile was filtered for CNAs > 3Mb in size, both profiles showed a similar pattern, confirming that the cell line was not altered after manipulation. According to the 180K aCGH profile, the following chromosomal aneuploidies and CNAs were called within the resolution range of the subsequent sequencing results (>3Mb): a deletion of an entire X-chromosome, a distal deletion of ±72Mb on

5q21.3q35.3, a distal deletion of ±45Mb on 6q22.31q27, a ±26Mb duplication of 13q33-q33.3 and deletions of respectively 13Mb and 3Mb on 16p13.3-p13.12 and 16q24.2q24.3. These CNAs were used as a reference for comparison with the MPS analyses.

4.2. Yield after WGA and library preparation

Figure 3 compares the WGA product yield of both tested WGA methods. The final volume of all samples was the same. Both WGA methods resulted in a similar yield after amplification of the samples containing 1 cell. The yield after amplification with SurePlex was significantly higher than the yield after MALBAC amplification when started from samples of 3 (34.7±6.1 ng/µl vs. 19.9±2.1 ng/µl) or 5 cells (31±4.8 ng/µl vs. 17.7±5 ng/µl).

For the libraries that were prepared using enrichment PCR, there was no significant difference in the amount of sequence-able fragments measured by qPCR for MALBAC or SurePlex amplified samples (14.8±3.7 nM and 18.5± 6.3 nM for MALBAC and SurePlex amplified samples, respectively). In contrast, for the PCR-free library preparations, a significant difference was detected between the samples with MALBAC (1.1±0.6 nM) and SurePlex amplification (4.6±1.5 nM).

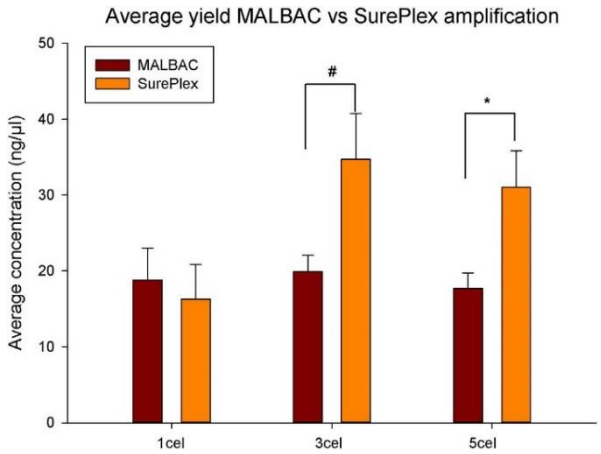

Figure 3: Average yield after MALBAC and SurePlex amplification for the different amounts of starting material used.

The difference between MALBAC and SurePlex within each group was tested with a t-test. One-tailed p-values are #: p =0.000305; *: p=0.00352. 1 cell N=6; 3 cell N=9; 5 cell N=6.

4.3. Sequencing quality

With a density of 140K/mm^3 and a total (passed-filter) read count of 324.76M, the run quality was within expectations with 87% passing the quality threshold of 30, a Full width at half maximum (FWHM) of 3 and a 1.66% alignment of the PhiX control. After adaptor and quality trimming and mapping of the reads, an average of 12,708,048 reads of ±30bp was mapped per sample, resulting in an average coverage of 0.1X per sample. The PCR-free SurePlex prepped samples had a lower number of reads mapped, compared to the other samples. While all other samples contributed on average to 14,013,601 reads per sample, these samples only had 3,569,175 reads on

average mapped per sample (coverage of 0.03X). To allow comparison between PCR-free libraries and enrichment PCR amplified libraries, the latter were randomly down-sampled to a comparable raw read count.

4.4. Difference in read mapping between MALBAC and SurePlex.

When comparing the mapping results within each protocol from the samples with a different number of input cells, no significant differences were detected in the relative number of uniquely, non-uniquely and unmapped reads ($p>0.05$). A significantly higher percentage of reads, generated from the samples amplified with MALBAC, mapped uniquely compared to the percentage of uniquely mapped reads from samples amplified with SurePlex (82.8± 1.4% vs 76.1± 1.6 %, respectively) (Figure 4). This also holds true for the MALBAC and SurePlex amplified samples that were not enriched by PCR during library preparation (81.1 ± 2.4% vs 69.8 ± 2.3%, respectively). The percentage of uniquely mapped reads was significantly higher in the SurePlex amplified samples compared to the SurePlex amplified samples prepared without enrichment PCR. No significant difference was found for the MALBAC samples prepared with enrichment PCR versus the PCR-free MALBAC amplified samples.

The distributions of the GC content per read showed, for both MALBAC and SurePlex amplified samples, a higher mean GC-content than the GC-content in the human genome, around 46% and 45% vs 42.4% for MALBAC and SurePlex, respectively (Supplementary fig S3). Omission of the enrichment PCR during library preparation resulted for both amplification protocols in slightly lower average GC-contents (43% for both MALBAC and SurePlex), yet the distributions were less well-shaped (Supplementary fig S3).

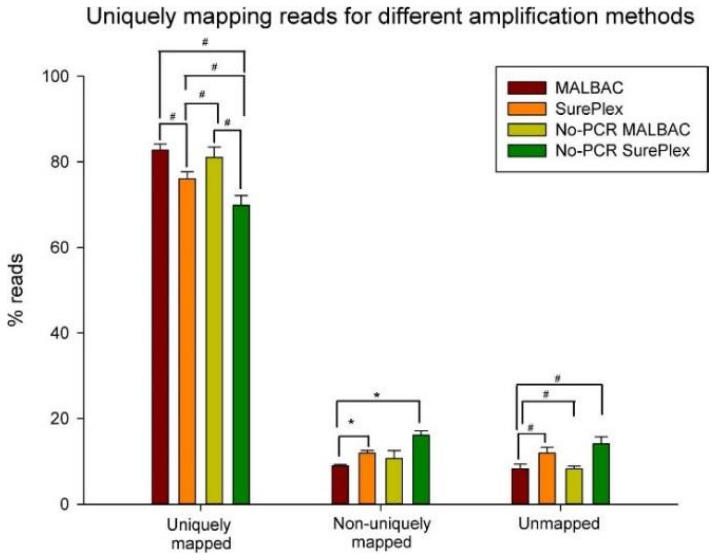

Figure 4: Scheme of read mapping after different amplification methods

MALBAC amplified samples have more uniquely mapped reads compared to SurePlex amplified samples. Samples were combined for the different starting amounts. Statistical analysis was performed with a one-way ANOVA followed by a Bonferroni t-test for multiple comparison. When comparing the percentages of non-uniquely mapped samples, the equal variance test failed. Here an ANOVA on ranks was performed followed by Dunn's method for multiple comparison. #: $p<0.001$ and *: $p<0.05$.

4.5. Read distribution across the genome

The variance in read distribution across the genome was significantly different between MALBAC and SurePlex amplified samples. The number of reads per 1Mb bin in MALBAC amplified samples varied more across the genome as compared to SurePlex amplified samples. This was the case for 1 cell, 3 cells and 5 cell samples (Table 1). The variability in mapping had the consequence that a lot of bins, in the MALBAC amplified samples, fell outside of the range expected for diploidy, even in regions where the Loucy genome is diploid. This was not observed in the SurePlex amplified samples, were a more smooth read distribution was observed.

Estimates of variance		
condition	mean	standard
MALBAC 1 cell	0.165	0.03
MALBAC 3 cells	0.138	0.01
MALBAC 5 cells	0.146	0.01
MALBAC no PCR	0.120	0.01
SurePlex 1 cell	0.083	0.01
SurePlex 3 cells	0.077	0.01
SurePlex 5 cells	0.073	0.00
SurePlex no PCR	0.064	0.00
Statistical differences in variance		
comparison	p-value	
MALBAC 1 cell vs	0.0239	
MALBAC 3 cells vs SurePlex 3 cells	0.0031	
MALBAC 5 cells vs SurePlex 5 cells	0.0007	
MALBAC no PCR vs SurePlex	0.0032	

Table 1: Estimates of variance (mean and standard deviation) and statistical differences in variance for the different tested conditions. "no PCR" indicates the absence of an enrichment PCR during library preparation.

4.6. Detection of chromosomal aneuploidy and copy number variants

The first way to detect CNAs is using an algorithm such as used by ReadDepth. Next to this, CNAs can also be represented as a graphical profile (Figure 5), allowing a more manual interpretation. The choice for 1Mb bins allowed us to detect CNAs at least 3Mb in size. Analysis of the MALBAC amplified samples resulted in many false positive CNA calls random across the genome, which were not observed on the reference aCGH profile (Table 2; Supplementary Table 1). Only one of the MALBAC amplified samples resulted in detection of all CNAs that were present according to the aCGH reference (Table 2; Supplementary Table 1). Most of the samples missed more than one of the expected CNAs. On the other hand, of all samples amplified with SurePlex, only two gave an incomplete detection of the CNAs and only a few false positive CNAs were detected. Figure 5 shows the CNA profiles of two 3-cell samples amplified with either SurePlex (Figure 5a) or MALBAC (Figure 5b). The profile of the SurePlex samples is smoother and the expected CNAs are clearly observed. The CNA profiles of all samples used during this

experiment are shown in Supplementary fig. S4. These results show a sensitivity for calling the correct CNA equal to 59.3% ±22.2% (mean ± standard deviation) for MALBAC amplified samples and 94.4% ±11.8% for SurePlex amplified samples. The difference between both methods, is also reflected in the PPV, with a PPV of 42% ±12.3% and 77.7% ±11.8% for MALBAC and SurePlex amplified samples, respectively.

Number of	Expected CNA calls according to reference array (≥3Mb) (18)			False positive calls (0)		
3X	**1cell**	**3cell**	**5cell**	**1cell**	**3cell**	**5cell**
MALBAC	9	10	13	16	13	14
SurePlex	13	18	18	6	4	5
No-PCR MALBAC		9			8	
No-PCR SurePlex		14			0	

Table 2: Number of expected calls and false positives made by all samples.

Expected calls were: deletions in chromosomes X, 5, 6, 9 and 16 and duplication in chromosome 13 as expected by array. Calls were of 3Mb and bigger expected. Calls were summed for the samples that started with the same amount of cells.

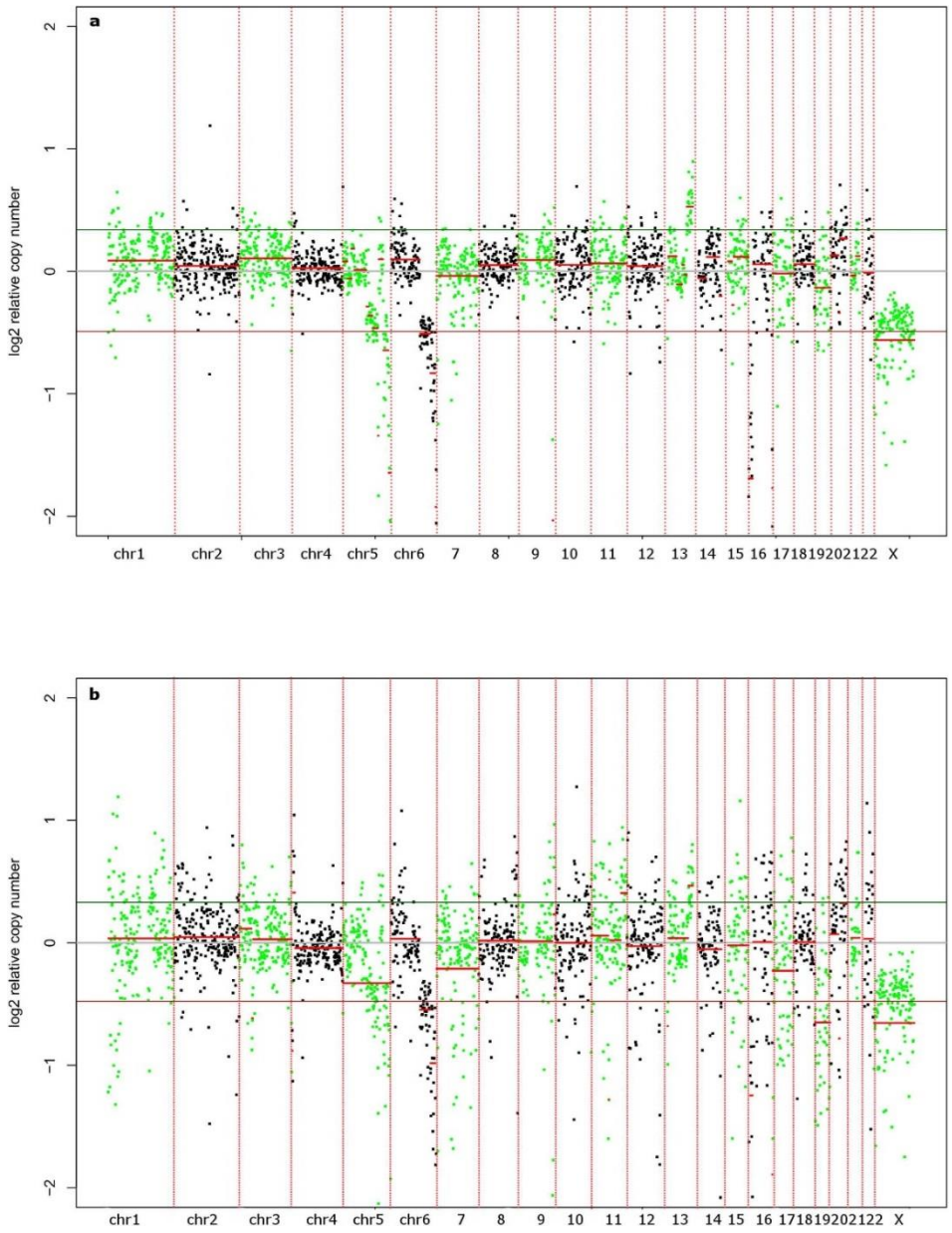

Figure 5: Samples amplified with SurePlex are better suited for detection of aneuploidies and CNAs.

A) All aCGH-verified deletions in chromosomes X, 5, 6, 9 and 16 and duplication of 13 are only detected in SurePlex amplified samples. B) MALBAC amplified samples show, because of their bigger variability, false positives. Each dot on the plots represents an equally sized bin of 1Mb. Separate chromosomes (from 1 to 22 and X) are colored green/black alternatingly. The X-axis indicates $\log_2$(copy number / 2), estimated based on the number of reads per bin. A $\log_2$(copy number / 2) equal to zero corresponds to a copy number of 2, as would be expected for a diploid genome. Theoretically for an insertion a $\log_2$ (copy number/2) of 0.5 is expected, whereas for a deletion a $\log_2$ (copy number/2) of -1 is expected. The red and green horizontal lines represent the threshold for detection of insertion or deletion, respectively. The brighter red line combines the bins with equal means.

4.7. The influence of a PCR-free library preparation on read distribution and CNA detection

The variance in read distribution across the genome was significantly different between enrichment PCR amplified and PCR-free samples. The number of reads per 1Mb bin in the PCR-free SurePlex samples varied less across the genome compared to enrichment PCR amplified SurePlex samples (Table 1). The detection of CNAs was comparable at this resolution, yet slightly more consistent in PCR-free SurePlex samples compared

to enrichment PCR amplified SurePlex samples (Figure 6). Although the X-chromosome monosomy was not called by ReadDepth, on the graphical profiles it can be distinguished. MALBAC amplified samples with subsequent PCR-free library preparation also resulted in improved MALBAC variation, but still a lot of false positive CNAs were detected in these libraries. CNA calling in SurePlex amplified samples with PCR-free library preparation has a PPV of 100% (±0%; mean ± standard deviation) and a sensitivity of 77.8% (±9.6%). CNA calling in the MALBAC amplified PCR-free library preparation samples has a PPV of (50% ± 26.8%) and a sensitivity of (50% ± 33%).

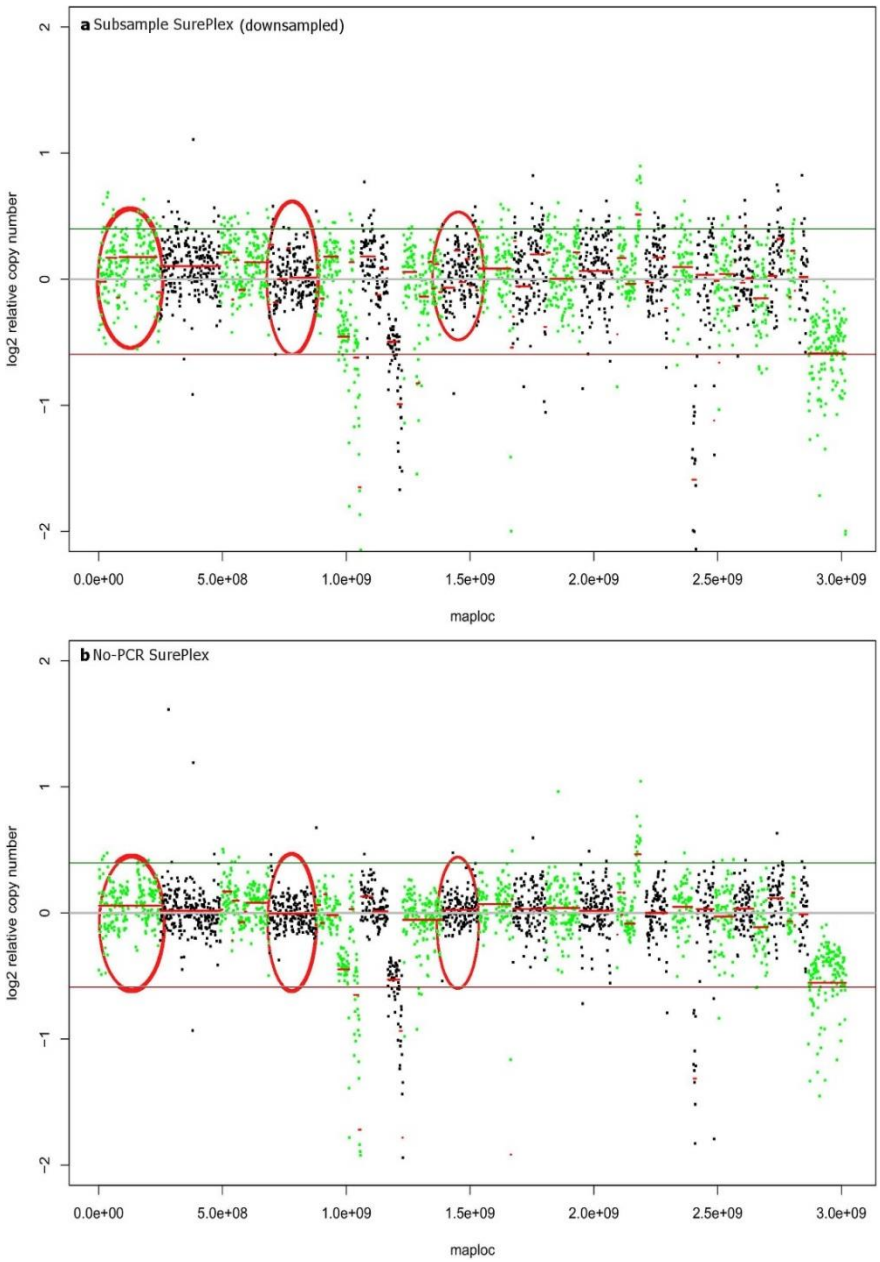

Figure 6: Omitting enrichment PCR during library preparation leads to smoother CNA profiles

As a result of the decreased variation, copy number estimation is more consistent across chromosomes, for instance in chromosome 1, 4 and 8 (red circles). This will be an important benefit if screening at higher resolutions is performed. To allow direct comparison, 'SurePlex PCR' samples were randomly downsampled to obtain a similar number of raw reads as 'SurePlex no-PCR' samples.

5. Discussion

SurePlex amplification has already proven its efficiency in combination with the 24Sure aCGH protocol for PGD purposes. During aCGH, amplification bias could partially be overcome by using the same WGA method for both sample and reference. However, due to the rather random nature of the bias introduced by WGA, the possibility of bias cannot be completely eliminated (173). Because of the nature of the detection of aneuploidies and CNAs from MPS data, it is not necessary to sequence a reference with the samples every time. This, however makes it even more important to obtain an unbiased amplification. De Bourcy *et al.* (2014), observed that PCR-based methods like MALBAC and NEB-WGA, are better suited for CNA detection than MDA methods because of their low variability. NEB-WGA is similar to the SurePlex WGA method used in this study, while the MALBAC WGA method of De Bourcy *et al.* (2014) is comparable, yet not entirely similar, to the MALBAC WGA method used in this study. In the present study, MALBAC (Yikon Genomics) and SurePlex (Bluegnome), both commercial kits, were compared for their usability in CNA detection in a more complex, say diploid human genome, setting that has to our knowledge not been done before.

The reference aCGH used for this study was performed with unamplified genomic material, thus avoiding the bias introduced by WGA. The resolution aimed by the sequencing during this study, is in the range of state-of-the-art PGD with aCGH. With 1Mb bins, CNAs of 3Mb and larger should be successfully detected by ReadDepth. However, as stated in the results, some smaller CNA can also be called if the variation in that specific region is low. We were, for instance, able to detect a deletion of 2.5 Mb at chromosome 9 (q34.11q34.12), which was also detected, and thus confirmed, on the 180K and 1Mb aCGH. In the sequencing results this particular deletion was called as a 3Mb CNA because sequencing is only accurate down to 1Mb.

Based on raw read count, an average genome coverage of approximately 0.3x was obtained for most samples. This theoretical calculation of the coverage gives an indication of how much of the human genome could theoretically be covered with a certain number of reads of a given length. However, after adaptor and quality trimming and mapping of the reads, an actual coverage of approximately 0.1X was obtained, except for the PCR-free SurePlex samples, for which a coverage after mapping of only 0.03X was obtained. It was shown that MALBAC amplified DNA samples yielded a significantly higher amount of uniquely mapped reads compared to SurePlex amplified samples. If these uniquely mapped reads are distributed uniformly along the genome, this would indicate that the MALBAC amplified samples cover the reference genome better, potentially increasing the accuracy in which CNAs can be detected. However, the distribution of the reads along the different bins in every chromosome was not uniform for the MALBAC amplified samples (Table 1). Indeed, the variance in read counts per 1Mb bin across the genome was

significantly higher compared to the SurePlex samples, suggesting that certain loci in the genome must be over- or under-amplified during MALBAC amplification.

MALBAC has been reported to have strong GC biases (168). Indeed, when studying the distribution of the GC-content per read, MALBAC seems to prefer more GC-content rich regions for amplification. Yet, this bias seems also to be prevalent in the reads originating from SurePlex amplified samples. Enrichment PCR during library preparation seems to amplify this GC bias effect, i.e. GC-bias is less pronounced in samples that did not undergo enrichment PCR compared to samples that did. However, where usually a clear Gaussian distribution can be expected, the distribution for the samples that were not enriched by PCR is less well-shaped, i.e. no clear maximum/mean can be distinguished.

Bias caused by over- or underrepresentation of certain parts of the genome, will most likely lead to false interpretations of the copy number status of chromosomal regions. This means that the variability in read distribution across the whole genome is directly related to the suitability to detect CNAs. The smaller the variation, the bigger the possibility that a value lying outside the threshold barriers is a true CNA. The thresholds for diploidy were redefined for every sample based on their negative binomial distribution, but did remain comparable between the samples. Variations in copy number were called if the number of alleles exceeded these boundaries. For only one of the MALBAC amplified samples, the MPS-CNA profile was similar to the reference aCGH profile. For SurePlex amplified samples on the other hand, all the expected CNAs were detected in the majority of the samples (7 out of 9). The variability between different bins in the MALBAC samples was too high to distinguish whether regions were actually underrepresented because they were deleted in the original genome or because of amplification bias. In addition, for the MALBAC amplified samples, quite some false positive results were called that were not visible on the reference array. For instance, chromosome 19 aberrations, a false positive recurrently appearing on aCGH (174), was called for almost all MALBAC amplified samples, but for none of the SurePlex amplified samples. Moreover, calls made for the MALBAC amplified samples were not very consistent across the three replicates, especially for 1 and 3 cell samples. Although such inconsistency was also observed across the replicates of the 1 cell samples amplified with SurePlex, less false positive calls were made compared to the MALBAC amplified samples. In the two cases that not all expected CNAs were called, the correct profile could still be deducted from the graphical profile. The opposite does also occur, where in one SurePlex amplified 3 cell sample a duplication in chromosome 20 was called by ReadDepth, but on the graphical profile this could not be observed. These observations suggest that for good practices both calls made by the ReadDepth algorithms and manual visual inspection of the graphical profiles should be considered. Nowadays, aCGH profiles in PGD are interpreted and corrected based on recurrent artifacts, i.e. aberrations that are present in most profiles but which are known not to have any impact on the correct development of the embryo. Such artifacts may result from the used technique and are frequently observed around

telomeric and centromeric regions of the chromosome. In this study however, information of such artifacts was not available and thus not taken into account to correct the calls. Nevertheless such information could be obtained by sequencing multiple normal, non-aberrant genomes and screening for recurrent aberrations. In general, this study shows that even without a reference genome the expected calls can be made, although a few false positives were also called.

The inconsistency observed between different replicates of 1 cell samples could possibly be explained by the cell cycle status of the amplified cells. More evidence is growing that cells that are in S-phase give a more scattered profile because of the replication status of the DNA (54). Samples containing multiple cells could contain cells that are in a different cell cycle status, which diminishes the influence of the individual cell status.

In the PCR-free MALBAC and PCR-free SurePlex amplified samples, similar overall differences could be observed between both WGA methods. The PCR-free MALBAC amplified samples had again a significantly higher amount of uniquely mapped reads but at the same time also a significantly higher variance in read counts per bin across the genome. This suggests that the enrichment PCR did not cause the difference observed between the two amplification methods. However, omitting the PCR shows an even lower, significant, variance in read distribution across the genome. Still, the difference with the normal diploid parts on the graph was obvious. Also the graphical profile is smoother without the use of enrichment PCR. This might become even more important to detect CNAs at a higher resolution and thus smaller bin size. Generally, these results suggest that at least part of the bias in MPS data for CNA detection could be eliminated by avoiding an enrichment PCR during library preparation.

Although the detection of CNAs was performed with ReadDepth, other bioinformatics tools exist for calling CNAs without the need of a reference genome. Some of them are described in the review of Duan *et al.,* who compare six different tools in different settings (172). ReadDepth seemed to perform best in most of the conditions tested in this review (172). However, the tool described by Baslan *et al.*, which should be more specific for single cell analysis (175), was not considered in this review. Although this tool is quite similar to ReadDepth, it might be expected that in a setting with higher resolution, and thus much less reads per bin, where the bias introduced by WGA will be more prominent, the tool might perform better in calling CNAs compared to ReadDepth. Another recently published tool, QDNAseq, might also have that advantage over ReadDepth, as it uses a blacklist to filter chromosomal regions with anomalous behavior, such as satellites, centromeric and telomeric repeats, reducing the noise level of the data (160).

6. Conclusion

In conclusion, we observed that for CNA detection, the SurePlex protocol is better suited than the MALBAC procedure. MALBAC amplified samples show a high non-uniformity across the genome, which leads to false positive CNAs. This

is especially true when starting from single cells. SurePlex amplification has shown its value for single cell chromosomal CNA detection, although for PGD purposes a minimal 3 cell starting amount is recommended. It has also been shown that omitting enrichment PCR during library preparation, will lead to a more uniform coverage of the genome. This may become more important if sequencing depth is being increased to increase resolution.

7. Supplementary information

Supplementary figure S1

1Mb aCGH profile of the Loucy cell line determined from a 3 cell sample amplified with SurePlex. The profile confirms the profile determined prior to the start of the experiments. CNAs of 3Mb and more can be detected on this profile. Since the reference genome used for this array was a male genome, the X chromosome deletion was observed as normal while the Y chromosome is shown as a deletion.

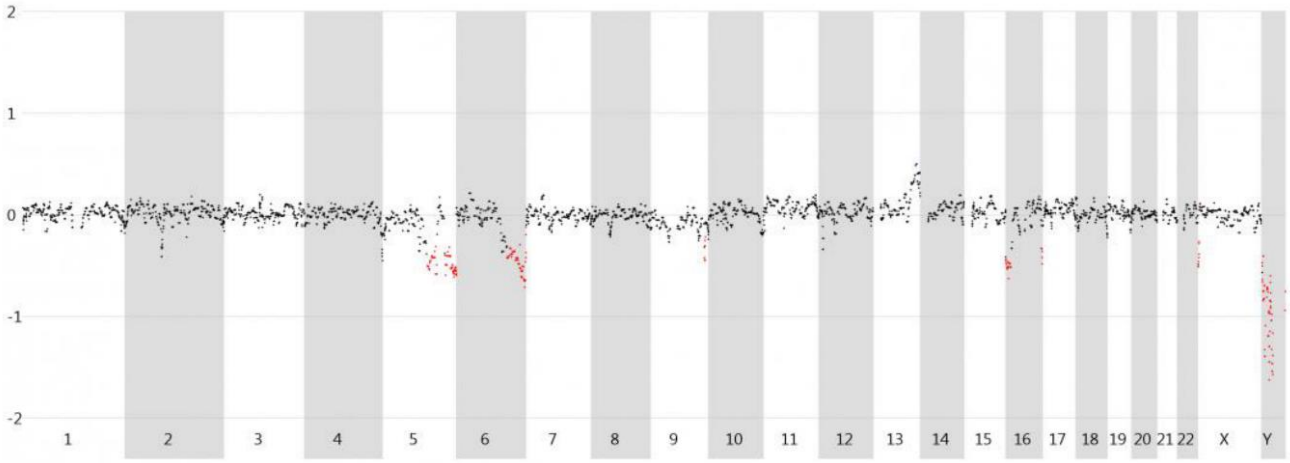

Supplementary figure S2: Sequence content across all bases

The percentage of each base at the different bp positions on the reads is shown in this graph. A) For the MALBAC samples a slightly irregular pattern is observed for the first 10 bases. The last base shows a skewed pattern and will be trimmed. B) The SurePlex samples have a very irregular pattern for the first 30 bases indicating that the adapter probably consists of mainly G and T. This passage, together with the last base, will be trimmed.

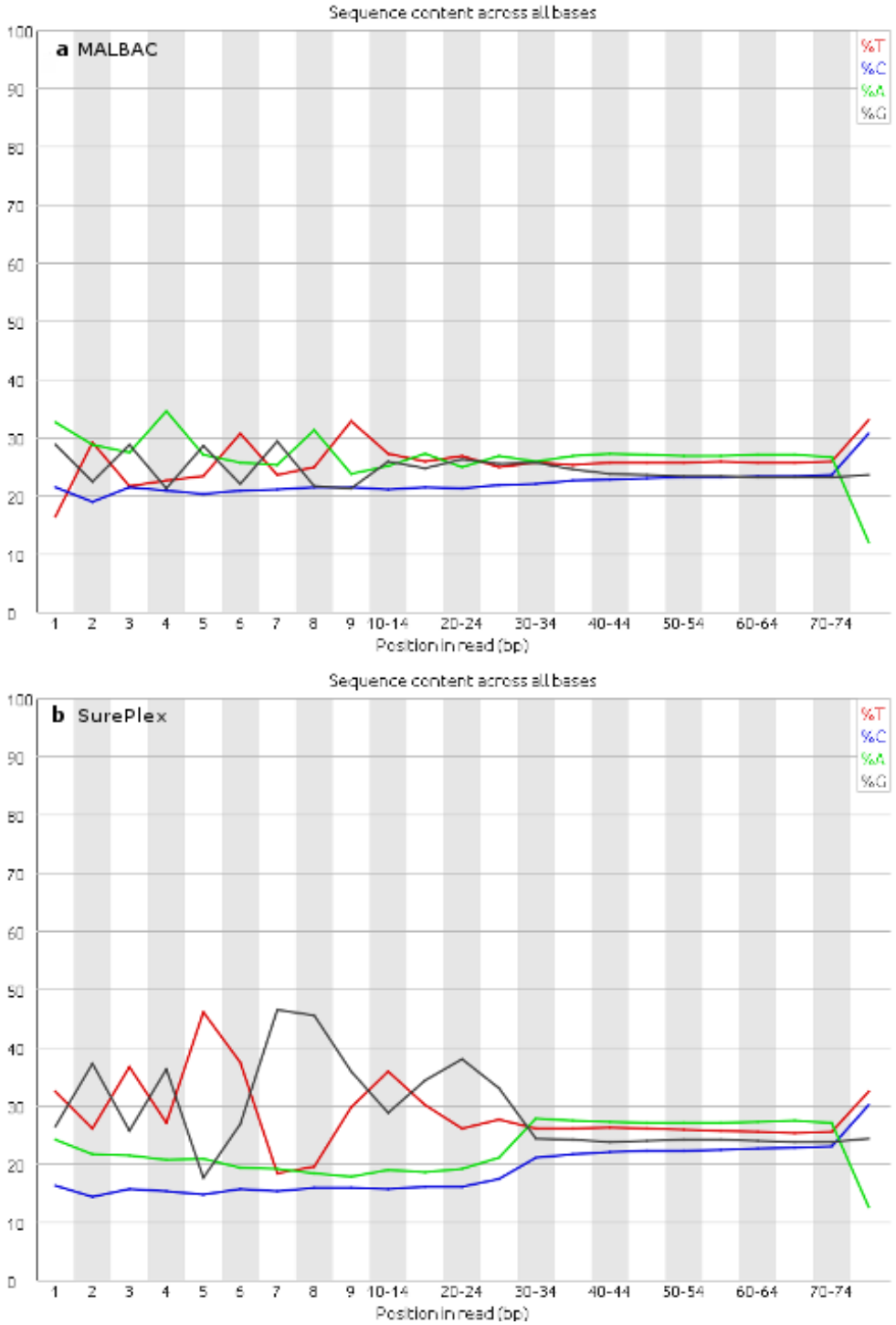

Supplementary fig. S3: Distribution of GC content per read

MALBAC and SurePlex seem to prefer more GC-content rich regions for amplification. Enrichment PCR during library preparation seems to amplify this GC bias effect, i.e. GC-bias is less pronounced in samples that did not undergo enrichment PCR compared to samples that did. However, where usually a clear Gaussian distribution can be expected, the distribution for the samples that were not enriched by PCR is less well-shaped, i.e. no clear maximum/mean can be distinguished. The red vertical line shows the normal GC content of the human reference genome

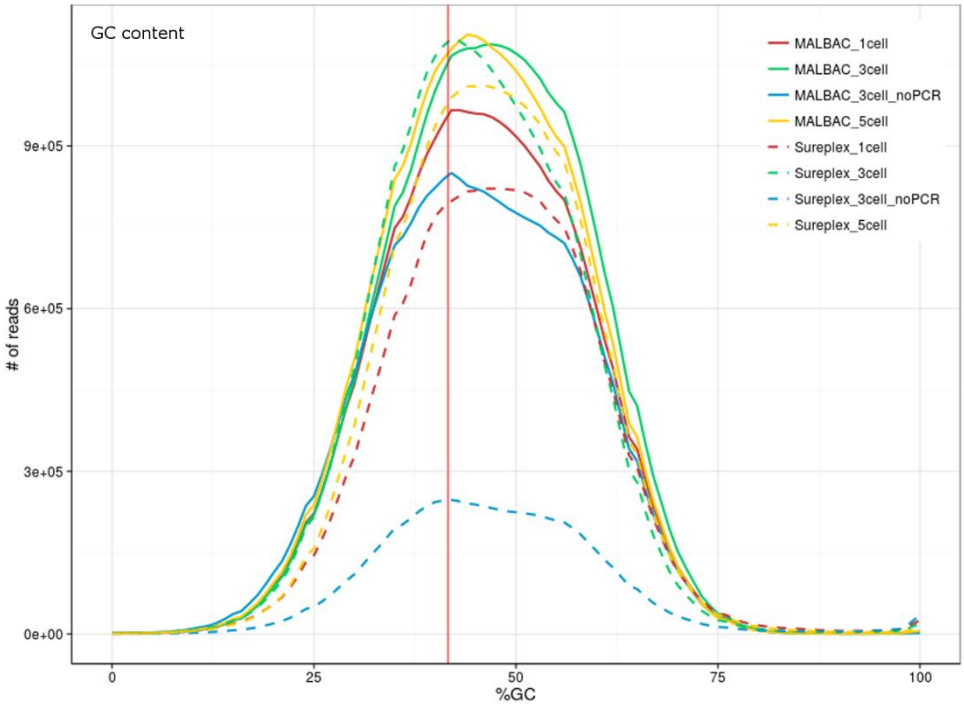

Supplementary fig. S4: Overview of the CNA profiles of all samples

The CNA profiles of all samples used in this study are shown here. These CNA profiles are similar to the profiles shown in figure 6. The very low copy number of the last part of chromosome 9 will fall out of the range of these graphs, but is present in al SurePlex samples.

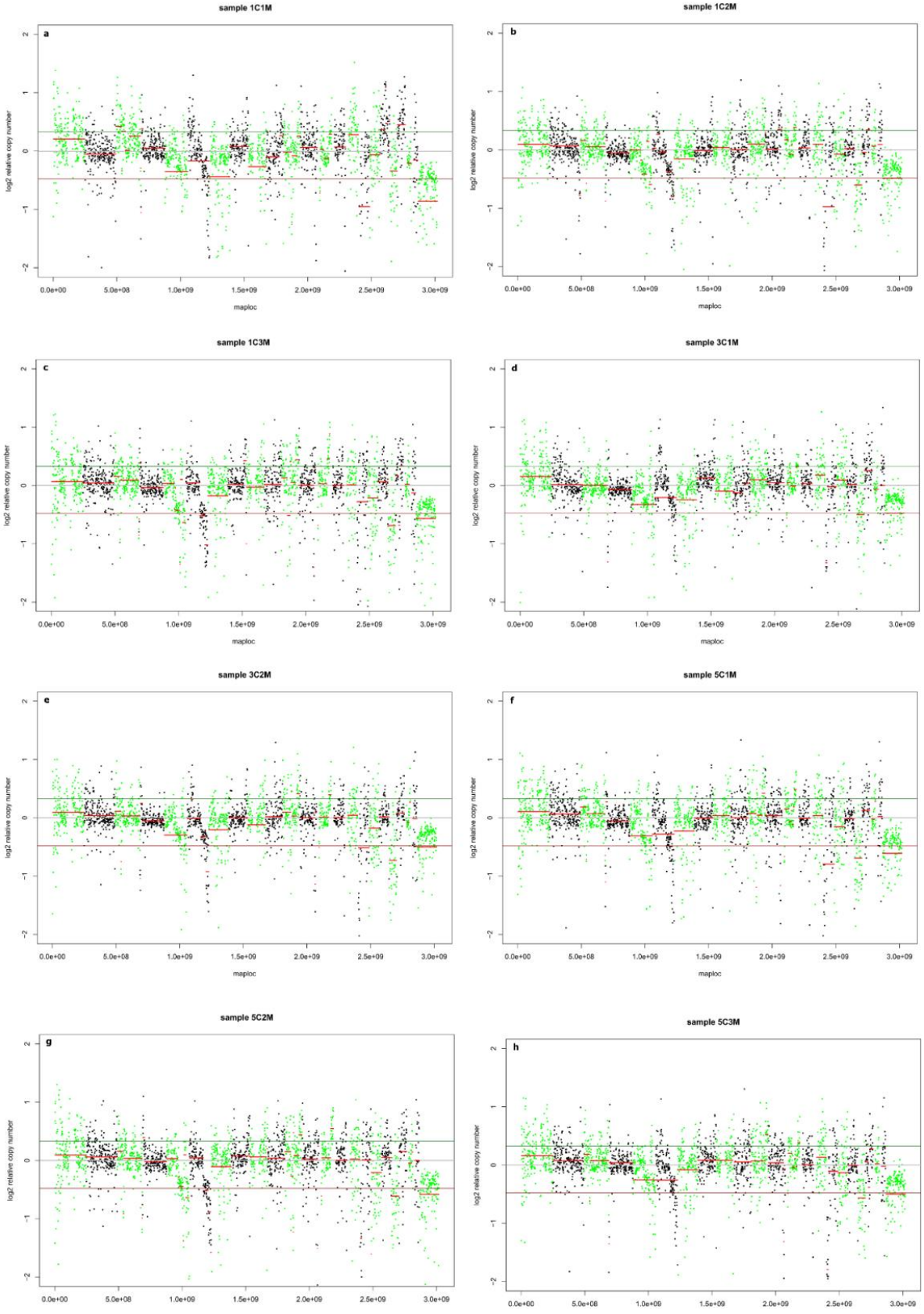

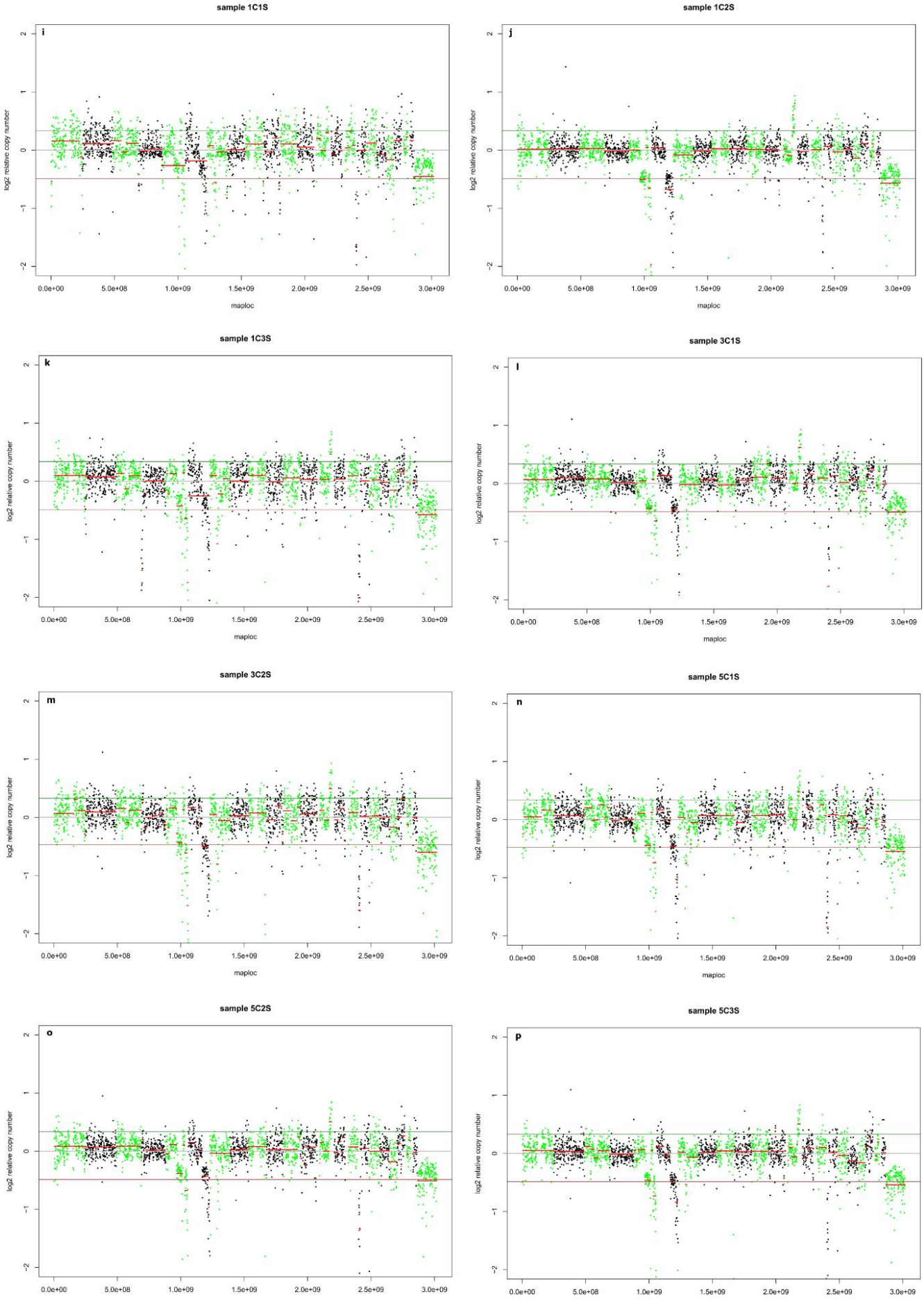
sample 1C1S
i
sample 1C2S
j
sample 1C3S
k
sample 3C1S
l
sample 3C2S
m
sample 5C1S
n
sample 5C2S
o
sample 5C3S
p
log2 relative copy number
maploc
0.0e+00
5.0e+08
1.0e+09
1.5e+09
2.0e+09
2.5e+09
3.0e+09

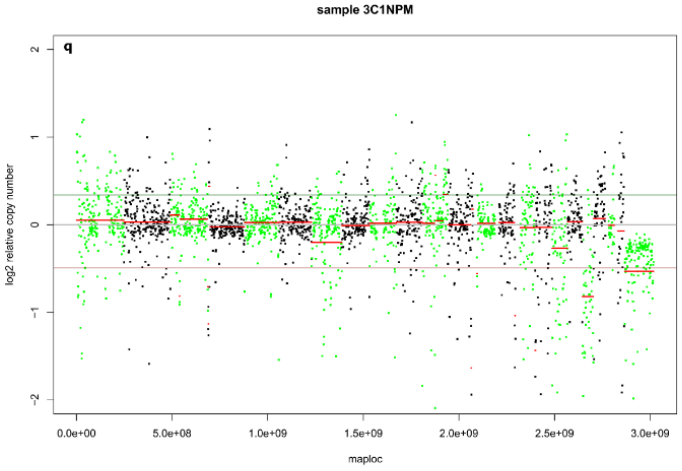
sample 3C1NPM
q
log2 relative copy number
maploc

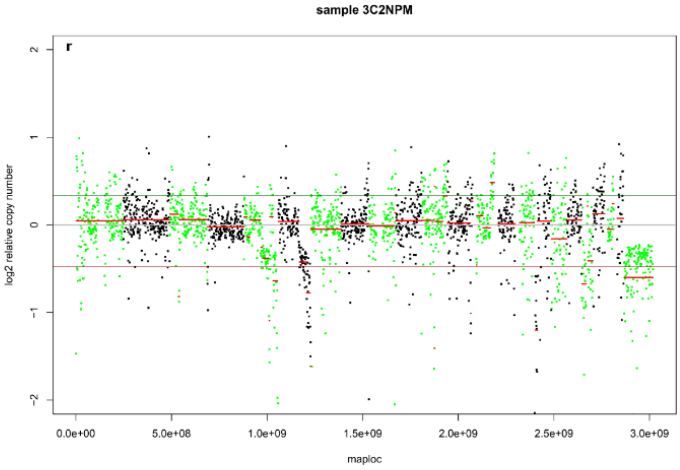
sample 3C2NPM
r
log2 relative copy number
maploc

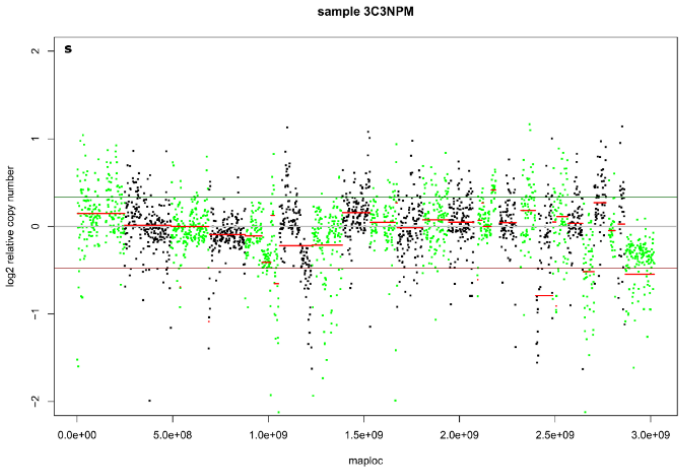
sample 3C3NPM
s
log2 relative copy number
maploc

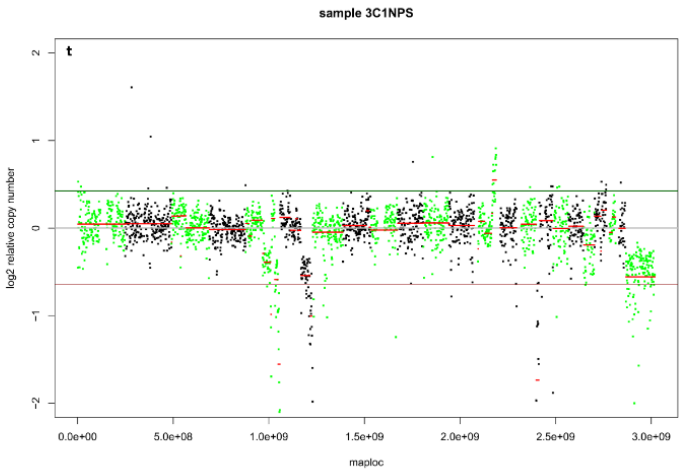
sample 3C1NPS
t
log2 relative copy number
maploc

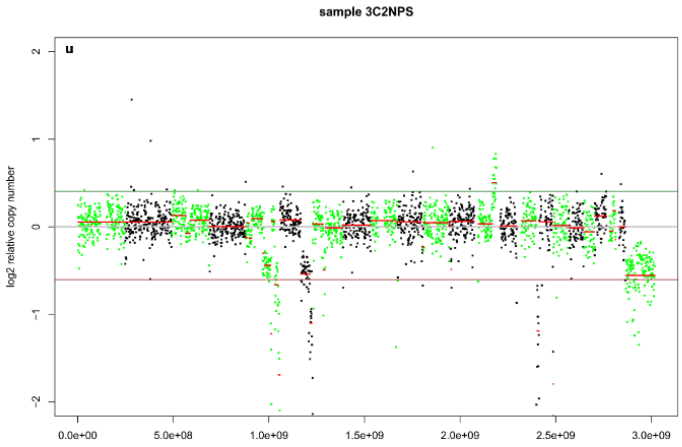
sample 3C2NPS
u
log2 relative copy number

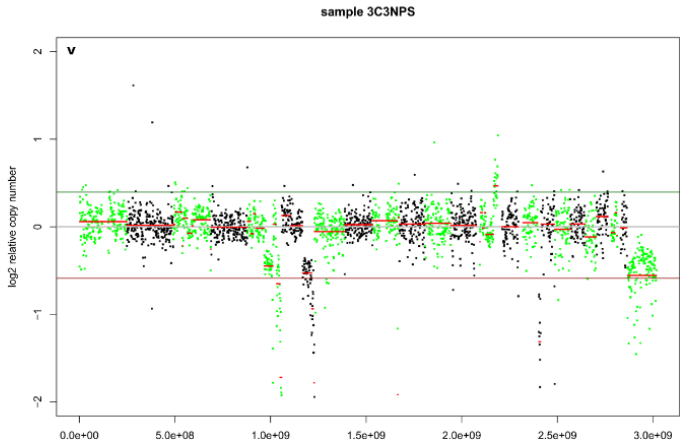
sample 3C3NPS
v
log2 relative copy number

Supplementary table S1: List of all CNAs detected by ReadDepth

CNAs given in grey are the ones that are expected to be detected. The CNAs given in de white columns are false positive calls if compared to the reference array.

	detected in																								
aberration	aCGH	1cell MALBAC rep1	1cell MALBAC rep2	1cell MALBAC rep3	3cell MALBAC rep1	3cell MALBAC rep2	3cell MALBAC rep3	5cell MALBAC rep1	5cell MALBAC rep2	5cell MALBAC rep3	1cell SurePlex rep1	1cell SurePlex rep2	1cell SurePlex rep3	3cell SurePlex rep1	3cell SurePlex rep2	3cell SurePlex rep3	5cell SurePlex rep1	5cell SurePlex rep2	5cell SurePlex rep3	3cell MALBAC noPCR rep1	3cell MALBAC noPCR rep2	3cell MALBAC noPCR rep3	3cell SurePlex noPCR rep1	3cell SurePlex noPCR rep2	3cell SurePlex noPCR rep3
5q-	✓		✓	✓					✓		✓	✓	✓	✓	✓	✓	✓	✓	✓		✓	✓	✓	✓	✓
6q-	✓		✓	✓		✓	✓		✓			✓		✓	✓	✓	✓	✓	✓		✓		✓	✓	✓
9q-	✓							✓	✓	✓	✓	✓	✓	✓	✓	✓	✓	✓	✓		✓			✓	✓
13q+	✓		✓	✓	✓	✓	✓	✓	✓	✓	✓	✓	✓	✓	✓	✓	✓	✓	✓		✓	✓	✓	✓	✓
16p-	✓				✓		✓		✓	✓	✓	✓	✓	✓	✓	✓	✓	✓	✓				✓	✓	✓
Xmono	✓	✓	✓	✓	✓	✓	✓	✓	✓	✓		✓	✓	✓	✓	✓	✓	✓	✓	✓	✓	✓			
1p-											✓														
2q-			✓																						
3p+		✓																							
3p-			✓			✓	✓	✓	✓	✓										✓	✓				
4p+									✓																
4p-													✓												
7m-											✓		✓		✓		✓		✓						
8q+				✓																					
10q-											✓														
10m+					✓																				
11q+				✓		✓	✓	✓	✓	✓				✓						✓					
11m-		✓		✓				✓	✓																
12q+			✓																						
12q-						✓		✓				✓		✓				✓	✓						
13p-		✓			✓																				
15q-																				✓					
16p-							✓																		
16mono			✓			✓		✓														✓			
18m+															✓										
18tris		✓																							
19p-																					✓				
19mono				✓	✓	✓	✓	✓	✓	✓										✓		✓			
20q+			✓	✓													✓								
20m-				✓			✓																		
20tris		✓																							

Chapter IV: Shallow whole genome sequencing is well suited for the detection of chromosomal aberrations in human blastocysts

Lieselot Deleye[#,1], Annelies Dheedene[#,2], Dieter De Coninck[1], Tom Sante[2], Christodoulos Christodoulou[3], Björn Heindryckx[3], Etienne Van den Abbeel [3], Petra De Sutter[3], Dieter Deforce[1], Björn Menten[$,2], Filip Van Nieuwerburgh[$,1]

[1.] Laboratory of Pharmaceutical Biotechnology, Ghent University, Ottergemsesteenweg 460, 9000 Ghent, Belgium
[2.] Center for Medical Genetics, Ghent University, De Pintelaan 185, 9000 Ghent, Belgium
[3.] Department for Reproductive Medicine, Ghent University Hospital, De Pintelaan 185, 9000 Ghent, Belgium
[#,$] similar in author order: LD was responsible for the sequencing part of the study, AD was responsible for the aCGH part.

Fertility Sterility; https://doi.org/10.1016/j.fertnstert.2015.07.1144; Accepted 6 July 2015

1. Abstract

Preimplantation genetic diagnosis (PGD) for chromosomal rearrangements is widely used to avoid transferring embryos with genomic aberrations. Currently, genomic microarrays are predominantly used for the detection of unbalanced structural abnormalities and aneuploidies in embryos from parents at risk. In this study we evaluate whether massive parallel sequencing (MPS) can be used in PGD for detecting chromosomal abnormalities.

15 patients with a balanced structural rearrangement were included in the study: 8 reciprocal translocations, 3 Robertsonian translocations, 2 inversions and one insertional translocation. In total, 6 normal embryos and 41 abnormal embryos were included in the cohort. Low coverage MPS on a NextSeq 500 (Illumina) and Ion Proton (Life Technologies) instrument was performed in parallel for 47 trophoblast amplified samples. All aberrations previously detected with aCGH could be readily detected in the MPS data and were called correctly. The smallest detected abnormality was a 5 Mb deletion/duplication hence equaling or even exceeding the resolution of the routinely used microarrays. Thereby, this study demonstrates that MPS on a NextSeq 500 or Ion Proton instrument can both be applied for the detection of chromosomal abnormalities in PGD embryos and MPS can serve as a more cost-effective and flexible technology for PGD compared to aCGH.

2. Introduction

Chromosomal abnormalities in early embryonic development can give rise to implantation failure, early spontaneous abortions and/or fetuses with multiple congenital anomalies. For couples with a known balanced or unbalanced chromosomal rearrangement, preimplantation genetic diagnosis (PGD) can be offered to select against unbalanced chromosomal aberrations in the embryo during assisted reproductive technology (ART) (24). At the same time, it is well established that early stage embryos suffer from a high rate of (mosaic) aneuploidy, reducing embryo survival, implantation potential and hence the success rate of ART (25).

In the past, Fluorescent In Situ Hybridization (FISH) has been widely used to screen for chromosomal imbalances in the embryos (27). With FISH, the chromosomes involved in the translocation can be evaluated for unbalanced rearrangements at the single cell level. However, for every single case, an individual laboratory genetic work-up is needed to optimize the protocol before starting the PGD procedure (27, 176).

In recent years, array Comparative Genomic Hybridization (aCGH) has replaced FISH for PGD in translocation carriers. ACGH is a valuable technology in the context of PGD, since all chromosomes can be interrogated in a single experiment. There is no need for optimization of the PGD test in advance and besides chromosomal aberrations due to the (balanced) chromosomal rearrangement in the parent, also other aneuploidies or large copy number variations (CNV) can be detected. ACGH and other comprehensive screening methods such as real-time PCR and

SNP-arrays, allow improved embryo diagnosis before transfer to the uterus and have proven their clinical utility (20, 61, 177, 178).

Embryonic aneuploidy detection is not only valuable in a PGD setting. Recent evidence suggests that also patients with normal karyotypes who have recurrent miscarriages can benefit from comprehensive chromosome screening of the embryo (20). Currently, randomized controlled trials (RCTs) are ongoing to evaluate the use of preimplantation genetic screening (PGS) in those patients and these studies might prove that comprehensive chromosome screening could increase the implantation and pregnancy rate (20, 61).

Although aCGH proved its value, its rather limited resolution and the relative high cost are a disadvantage (32). For cryptic chromosomal rearrangements, the current resolution of approximately 10 Mb can be shortcoming. These issues could be addressed using massively parallel sequencing (MPS). Shallow or low-pass whole genome sequencing is used when no full genome coverage is needed. This technique can be used for detection of aneuploidy and/or chromosomal imbalances. The rapid development, dropping costs, and the possibility of screening at higher resolution, make MPS an attractive alternative to further increase the success rate of PGD and/or PGS after ART. Some proof of concept studies have shown the possibilities of shallow whole genome sequencing in a PGD/PGS setting (32, 163, 164, 179). However, most of these studies focused on aneuploidy detection and the resolution remained rather limited.

A recent important evolution in PGD is the time point for embryo biopsy. While cleavage stage biopsy, taking one or two blastomeres from the embryo on day 3, has long been the gold standard, recently a shift towards blastocyst trophectoderm biopsy on day 5 has occurred.

The present study evaluates the use of MPS for PGD on trophectoderm cells of blastocysts, making a comparison with aCGH in terms of accuracy. With this study, we aim to add evidence that MPS is a valuable and efficient substitute for aCGH, with the potential of being more cost efficient, and with a resolution that is more appropriate for PGD in translocation carriers.

3. Materials and methods

3.1. Study design

In the present study, 15 patients with a balanced structural chromosomal rearrangement were enrolled. The aberrations included 8 reciprocal translocations, 4 Robertsonian translocations, 2 inversions and one insertional translocation (Table 1). Maternal age ranged from 27 to 41 years (mean 33,5 years). Retrieved oocytes underwent intracytoplasmic sperm injection (ICSI) and trophectoderm biopsies were performed on day 5 or 6. After WGA of the DNA from the trophectoderm cells, 24sure+ aCGH was performed for PGD. DNA amplified material from 47

embryos that were found abnormal with aCGH or did not implant after transfer were selected for MPS. In this validation study we evaluated whether MPS is able to detect small but relevant chromosomal aberrations in a PGD setting. The 47 embryos were selected from a larger clinical cohort of 141 embryos in total and were specifically selected based on different sizes of the involved translocated segments and aneuploidy of different chromosomes. This study cohort represents a variety of clinical relevant chromosomal aberrations in a PGD setting.

After aCGH, we analyzed the remaining amplified DNA with shallow whole genome sequencing on both an Illumina NextSeq500 platform and an Ion Proton sequencer. Results from MPS were subsequently compared with the previously generated aCGH results (Figure 1).

The aCGH analysis was performed between September 2014 and December 2014. Ion Proton and NextSeq500 sequencing was performed simultaneously at the beginning of 2015.

Our institutional review board approved this study (EC/UZG/2015/0108) and informed consent was obtained from all patients included in this study.

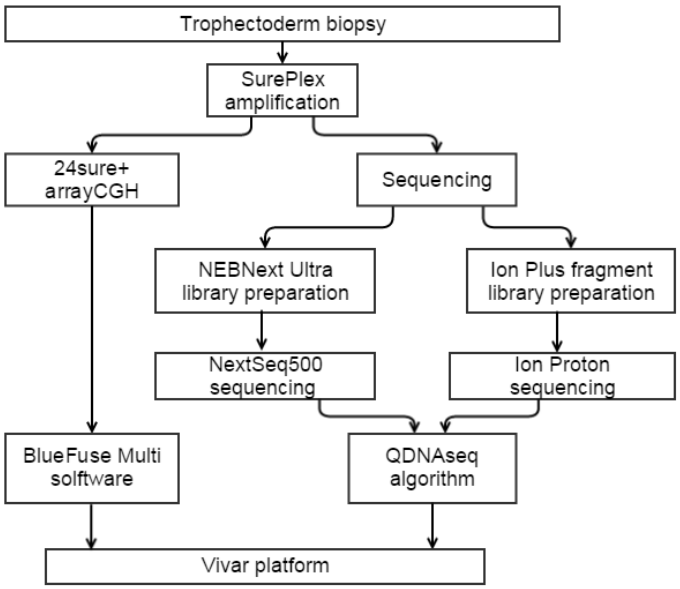

Figure 1: Schematic overview of the experimental design of this study.

After whole genome amplification of trophectoderm biopsies, routine microarray analysis was performed. Remaining amplified DNA was used to sequence samples on a NextSeq 500 and Ion Proton sequencer in parallel.

3.2. Oocyte retrieval and blastocyst biopsy

Controlled ovarian hyperstimulation of this study's patients was performed according to age, anti-Müllerian hormone levels and previous response. The gonadotrophins used were either a recombinant follicle stimulating hormone (FSH) (Gonal F, Merck Serono) or a urinary FSH (Menopur, Ferring Pharmaceuticals) at daily doses between 150 and 300 U. When an agonist protocol was followed, 0.1 mg triptorelin (Decapeptyl, Ipsen) was administered

subcutaneously for 7 days starting on cycle day 1, and gonadotrophins were started on cycle day 3. In case an antagonist protocol was necessary, gonadotrophins were started on cycle day 3, and 0.25 mg cetrorelix (Cetrotide, Merck Serono) was injected subcutaneously as a daily dose from the 6th day of stimulation until the day of oocyte maturation triggering. The course of stimulation was followed by ultrasound monitoring. As soon as 50% of the follicles were > 10-18 mm in diameter, oocyte maturation and retrieval was performed according to Vandekerckhove *et al.* 2014 (180).

After ICSI, oocytes were cultured in 25µl drops of IVF-cleavage-medium (COOK) in the microwells of Embryoslides (Vitrolife) and overlaid with 1,2 ml of mineral oil. Embryoslides were placed in the EmbryoScope (Fertilitech) at 37°C in 5% O_2 and 6% CO_2. On the 3rd day of embryo development, the zona pellucida was breached using a series of laser pulses (Zilos-TK, Hamilton Thorne) to assist trophectoderm herniation and the medium of the microwells was refreshed with IVF-blastocyst-medium (COOK). On the 5th or 6th day of development, good quality blastocysts, according to the criteria of Gardner and Schoolcraft (181) (>grade 3BB) with herniating trophectoderm underwent laser-assisted biopsy (Zilos-TK, Hamilton Thorne) using a 28-32 µm inner diameter biopsy micropipette (Origio). The biopsied cells (min. 1 cell and max. 9 cells; average, 4.3 cells) were washed with PBS (AMRESCO, USA) and polyvinylpyrrolidone (COOK), placed in 0.2 ml sterile PCR tubes and kept in -20°C until genetic screening. Embryos were vitrified on the day of the biopsy with the Vitrification Freeze kit (Irvine Scientific, USA).

3.3. SurePlex WGA

Cell lysis and amplification of 47 biopsied blastocyst samples, was performed following manufacturer's instructions using the SurePlex Amplification system (Illumina Bluegnome, Cambridge, United Kingdom). 2.5µl of control DNA (G1521; Promega, USA; 187ng/µl) was used at a concentration of 25pg/µl. The blank was equal to 2.5µl of PBS. Evaluation of amplification was performed on a Labchip GX (CaliperLife Sciences) instrument. All samples for sequencing were purified according to the manufacturer's protocol of the Genomic DNA Clean & Concentrator kit (version 1.0.0, Zymo Research, Irvine, USA) with 5X binding buffer. Samples that were analyzed with aCGH were not purified. Concentration was measured using Qubit dsDNA High Sensitivity Assay kit (Life technologies, Carlsbad, USA).

3.4. ACGH

The WGA products were processed following manufacturer's protocol (Illumina, Bluegnome) and hybridized on 24sure+ arrays. A male reference sample was used for all tested embryos.

Briefly, amplified samples and reference DNA were labeled with Cy3 and Cy5 fluorophores, respectively, during 4 hours at 37°C. After combining sample and reference with Cot1 DNA, the mixture was precipitated for minimum 20 minutes at -80°C. The pellets were resuspended in pre-warmed hybridization buffer and hybridized on a 24sure+

array for 16h (overnight) at 42°C. After washing, microarrays were scanned on an Agilent G2565CA microarray scanner. Data were analyzed using the BlueFuse Multi software (Illumina) and visualized in ViVar (182).

3.5. Fragmentation

One hundred ng of the purified WGA product was fragmented to an average size distribution of 200bp with the S2 Focused Ultrasonicator with Adaptive Focused Acoustics (AFA) technology (Covaris, Woburn, USA). All samples were diluted in Tris-EDTA buffer (TE-buffer) to a volume of 130µl in microTUBES (Covaris, Woburn, USA). The guidelines for fragmentation to 200bp were followed (duty cycle of 10%, intensity of 5 and 200 cycles/burst), but the fragmentation time was prolonged to 190sec based on previous experience. Subsequently, samples were divided in two aliquots, one for Illumina sequencing and one for Ion Proton sequencing.

3.6. Sequencing on NextSeq500

Libraries of the fragmented samples were created using NEBNext Ultra DNA Library Prep (Chapter 2B, New England Biolabs, Ipswich, USA), following manufacturer's protocol with modifications as described here. After incubation with the USER enzyme, a DNA purification step (Zymo Genomic DNA Clean & Concentrator) was included before the size selection step. Size selection was performed with the E-Gel iBase Power system (Invitrogen) using an E-gel EX 2% agarose gel and a 1kb Plus DNA ladder (Thermo Fisher Scientific, Waltham, USA). For all samples, fragments with a size of ±300bp were cut from the gel and DNA was recovered using the Zymoclean gel DNA recovery kit (Zymo research). The size selected DNA samples were then subjected to an enrichment PCR using NEBNext Multiplex Oligos for Illumina (Index Primers Set 1 and 2) according to the protocol, with addition of tRNA to minimize the loss of DNA via tube interaction. The quality of the different samples was assessed with the Agilent High-Sensitivity DNA kit (Bioanalyser, Agilent Technologies, California, USA).

Before sequencing the samples, the amount of sequence-able library fragments was determined by performing a qPCR according to the Sequencing Library qPCR Quantification kit (Illumina, San Diego, USA). Samples were diluted to 10nM with elution buffer (EB buffer) (QIAGEN, Hilden, Germany). The control template used for the standard curve was a PhiX control library (10nM). Finally, single-end index 75bp sequencing was performed on a high-output flowcell on a NextSeq500 (Illumina, California, USA). Samples with different indexes were pooled at 4nM each and diluted to a final concentration of 2.3pM. 24 samples were multiplexed on one flowcell. The complete protocol from library construction to data analysis takes 23 hours.

3.7. Sequencing on Ion Proton

Library construction was performed according to the Ion Plus Fragment Library Kit (Life Technologies). Briefly, end-repair of the amplified DNA was performed with T4 DNA polymerase and T4 polynucleotide kinase. Ion Proton compatible adapters with barcodes were ligated to the WGA DNA using DNA ligase. Libraries were amplified using

Platinum PCR SuperMix High Fidelity in a thermal cycler (5 min 95°C, [15 sec 95°C, 15 sec 58°C, 1 min 70°C] 9 cycles). Libraries were purified using Agencourt AMPure XP beads (Beckman Coulter). After the amplification double size selection was performed using Agencourt AMPure XP beads (Beckman Coulter) for removal of residual adaptors and primers. Libraries were quantified with the Ion Library Quantitation Kit (Life Technologies). Template preparation and PI chip loading was performed on Ion Chef (Life Technologies) using 60 pM of equimolar pooled libraries. Six samples were pooled on one PI chip and sequenced on an Ion Proton instrument using 400 flows. The complete protocol from library construction to data analysis takes 26 hours.

3.8. Data analysis

Reads were aligned to the human genome hg19, assembly GRCh37, using the Burrow-Wheeler-Aligner Maximal Exact Matches (BWA-MEM) v0.7.5a-r405 algorithm (183) and converted to BAM files using SAMtools v0.1.19 (170). Subsequent data analysis for CNV detection was performed using QDNAseq (160). This tool is implemented in R (184) and normalizes, after removal of non-uniquely and poorly mapped reads, the number of reads mapped in non-overlapping, fixed size windows for bias in GC-content and mappability simultaneously. Moreover, QDNAseq uses a "blacklist" of genomic regions. This blacklist, based on the ENCODE Project Consortium (185), contains information on chromosomal regions with anomalous behavior, especially regions with known repeat elements, such as satellites, centromeric, and telomeric repeats. QDNAseq uses the blacklist to exclude these regions from the analysis. After GC-content and mappability normalization, read counts are median normalized, after which a circular binary segmentation algorithm detects breakpoints between the windows, and groups them between breakpoints in segments with equal copy number.

Different window sizes (100kb, 250kb, 500kb and 1Mb) were evaluated for CNV detection. Each genome profile (line view and chromosome view) was manually checked for aberrations.

To determine the minimum number of reads necessary to detect CNVs successfully, raw reads were randomly downsampled to levels 2-10 times lower than the original number of raw reads. This downsampling was performed using the seqTK toolkit (https://github.com/lh3/seqtk). For each sample, another random seed was used.

The profiles of all samples used in this study can be found online in ViVar (182), a platform for the automated analysis and visualization of microarray and sequencing data. For this study, we incorporated the QDNAseq algorithm in ViVar, enabling easy comparison of the sequence profiles and array data. All results can be found on ViVar: http://cmgg.be/ViVar/.

4. Results

4.1. MPS specifications

Twenty-four samples were pooled on one NextSeq500 run, whereas 6 samples were combined on a single Ion Proton PI chip. This resulted in an average of 11 and 10 million uniquely mapped reads per sample for NextSeq 500 and Ion Proton, respectively. An average coverage of 0.3x resp 0.4x per sample was obtained (mean read length NextSeq500 = 75 bp, mean read length Ion Proton = 123 bp).

4.2. Aberrations detected with MPS

MPS results for the 47 analyzed samples were evaluated in ViVar and interpretation of the genomic profiles (line views) was performed with knowledge of the parental karyotype, but blindly from the earlier generated aCGH results (Table 1).

The genetic diagnosis of all samples was the same for aCGH and both MPS technologies. The chromosomal changes detected by MPS were concordant with those detected by aCGH in all embryos, as all structural and numerical aberrations identified by aCGH were also identified by MPS, hence the sensitivity is 100%. Vice versa, no new aberrations have been detected with MPS giving a specificity of 100%.

The 500kb window size during QDNAseq analysis proved to give the most appropriate resolution for our analysis. While the 1Mb window smoothed the signals to much, hampering the proper detection of smaller aberrations, the 250kb windows and smaller windows resulted in the identification of several smaller aberrations that were recurrent across different unrelated samples, probably due to artefacts during the WGA.

Results from NextSeq500 and Ion Proton sequencing were concordant: QDNAseq line views are almost indistinguishable between both technologies, independent of the chosen window size (See example in Figure 2). All aberrations were detected by both technologies. The size of these aberrations was also identical between the two technologies. For an overview of all samples, following link to ViVar can be used: ViVar: http://cmgg.be/ViVar/.

Five of the 47 analyzed embryos, gave a normal profile without any detectable structural or numerical aberration. The other 42 embryos showed one or several abnormalities. In total, 54 structural abnormalities (31 deletions and 23 duplications) were detected in 27 embryos. Additionally, 17 monosomies and 16 trisomies were observed in 25 embryos. Twenty-three embryos showed a duplication together with a deletion in concordance with an unbalanced, derivative chromosome related to the parental rearrangement. Of these, 9 embryos showed additional aneuploidies or copy number aberrations together with the unbalanced translocation. Of note, and in line with previous studies, 19 embryos did not show the expected parental rearrangement, but showed aneuploidies or copy number aberrations of/in chromosomes not involved in the parental rearrangement, illustrating the importance of whole genome analysis.

Chromosomal aberrations present in the study cohort.

Patient no.	Parental karyotype	Embryo	Embryonic profile
1	46,XX,inv(5)(p15.1q13.3)	embryo1	*del 6q16.1q27, monosomy 9*
		embryo2	*monosomy 2, monosomy 16*
		embryo3	*monosomy 16*
		embryo4	*dup 16q11.2q24.3*
		embryo5	normal
2	46,XX,t(9;16)(p24.1;p12.3)	embryo1	**del 9p24.3p24.2, dup 16p13.3p12.3**
		embryo2	*trisomy 11, monosomy 16*
		embryo3	*monosomy 4, monosomy 7*, **del 9p24.3p24.2, dup 16p13.3p12.3,** *trisomy 18*
		embryo4	*monosomy 12, trisomy 22*
		embryo5	*trisomy 16*
		embryo6	*trisomy 16*
		embryo7	**dup 9p24.3p24.2, del 16p13.3p12.3**
		embryo8	**del 9p24.3p24.2, dup 16 p13.3p12.3**, *trisomy 21, trisomy 22*
		embryo9	**dup 9p24.3p24.2, del 16p13.3p12.3**
		embryo10	*monosomy 8*
3	45,XX,der(13;14)(q10;q10)	embryo1	*dup 4q22.3q35.2*
		embryo2	*monosomy 21*
4	46,XX,t(1;16)(q24;q23)	embryo1	**dup 1q24.3q44, del 16q23.1q24.3**
		embryo2	normal
5	46,XY,t(2;6)(q11.1;p25)	embryo1	**del 2q11.1q37.3**
6	46,XX,t(16;20)(p11.2;q13.2)	embryo1	**dup 16p13.3p11.2, del 20q13.2q13.3**
		embryo2	*trisomy 4*, **dup 16p11.2q24.3, del 20p13q13.2**, *trisomy 22*
		embryo3	*trisomy 19*
		embryo4	**dup 16p11.2q24.3, del 20p13q13.2**
		embryo5	*del 1p12q44, trisomy 6,* **dup 16p25.3p11.2, del 20q13.2q13.3**
		embryo6	*del 10p11.21q22.2,* **del 16p13.3p12.1, dup 20q13.2q13.33**
		embryo7	normal
7	45,XY,der(13;14)(q10;q10)	embryo1	*trisomy 9, del 13q32.1q34*
8	46,XY,inv(13)(q14.11q34)	embryo1	**del 13q14.11q34**
		embryo2	trisomy 16
9	45,XY,der(13;14)(q10;q10)	embryo1	*del 2p25.3p21, del 2q22.1q37.3, trisomy 4,* **trisomy 13**, *del 20q13.1q13.1, monosomy 21, del 22q12.3q13.3*
		embryo2	*monosomy 16*
		embryo3	*monosomy 17*
		embryo4	normal
10	46,XY,ins(14;6)(q23.2;q23.2q24.3)	embryo1	**dup 6q23.2q24.3**
11	46,XX,t(1;21)(p13.3;q11.2)	embryo1	**del 1p21.3q44**, *trisomy 16,* **dup 21q11.2q21**
		embryo2	**dup 1p36.3p21.3**, *del 12q24.2q24.3, monosomy 13,* **dup 21q11.2q21.2**
12	46,XY,t(3,5)(p14.2;q14.1)	embryo1	*monosomy 7, monosomy 16*
		embryo2	**del 3p26.3p12.1, dup 5q14.3q35.3**
		embryo3	**dup 3p26.3p12.1, del 5q14.3q35.3**
13	46,XY,t(7;13)(q22;q21.2)	embryo1	**del 7p22.3q22.1, dup 13q12.1q21.3**
		embryo3	**del 7q22.1q36.3, dup 13q21.3q34**
14	46,XX,t(5;16)(q11.1;q11.2)	embryo1	*monosomy 2*
		embryo2	**del 5p15.3q11.2, dup 16p13.3p11.2**
		embryo3	*trisomy 16*
		embryo4	**dup 5p15.33q11.2, del 16p13.3p11.2**, *monosomy 22*
15	45,XX,der(15;22)(q10;q10)	embryo1	normal

Note: All aberrations that are related to the parental karyotype are in bold; aberrations not directly related to the parental rearrangements are in italics.

Deleye. Massive parallel sequencing in PGD. Fertil Steril 2015.

Table 1: Chromosomal aberrations present in study cohort

Although all structural aberrations could be detected by both aCGH and MPS, MPS showed a slightly higher resolution and signal-to-noise ratio. Accordingly, the smaller aberrations could be identified more clearly as illustrated in Figure 3. The examples in Figure 3 are further discussed in detail in the discussion section of this article.

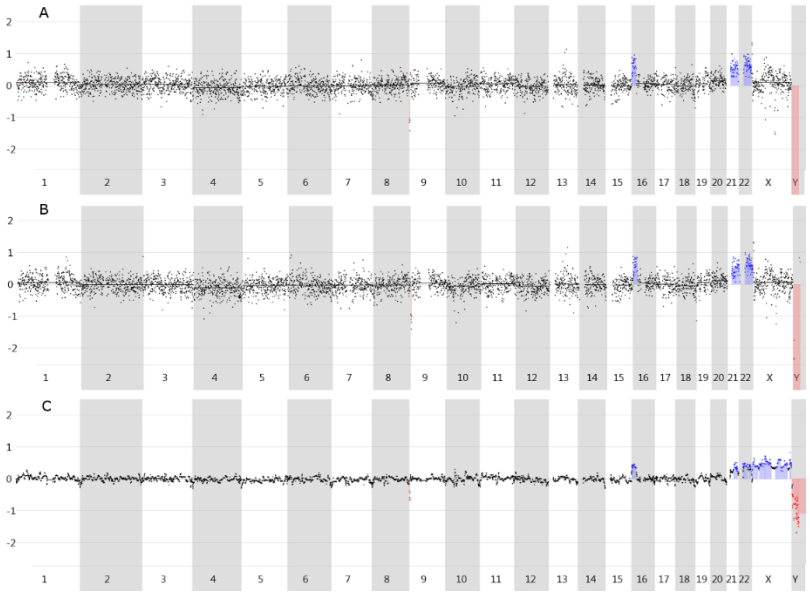

Figure 2: Comparing aCGH and MPS profiles for chromosomal aberrations.

Genomic profiles from Patient 2 embryo 8 generated with (A) NextSeq500 sequencing, (B) Ion Proton sequencing and (C) aCGH. The blue color indicates a duplication or trisomy, while the red color indicates a deletion or monosomy. All sequencing results were analyzed with a female reference while a male reference was used in the aCGH experiments. The aCGH profiles were analyzed with a 1Mb distance between the probes, which leads to a smoother line compared to the 500kb windows from sequencing results.

4.3. Resolution limited by number of reads or by WGA amplification bias?

The average number of reads per sample was higher than actually needed for correct detection of the aberrations present in the samples. The minimal number of reads that would still lead to the same result can be imputed by random selection of reads across the genome (downsampling of the sequencing reads). With only 1/10th of all reads remaining, all aberrations could still be detected. Even the very small duplication as shown in figure 3b, is still detected after a 10x downsampling. We can conclude that with ±1.6 million reads we still achieve the resolution necessary for this sample set (4.5 Mb resolution) (Supplementary figure 1). Although it is expected that a higher read count will lead to a higher resolution, we saw an increase in false positive results (see above) when reducing the analysis window to a size that is required to call copy number aberrations at a higher resolution. This shows that the minimal resolution for detection of chromosomal aberrations is probably limited by the WGA and not by the number of reads.

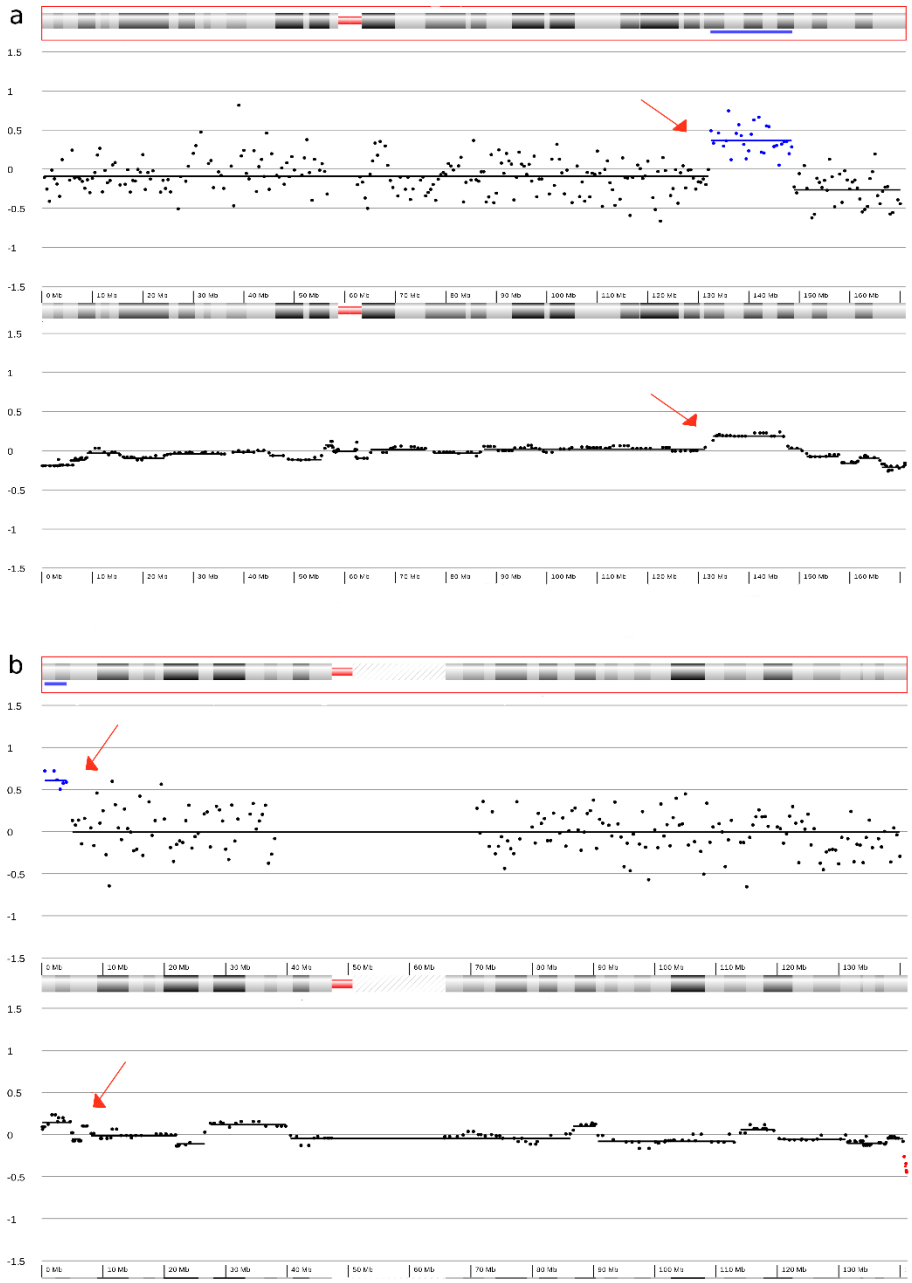

Figure 3: The resolution and signal-to-noise is more appropriate for MPS analysis.

(A) Sequencing (top) and aCGH (bottom) profile of chromosome 6 from Patient 10 embryo 1. The 6q23.2q24.3 duplication due to the paternal insertional translocation (46,XY,ins(14;6)(q23.2;q23.2q24.3)) is more clearly detected on the MPS profiles than on the array profile. (B) Sequencing (top) and aCGH (bottom) profile of chromosome 9 from Patient 2 embryo 7. The 4.5 Mb duplication on chromosome 9 is unequivocally apparent in the MPS data whereas less obvious in the array profile. The abnormalities were highlighted with red arrows.

5. Discussion

In the present study we evaluated the use of MPS in PGD for chromosomal aberrations. We thoroughly compared aCGH data from 47 embryos with data generated on the same amplified samples using shallow whole genome sequencing on both an Illumina and Ion Torrent instrument. All aberrations previously detected with aCGH could

be identified by MPS. There was no difference in the detection capacity between the NextSeq500 and Ion Proton instrument.

Microarrays are widely used in PGD and are considered the gold standard for the detection of chromosomal aberrations in embryonic samples. However, a major drawback of microarrays is the high cost per sample. We show that multiple PGD samples can be multiplexed in one MPS run. The PGD samples could also be multiplexed with sequencing libraries from other samples such as NIPT and exome sequencing samples. MPS technology and workflows can thus be flexibly applied to a range of samples. Depending on the sample throughput, MPS can be a cost-effective alternative compared to aCGH. Furthermore, we show that less sequencing reads than generated in this validation study can be used to obtain the same resolution.

According to our downsampling experiment, the minimal amount of sequencing reads to obtain a 4.5Mb resolution in PGD (smallest aberration present in our data set), is 1.6 million reads per sample. This number of reads is much higher compared to what is needed in MPS experiments on non-amplified DNA for copy number analysis. Probably due to the amplification bias introduced by the WGA protocol more reads are needed to obtain a similar resolution (186). Although several new WGA methods have been described, we –and others- have shown that the SurePlex method used in this study introduces the least amplification bias (187) (Chapter III). Although MPS is a technique that allows scaling, the WGA is currently the limiting factor in achieving higher resolution copy number profiles when starting from a single or a limited number of cells. According to the binomial distribution, higher read counts would lead to higher resolutions. However, looking at a higher resolution by using smaller windows introduced artefacts originating from WGA representation bias.

This validation study nicely demonstrates that for some samples the resolution of the commonly used BAC arrays is suboptimal. Although current WGA methods limit the resolution in both aCGH and MPS, with MPS the resolution can be increased (e.g., by lowering the analysis window size) for patients with known cryptic aberrations while restricting the analysis to the chromosomal segments of interest to avoid false positive results genome-wide. Illustrative are two different cases (Patient 2 and 10) in the present study. Both patients had a small balanced rearrangement in one of the parents. In Patient 10, embryo 1 has a 16.5 Mb duplication on chromosome 6 due to an insertional translocation in the father-46,XY,ins(14;6)(q23.2;q23.2q24.3). This couple was enrolled for PGD following a pregnancy where amniocentesis showed an aberrant prenatal microarray profile with a 16.5 Mb duplication on chromosome 6. Only with knowledge of this previous prenatal result, the insertion could be detected in the embryo by aCGH. The duplication is not called automatically by the BlueFuse software and although the 24sure+ arrays have a higher coverage of BAC probes near the telomeres and centromeres, the resolution in between is rather limited. The duplication is, however, clearly visible in the MPS data (Figure 3a). Another example of a small relevant

aberration is observed in Patient 2 embryo 7, where the terminal duplication of 4.5 Mb on the p-arm of chromosome 9 is only vaguely detectable by aCGH, but is very clearly revealed by sequence analysis (Figure 3b). Those two examples show that for some cases the resolution of the commonly used microarrays can be a limiting factor for PGD.

Concerns are raised about the ideal resolution for preimplantation analysis (36). The detection of Variants Of Unknown Significance (VOUS) should be avoided at this time, as this can potentially lead to discarding normal embryos. We therefore chose to limit the resolution of our analysis to ±3 Mb. Larger aberrations are very likely to be pathogenic and selecting against these larger aberrations can enhance conceiving a normal pregnancy. Depending on the parental karyotype and the imbalances involved, one could however adjust sequencing depth to obtain the needed resolution. The window size used during data analysis is another important element influencing the resolution of CNV detection. While smaller windows will be able to detect smaller CNVs, the amount of false positive calls will also increase. In the present study, we noticed that artefacts were apparent in smaller window sizes (100kb and 250kb windows). Of note were two recurrent artefacts that were present in several embryonic samples from different cases using the smaller window sizes: a duplication at 10q22.2q23.1 and a deletion in 17q22q24.1. Both aberrations were present in the NextSeq 500 and Ion Proton data. These aberrations are very likely the result of a bias in the genomic representation introduced by WGA. Therefore, for clinical use of MPS in PGD we consider 500kb as the most appropriate window, giving the best trade-off between sensitivity and specificity. The 500kb moving window allowed clear detection of all clinically relevant aberrations, yet excluding false positive calls.

MPS is a labor-intensive technique and library construction is quite a lengthy protocol that consists of multiple steps. Automation of the library preparation can diminish the hands-on time and increase the throughput. MPS for PGD with fresh embryo transfer can, however, be problematic due to the limited available timeframe. The introduction of trophectoderm biopsy and major improvements in cryopreservation, using the closed blastocyst vitrification system, are revolutionary innovations for PGD (61-63). First, more time available to perform the genetic analysis and potentially discuss difficult cases. Upon failure of the sequencing, the MPS protocol can be easily repeated or even a re-biopsy can be considered. Dimitriadou *et al.* showed that the quality of aCGH results on single cells is dependent on the phase in the cell cycle (54). ACGH on S-phase cells shows a more fluctuating profile than cells in the G-phase, which can lead to misdiagnosis. More cells can be biopsied from blastocysts which leads to a better and more uniform amplification. Cell cycle discrepancies are smoothed, ultimately leading to better results and hence, a more confident genetic diagnosis (54). An additional advantage of trophectoderm biopsy is the decreased risk of damaging the embryo. It has been shown that taking more than one cell from a cleavage stage embryo decreases the survival rate of the embryo, whereas this is not the case for trophectoderm biopsy (48, 61).

Furthermore, it has been shown that cleavage stage embryos contain more aneuploidies and show a higher rate of mosaicism for numerical and structural chromosomal aberrations (55). This can lead to both false positive and false negative results (58). This makes genome-wide chromosome analysis on day 3 embryos less meaningful. Genomic activation of the embryo sets in at day 3 and in this way DNA damage and response pathways will be activated. This will lead to the loss of some or even most of the abnormal embryos (58-60). Due to this natural selection against genomic abnormal embryos, genetic testing is needed for fewer, high quality embryos at the blastocyst stage. Although we use day 5 biopsy in this study, there is still a low chance of mosaicism for aneuploidies or structural abnormalities in the embryo. Since only a few cells are biopsied, mosaic embryos could potentially be missed. If the mosaicism is present in the biopsied cells, it is possible to detect mosaicism with aCGH as well as sequencing, depending on the percentage of abnormal cells vs normal cells. Although trophectoderm biopsy, combined with PGD, hampers fresh embryo transfer and implies vitrification of the embryos, it was recently shown that embryo transfer after freezing and transfer in a natural menstrual cycle leads to better IVF outcomes than fresh embryo transfer (63, 188). All these issues make trophectoderm biopsies the preferred approach for PGD for chromosomal aberrations.

This study also shows that shallow whole genome sequencing enables the unambiguous identification of aneuploidies and copy number aberrations in embryonic samples. Randomized control trials are currently being performed to evaluate whether aneuploidy screening shows added value in ART (19). The used technologies can be easily implemented for PGS and will allow reliable detection of aneuploidies of all chromosomes.

Furthermore we show, for the first time, that both Illumina (NextSeq500) and Ion Torrent (Ion Proton) sequencing technologies can both be used for the detection of chromosomal aberrations in embryos. Most clinical, genetic laboratories have access to one of these benchtop sequencers and the used protocols can be easily implemented. We could not determine any difference between both MPS techniques, and as such, they can be used equally. We prove that all aberrations detected by aCGH are also detectable by MPS, even the smaller ones and this for 42 abnormal samples. For the data analyses, QDNAseq or other published read depth algorithms can be used (159, 175). Due to the ease of use and the incorporation of the blacklisted regions, we prefer the QDNAseq algorithm.

6. Conclusion

We demonstrated that shallow whole genome sequencing on trophectoderm biopsies is a preferable alternative for the detection of chromosomal structural and numerical abnormalities in PGD embryos. MPS results are completely concordant with current aCGH techniques and provide slightly higher signal-to-noise ratio and resolution. The resolution of the MPS assay can be scaled by generating more or less reads, but resolution of <3Mb is hampered by WGA representation bias.

Link to data:
ViVar: http://cmgg.be/ViVar/

7. Supplementary information

Supplementary figure 1: Only 1/10nd of the reads is needed for detecting the chromosomal aberrations of 4.5 Mb and more.

To determine the minimum number of reads necessary to detect copy number aberrations successfully, raw reads were randomly downsampled to levels, respectively, 2 to 10 times lower than the original number of raw reads. (7) Original genomic MPS profile of Patient 2 embryo 7, (1) Genomic MPS profile of Patient 2 embryo 7 with the 10x less reads. All aberrations from the original sample could still be detected after downsampling.

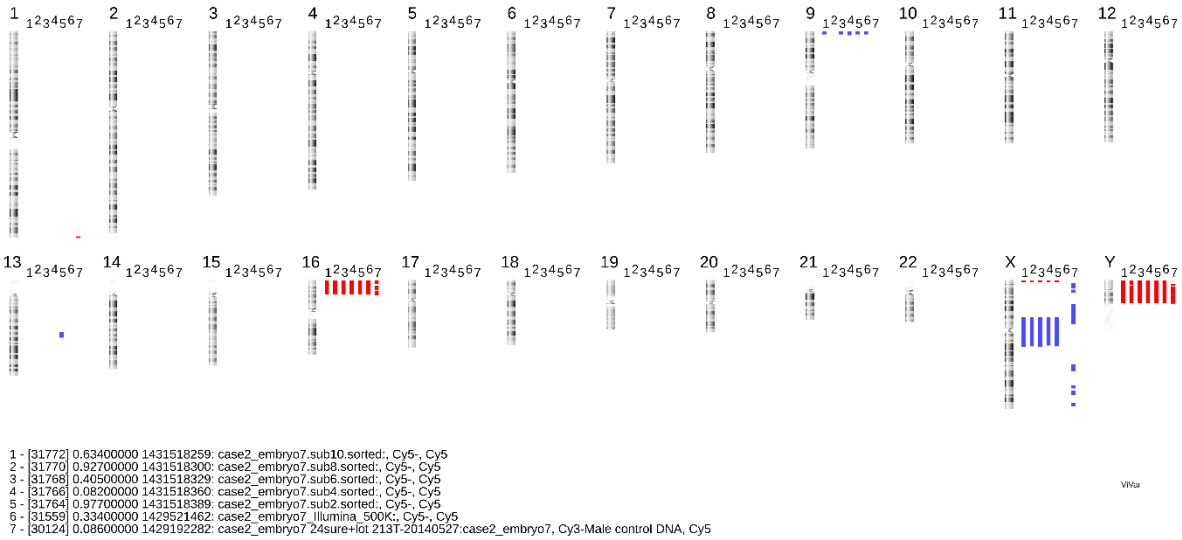

Chapter V: Genome-wide copy number alteration detection in preimplantation genetic diagnosis

Lieselot Deleye[1], Dieter De Coninck[1], Dieter Deforce[1], Filip Van Nieuwerburgh[1]

[1]Laboratory of Pharmaceutical Biotechnology, Ghent University, Ottergemsesteenweg 460, 9000 Ghent, Belgium

Chapter in book **"Next generation sequencing: Methods and Protocols"**;
Editors: Steven R. Head, Phillip Ordoukhanaian and Daniel R. Salomon;
Published in *Springer* 2018.; 10.1007/978-1-4939-7514-3..

1. Abstract

Shallow whole genome sequencing has recently been introduced for genome-wide detection of chromosomal copy number alterations (CNAs) in preimplantation genetic diagnosis (PGD), using only 4–7 trophectoderm cells biopsied from day-5 embryos. This chapter describes the complete workflow, starting from whole genome amplification (WGA) on isolated blastomere(s), up to data analysis for CNA detection. The process is described generically and can also be used to perform CNA analysis on a limited number of cells (down to a single cell) in other applications. This unique description also includes some tips and tricks to increase the chance of success.

2. Introduction

Massively parallel sequencing (MPS)-based preimplantation genetic diagnosis (PGD) has been the subject of several studies in recent years (30, 32, 163, 179). Those studies show the advantages of MPS over current methods, such as array Comparative Genomic Hybridization (aCGH), for detecting chromosomal aberrations in PGD (30, 32, 163). Although aCGH proved its value, its rather limited resolution and the relative high cost are a disadvantage (32). Shallow or low-pass whole genome sequencing can address these issues (30) (Chapter IV). Chapter IV concluded that shallow whole genome sequencing on trophectoderm biopsies is a preferable alternative for the detection of chromosomal structural and numerical abnormalities in PGD embryos (30). MPS-based PGD was able to detect chromosomal aberrations, equal or larger than 3Mb, in 47 blastocysts of 15 patients with a better resolution and signal-to-noise ratio compared to aCGH-based PGD (30) (Chapter IV). Although no large clinical trials on the long-term clinical advantages of embryo selection using MPS have been reported yet, a few cases of birth of a healthy baby are known (31, 32).

Embryo implantation fitness is determined using only 4–7 trophectoderm cells biopsied from day-5 embryos (48, 55, 58). Whole genome amplification (WGA) is needed to amplify the DNA from those cells before downstream analysis. Especially with such low amounts of input DNA, some WGA methods will lead to unbalanced amplification with over- and under-representation of genomic regions. Bias introduced during this amplification process, may lead to misinterpretations of the genomic profile (187) (Chapter III). Choosing the correct method for amplification depends on the application (130): PCR-based methods are better suited for chromosomal aberration detection compared to multiple displacement amplification (MDA) methods, because they give a more balanced genomic amplification. In Chapter III, two state-of-the-art PCR-based WGA methods were compared to study their applicability for copy number alteration (CNA) detection using MPS (187). In this study, PicoPLEX/SurePlex (Rubicon Genomics Inc., MI 48108, USA / BlueGnome Ltd., Mill Court, Great Shelford, Cambridge, UK) proved to be better suited for CNA analysis using MPS compared to Multiple Annealing and Looping Based Amplification Cycles (MALBAC) (Yikon genomics, Beijing, China). SurePlex WGA is more uniform across the genome, leading to less false positive

and false negative CNAs. SurePlex WGA has been successfully applied in clinical MPS-based PGD with correct detection of CNAs with a resolution of 3Mb (30) (Chapter IV).

CNA analysis starting from a limited number of DNA has several applications. Therefore, a detailed description of this method is useful. In this chapter, the workflow is described in detail as it would be executed for PGD. The general techniques described are from standard protocols, but important changes to these standard protocols were introduced to optimize the results. The note section, listing some tips and tricks, is important to increase the chance of success. The complete procedure, starting from a few cells and ending up with a CNV profile of the DNA, has never been described in such great detail before. The workflow, as described, has proven its success in detecting CNV up to 3Mb starting from 4-6 blastocysts.

The protocol starts with WGA on a few cells. Based on previous results, the SurePlex WGA kit was the method of choice for WGA (187) (Chapter III). SurePlex might be replaced with another WGA method, but this might have a significant influence on the results. The genomic coverage, sequence error rate, yield, and representation bias might differ, possibly leading to more/less accurate CNA detection and/or a higher/lower CNA detection resolution. Changing from SurePlex to PicoPLEX should not influence the results, since both kits basically have the same underlying method. The amplified DNA is fragmented to fragments of 200bp using sonication. Subsequently, Illumina sequencing libraries are prepared from the fragmented DNA using NEBNext Ultra 2 library preparation kit. This kit is suited for DNA input amounts as low as 500pg. The needed library preparation method depends on the downstream sequencing technology. In this protocol, Illumina NextSeq500 sequencing is described. Ion Torrent sequencing will show similar results as demonstrated in chapter IV (30).

3. Materials

3.1. Whole genome amplification

1. DNA Lo-bind 0.2ml or 1.5ml tubes.
2. Filter tips
3. Positive control (genomic DNA at a known concentration): diluted to 30pg/µl in Molecular Bio-grade water (Note 1).
4. Phosphate Buffered Saline (PBS).
5. SurePlex/PicoPLEX WGA kit for single cell whole genome amplification, Rubicon Genomics, store at -20°C (Note 2).
6. Thermocycler with heated lid at 105°C.
7. Purification kit: Genomic Clean &Concentrator, Zymo Research, store at room temperature. Binding buffer and Wash buffer are provided.
8. Benchtop microcentrifuge.
9. Thermomixer at 65°C.

10. Quality control using capillary gel electrophoresis: Agilent High-Sensitivity DNA kit (lab-chip), Bioanalyser 2100, Agilent Technologies.
11. Concentration measurement: Qubit dsDNA High Sensitivity Assay kit.

3.2. Fragmentation of purified WGA product

1. DNA Lo-bind 0.2ml tubes.
2. Filter tips
3. Fragmentation of DNA by sonication: Covaris S2 Focused Ultrasonicator with Adaptive Focused Acoustics technology (Covaris).
4. MicroTUBES (Covaris)
5. 1/5 X Tris-ethylenediaminetetraacetic acid (EDTA) buffer: 0.5ml 20 X TE buffer, 49.5ml molecular bio-grade water.

3.3. Library preparation

1. DNA Lo-bind 0.2ml or 1.5ml tubes.
2. Filter tips
3. All buffers mentioned during the downstream protocol are derived from the NEBNext Ultra II kit, Bioké. Store at -20°C. (Note 3)
4. Thermocycler with adjustable heated lid.
5. Thermomixer for 0.2 and 1.5ml tubes.
6. Purification kit: Genomic Clean & Concentrator (Zymo Research), store at room temperature. Binding buffer and Wash buffer are provided.
7. Benchtop microcentrifuge.
8. Size selection: E-Gel 2% EX agarose gel, 1kb plus DNA ladder and E-gel ibase power system (Thermo Fisher Scientific).
9. Purification from gel: Zymoclean gel DNA recovery kit, Zymo Research, store at room temperature.
10. Dark Reader blue light Transilluminator
11. 10ng/µl yeast tRNA
12. Purification after enrichment PCR: magnetic beads, Agencourt AMPure XP beads, store at 4°C, magnetic particle concentrator (MPC).
13. 80% ethanol: 40ml 100% ethanol with 10ml molecular bio-grade water. This can be kept at 4°C for two weeks.

3.4. Library quality control and quantification

1. Quality control using capillary gel electrophoresis: Agilent High-Sensitivity DNA kit (lab-chip), Bioanalyser 2100, Agilent Technologies.
2. Quantification of adapter-ligated fragments: Sequencing library qPCR quantification guide (Illumina)
3. Illumina sequencing kit (Note 4).

4. Method

Carry out all procedures at room temperature unless otherwise specified.

4.1. Whole genome amplification

1. Isolate the necessary amount of cells in less than 2.5µl of cell medium or PBS in a 0.2ml tube (Note 5).
2. Dilute with the appropriate volume of Cell Extraction Buffer to achieve a total sample volume of 5µl (Note 6).
3. Prepare a positive and negative control. Take 2.5µl of PBS as negative control and take 2.5µl of the diluted positive control.
4. Prepare an extraction cocktail for at least 5 samples (positive and negative control included) (Note 7). Combine 24µl of Extraction Enzyme Dilution Buffer and 1µl of Cell Extraction Enzyme in a 0.2ml tube and mix by flicking the tube. Add 5µl of this cocktail to each sample (Note 8). Incubate the samples immediately in a pre-programmed thermocycler:

10min 75°C
4min 95°C
Hold 10°C

Proceed immediately.

5. Prepare a pre-amp cocktail for at least 5 samples. Combine 24µl of Pre-Amp buffer and 1µl of Pre-Amp Enzyme in a 0.2ml tube and mix by flicking the tube. Add 5µl of the cocktail to each sample (Note 8). Incubate the samples in a pre-programmed thermocycler:

2min 95°C
15sec 95°C
50sec 15°C
40sec 25°C
30sec 35°C
40sec 65°C
40sec 75°
} 12 cycles
Hold 4°C

6. Place the samples on ice before use.
7. Prepare the Amplification Cocktail as instructed. Combine 34.2µl nuclease-free water/sample, 25µl Amplification buffer/ sample and 0.8µl Amplification enzyme/sample in a 0.2ml tube. Mix by flicking the tube and add 60µl to each sample tube. Incubate the samples in a pre-programmed thermocycler:

2min 95°C
15sec 95°C
1min 65°C
1min 75°C
} 14cycles
Hold 4°C

8. Vortex the samples and spin down
9. Purify the samples on spin columns. As an efficient example, Zymo Genomic Clean and Concentrator has been described below.
10. Place nuclease-free water at 65°C in a thermomixer.
11. Add 375µl Binding buffer to each sample and transfer this mix to the spin column (Note 9).
12. Centrifuge at 11000 RPM for ± 25sec.
13. Discard the flow-through and pat the collector tube dry. Re-use the same collector tube.
14. Wash the spin columns with 200µl Wash buffer.
15. Centrifuge at 11000 RPM for ± 25sec.

16. Repeat step 14.
17. Centrifuge at 11000 RPM for ± 1min (Note 10).
18. Transfer the spin columns to a new 1.5ml tube.
19. Elute the DNA in ±32µl of the pre-warmed molecular biology grade water (Note 11) and incubate for 1min at room temperature.
20. Centrifuge at 11000 RPM for ± 35sec.
21. Remove the spin column and store the 1.5ml tubes at -20°C or perform a quality/quantity check before storing. Measure the concentration with Qubit (Note 12). Analyze the sample on a high sense Agilent lab-chip (Note 11).

4.2. Fragmentation of purified WGA product

1. Dilute ±100ng of the WGA product with 1/5 TE buffer in 130µl in microTUBES.
2. Adjust the settings of the Covaris S2 for a 200 bp fragmentation: duty cycle of 10%, intensity of 5, 200 cycles/burst and a treatment time of 190s (Note 14).

4.3. Library preparation

1. Make sure the heated lid of the thermocycler is set on 75°C.
2. Add 7µl of End repair reaction buffer to empty 0.2ml tubes. Transfer 50µl of each fragmented sample into a 0.2ml tube with buffer. Add 3µl of End prep enzyme mix to each sample and mix by flicking the tube. Incubate the samples immediately in the pre-programmed thermocycler with heated lid on 75°C:

30min 20°C
30min 65°C
Hold 4°C

Proceed immediately

(During incubation, put a thermomixer at 20°C and pre-program another thermocycler at 37°C with a heated lid at 47°C. Make sure the temperature of the thermocycler is already at 37°C when the samples are inserted. If DNA input was less than 100ng, dilute the adapter to a finale concentration of 1.5µM (Note 15).)

3. Add 30µl ligation master mix, 1µl ligation enhancer and 2.5µl diluted adapter to each sample in this respective order (Note 16). Mix by flicking the tube and incubate 15min at 20°C in a thermomixer.
4. Add 3µl USER enzyme to each sample and incubate 15min at 37°C in a thermocycler with heated lid at 47°C.
5. Purify the samples on spin columns, such as described above. Place nuclease-free water at 65°C in a thermomixer.
6. Add 482.5µl Binding buffer to each sample and transfer this mix to a spin column (Note 9).
7. Follow step 12-18 as in part 4.1.
8. Elute the DNA in ±22µl of the pre-warmed nuclease-free water (Note 17) and incubate for 1min at room temperature.
9. Centrifuge at 11000 RPM for ± 35sec and remove the spin column (Note 18).
10. Perform size selection using E-gel EX 2% agarose gels. Dilute the DNA ladder ¼ in 20µl water. Add all samples individually to a separate gel-slot, alternated with a ladder every 3 or 4 samples. Choose the 1-2% gel program on the ibase (10min) and run the gel.

11. Remove the gel from its case and visualize using a Dark Reader blue light transilluminator. Cut the gel at the desired height to retrieve the DNA (Note 19).
12. Dissolve the gel in 300µl ADB buffer (Zymo gel purification) at 55°C in a thermomixer for at least 10min. When the gel is completely dissolved, purify on spin columns as described above in 4.1. However, change the elution volume to 17µl.
13. Next, enrich the samples carrying adapters. Each sample is assigned an index (Note 20). Transfer the samples to a 0.2ml tube and add 1µl of tRNA (Note 21). Add 3µl of the assigned index primer and 3µl of universal primer to each sample. Finally, transfer 25µl of HF 2X PCR master mix to each sample. Mix by flicking the tube and immediately incubate in a pre-programmed thermocycler:

30sec	98°C	
10sec	98°C	} 9 cycli (Note 22)
75sec	65°C	
5 min	65°C	
Hold	4°C	

While waiting: put the magnetic beads at room temperature.

14. Purify the sample using magnetic beads (Note 23). Mix the samples with 45µl beads and leave at room temperature for 6min.
15. Put on a MPC until the liquid is clear and remove supernatant
16. Wash the beads with 200µl 80% ethanol while on MPC and wait 30sec before removing supernatant.
17. Repeat step 18
18. Make sure all supernatant has been removed, in order to facilitate the air-drying process. Air-dry the samples until cracks are visible between the beads (Note 24).
19. At 22µl nuclease-free water to each sample and remove from MPC. Mix well until sample and beads are a homogeneous mixture. Leave at room temperature for 3min.
20. Put on MPC until clear and transfer the supernatants to new 0.2ml tubes. Make sure no beads are transferred.

4.4. Library quality control and quantification.

Library quality control is performed by capillary gel electrophoresis on a Bioanalyzer High sense labchip. The result is displayed as an electropherogram (EPG) showing intensity in function of fragment-size distribution. The library should contain DNA fragments of ±300 bp. Figure 1a shows an EPG of a good quality library. The other two smaller peaks represent the internal standards (upper and lower marker). The intensity of the library informs about the concentration of the library (Note 25). A peak visible around 85bp, as the one shown in figure 1b, indicates the presence of primer-dimers (Note 26).

The quantification of adapter-ligated fragments in the library is performed by qPCR. Only fragments carrying an adapter will bind to the flowcell, and therefore will be sequenced (Note 27). QPCR is performed as recommended by Illumina. Make sure the libraries are diluted to fit the standard curve used for qPCR. The concentration measured after qPCR reflects the amount of DNA that can be sequenced.

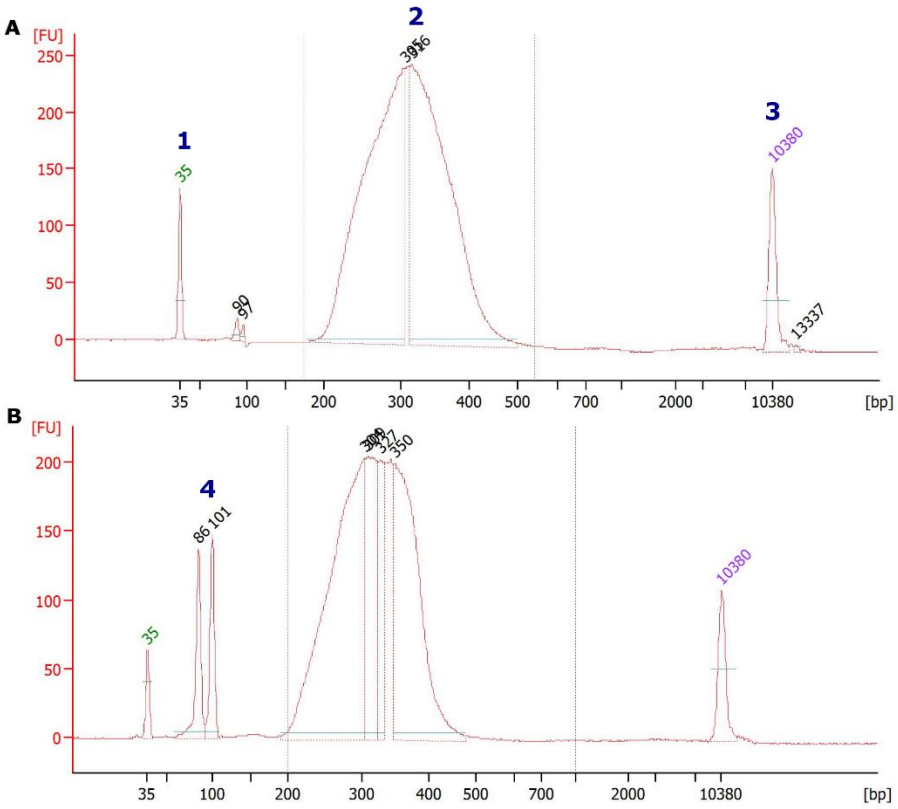

Figure 1: Library quality control.

A) An electropherogram of a good quality library with a fragment length of ±300bp. (1) Lower marker, (2) Library, (3) Upper marker. B) An electropherogram of a library with primer-dimers (4).

The libraries are further prepared for sequencing using the standard Illumina protocols. Sequencing is performed on a NextSeq500 using a high output flowcell for single read and 75 cycles. The sequencing run will last for about 11 hours.

4.5. Data analysis

Several tools and programs are available to detect CNAs using shallow, genome-wide massively parallel sequencing data (172, 189). However, most of these tools only handle a certain part of the analysis. It requires bioinformatics knowledge to handle and combine these different tools to perform CNA detection starting from raw sequencing data. Recently, ViVar (182) was developed to provide a user-friendly web-based analysis platform that handles all necessary steps in a comprehensive way. This platform is freely available at https://www.cmgg.be/ViVar/. Download and installation instructions are also provided at this web URL.

ViVar offers an easy-to-use and straightforward interface which enables the analysis from raw sequencing data, obtained from the sequencer as .fastq files, for detection of CNAs:

1. Select 'Projects' from the top navigation bar (Figure 2).
2. Click the 'New project' button to create a new project (Figure 2).
3. Click the 'Save' button after filling out the project's information to save the new project.

4. One can now find the new project in the list, which is accessed by selecting 'Projects' from the top navigation bar (Figure 2).
5. By clicking on the new project's name, a page containing the experiments for that project will be loaded. In ViVar, each experiment consists of a single sample.
6. To create a new experiment, click the 'New experiment' button.

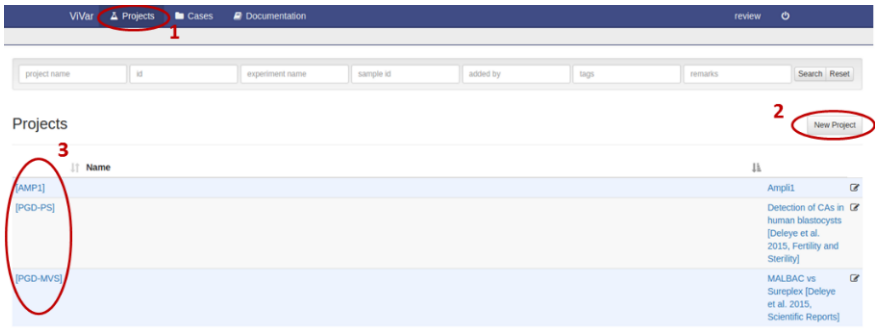

Figure 2: Creating a new project in ViVar.

First, select 'Projects' from the top navigation bar (1), then click the 'New project' button to create a new project (2). After filling out the project's information, the newly created project will appear in the projects list (3).

7. Choose 'Sequencing data' by clicking the 'Next' button in the 'Sequencing data' field (Figure 3).

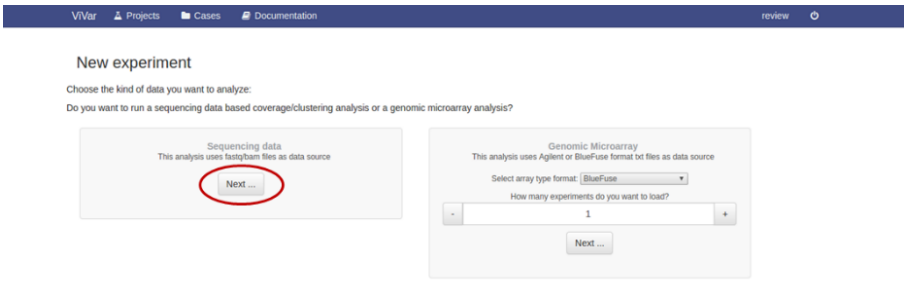

Figure 3: Starting a new sequencing experiment on ViVar.

A new experiment/analysis based on massively parallel sequencing data can be started by clicking the 'Next' button in the 'Sequencing data' field (red circle).

8. From the drop-down list select the project you want to add a new experiment to (Figure 4).
9. Add data to an experiment by selecting the samples you want to analyze. You can select multiple samples at once (Figure 4).
10. Next, choose the organism from which the samples originate (Figure 4).
11. Then, also select the version of the reference genome you want to use for the analysis from the drop-down list (Figure 4).
12. Finally, in the 'Depth of Coverage' field, select the bin size you want to use for the analysis (see description of this parameter below), switch the tumble button from 'OFF' to 'ON' and click the 'Next…' button to start the analysis (Figure 4).

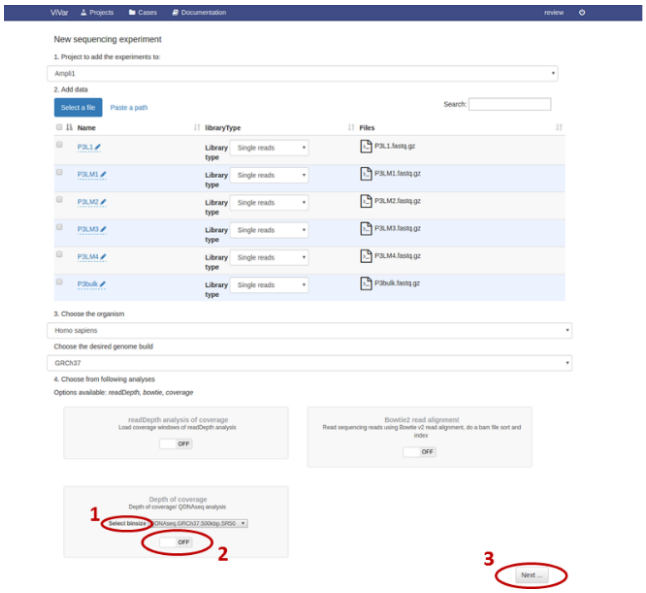

Figure 4: Setting the parameters for a new analysis in ViVar.

Once a new analysis based on massively parallel sequencing data has been created, parameters for the analysis can be specified: the project to which the experiment should be added, the sample(s) which should be analyzed, the reference genome which should be used in the analysis, and the bin size (1). Analysis can be started by switching the tumble button from 'OFF' to 'ON' (2) and clicking the 'Next...' button (3).

ViVar will now analyze the data in a fully automated manner. Briefly, it first uses Bowtie (190) to place the sequencing reads onto the reference genome. Then, using these mapped reads, it performs CNA detection using the QDNAseq algorithm (160). To this end, the genome is divided in non-overlapping fixed size parts, so called bins/windows. The size of these bins will determine the minimum size of the CNAs which can be detected. Generally, CNAs three to five times the size of the bins can be detected. The number of reads mapped to each bin will be determined. This number is influenced by certain factors, such as GC-content and mappability, for which the number of reads mapped per bin is normalized. After GC-content and mappability normalization, read counts are median-normalized by dividing the number of reads in each bin by the median number of reads across all bins. As CNAs are assumed to be rare, the median number of reads across all bins is a fair estimate of the expected number of reads per window for a perfectly diploid genome. As such, the median-normalized read counts represent a measure for the deviation from diploidy for each window and a copy number (CN) estimate is calculated using the following formula: CN= 2(read count/median read count). Then, a circular binary segmentation (CBS) algorithm (161) is applied which groups bins into larger contiguous regions with an equal CN. The mean of read counts of the windows contained in the segments are used as an estimator of the copy number of the whole segment. After this segmentation, CNAs are called when the segment's $\log_2$(CN/2) surpasses a certain threshold. This threshold can be specified by the user in ViVar (see further). Based on literature review and own experience a threshold of +/- 0.35 performs well.

After the analysis has been finished, ViVar offers some powerful visualizations of the data: line profile plots, karyo plots, genome heatmaps, etc. (Figure 5). The procedure to obtain these visualizations is always similar:

- Select 'Projects' from the top navigation bar
- Click on the project of interest. A list of experiments within the project is now shown.
- Select the experiment you want to visualize by ticking the checkbox in front of the experiments name (Figure 6).
- Select, from the dropdown list at the top of the screen, the visualization of interest.
- Some visualizations, such as the karyo plots, can handle multiple simultaneous experiments.
- Finally, certain visualization and analysis settings, such as color schemes and thresholds for calling CNAs can be adjusted by clicking on 'criteria' in the upper right corner of the visualization screen.

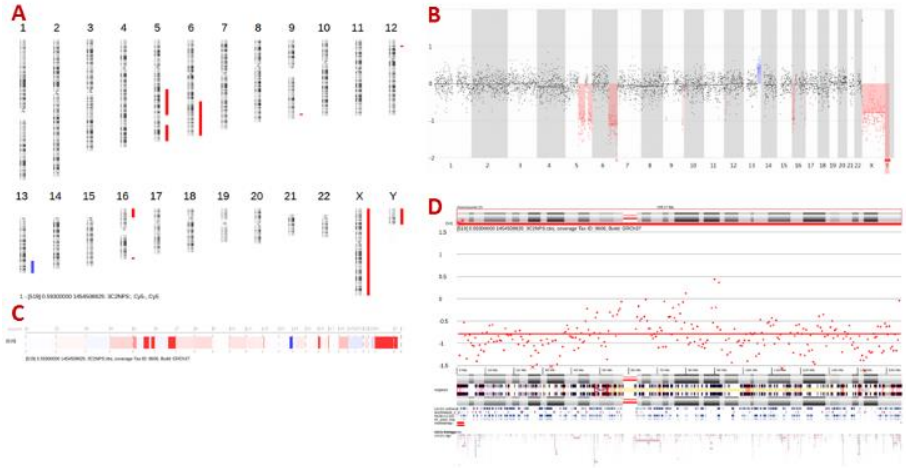

Figure 5: Some of the visualizations possible with ViVar.

Karyo plot (A); line view plot (B); genome heatmap (C); and chromosome view (D).

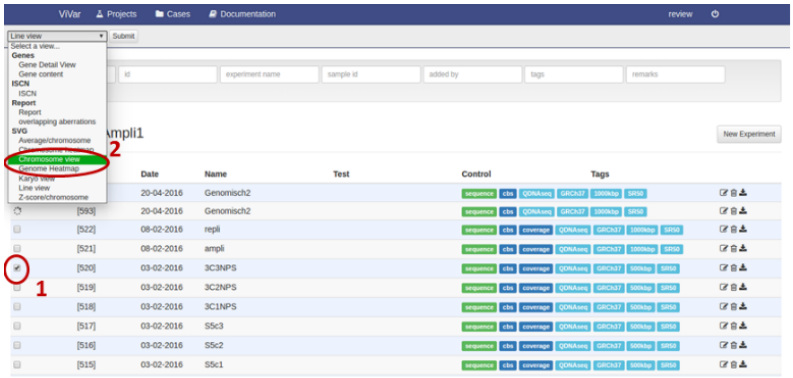

Figure 6: Visualizing results in ViVar.

Results can be visualized in ViVar by ticking the checkbox in front of the name of the experiment you want to visualize (1) and choosing the visualization of interest from the dropdown list (2).

5. Notes

1. The amount of DNA in the positive control is equivalent to 5 cells.

2. All buffers used during the downstream protocol are derived from this kit. Buffers must be vortexed before use, but never vortex enzymes. Always keep enzymes on ice.

3. Another library preparation method for Illumina, without the enrichment PCR step, is a valid alternative for the described method. Omitting the PCR-step will lead to a more uniform coverage of the genome (187) (Chapter III). However, this TruSeq PCR-free library prep kit requires more input material, which might pose a limitation for some applications. Replacing the NEBNext Ultra II kit with the NEBNext Ultra 1 version, will not change the outcome.
4. The type of kit depends on the number of samples and the coverage aimed. Here: Illumina NextSeq500 high output kit v2 (75 cycles).
5. A) Blastocysts are kept at -20°C after biopsy until genetic analyses. Cells isolated from a cell culture are snap frozen in N_2 immediately after collection and stored at -80°C until further use.
   B) Other start material, such as fixed or microdissected cells, might lead to different results and might need some optimization.
6. This mix can be stored at -80°C. However, it is recommended to proceed immediately.
7. To avoid pipetting errors when pipetting very small volumes, prepare the mix for at least 5 samples.
8. To avoid the loss of cell material, do not touch the liquid already present in the tube while adding the cocktail.
9. To increase binding of the DNA, add 5 X Binding buffer (ratio 1:5).
10. Make sure no residual wash buffer/ethanol is left, because this might lead to a suboptimal elution of the DNA. Centrifuge again if necessary.
11. Elution with *pre-warmed* water will lead to a better elution of the DNA. The elution volume depends on the downstream application. Make sure to get rid of the air-bubbles in your tip that arise because of the temperature difference. Pipet the water straight on top of the column.
12. Other assays based on fluorescent DNA stains can also be used to measure the concentration. However, spectrophotometric techniques such as Nanodrop are less accurate because the UV signal is not specific to DNA.
13. If the negative control shows a similar result on Qubit and Agilent as the samples, some contamination might have occurred during the WGA procedure. In this case, samples might contain more amplified contaminated material than amplified template. If both samples and positive control show negative results, the PCR reaction during WGA might have failed. If the positive control looks fine, but one (or more) of the samples is negative, that specific sample probably lacked template at the start.
14. The treatment time might need to be slightly adjusted depending on the specific instrument and water bath temperature.
15. The dilution needs to be made fresh.

16. Do not mix the three components in advance, since this might create adapter-dimers. The adapter ligation could be suboptimal, since a large part of the adapters are already ligated to each other. Add the three components sequentially to one sample, then add the three components sequentially to the next sample, etc. Avoid a big time difference between the first and last sample, since the reaction already starts at room temperature.
17. The elution volume is important for the next step.
18. At this point, the sample could be stored at -20°C. However, long time storage might negatively affect the concentration of library with intact sequencing adapters.
19. Make sure to change scalpel between each sample. If DNA concentrations are low, samples might be nearly invisible under the dark reader. Retrieve the samples between 200 to 400bp.
20. Make sure each sample is assigned a unique index. The specific combination of indexes is only important if less than 7 samples are pooled (see kit documentation). Dual-indexing is used when more than 24 samples are pooled.
21. In samples were template DNA concentrations are rather low, tRNA is added as a carrier that will adsorb to most of the tube wall, resulting in more concentrated template DNA in the rest of the tube. Higher concentration increases the efficiency of primer annealing to the template. More template will be efficiently amplified and the amount of primer-dimers will decrease.
22. The number of cycles depends on the input amount of DNA. Decrease the number of cycles if possible, to decrease amplification bias.
23. Make sure the beads are well mixed before use. When removing supernatant, check your tip for beads. If beads are visible, transfer the liquid back into the right tube and wait again until the liquid is clear.
24. The protocol states not to dry the beads until they are cracked. Nevertheless, based on our experience, the elution efficiency increases when the ethanol is completely evaporated.
25. The intensity of both internal standards should be similar. If this is not the case, the concentration measurements are not reliable.
26. Intense primer-dimer peaks should be removed from the library. They will skew qPCR results, because they also contain the binding place for the qPCR primers and thus yield an unreliable quantification of adapter-ligated fragments. The dimers are removed by size selection on gel, as described before. The bright band of 200-400bp is cut from the gel and the dimers are left behind nearly at the end of the gel. Primer-dimers might also be avoided by decreasing the primer input during enrichment PCR or decreasing the amount of samples prepared simultaneously. They will compete with the library-fragments for binding places on the flowcell. Only fragments carrying the correct adapters on both ends will bind to the flowcell. A peak at ±125bp

on the EPG indicates the presence of adapter-dimers. Measuring the amount of DNA from the library that will actually bind to the flowcell is essential to overcome over- or underclustering during the sequencing run and can only be achieved using qPCR.

27. When the fragment length between the samples and PhiX is different, a size correction is performed on the measured concentration after qPCR. PhiX has a fragment length of 500bp, whereas the samples have fragment lengths of only 300 bp. For size correction, the measured concentration is multiplied by the ratio of PhiX length over library length.

Chapter VI: Performance of a TthPrimPol-based whole genome amplification kit for copy number alteration detection using massively parallel sequencing

Lieselot Deleye[1], Dieter De Coninck[1], Annelies Dheedene[2], Petra De Sutter[3], Björn Menten[2], Dieter Deforce[1,#], Filip Van Nieuwerburgh[1,#]

[1]Laboratory of Pharmaceutical Biotechnology, Ghent University, Ottergemsesteenweg 460, 9000 Ghent, Belgium.
[2]Center for Medical Genetics, Ghent University, De Pintelaan 185, 9000 Ghent, Belgium.
[3]Department for Reproductive Medicine, Ghent University Hospital, De Pintelaan 185, 9000 Ghent, Belgium.
[#]These authors contributed equally.

Scientific Reports | 6:31825 | DOI: 10.1038/srep31825; Published 22 August 2016

1. Abstract

Starting from only a few cells, current whole genome amplification (WGA) methods provide enough DNA to perform massively parallel sequencing (MPS). Unfortunately, all current WGA methods introduce representation bias which limits detection of copy number aberrations smaller than 3Mb. A recent WGA method, called TruePrime single cell WGA, uses a recently discovered DNA primase, TthPrimPol, instead of artificial primers to initiate DNA amplification. This method could lead to a lower representation bias, and consequently to a better detection of CNAs. The enzyme requires no complementarity and thus should generate random primers, equally distributed across the genome. The performance of TruePrime WGA was assessed for aneuploidy screening and CNA analysis after MPS, starting from 1, 3 or 5 cells. Although the method looks promising, the single cell TruePrime WGA kit v1 is not suited for high resolution CNA detection after MPS because too much representation bias is introduced.

2. Introduction

Several whole genome amplification (WGA) methods exist to amplify DNA extracted from a limited number of cells, yielding the necessary amount of DNA required to perform massively parallel sequencing (MPS) (130, 191). The different WGA methods each have their advantages and disadvantages in terms of genome coverage, representation bias, error rates, yield and robustness. The most appropriate method should be selected based on its intended application. A recent study suggests that multiple displacement amplification (MDA) methods are better suited for single nucleotide polymorphism (SNP) detection while PCR-based methods are the better option for copy number aberration detection (130). MDA methods use the high-fidelity phi29 polymerase, leading to less nucleotide errors in the amplified sequences, while PCR-based methods tend to give a more balanced genomic amplification. In Chapter III, we compared two state-of-the-art PCR-based WGA methods to study their applicability for CNA detection using MPS (187). In that study, PicoPLEX/SurePlex (Rubicon Genomics Inc., MI 48108, USA / BlueGnome Ltd., Mill Court, Great Shelford, Cambridge, UK) proved to be more suitable for CNA detection compared to Multiple Annealing and Looping Based Amplification Cycles (MALBAC) (Yikon Genomics, Beijing, China). MALBAC amplified samples showed a less uniform read distribution across the genome (i.e. more representation bias), leading to more false positive and false negative CNA detections. SurePlex amplified samples lead to accurate detection of CNAs with a resolution of 3Mb. In another study, SurePlex WGA proved its efficient amplification of DNA from 4-6 blastocyst cells for downstream MPS with a reliable detection of chromosomal aberrations down to 3Mb (30) (Chapter IV). Nevertheless, results show that the WGA representation bias is still a limiting factor in achieving higher resolution copy number profiles when starting from a single or a limited number of cells (30). In order not to call over- or underamplified regions as CNAs, the read counts need to be averaged out in genomics windows of at least 500kb (30) (Chapter IV), leading to a 3Mb resolution for CNA detection (see also Methods section). With less representation bias, smaller windows and a higher resolution could be used. Accurate detection of CNAs from

amplified DNA is of importance for applications such as preimplantation genetic diagnosis (PGD), in which day-5 embryos are screened for CNA using of 4-6 trophectoderm cells (30) (Chapter IV). Cell-based liquid biopsy both in cancer and prenatal diagnosis, is another emerging field where accurate, high resolution CNA detection starting from a limited number of cells is invaluable.

A WGA method called TruePrime single cell WGA (Sygnis, Heidelberg, Germany) uses a DNA primase, TthPrimPol, which synthesizes primers for Phi29 DNA polymerase, so that no artificial primers need to be added to the reaction (192). After primer synthesis by TthPrimPol, Phi29 polymerase performs polymerization and strand displacement as in a classical MDA. The non-artificial primers, which could lead to a lower representation bias, combined with the high-fidelity of Phi29, could theoretically lead to an ideal WGA method.

The goal of the present study was to assess the performance of TruePrime WGA for aneuploidy screening and high resolution copy number analysis, starting from a limited number of cells, using MPS. The variability in distribution of the reads across the genome and the ability to correctly detect chromosomal aneuploidies and large CNAs was assessed and the results were compared to the study of Chapter III (187), in which the performance of PicoPLEX/SurePlex and MALBAC WGA was studied in a similar setting.

3. Material & Methods

3.1. Experimental design

This study was performed on cells derived from the female Loucy cell line (DSMZ, ACC394) (169) . A reference 180K aCGH profile (Agilent Technologies) was obtained from unamplified genomic DNA from this cell line (Figure 1). According to the 180K aCGH profile, the following chromosomal aneuploidies and CNAs were called within the resolution range (≥3Mb) of the subsequent sequencing results: a deletion of an entire X-chromosome, a distal deletion of ±72Mb on 5q21.3q35.3, a distal deletion of ±45Mb on 6q22.31q27, a ±26Mb duplication of 13q33-q33.3 and deletions of respectively 13Mb and 3Mb on 16p13.3-p13.12 and 16q24.2q24.3. These CNAs were used as a reference for comparing with the MPS analyses. The cell line was grown in suspension which allowed for isolation of individual cells. Samples consisting of 1, 3 or 5 cells, in triplicate, were collected using micromanipulation. These samples were used to perform TruePrime WGA, Illumina library preparation with enrichment PCR and sequencing. In parallel, triplicate samples consisting of 3 cells were subjected to TruePrime WGA, PCR-free Illumina library preparation and sequencing to comparatively study the effect of enrichment PCR on representation bias (Figure 2).

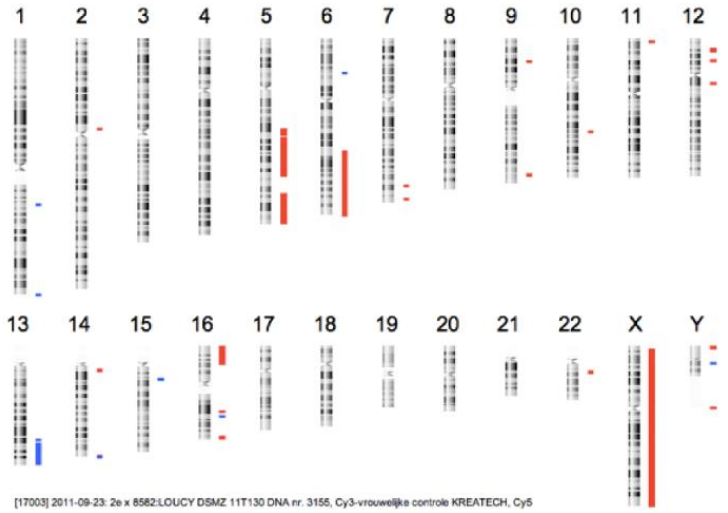

Figure 1: 180 K aCGH of genomic DNA from the female Loucy cell line.

This profile shows all CNAs detected in the female Loucy cell line up to a resolution of 50 kb. Red bars indicate deletions and blue bars indicate insertions. The deletions in chromosomes X, 5, 6, and 16 and duplication in chromosome 13, all with a size of ≥3 Mb, were the CNAs expected to be detected by the sequencing results.

A negative control was used during WGA to control for contamination of the samples. A sample containing 26pg high quality DNA was used as a positive control during WGA. This positive control was performed to check the yield of the WGA procedure on a sample with high quality input DNA, excluding possible suboptimal conditions due to the cell manipulation and extraction steps. The positive control serves as reference of the optimal WGA product yield and could be used as a troubleshooting tool in case the cell samples would yield no (or low) amounts of WGA product. Library preparation, sequencing and data analysis were performed in parallel with other similar samples (routine samples amplified with SurePlex WGA, not belonging to present study) to rule out failing steps after WGA amplification.

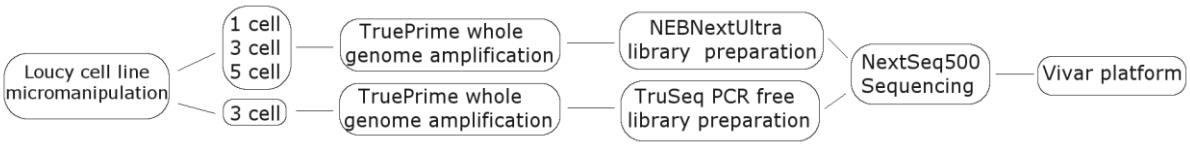

Figure 2: Experimental design.

Schematic overview of the experimental design of the study. Samples containing 1, 3 and 5 cells were taken from the Loucy cell line using micromanipulation. Next, the DNA of these individual samples was amplified with the TruePrime WGA kit. The WGA product of 1, 3 and 5 cell samples was used to perform an Illumina library preparation with enrichment PCR. In parallel, WGA product of 3 cell samples was used to perform a PCR-free Illumina library preparation. This experiment was done in triplicate for all sample types.

3.2. Growth and isolation of cells

The cells were grown in Roswell Park Memorial Institute (RPMI-1640) medium (Life Technologies, Carlsbad, USA), supplemented with 10% fetal bovine serum (Life Technologies, Carlsbad, USA). For optimal growth, they were kept at a temperature of 37°C and a 5% CO_2 level. A known amount of cells was isolated with an ergonomic denuding

handle from STRIPPER (Origio, Måløv, Denmark) and MXL3-100 needles with a diameter of 100 µm (Origio, Måløv, Denmark). A serial dilution with sterile phosphate buffered saline (PBS) (Life Technologies, Carlsbad, USA) spots was performed on a Petri dish (5.5cm) under an Axiovert 25 light microscope (Zeiss, Jena, Germany), until the desired amount of cells for isolation was obtained. All cells were collected in a maximum volume of 2.5µl. All samples were snap frozen in liquid N_2, immediately after collection.

3.3. TruePrime WGA

Cell lysis and amplification was performed using the TruePrime Single cell WGA kit (Sygnis, Heidelberg, Germany), following manufacturer's instructions. As a positive control, 1µl of 26pg/µl single-source male control DNA (NIST 2391C Component C DNA) was used. As a negative control, 1µl of PBS was used as input material. All samples were purified according to the manufacturer's protocol of the Genomic DNA Clean & Concentrator kit (version 1.0.0, Zymo Research, Irvine, USA) with 5X binding buffer. Concentration was measured using Qubit dsDNA High Sensitivity Assay kit (Life Technologies, Carlsbad, USA). The quality of the different samples was assessed with the Agilent 12000 (12K) DNA Assay kit (Bioanalyser, Agilent Technologies, California, USA).

3.4. Illumina library preparation

One hundred ng of the WGA product was fragmented to an average size distribution of 200bp with the S2 Focused Ultrasonicator with Adaptive Focused Acoustics (AFA) technology (Covaris, Woburn, USA). All samples were diluted in 1/5X Tris-EDTA buffer (TE-buffer; stock 1X) to a volume of 130µl in microTUBES (Covaris, Woburn, USA). The programmed guidelines for fragmentation to 200bp were followed (Duty cycle of 10%, Intensity of 5 and 200 cycles/burst), but the fragmentation time was prolonged to 190s based on previous experience.

Subsequently, libraries of the fragmented samples were created using NEBNext Ultra DNA Library Prep (PCR 1.4A, New England Biolabs, Ipswich, USA), following manufacturer's protocol, with the exception of some minor modifications. After incubation with the USER enzyme, a DNA purification step (Zymo Genomic DNA Clean & Concentrator) was included before the size selection step. Size selection was performed with the E-Gel iBase Power system (Invitrogen) using an E-gel EX 2% agarose gel and a 1kb Plus DNA ladder (Thermo Fisher Scientific, Waltham, USA). For all samples, fragments with a size of ±300bp were cut from the gel, and DNA was recovered using the Zymoclean gel DNA recovery kit (Zymo Research). The size selected DNA samples were then subjected to an enrichment PCR using NEBNext Multiplex Oligos for Illumina (Index Primers Set 1 and 2 version 3.0) according to the protocol. tRNA was added to the reaction to minimize the loss of DNA via tube interaction. The quality of the different libraries was assessed with the Agilent High-Sensitivity DNA kit (Bioanalyser, Agilent Technologies, California, USA).

The PCR-free libraries were created entirely according to the TruSeq DNA PCR-free HT sample preparation kit (Illumina), which does not require an enrichment PCR. For each sample, 1µg of WGA product was used as input. From here onwards, these samples will be referred to as 'PCR-free' samples.

Before sequencing the samples, a library quantification was performed using a Sequencing Library qPCR Quantification kit (Illumina, San Diego, USA) to quantify the sequence-able DNA fragments containing the correct adapters. The control template used for the standard curve was a PhiX control library (10nM). The libraries from the different samples were equimolarly pooled, denatured and diluted to a final loading concentration of 2.1pM for sequencing. Finally, single-end index 75bp sequencing was performed on a high-output flowcell on a NextSeq500 (Illumina, California, USA).

3.5. Data analysis

Fastq files of the samples were automatically analyzed using the ViVar software (182). The ViVar software performs CNA detection using the QDNAseq algorithm (160). After removal of poorly mapped reads, this algorithm normalizes the number of reads, mapped in non-overlapping, fixed size windows, for bias in GC-content and mappability simultaneously. In addition, QDNAseq excludes anomalous genetic regions from the analysis making use of a "blacklist" based on information from the ENCODE Project Consortium (185). The blacklist contains chromosomal regions with known repeat elements, such as satellites, centromeres, and telomeres. After GC-content and mappability normalization, read counts were median-normalized by dividing the number of reads in each window by the median number of reads across all windows. As chromosomal aberrations were assumed to be rare, the median number of reads across all windows is a fair estimate of the expected number of reads per window for a perfectly diploid genome. As such, the median-normalized read counts represent a measure for the deviation from diploidy for each window and a copy number (CN) estimate is calculated using following formula: CN= 2(read count/median read count). Then, a circular binary segmentation (CBS) algorithm was applied which detects breakpoints between the windows, and groups them between breakpoints into larger contiguous regions with an equal CN. To this end, the CBS algorithm starts with the whole chromosome and segments it recursively by testing for change-points between such regions. The two-sample t-statistic is then applied to compare the mean of the read counts of the windows contained in one segment to the read counts of the windows in its adjourning segment. The mean of read counts of the windows contained in the segments, are used as an estimator of the CN of the whole segment. After this segmentation, CNAs are called when the segment's $\log_2$(CN/2) surpasses a threshold of +/- 0.35, corresponding to a CN greater than 2.55 or less than 1.57. These thresholds were chosen based on literature review and own experience (161). From previous experience, a window size of 1Mb should be ideal to detect chromosomal aberrations of 3 Mb and bigger (187) (Chapter III). Analyzed data was visualized as line plots, in which windows are ordered along the x-axis by their genomic positions, and the y-axis shows the median normalized $\log_2$

transformed read counts, i.e. the $\log_2$(CN/2). Chromosomes are identified along the x-axis by an alternating white and blue background color. Each dot on the profiles represents a different window and the horizontal lines refer to the segments. Each genomic profile was manually checked for aberrations.

3.6. Read distribution analysis

The read distribution in the samples was further analyzed using Integrative Genomics Viewer (IGV) (193). The BAM file of a sample was uploaded and hg19 was selected as the human reference genome. Next, a region was selected to zoom-in until the individual reads were visible. The selected regions covered a 1Mb window or one dot on a line profile on ViVar. Windows with a very high, low or average CN were investigated.

3.7. Data dereplication

Reads of which the start is mapped to the same genome position were dereplicated from the BAM files (containing the mapped reads) using a Python script. From a group of reads with an identical start position, only one is kept. Reads with an identical sequence are thus also dereplicated.

3.8. Sensitivity and positive predictive value

The sensitivity was defined as the number of true positive calls divided by all CNAs present in the reference (See details in Experimental design section). The positive predictive value (PPV) was defined as the number of true positive calls divided by the total number of calls (true positive + false positive). True positives are CNA calls that refer to a chromosome region that differs at most 10% in size from the corresponding CNA in the reference: When e.g. a complete chromosome is called, and only a part of that chromosome has a CNA in the reference, the call counts as a false positive.

3.9. Statistical analysis of the read count variance

For each sample, the read count variance observed between the windows across the whole genome is calculated using formula (1): $\frac{\sum_i^{N-1}\left(\left(\frac{x_i}{a}\right)-\left(\frac{x_{i+1}}{a}\right)\right)^2}{N}$ where 'N'is the number of windows, 'x_i'the read count in window i, 'x_{i+1}' the read count in the next window $i+1$and 'a'the average of the read counts in all windows (160, 193). In this formula, the read count in each window is scaled by factor 'a', normalizing the result for the total number of reads that was sequenced for the sample. This measure was calculated for each sample. A Welch's t-test for unequal variances was performed to compare all 12 (3 repeats each of 1-, 3- and 5-cell samples + 3 3-cell PCR-free samples) TruePrime amplified samples *versus* all 12 analogous SurePlex amplified samples reported in Chapter III (187). A similar analysis was performed using the dereplicated TruePrime data. P-values smaller than 0.05 were considered statistically significant.

4. Results

4.1. Sample quality and yield after WGA

All samples had a similar electropherogram (EPG) on a 12K chip after WGA (Supplementary File 1). The DNA fragments resulting from amplification had an average length of 5kb. The negative control showed a flat EPG and the positive control an EPG similar to 5 cell samples.

The WGA yield increased with increased amounts of DNA input material. The average output after WGA on 1, 3 and 5 cells was respectively 1684±120.4 ng (mean ± standard deviation), 2470±88.6 ng and 2629±38.7 ng. The positive control yielded an output of 2387 ng, while the negative control had an output of 22 ng. This small amount of WGA product in the negative control is considered normal for negative control WGA products.

4.2. Sequencing run statistics

The quality control parameters of the sequencing libraries were flawless. Supplementary File 2 shows the Agilent Bioanalyser 2100 results of the individual libraries (A), as well as the qPCR library quantification results (B). The Bioanalyser results have a library size distributions within the range of 200-1000 bp, which is suitable for clustering on the Illumina flowcell. The qPCR results show a variable but adequate amount of sequence-able library within the expected yield range for NEBNext Ultra library preparations. Based on these results the libraries were equimolarly pooled. The overall sequencing run quality was good: a Q30 of 90.1±0.5, a density of 269.25±1.3 K/mm^2 and a full width at half maximum (FWHM) of 3. On average 34 million passed filter reads were obtained per sample, corresponding with an average read depth of 0.8 per sample, if all reads could be mapped. This number of reads is a multitude of what is needed to perform CNA detection at a 3 Mb resolution (30) (Chapter IV). Supplementary File 3 shows an elaborate sequencing run-statistics quality control report. On average 96.3% of the reads mapped to the reference human genome, of which 97.8% mapped uniquely to the reference. The actual average read depth and coverage, calculated after mapping, are 0.77 and 0.04 respectively. Raw sequencing data (FASTQ files) has been deposited in the NCBI Sequence Read Archive under project accession number PRJNA318625.

4.3. Visualization of the data on ViVar

The results of the data analysis workflow were plotted on a graphical line profile using the ViVar software. A uniform distribution of the reads over the windows across the genome (except for the parts with a CNA) would be the preferred result. However, the read counts per window from our samples were extremely irregular across the genome (Figure 3a). Although all profiles were similar within and between the 1, 3 and 5-cell samples, the exact regions showing over- or under-representation were different from sample to sample. The line plots of all samples are available in Supplementary File 4. A consequence of the uneven distribution of the reads is that a lot of window segments had a CN greater than 2.55 or less than 1.57, leading to falsely called CNA in regions where the Loucy

genome is known to be diploid. The expected chromosomal abnormalities could also not be deduced from the line profiles. The sensitivity for TruePrime amplified samples was 18.5% ± 5.6% (mean ± standard deviation), whereas for SurePlex amplified samples this was 94.4% ± 11.8%2. Except for the deletion of chromosome X, which was called correctly in all samples, only one other CNA was called correctly in one of the TruePrime samples. Most often, complete chromosome aneuploidies were called instead of only the chromosomal parts that show a CNA in the reference. Both WGA methods, also resulted in a significantly different PPV of 8.43% ± 3.16% and 77.7% ± 11.8% for TruePrime and SurePlex respectively. The distinctive difference between the PPV of TruePrime and SurePlex is due to the presence of a lot more false positives after TruePrime WGA than after SurePlex WGA.

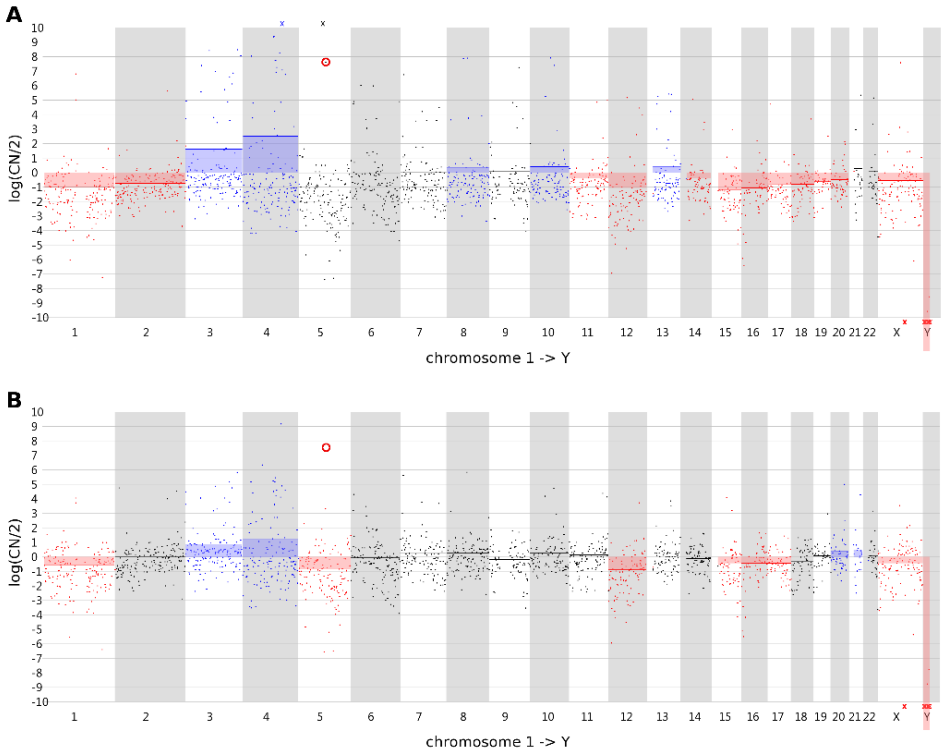

Figure 3: CNA profiles before and after dereplication of the data.

a) A line profile of sample '3 cells, replicate 1', before dereplication, including the 'outlier' windows such as the one in the red circle. b) The same line profile after dereplication shows some improvement. High outliers such as the one in the red circle are no longer present. However, windows with a very low CN were still observed and the CNA profile is still littered with deletions and insertions. The blue color indicates a duplication or trisomy, whereas the red color indicates a deletion or monosomy.

4.4. Statistical analysis of the read count variance

The variance of the read counts per window across the genome for the current TruePrime samples is a lot higher compared to the variance in the SurePlex samples from Chapter III (187) (p= 0.015; Figure 4). A similar observation was made when comparing the dereplicated TruePrime data with the SurePlex data (p= 0.052; Figure 4). A table containing the calculated variances for SurePlex and TruePrime amplified samples can be found in Supplementary File 5.

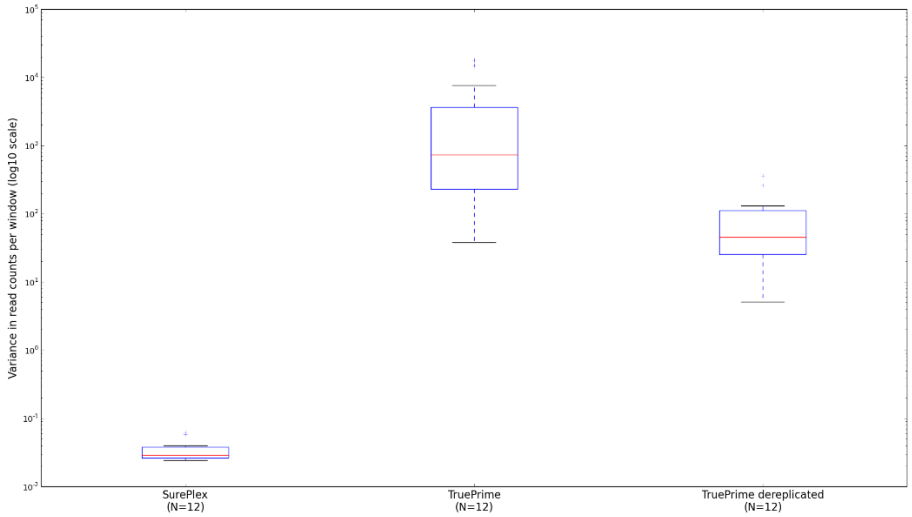

Figure 4: Boxplots of the variances in read counts per window across the genome.

Boxplots are shown for all TruePrime samples, the dereplicated TruePrime samples and SurePlex samples reported in Chapter III (187).

4.5. Visualization of read alignment in IGV

To explain why some windows had extremely high read counts, a better insight into the read distribution within these windows was needed. Two windows were analyzed in detail using IGV, one having a CN close to 2 (CN= 1.9) and one 'outlier' (CN= 89.9) on chromosome 3 of a 5-cell sample amplified with TruePrime. The first window did not show the random equal distribution of reads expected from a low-pass sequencing. A lot of regions, larger than could be expected for a random distribution of reads across the window, showed a complete lack of reads (Figure 5a), whereas other regions showed small clusters of reads (Figure 5b). The 'outlier' window showed a massive buildup of reads over a region of 48 kb, halfway the window (Figure 5c).

Supplementary File 6 shows the read distribution of a few representative regions, comparing the previously studied SurePlex WGA and the currently studied TruePrime WGA. SurePlex WGA shows a much more even distribution of the reads compared to TruePrime WGA.

Figure 5: Read alignment in IGV.

A print-screen is shown for 3 different 14kb regions on chromosome 3 of sample '5 cells replicate 2'. The read alignment to the reference genome hg19 is illustrated for these regions. a) A region in a window close to the baseline (CN= 1.9) with a complete lack of reads. b) A small clustering of reads in another region of this window. c) A massively buildup of reads in a 48kb wide region in an 'outlier' window with a CN of 89.9. Only a part of this buildup is shown here.

4.6. Read distribution across the genome and CNA detection on dereplicated data

When sequencing at an average read depth below 1, only a minor fraction (< 1%) of the reads should have the same starting position when there is no representation bias. When the number of mapped reads obtained for the individual samples (ranging between 2.2E+07 and 5.5E+07) in this study, would be randomly distributed over the genome, approximately 0.4 to 0.9% of the reads would not have a unique starting position. A lot of the representation bias introduced during TruePrime sequencing is caused by regions which are highly covered with duplicate or overlapping reads. We explored if the analysis could benefit from the removal of reads with the same starting position. Only 22% ± 12% of the originally mapped reads were left after dereplication. The dereplicated data resulted in a lower read count variability across the genome and a reduced number of positive outliers (Figure 3b). Still, the variability is higher in the TruePrime results compared to the SurePlex results (Figure 4). As a consequence, the CNAs could still not be correctly deduced from the profile. The sensitivity and PPV did not change substantially.

4.7. Library preparation without enrichment PCR

Omitting the enrichment PCR during library preparation did not influence our results. The results showed very similar profiles to the samples that were amplified, including the large read variability and the inadequacy to detect the CNAs (Supplementary File 4). Also after dereplication, the results were similar to the enriched samples.

5. Discussion

The new TruePrime WGA kit looks very promising from a theoretical point of view and should introduce less representation bias. However, during this study the advantage of this kit over other WGA methods for the detection of CNAs could not be demonstrated. A proper CNA detection using MPS was not possible on samples amplified with this kit. In Chapter III, SurePlex WGA was considered most suitable for this application (187). The results from the current study were compared to these previously generated SurePlex WGA results.

Several factors, other than the TruePrime WGA, that could lead to representation bias were ruled out. The setup of this study was equal to the study in Chapter III (187), except for the WGA method used. The same cell line and cell isolation techniques were used. All EPG profiles of the WGA samples were similar and showed the expected pattern according to the manufacturer. No contamination was introduced during the preparation of the samples, as indicated by the flat EPG of the negative control. The WGA amplification was successful in terms of yield, as all samples and the positive control produced adequate amounts (> 1µg) of WGA product. Library preparation, sequencing and data analysis were performed in parallel with other similar samples (routine samples amplified with SurePlex WGA, not belonging to present study). These samples yielded the expected results with a representation bias as reported in Chapter III (187) (data not shown), ruling out that steps following the WGA are introducing the observed representation bias. The kit was stored at -20°C, as recommended by the manufacturer, and this for two months. The use of a kit derived from an exceptional bad batch was excluded, as a second kit from a different batch led to the same results.

The yield after amplification was quite high: Compared to the SurePlex study, the lowest yield was 1.4 times higher than the lowest yield with SurePlex WGA (1684±120.4 ng vs 1212.1±99.9 ng). The high TruePrime WGA yields would enable the use of this WGA material for multiple simultaneous applications.

The sequencing run from these samples was of high quality and the created reads were almost exclusively composed of human genomic material, as on average 96.3% mapped to the human genome of which 97.8% mapped uniquely. In this respect, the TruePrime amplified samples perform better than samples amplified with SurePlex or MALBAC. However, these mapping results disclose no information regarding the uniformity of read distribution. A high mapping rate does not implicate an equal distribution of these reads across the genome. This was already clear in a previous study, where MALBAC had significantly higher mapping rates compared to SurePlex, but the read

distribution for MALBAC was less uniform compared to SurePlex. Unfortunately, TruePrime WGA causes an even less uniform read distribution compared to this previous study. The per-window read count shows extreme outliers. As a consequence of this non-uniform read distribution, the expected CNA profile of the Loucy cell line could not be detected.

A thorough data review in IGV led to a better understanding of the read distribution within these 'outlier' windows. The reads of these outliers clustered together in some regions within the window. Although windows with 'normal' CN values did not show such clustering, the read distribution was still highly non-uniform within these windows. When low-pass sequencing is performed, reads should be uniformly distributed across the genome, with regular intervals and without clustering. A uniform, unbiased read distribution is necessary for a reliable CNA determination, because over- and underrepresentation due to the WGA will disturb the CNA determination.

In an effort to make the data more suitable for CNA detection, the outliers were filtered from the data by removing reads with the same starting position from the data. Hereby, identical sequences, commonly caused by enrichment PCR, are dereplicated. Reads with the same genomic mapping position, but that do not necessarily have the same length, are also dereplicated. This could have been caused by preferential binding of the TthPrimPol primase to certain regions. After dereplication, only 22% of the reads remained, highlighting the magnitude of the problem of duplicated reads in a situation were almost no reads with the same starting position were expected. Nevertheless, a highly non-uniform read distribution remained after dereplication, albeit with slight improvements. As a consequence of this non-uniform read distribution, the expected CNA profile for the Loucy cell line could still not be detected. It is of concern that true positive duplications could also be removed when reads with the same starting position are removed. This is not be the case in shallow whole genome sequencing with a coverage below 1x. When the reads would be randomly distributed over the genome, less than 1% of the reads would have the same starting position. Even in duplicated regions, very few reads with the same starting position are to be expected.

Enrichment PCR and PCR-free libraries yielded the same results, showing that the enrichment PCR during library prep was not causing the representation bias. The amount of input DNA for the WGA was also not influencing the results, as the results for 1-, 3- and 5-cell were similar.

It is not clear what is causing the representation bias. The main difference between the TruePrime WGA and other WGA methods is the use of TthPrimPol primase instead of primers. A primase should randomly bind to the DNA, because no complementarity is required. If this primase favors some regions over others, this could lead to over- and under amplification of these regions, exactly as in our results. We, however, see that the overrepresented regions are different from sample to sample, suggesting that the primase is not systematically favoring the same DNA regions. Possibly, too few (random) primers are formed, leading to underrepresented regions. The ones that

are formed, are heavily amplified and lead to extremely overrepresented regions. We hope that our study can provide insights that can help to improve this technology, leading to WGA with less representation bias.

6. Conclusion

The single cell TruePrime WGA kit version 1 is not suited for CNA detection after MPS. Representation bias seemed to be introduced during amplification, resulting in over-and underrepresentation of genomic regions.

7. Supplementary information

Supplementary file 1: Agilent Bioanalyser 2100 12K electropherograms of TruePrime WGA products from all samples.

All samples have a similar profile, with an average fragment length of ± 5kb. The negative control, in which the template was substituted with PBS, the electropherogram signal is a flat line, indicating the absence of DNA amplification. The positive control showed a similar profile to the other samples. In this positive control, the template was 26pg of DNA from the 2391C Component C. The Y-as shows the fluorescence intensity, which is an indicator for the amount of DNA present. The X-as shows the fragment length in base pairs.

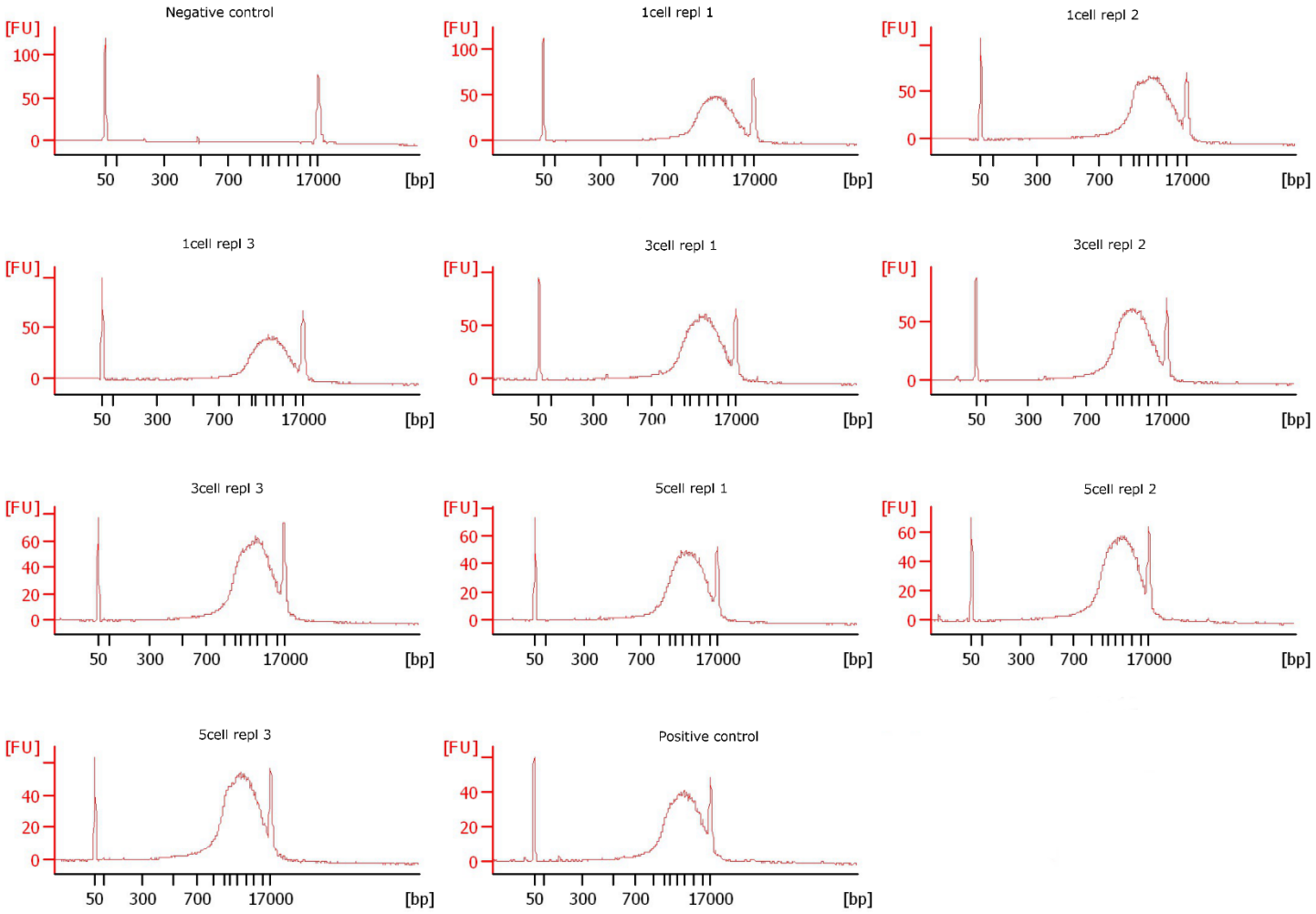

Supplementary file 2: Agilent Bioanalyser 2100 electropherograms (A) and qPCR library quantification results (B) of the sequencing libraries.

Samples 1 to 9 were prepped using the NEBNext ultra library preparation kit. The last 3 samples were prepped using the TruSeq DNA PCR-free HT library preparation kit. Sample 5cell repl 2 shows a high primer-dimer peak, which has subsequently been removed using a 2% EX E-gel size selection.

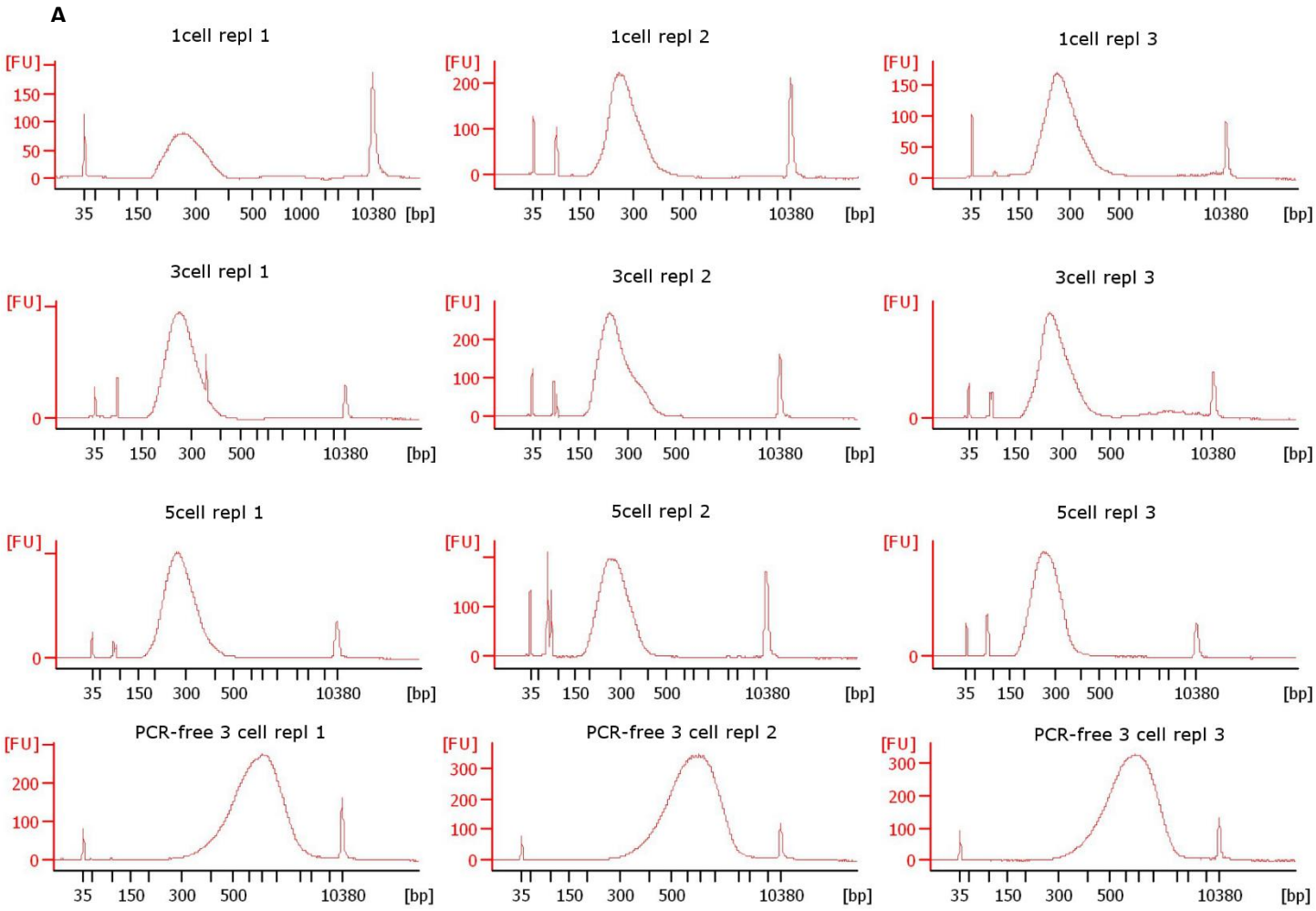

B

Samples	Concentration diluted library (nM)
1cell repl 1	3.7
1cell repl 2	9.4
1cell repl 3	7.9
3cell repl 1	5.7
3cell repl 2	6.3
3cell repl 3	8.9
5cell repl 1	9.6
5cell repl 2	4.7
5cell repl 3	15.7
PCR-free3cell repl 1	5.8
PCR-free3cell repl 2	5.4
PCR-free3cell repl 3	6.1

Supplementary file 3:

Sequencing quality control report and read mapping statistics. The information in the table displays the average over the 4 lanes. The run was performed on a total of 20 samples.

Density (K/mm^2)	269.25±1.3
Clusters past filter (%)	83.2±0.7
Reads past filter/lane (x10^6)	145±1.8
Total read count past filter(x10^6)	581.63
Reads/sample (x10^6)	29.1
Q30 (%)	90.1±0.5

Mapping statistics	number of past filter reads	number of mapped reads	average depth	standard deviation depth	coverage
1 cell replicate 1	26,876,572	26,485,659	0.62	181.35	0.017038
1 cells replicate 2	21,931,292	21,690,048	0.51	38.87	0.021864
1 cells replicate 3	28,375,813	26,675,758	0.61	227.65	0.029697
3 cells replicate 1	36,862,692	36,145,552	0.84	228.08	0.034895
3 cells replicate 2	42,893,602	41,766,495	0.97	187.97	0.0236
3 cells replicate 3	30,007,070	29,259,675	0.68	134.71	0.042562
5 cells replicate 1	58,193,351	54,676,410	1.25	661.60	0.058997
5 cells replicate 2	34,894,399	33,703,063	0.79	233.71	0.071542
5 cells replicate 3	29,382,392	28,768,667	0.68	91.36	0.060076
PCR-free 3 cells replicate 1	39,486,483	37,063,877	0.85	475.55	0.042761
PCR-free 3 cells replicate 2	33,362,926	32,478,336	0.76	146.33	0.021173
PCR-free 3 cells replicate 3	29,333,156	27,753,005	0.64	257.43	0.03613

Supplementary file 4: ViVar line plots of all samples

TruePrime 1cell repl 1

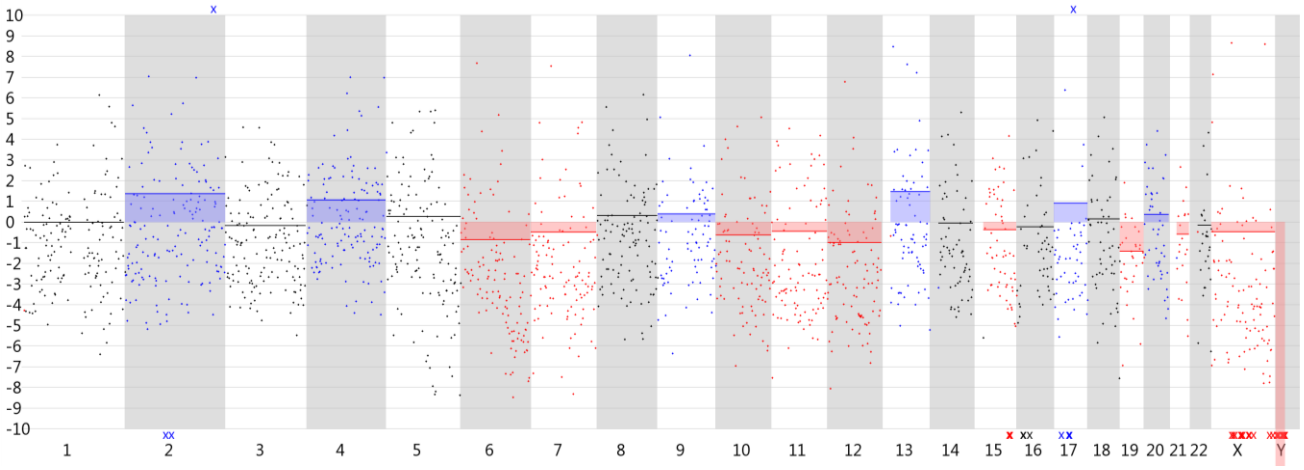

TruePrime 1cell repl 2

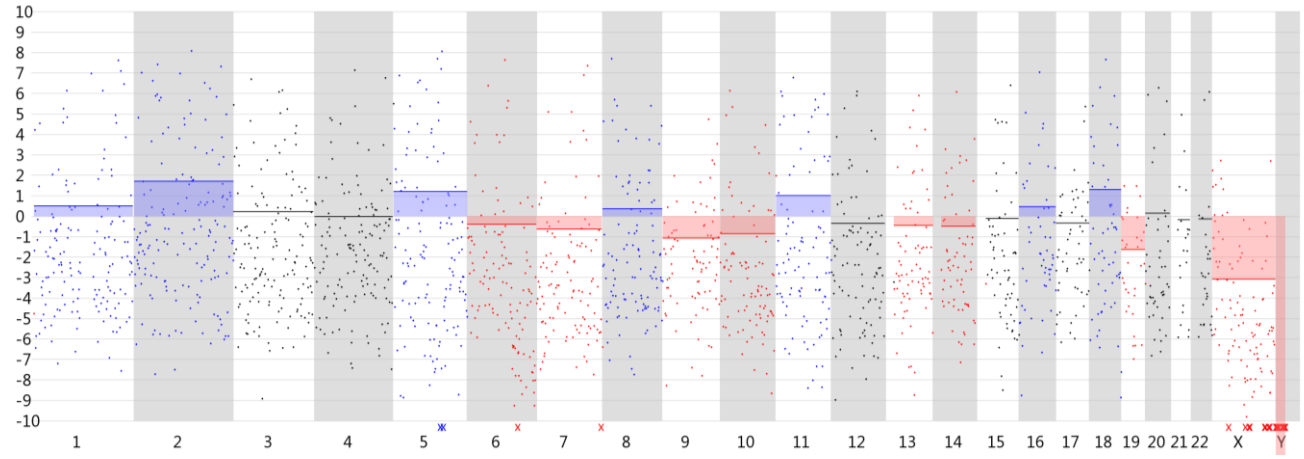

TruePrime 1cell repl 3

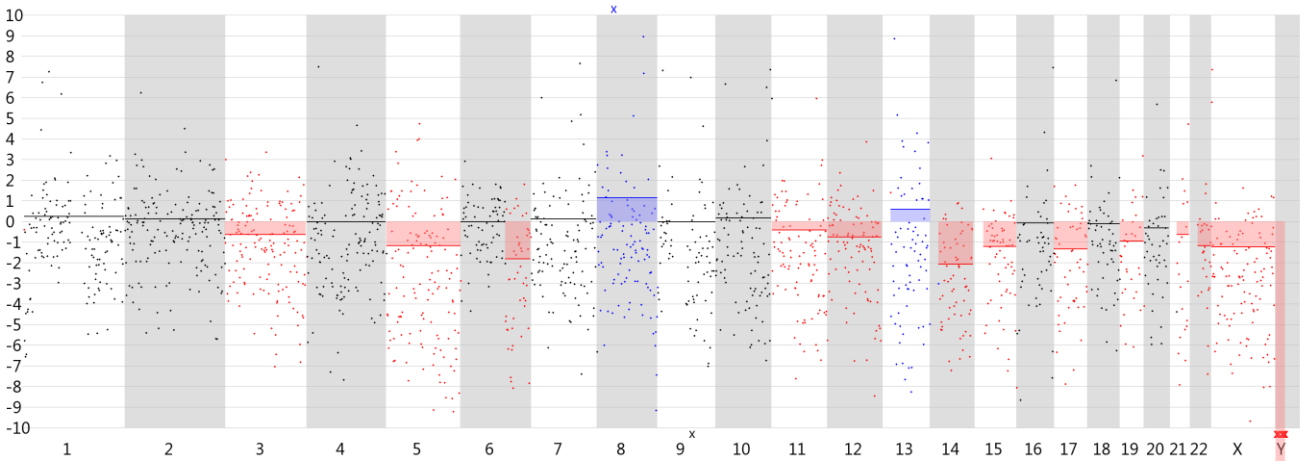

TruePrime 3cell repl 1

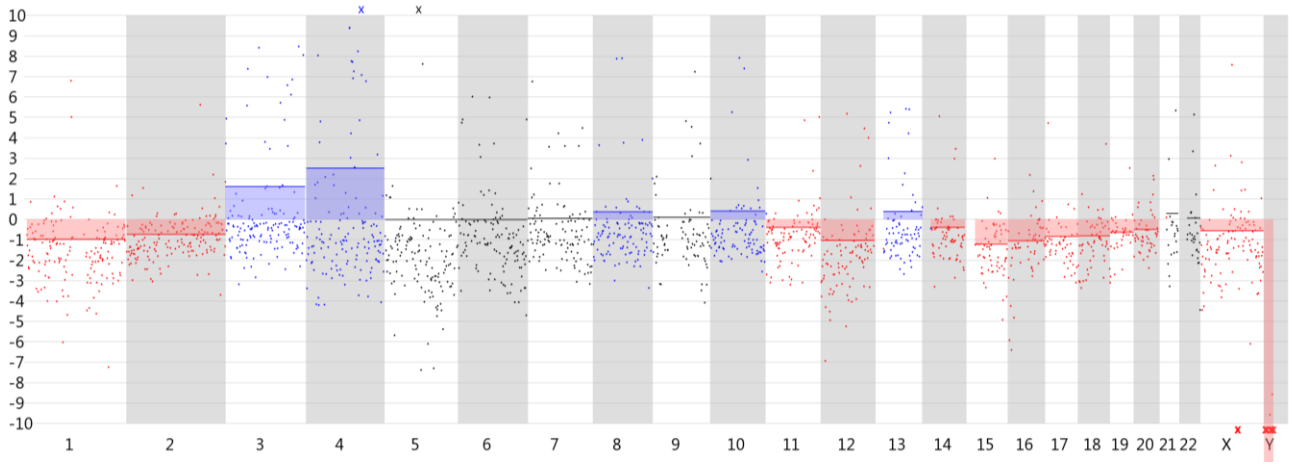

TruePrime 3cell repl 2

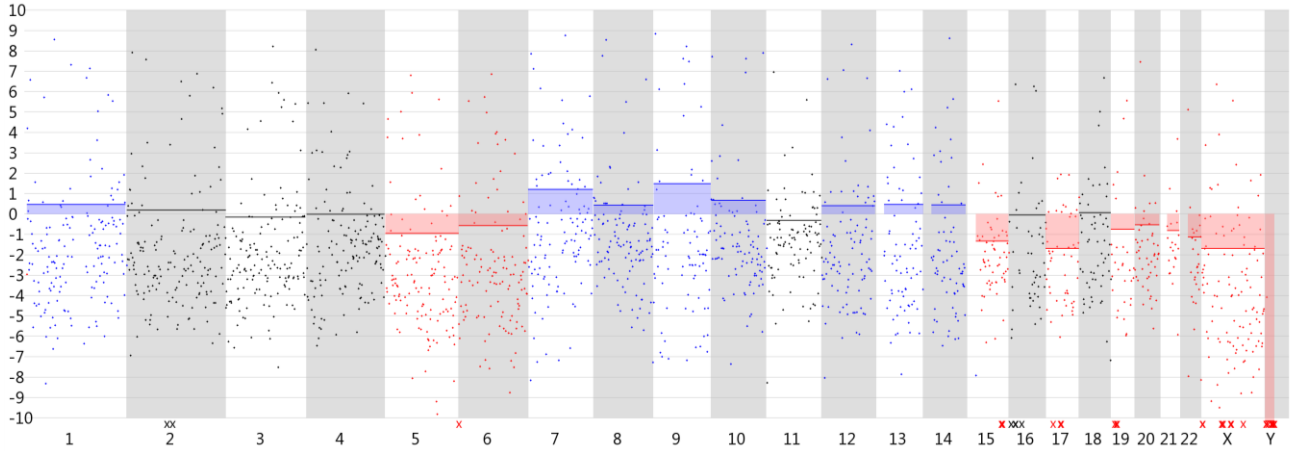

TruePrime 3cell repl 3

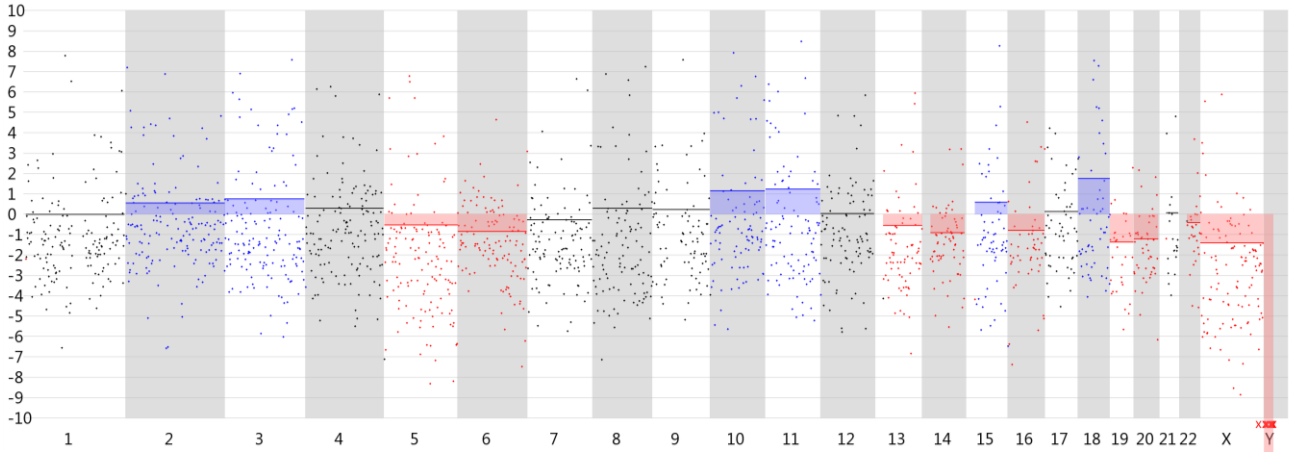

TruePrime 5cell repl 1

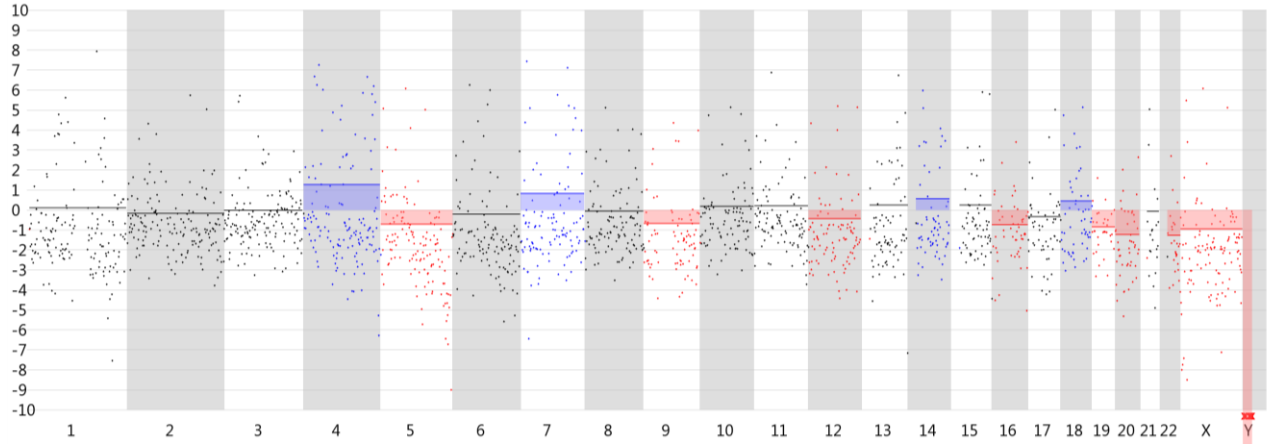

TruePrime 5cell repl 2

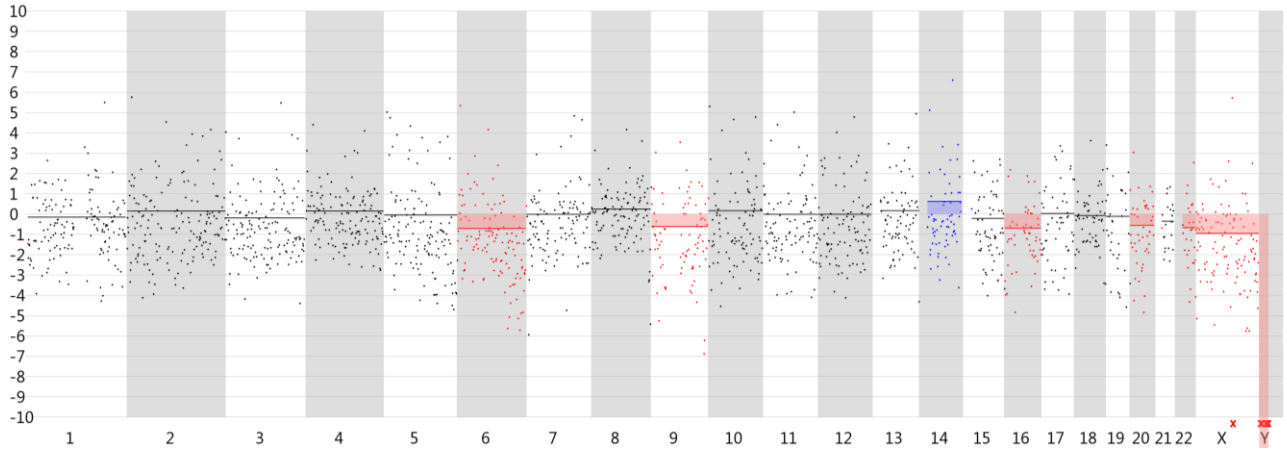

TruePrime 5cell repl 3

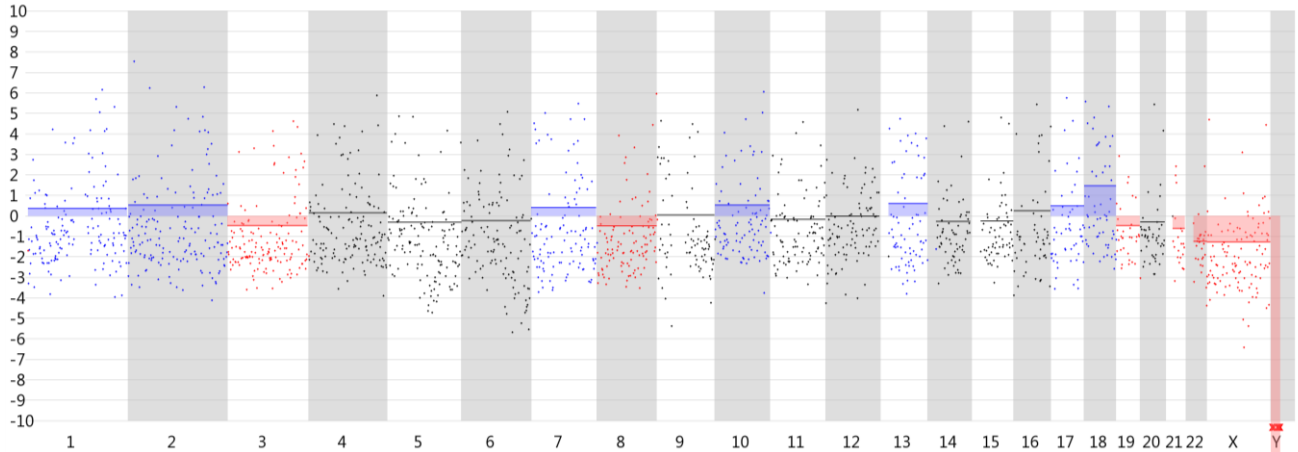

PCR-free 3cell repl 1

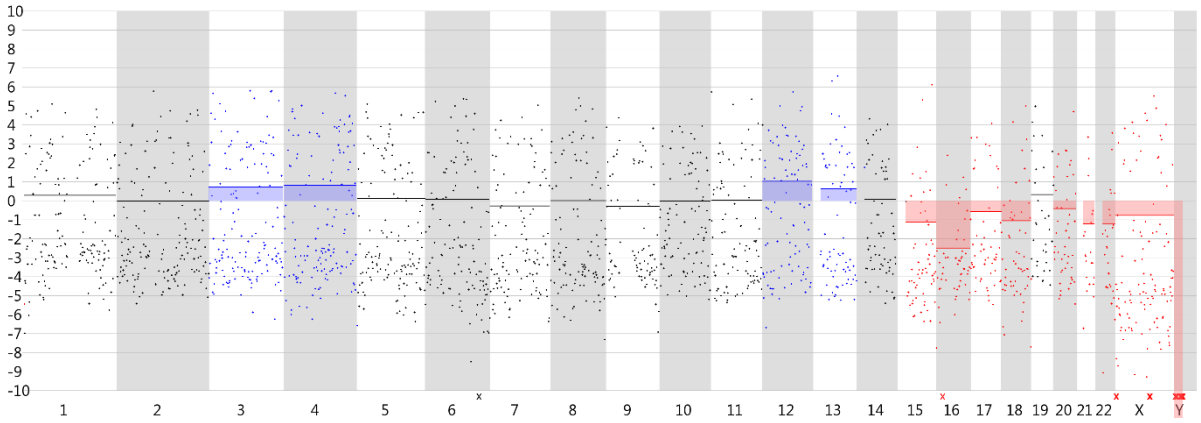

PCR-free 3cell repl 2

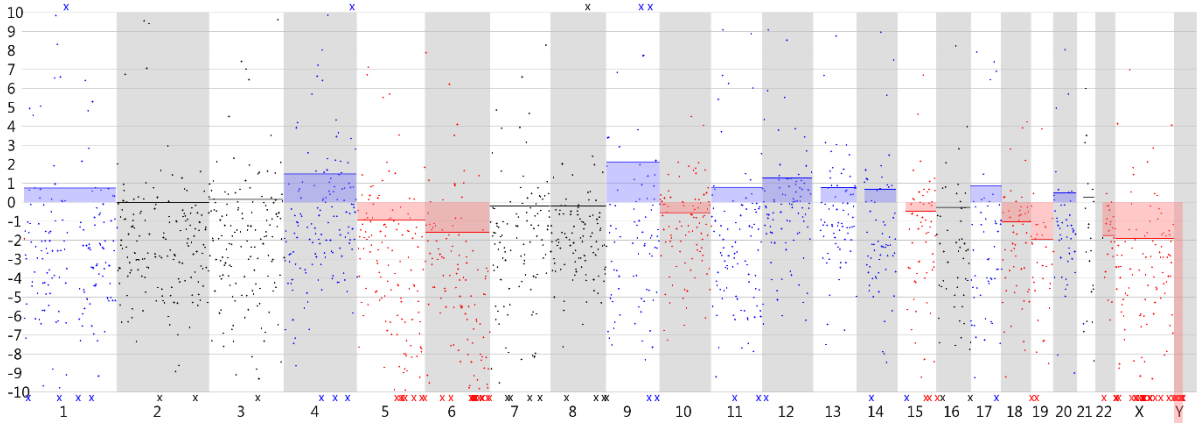

PCR-free 3cell repl 3

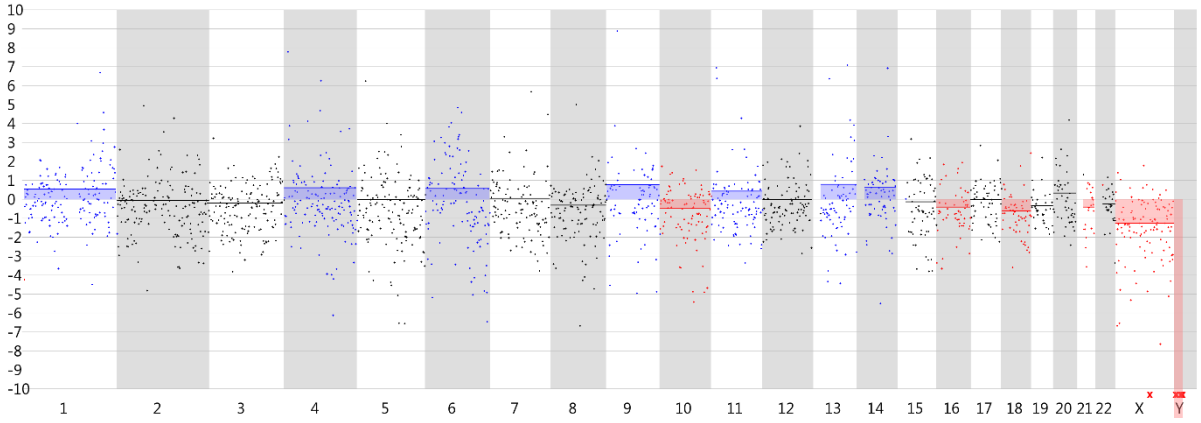

Supplementary file 5: Read count variance between the windows across the whole genome for TruePrime and SurePlex amplified samples.

	SurePlex	TruePrime	TruePrime dereplicated
1cell repl 1	4.84	1.24E+20	7.96E+09
1cell repl 2	1.48	1.58E+14	5.43E+10
1cell repl 3	7.79	1.91E+18	5.94E+11
3cell repl 1	2.16	1.78E+21	9.14E+15
3cell repl 2	3.00	5.29E+15	7.36E+12
3cell repl 3	1.43	5.59E+14	2.41E+10
5cell repl 1	3.39	3.64E+13	1.67E+06
5cell repl 2	3.97	6.41E+10	6.69E+07
5cell repl 3	1.52	4.78E+12	1.05E+09
PCR-free 3cell repl 1	2.02	9.39E+10	7.35E+08
PCR-free 3cell repl 2	1.36	2.87E+19	8.14E+12
PCR-free 3cell repl 3	1.51	2.22E+15	2.26E+10

Supplementary file 6 Read distribution of a few representative regions, comparing the previously studied SurePlex WGA and the currently studied TruePrime WGA.

a) In the SurePlex amplified sample were the reads uniformly distributed across the different windows. The TruePrime samples showed large empty regions alternated with regions of clustered reads. b) Some regions show massive clustering after TruePrime amplification.

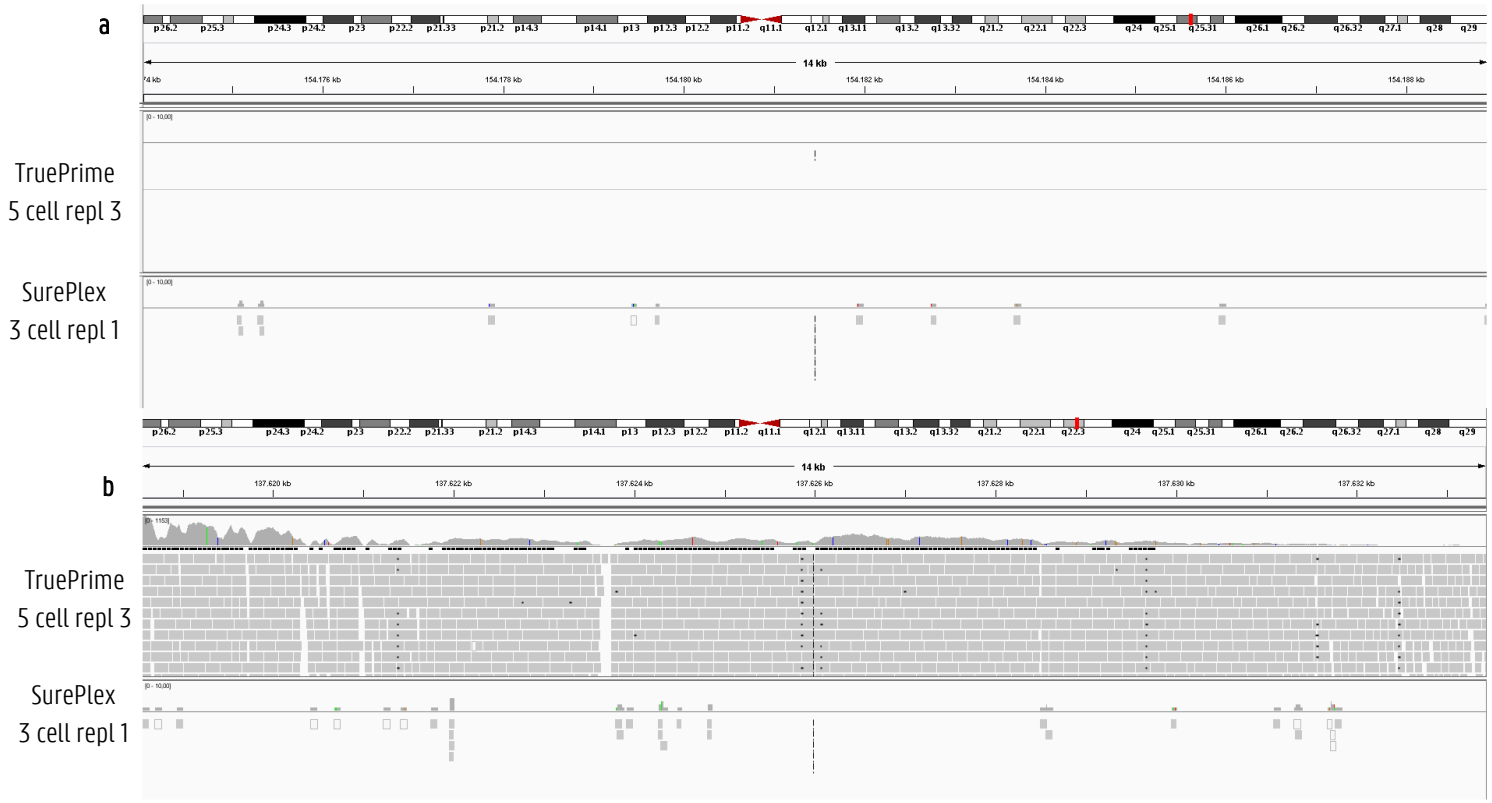

Chapter VII: Performance of four modern whole genome amplification methods for copy number variant detection in single cells

Lieselot Deleye[1], Laurentijn Tilleman[1], Ann-Sophie Vander Plaetsen[1], Senne Cornelis[1], Dieter Deforce[1,#], Filip Van Nieuwerburgh[1,#]

[1]Laboratory of Pharmaceutical Biotechnology, Ghent University, Ottergemsesteenweg 460, 9000 Ghent, Belgium.
[#]These authors contributed equally.

Scientific Reports | 7: 3422 | DOI:10.1038/s41598-017-03711-y; Published 13 June 2017.

1. Abstract

Whole genome amplification (WGA) has become an invaluable tool to perform copy number variant (CNV) detection in single, or a limited number of cells. Unfortunately, current WGA methods introduce representation bias that limits the detection of small CNVs. New WGA methods have been introduced that might have the potential to reduce this bias. We compared the performance of PicoPLEX DNA-Seq (Picoseq), DOPlify, REPLI-g and Ampli1 WGA for aneuploidy screening and copy number analysis using shallow whole genome massively parallel sequencing (MPS), starting from a single or a limited number of cells. Although the four WGA methods perform differently, they are all suited for this application.

2. Introduction

Whole genome amplification (WGA) has become an invaluable tool to perform massively parallel sequencing (MPS) in applications where only a limited number of cells is available. Well-known examples of such applications are: preimplantation genetic diagnosis (PGD), cell-based non-invasive prenatal testing (NIPT) (110) and liquid biopsy of circulating tumor cells (CTCs) (194-196) Several WGA methods exist to amplify DNA extracted from a limited number of cells, yielding the necessary amount of DNA required to perform MPS (130, 191). The different WGA methods each have their advantages and disadvantages in terms of genome coverage, representation bias, error rates, yield and robustness.

The best WGA method per se does not exist, because the downstream application is also important to determine the ideal method (130). Some WGA methods have already been compared for specific applications (30, 130, 187, 197-199). Multiple displacement amplification (MDA) methods are better suited for single nucleotide polymorphism (SNP) detection while PCR-based methods are the better option for copy number variant (CNV) detection (130). MDA methods use the high-fidelity phi29 polymerase, reducing nucleotide errors in the amplified sequences, while PCR-based methods tend to give a more uniform amplification across the genome. For the detection of CNVs, SurePlex WGA has proven its efficiency in clinical settings such as PGD (30, 32, 163). However, results show that the WGA representation bias is still a limiting factor, hampering higher resolution copy number profiles when starting from a single or a limited number of cells (30) (Chapter IV). Fortunately, new WGA methods are being introduced that might have the potential to reduce this bias. In this study, we compared four different commercially available WGA methods for their suitability to detect CNVs after MPS.

A first method, REPLI-g single cell WGA, is a well-established MDA method (130, 200). In a study comparing 5 different WGA methods, REPLI-g had the lowest false positive rate and was well-suited for detection of CNVs and

single nucleotide variations (SNVs) (200). This two-step protocol includes an amplification step of 8h, but the hands-on time is short.

A second method, Ampli1 WGA (Silicon Biosystems, Castel Maggiore, Italy), has already proven its efficiency for CNV and STR analysis in prenatal diagnosis (110). Ampli1 is based on a ligation-mediated PCR following a site-specific DNA digestion. Usage of non-random primers is one of the factors leading to a more homologous coverage. Unfortunately, the protocol consists of many different steps and is time consuming.

PicoPLEX DNA-Seq (Picoseq) (Rubicon Genomics Inc., MI 48108, USA) and DOPlify WGA (Reproductive Health Science, Thebarton, Australia) are the two most recently developed methods. Picoseq is a method based on the PicoPLEX/SurePlex WGA technology (Rubicon Genomics Inc., MI 48108, USA/ BlueGnome Ltd., Mill Court, Great Shelford, Cambridge, UK) and does not only amplify the DNA of a sample but also results in an Illumina sequencing library for that sample. The amplification part is similar to PicoPLEX WGA, but during the second amplification step, Illumina adapters and barcodes are introduced. WGA and library preparation are performed in a single tube, decreasing possible handling errors, contamination, turnaround time and costs. The second new method, DOPlify WGA, uses an advanced Degenerate Oligonucleotide Primed PCR (DOP-PCR). The classical DOP-PCR does already exist for many years and was one of the first existing WGA technologies (201). It has two basic principles: degenerate base-pairing primers and a slowly increasing annealing temperature during PCR. The classical DOP-PCR uses Taq polymerase with a high error rate, and uses primers that lead to an incomplete coverage (126). An advanced DOP-PCR, such as DOPlify might circumvent the disadvantages of previous DOP-PCR by using new polymerases or primers and might thereby out-perform other recent WGA technologies. DOPlify is a short and easy two-step protocol of only 3 hours.

The objective of this study was to compare the performance of Ampli1, REPLI-g, Picoseq and DOPlify WGA in a shallow whole genome MPS workflow for CNV detection, starting from a limited number of cells. Samples of 1, 3 or 5 cells were collected from the Loucy cell line in triplicate using micromanipulation. The samples were prepared using 4 different WGA methods followed by Illumina PCR-free MPS library preparation. The variability of the read distribution across the genome and the CNV detection performance were compared.

3. Material & Methods

3.1. Experimental design

Figure 1 illustrates the experimental design of this study. Experiments were performed on cells from the lymphoblastoid Loucy cell line (DSMZ, ACC394) (169) . A CNV analysis has been performed on this cell line as part of the COSMIC project (202, 203). A reference 180K aCGH profile (Agilent Technologies) from unamplified DNA of a bulk sample of the cell line was available from a previous study (187) (Chapter III) (Supplementary Figure 1). The

following reference aneuploidies and CNVs (≥3Mb) were present: a deletion of an entire X-chromosome, two deletions of ±45Mb (consists of 6Mb and a 36.5Mb deletion interspersed by a 2.5Mb normal ploidy region) and 30Mb on respectively 5q14.3-q31.1 and 5q33.1-q35.3, a deletion of ±60Mb on 6q21-q27, a deletion of 3Mb on 12p13.31-p13.2, a ±26Mb duplication of 13q31.3-q34, and two deletions of 16Mb and 3Mb on respectively 16p13.3-p13.11 and 16q24.2q24.3. The COSMIC and 180K aCGH CNV analyses are completely concordant regarding these >3Mb insertions and deletions.

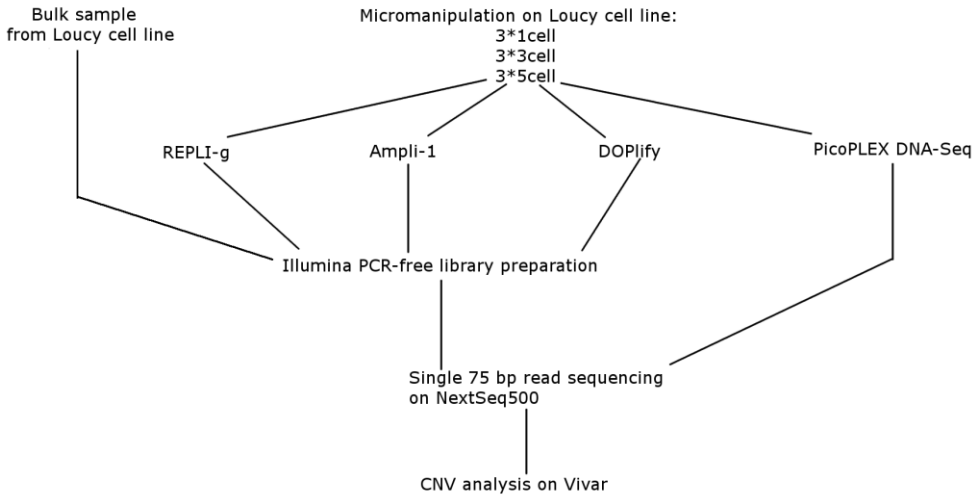

Figure 1: Experimental design.

Samples consisting of 1, 3 or 5 cells were collected from the Loucy cell line using micromanipulation for each WGA method in triplicate. Cells were amplified with either Ampli1, REPLI-g or DOPlify, followed by PCR-free Illumina library preparation and sequencing. A fourth method, Picoseq, performs WGA and library preparation simultaneously, without the need for a separate library preparation. A bulk DNA sample was extracted from $5*10^6$ Loucy cells using a column-based extraction method from Qiagen, also followed by PCR-free Illumina library preparation and sequencing.

The cell line was grown in suspension, which allows collection of individual cells. Samples containing 1, 3 or 5 cells were collected in triplicate using micromanipulation. These samples were used to perform WGA, PCR-free Illumina library preparation and sequencing. This was performed in parallel for three types of WGA methods. A fourth method, Picoseq, performs WGA and library preparation simultaneously, without the need for the PCR-free Illumina library prep. A bulk DNA sample of the Loucy cell line was also included in the study. The bulk DNA was treated in same way as the other samples, except for the amplification step.

A negative control, processed alongside the cell-containing samples, was used during all WGA methods to control for contamination. These negative controls contained the exact same reagents as the cell-containing samples, except that 1µl PBS instead of cells was added. A sample containing 1µl of male control DNA (Human Genomic DNA, Roche, stock solution of 0.2 mg/ml) with a concentration of 30pg/µl, was used as a positive control during each WGA method. This positive control was performed to check the yield of the WGA procedure on a sample with high quality input DNA, excluding possible suboptimal conditions due to the cell manipulation and extraction steps. This

sample could be used as a troubleshooting tool in case the cell samples would yield no (or low) amounts of WGA product.

The different WGA methods were compared to assess their suitability for downstream CNV analysis using shallow whole genome MPS (see other Material & Methods sections for details): A comparison of the DNA yield after WGA, the mappability of the reads and the variance in read counts per window across the genome was performed within and between the WGA samples. The CNV calling accuracy after WGA was evaluated by comparing the CNV calls in WGA samples with those called in the bulk DNA sample. As the WGA samples and the bulk sample are processed and analyzed entirely in the same way, except for the WGA step, this allows a comparison in which the effect of the WGA on CNV calling accuracy/resolution can be studied. The resolution is configurable and should be set considering the extent of representation bias and considering the average sequencing depth. A lower resolution, meaning that smaller CNVs will not be detected, allows for a better averaging/smoothing of representation bias introduced by the WGA and sequencing, avoiding incorrect CNV calls. We have shown before that the representation bias introduced by current WGA and sequencing methods is the limiting factor that is necessitating a resolution of 3Mb (30, 187) (Chapters III & IV). For this reason, we compare the CNV calls in WGA samples with those called in the bulk DNA sample at a resolution of 3Mb.

3.2. Growth and isolation of cells

The cells were grown in Roswell Park Memorial Institute (RPMI-1640) medium (Life Technologies, Carlsbad, USA), supplemented with 10% fetal bovine serum (Life Technologies, Carlsbad, USA) at a temperature of 37°C and a 5% CO_2 level. A known number of cells was collected with a denuding handle from STRIPPER (Origio, Måløv, Denmark) and MXL3-100 needles with a diameter of 100µm (Origio, Måløv, Denmark) from a serial dilution of medium with phosphate buffered saline (PBS). All cells were collected in a maximum total volume of 2.5µl and snap frozen in liquid N_2 immediately after collection. For the bulk DNA sample, DNA was extracted from $5*10^6$ cells using the DNeasy Blood & Tissue kit (Qiagen Hilden, Germany).

3.3. Ampli1 WGA, REPLI-g WGA, DOPlify WGA

Cell lysis and amplification was performed, using the Ampli1 WGA kit (Silicon Biosystems, Castel Maggiore, Italy), the REPLI-g single cell kit (Qiagen Hilden, Germany) or the DOPlify WGA kit (Reproductive Health Science, Thebarton, Australia) as described in the respective manufacturer's instructions. All samples were purified following the manufacturer's protocol of the Genomic DNA Clean & Concentrator kit (version 1.0.0, Zymo Research, Irvine, USA) with 5X binding buffer. Concentration was measured using the Qubit dsDNA High Sensitivity Assay kit (Life technologies, Carlsbad, USA).

3.4. PicoPLEX DNA-Seq

Cell lysis, amplification and library preparation was performed, using the PicoPLEX DNA-Seq kit (Rubicon Genomics Inc., MI 48108, USA) as stated in the manufacturer's instructions. All samples were purified with 50µl of Agencourt AMPure XP beads. The quality of the libraries was assessed with the Agilent High-Sensitivity DNA kit (Bioanalyser, Agilent Technologies, California, USA). This method will further be referred to as Picoseq.

3.5. TruSeq DNA PCR-free HT library preparation

The WGA products from Ampli1, REPLI-g, DOPlify and the bulk sample were fragmented to an average size of 350bp using the S2 Focused Ultrasonicator (Covaris, Woburn, USA) following the manufacturer's instructions (Duty cycle of 10%, Intensity of 5 and 200 cycles/burst, Duration 45 sec). Between 350ng and 1µg of WGA product was used as input for fragmentation. Sequencing libraries of the fragmented samples were prepared with the TruSeq DNA PCR-free HT library preparation kit (Illumina) on the IP-Star Compact (Diagenode, Seraing, Belgium). Library quantification was performed using a Sequencing Library qPCR Quantification kit (Illumina, San Diego, USA) to quantify the sequence-able DNA fragments containing the correct adapters (this was performed on the samples of all four methods). The libraries from the different samples were pooled equimolarly, denatured and diluted to a final loading concentration of 2.5pM for sequencing. Finally, single-end indexed 75bp sequencing was performed on a high-output NextSeq500 flow-cell (Illumina, California, USA).

3.6. Data analysis

Fastq files of the samples were automatically analyzed using the ViVar software (182). The ViVar software maps the reads using bowtie2 (190) with very sensitive-local setting and performs CNV detection using the QDNAseq algorithm (160). This algorithm divides the genome in equally sized windows (configurable; see below). The reads that map in these windows are counted and normalized for bias in GC-content and mappability. In addition, QDNAseq excludes anomalous genetic regions from the analysis making use of a "blacklist" based on information from the ENCODE Project Consortium (185). The blacklist contains chromosomal regions with known repeat elements, such as satellites, centromeres, and telomeres. After GC-content and mappability normalization, read counts were median-normalized by dividing the number of reads in each window by the median number of reads across all windows. As chromosomal aberrations were assumed rare, the median number of reads across all windows is a fair estimate of the expected number of reads per window for a perfectly diploid genome. As such, the median-normalized read counts represent a measure for the deviation from diploidy for each window and a copy number (CN) estimate was calculated using following formula: CN= 2(read count per window/median read count per window). Then, a circular binary segmentation (CBS) algorithm was applied which detects breakpoints between the windows, and groups them between breakpoints into larger contiguous regions with an equal CN. To this end, the CBS algorithm started with the whole chromosome and segments it recursively by testing for change-

points between such regions. The two-sample t-statistic was then applied to compare the mean of the read counts of the windows contained in one segment to the read counts of the windows in its adjourning segment. The mean read counts of the windows contained in the segments were used as an estimator for the CN of the whole segment. After this segmentation, CNVs were called when the segment's $\log_2$(CN/2) surpasses a threshold of +/- 0.35, corresponding to a CN greater than 2.55 or less than 1.57. These thresholds were chosen based on literature review and own experience (161). From previous experience (Chapter IV), a window size of 1Mb should be ideal to detect chromosomal variants of 3Mb and bigger (30). Typically, 3 neighboring windows with a significantly higher or lower read count are required to call a CNV. When 3 consecutive windows of 1Mb are needed to call a CNV, the detection limit is thus 3Mb. As the WGA methods in the current study might perform better than previously tested methods, results were also generated using 500kb windows, possibly lowering the detection limit. Analyzed data were visualized as line plots, in which windows are ordered along the x-axis by their genomic positions, and the y-axis shows the median normalized $\log_2$ transformed read counts, i.e. the $\log_2$(CN/2). Chromosomes are identified along the x-axis by an alternating white and grey background color. Each dot on the profiles represents a different window and the horizontal lines refer to the segments. Each genomic profile was checked manually for variants. Raw sequencing data are deposited in the NCBI Sequence Read Archive under project accession number PRJNA362886. On ViVar they are available under the project: Comparing four WGAs (https://holmes.ugent.be:9090/ViVar/)

3.7. Statistical analysis of the read count variance

For each sample, the average read count variance observed between the windows across the whole genome was calculated using following formula: $\frac{\sum_i^{N-1}\left(\left(\frac{x_i}{a}\right)-\left(\frac{x_{i+1}}{a}\right)\right)^2}{N}$ where '*N*'is the number of windows, 'x_i' the read count in window *i,* 'x_{i+1}' the read count in the next window *i+1* and *'a'* the median number of reads across all windows (160, 193). In this formula, the read count in each window was scaled by factor 'a', normalizing the result for the total number of reads that was sequenced for the sample. This measure was calculated for each sample. A one-way ANOVA was performed between the average read count variances of the four WGA methods. P-values smaller than 0.05 were considered statistically significant.

3.8. True and false positives

True positives are defined as the CNVs that are called in the bulk DNA aCGH & bulk DNA sequencing. Calls that are not present in these reference samples are considered false positives. Results of the WGA and the bulk DNA sequencing sample were compared using 1Mb windows and using 500Kb windows in the QDNAseq analysis. Within each comparison, the same window size is used for all samples. Individual cells from the same tissue or from the same cell line can show different CNVs (204, 205). Thus, some of the false positives and false negatives in the

individual cells (or in the limited number of cells samples) could have been caused by mosaicism in the Loucy cell line.

4. Results

4.1. DNA yield after WGA and DNA fragment-size

DNA yield after WGA was compared between Ampli1, REPLI-g and DOPlify. Yields of the 1-, 3-, and 5-cell samples do not differ significantly per method and are reported here as an average ± standard deviation. Picoseq does not yield amplified fragments, but results in sequence-ready libraries. Therefore, only the yield of adaptor-ligated fragments and not the entire DNA yield is important for this method. Ampli1 and DOPlify WGA resulted in a comparable yield of 19.2±6.9 ng/µl and 21.1±2.6 ng/µl (in 30µl), respectively. REPLI-g WGA has a significantly higher yield of 900.7±255 ng/µl (in 30µl). All negative controls contained a negligible amount of DNA after WGA, except the one amplified with REPLI-g. The concentration of 1000ng/µl in the latter was expected: Phi29 DNA Polymerase has an extremely high processivity and will extend primer-dimers that may be present in the reaction in the absence of specific template in the reaction, leading to unspecific high molecular weight amplification products. Samples with template, yield approximately the same amount of DNA as non-template controls. For all WGA methods, the yield of the positive control sample was similar to the 5-cell samples.

The average size of the DNA fragments after amplification varies between methods. REPLI-g has the longest fragments (> 10Kb), Picoseq the shortest (654±31.1 bp). Ampli1 and DOPlify result in fragments of respectively 740.1±27.6 bp and 957.3±87.2 bp. The WGA product is fragmented to ±350bp by sonication prior to sequencing.

4.2. Mapping statistics

The average sequencing depth was similar for all samples and was around 0.3X. An average depth of 0.3X exceeds the required average depth to call CNVs with a resolution of 3Mb. It has been shown before that the average depth can be reduced to 0.03X without becoming the limiting factor for the resolution: The representation bias introduced by the WGA and sequencing is the limiting factor that is necessitating larger window sizes (and thus a lower resolution) (30, 187) (Chapter III & VI). For the REPLI-g, Ampli1, DOPlify and Picoseq amplified samples, respectively 99.7±0.01%, 98.8±0.2%, 98.3±0.7% and 97±3.1% of the reads mapped to the human reference genome.

4.3. Variance in read counts per window across the genome

A uniform distribution of the reads over the windows across the genome (except for the parts with a CNV) is needed to be able to accurately call CNVs. Almost all the samples in this study had such uniform distribution. One 5-cell sample from Ampli1, as well as a 1-cell and 5-cell sample from DOPlify showed a distribution that cannot be used to call CNVs. The per-window read counts across the genome are so irregular that incorrect CNVs would be called across the entire genome (Supplementary Figure S2). Those three failures, as they are further referred to, were

excluded from any further analyses and are not included in the statistical analyses. Overall, the average variance in read counts per window across the genome was similar for all samples amplified with the same WGA method (Figure 2). Furthermore, this average variance was not significantly different between the four WGA methods (Figure 2). When the 1-cell, 3-cell and 5-cell samples were compared separately between all methods, they also showed no significantly different average variance (Supplementary Table S1; Figure 3). Although, statistically there was no difference, some observations were made. Picoseq seems to have a higher average read count variance for single cell amplification, with the highest difference in average variance between the three single cell samples amplified with this WGA (Supplementary Table 1; Figure 3A). For all WGA methods, the 3- and 5-cell samples tend to have a slightly lower average variance compared to single cell samples (Supplementary Table S1; Figure 3).

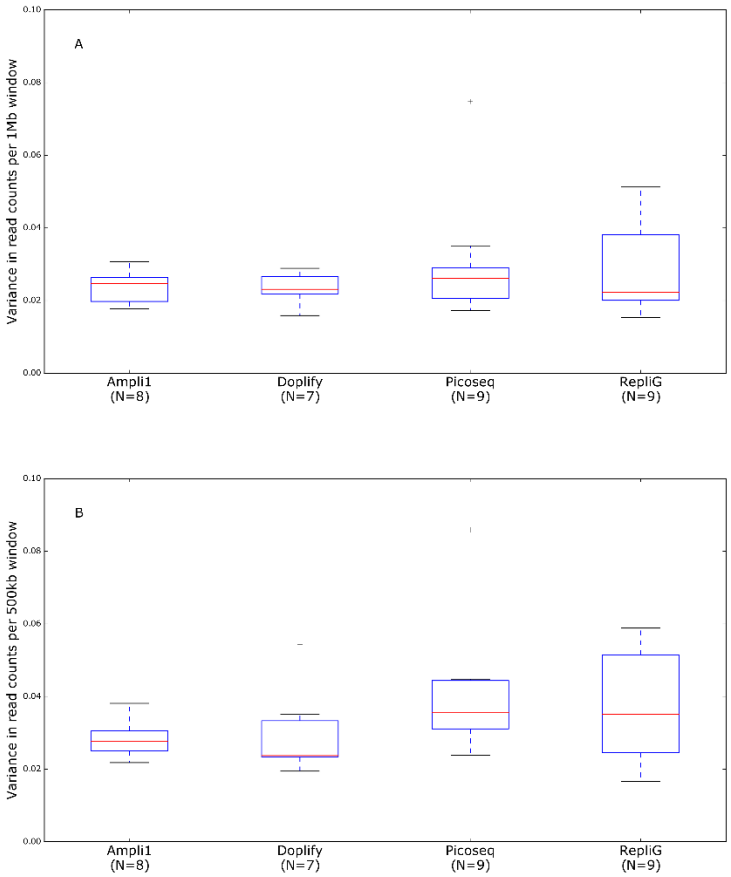

Figure 2: Boxplots of the average variance in read counts per window across the genome.

The boxplots show all samples per WGA method. A) Using 1Mb windows. B) Using 500Kb windows. The blue box contains the values between the first and third quartiles (Q1 and Q3). The black lines are the minimum and maximum, not considering outliers. Values that are more than 1.5 times the interquartile range (Q3-Q1) beyond the closest (Q1 or Q3) quartile were considered as outliers.

4.4. CNV line profiles with 1Mb windows

The 1Mb window line profiles of all samples are available online (https://holmes.ugent.be:9090/ViVar/) and in Supplementary Figure S3. One example of a 1Mb windows profile of a 3-cell sample is shown in Figure 4 for each WGA method. The 1Mb window profile of the sequenced bulk DNA reference sample (Figure 5A) showed all reference

CNVs (>3Mb), except the 3Mb deletion near the start of chromosome 12 and the 3Mb deletion at the end of chromosome 16. The same CNVs were called in almost all WGA samples. Every Picoseq sample showed the same CNVs. After DOPlify WGA, two samples failed to show a usable CNV profile, as mentioned above. In the other DOPlify amplified samples, the same CNVs were called. One sample failed after Ampli1 WGA and was excluded from further analysis. Three out of the 8 remaining Ampli1 samples showed no call for the 26 Mb insertion on chromosome 13. Nevertheless, the line profiles of these three samples all showed a slightly increased CN at the position of the insertion. The insertion on chromosome 13 was also missed in 2 out of 9 REPLI-g samples.

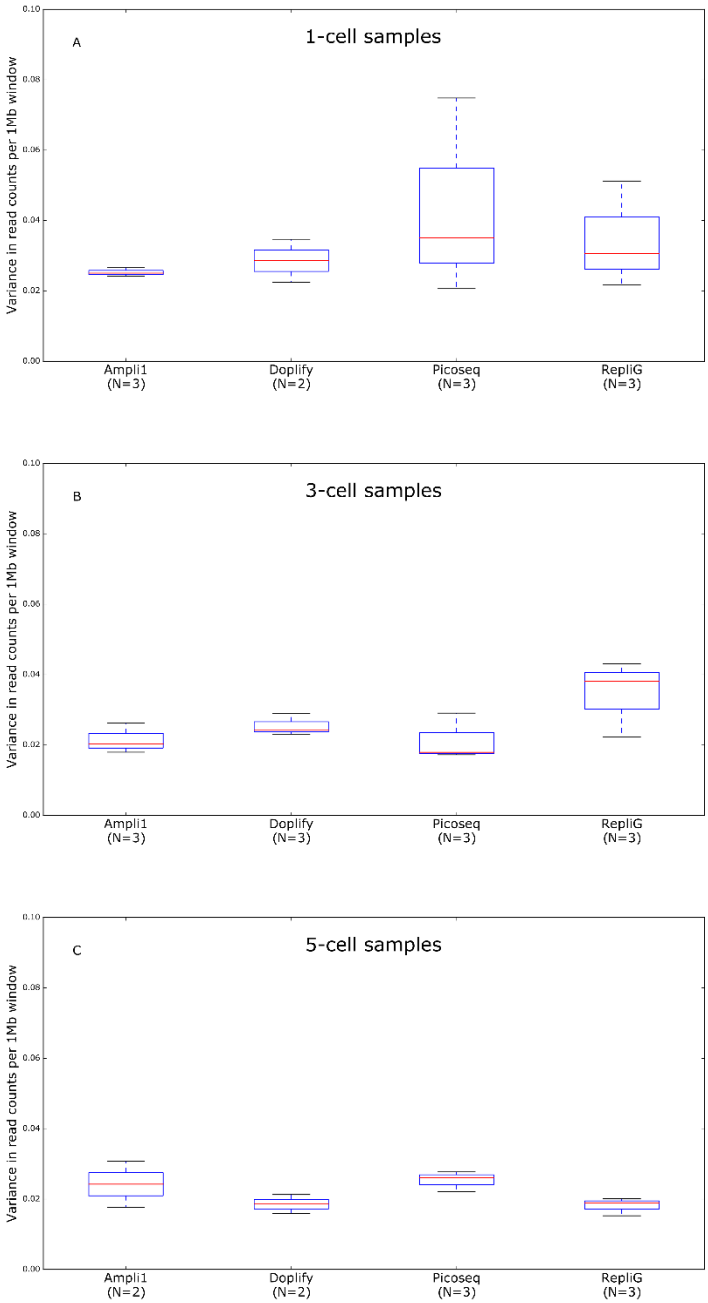

Figure 3: Boxplots of the variances in read counts per 1Mb window across the genome for 1-, 3- and 5-cell samples.

A) All 1-cell samples per WGA method, except the failed one. B) All 3-cell samples per WGA method. C) All 5-cell samples per WGA method, except the failed ones. The blue box contains the values between the first and third quartiles (Q1 and Q3). The black lines are

the minimum and maximum, not considering outliers. Values that are more than 1.5 times the interquartile range (Q3-Q1) beyond the closest (Q1 or Q3) quartile were considered as outliers.

Picoseq and DOPlify amplification did not only result in the same CNVs calls as the sequenced bulk sample, but did also result in no false positive calls. Analysis with Ampli1 and REPLI-g was slightly less accurate because some false positives were called. Only two Ampli1 amplified samples showed false positives, in contrast to five of the REPLI-g amplified samples. Overall, no specific trend in accuracy was observed in relation with the number of amplified cells. A table with the true and false positive calls per sample is shown in Supplementary Table S2.

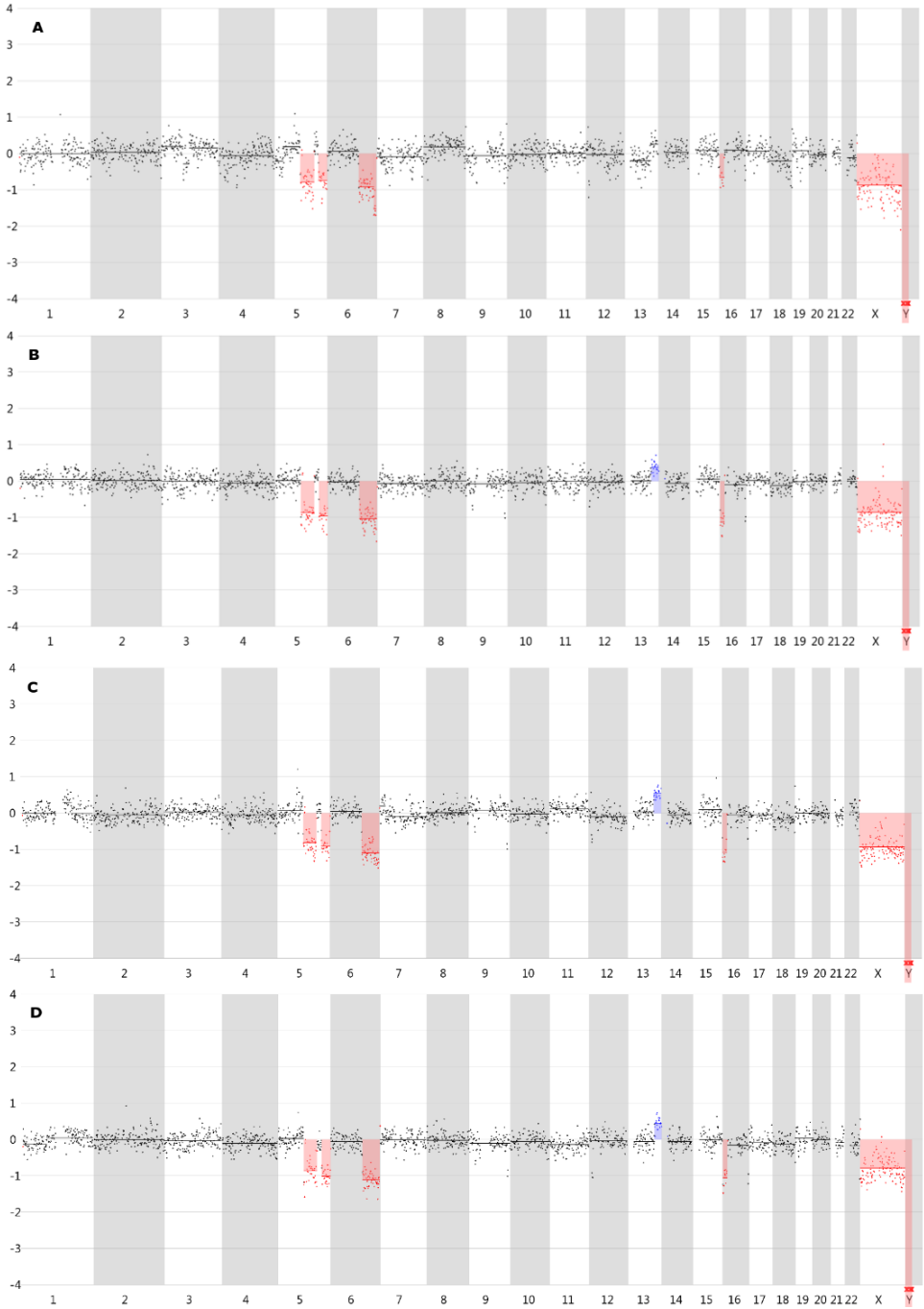

Figure 4: CNV line profiles generated with ViVar using 1Mb windows.

(A) A line profile of a 3-cell sample amplified with REPLI-g. (B) A line profile of an Ampli1 amplified 3-cell sample. C) A line profile of a DOPlify amplified 3-cell sample. D) A line profile of a Picoseq amplified 3-cell sample. The blue color indicates a duplication or trisomy, whereas the red color indicates a deletion or monosomy.

4.5. 1Mb window size versus 500kb window size

By analyzing the data with smaller windows, smaller CNVs could be detected. Supplementary Figure S4 shows the 500kb windows line profiles of all samples. The sequenced bulk reference sample showed all reference CNVs when the data was analyzed with a 500kb window size, except the 3Mb deletion near the start of chromosome 12 (Figure 5B). Compared with this result, Picoseq and DOPlify amplified samples still showed 100% concordance. Two Ampli1 amplified samples still missed the insertion on chromosome 13. One REPLI-g sample still missed the insertion on chromosome 13 and one other REPLI-g sample missed the 3Mb deletion at the end of chromosome 16.

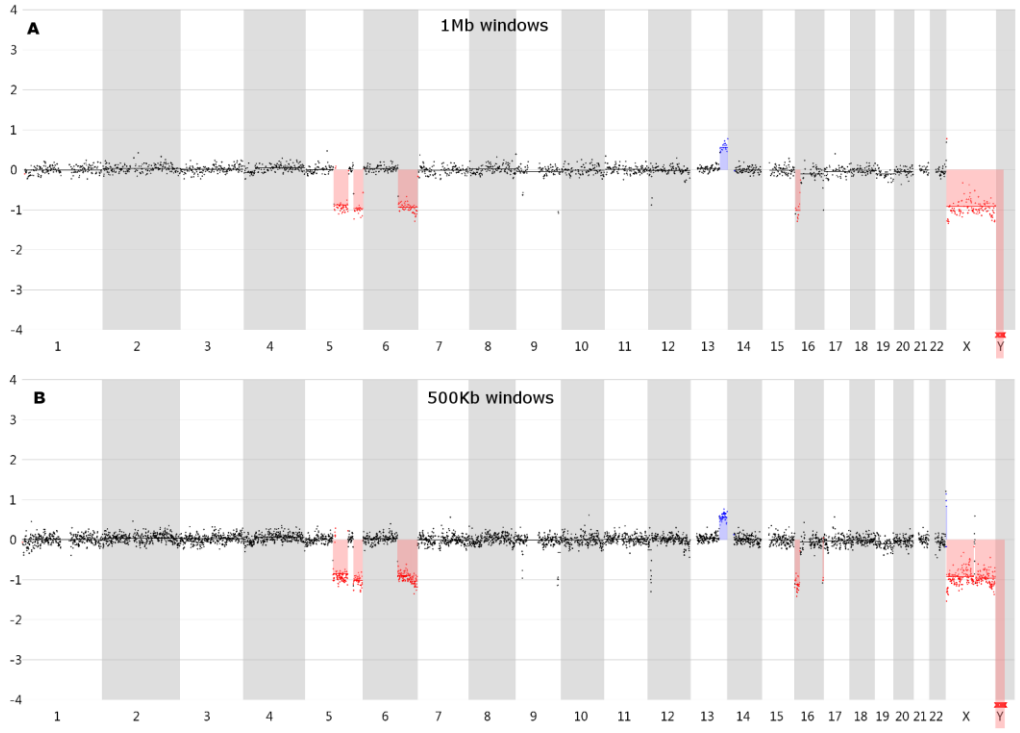

Figure 5: Line profile of the non-amplified bulk reference sample.

A) The line profile using 1Mb windows. B) The line profile using 500kb windows. The blue color indicates a duplication or trisomy, whereas the red color indicates a deletion or monosomy.

The 180K aCGH reference shows a 3Mb deletion near the start of chromosome 12. Although this deletion was not called in the bulk reference sample, the 500kb line profile (Figure 5B) clearly shows windows with lower read counts at this position in the genome. This deletion is called in all but one of the Picoseq samples, 5 out of 7 DOPlify samples, 4 out of 9 REPLI-g samples and 4 out of 8 Ampli1 samples. The 180K aCGH reference shows also a 1.5Mb Chr9p and a 2.5Mb Chr9q deletion. Although not called in the bulk reference sample, the 500kb windows profile (Figure 5B) clearly shows windows with lower read counts at these positions in the genome. The 1.5Mb Chr9p deletion is only called in one REPLI-g sample. The Chr9q deletion is called in 5 out of 9 REPLI-g samples and 2 out

of 7 DOPlify samples. Finally, the aCGH reference shows a small insertion and a small deletion on Chr16q. The 500kb windows line profile of the bulk reflects this, albeit not clearly. However, this deletion is called in 4 out of 8 Ampli1 samples and 1 out of 9 Picoseq samples.

Considering all other calls as false positives, Picoseq and DOPlify did not introduce any false positives in the 500kb windows analysis. Ampli1 amplified samples showed almost 2 times as much false positives with 500Kb windows compared to 1Mb windows. REPLI-g even showed 3 times more false positives compared to the analysis with 1Mb windows.

5. Discussion

In the present study, the performance of 4 different WGA methods was investigated to examine if they generate a WGA product from a limited number of cells that is suitable for CNV detection after shallow whole genome sequencing. All four methods are suitable for this goal, showing only minor differences in the results.

REPLI-g WGA resulted in the highest yield after amplification, enabling the use of this WGA material for multiple downstream applications. DOPlify and Ampli1 yielded only enough DNA to perform one PCR-free library preparation. Picoseq resulted in a sequencing-ready library, using a single-tube reaction. After library preparation, only the yield of adaptor-ligated, sequence-able fragments is of essence.

All WGA methods showed a high percentage of reads mapping to the human genome. In this respect, the four WGA methods showed similar results. All methods showed a uniform distribution of reads across the genome with a similar average variance in read counts per window across the genome. Ampli1 failed to amplify one 5-cell sample and DOPlify failed to amplify a 1-cell and a 5-cell sample. The reason for this failure is unclear. It is possible that these protocols are less robust or the input material was of bad quality. The latter is unlikely since all cells were isolated simultaneously. The WGA products and sequencing libraries of these failed samples showed a similar size distribution as the successful samples during the quality check using an Agilent bioanalyser and could thus not be excluded before sequencing. As we are working with a cancer cell line, the occurrence of chromothripsis might also explain the results. Nevertheless, the true

The accuracy to detect CNVs showed some discrepancies between the four tested methods. When using 1Mb windows, DOPlify and Picoseq samples detected 100% of the CNVs that were also detected in the sequenced bulk sample. The sensitivity to detect CNVs was lower for Ampli1 and REPLI-g. In some of these samples the 26Mb insertion on chromosome 13 was not called. Nevertheless, the size of this insertion is well above the threshold of 3Mb which is approximately the detection limit when using 1 Mb windows. Using 1Mb windows, both DOPlify and Picoseq had a CNV profile with only the expected CNVs and without false positives. A few false positives were

detected in Ampli1 amplified samples and even more were detected in REPLI-g amplified samples. Although this is not obvious from the line profiles, nor the average variance in read counts in windows across the genome, the (local) CNV signal-to-noise ratio seems to be lower in the Ampli1 and REPLI-g amplified samples. The metric of the average variance in reads counts in windows across the whole genome is indeed not a good metric to show possible variance in specific smaller regions of the genome.

In an effort to increase the resolution and to detect smaller CNVs, an analysis using 500kb windows was performed. Also in this analysis Picoseq and DOPlify excelled, leading to the highest number of detected true positives without detection of false positives. While additional true positives were also detected in the Ampli1 and REPLI-g amplified samples, the number of false positives increased substantially in the high-resolution analysis.

6. Supplementary information

Supplementary Figure S1: 180K aCGH of bulk DNA from the Loucy cell line.

This profile shows all CNVs detected in the female Loucy cell line with a resolution of 50kb. Red bars indicate deletions and blue bars indicate insertions.

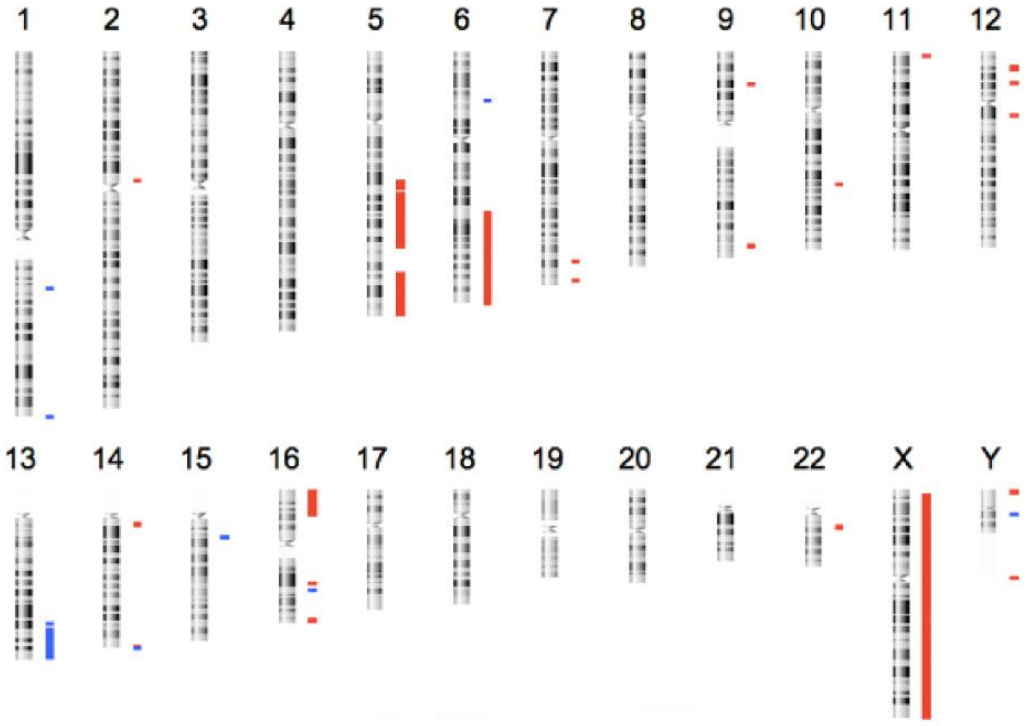

Supplementary Figure S2: Failed samples with an unusable CNV profile.

A) An Ampli-1 amplified 5-cell sample. B) & C) A DOPlify amplified 1-cell and 5-cell sample.

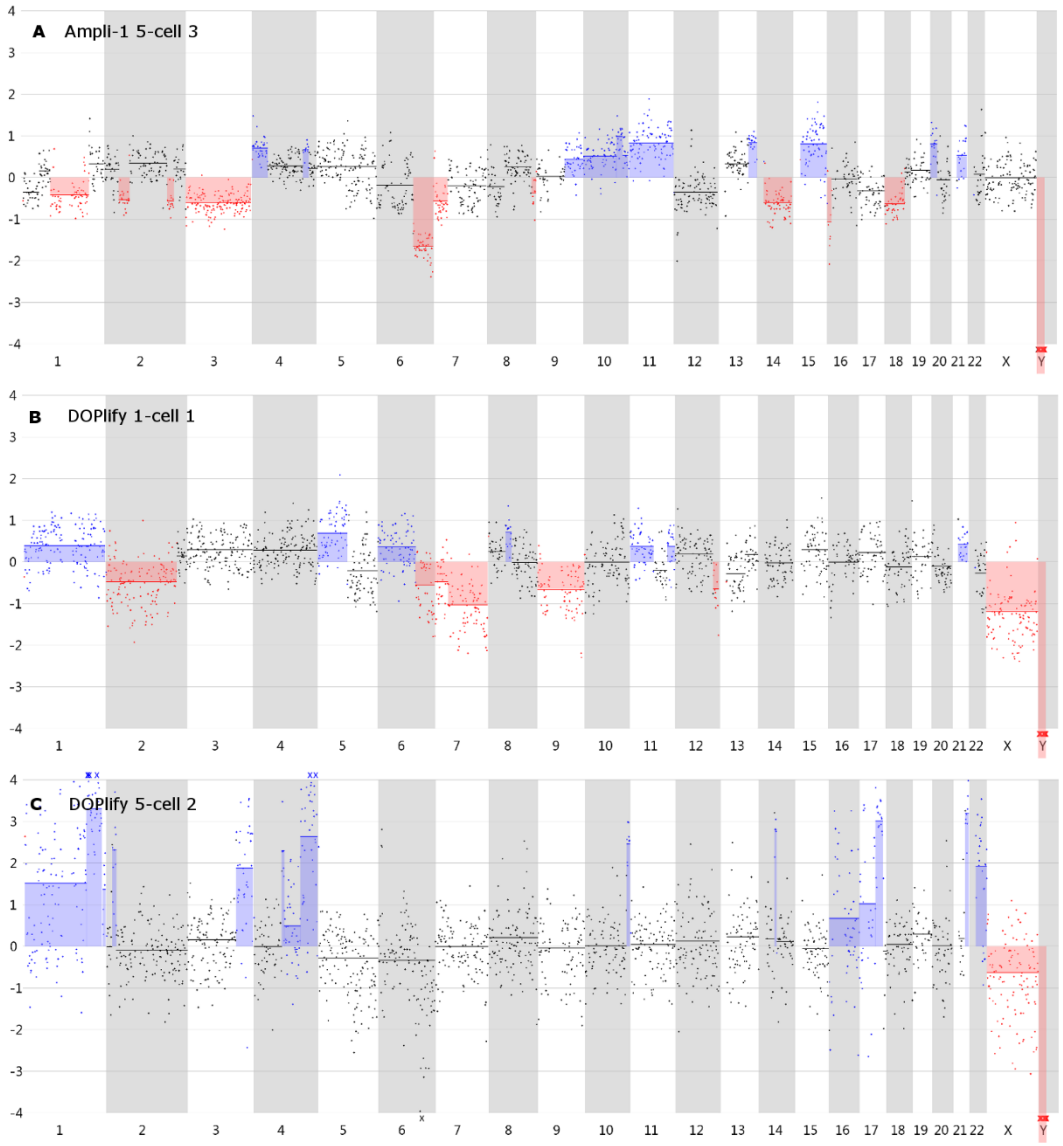

Supplementary Table S1: Average read count variances across the genome in 1Mb and 500kb windows.

		1Mb	500Kb
Ampli-1	1 cell	0.025±0.001	0.029±0.003
	3 cell	0.022±0.004	0.026±0.002
	5 cell	0.024±0.009	0.030±0.012
REPLI-g	1 cell	0.035±0.150	0.034±0.015
	3 cell	0.034±0.110	0.048±0.012
	5 cell	0.018±0.002	0.019±0.004
DOPlify	1 cell	0.029±0.009	0.045±0.014
	3 cell	0.025±0.003	0.026±0.005
	5 cell	0.019±0.004	0.021±0.003
Picoseq	1 cell	0.044±0.028	0.054±0.029
	3 cell	0.021±0.007	0.032±0.110
	5 cell	0.025±0.003	0.036±0.004

Supplementary Figure S3: CNV line profiles of all samples for a 1Mb window. REPLI-g CNV profiles

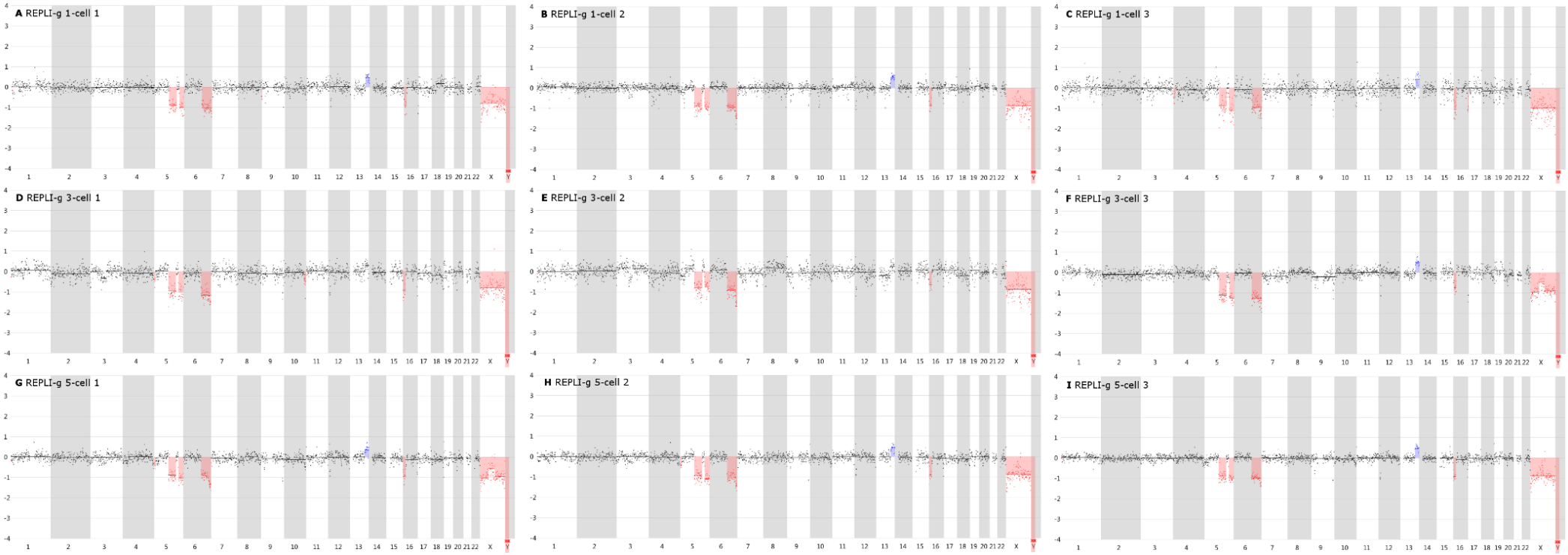

Supplementary Figure S3: CNV line profiles of all samples for a 1Mb window. Ampli-1 CNV profiles

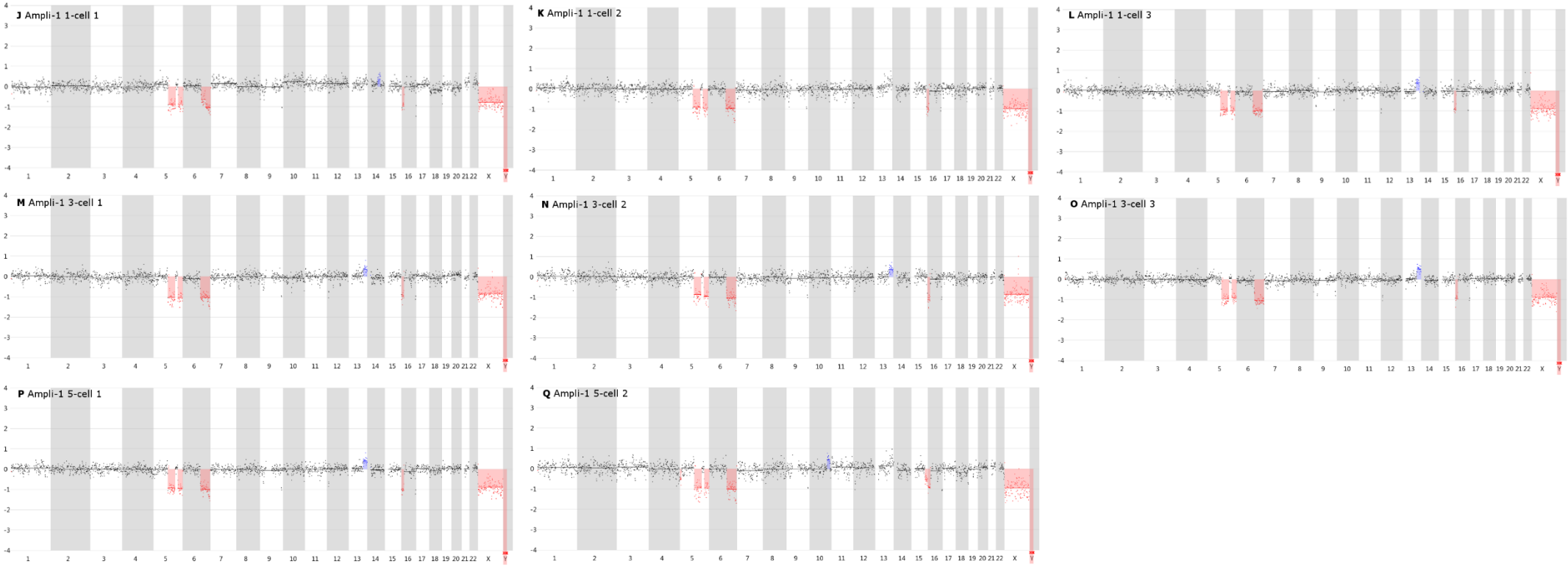

Supplementary Figure S3: CNV line profiles of all samples for a 1Mb window. DOPlify CNV profiles

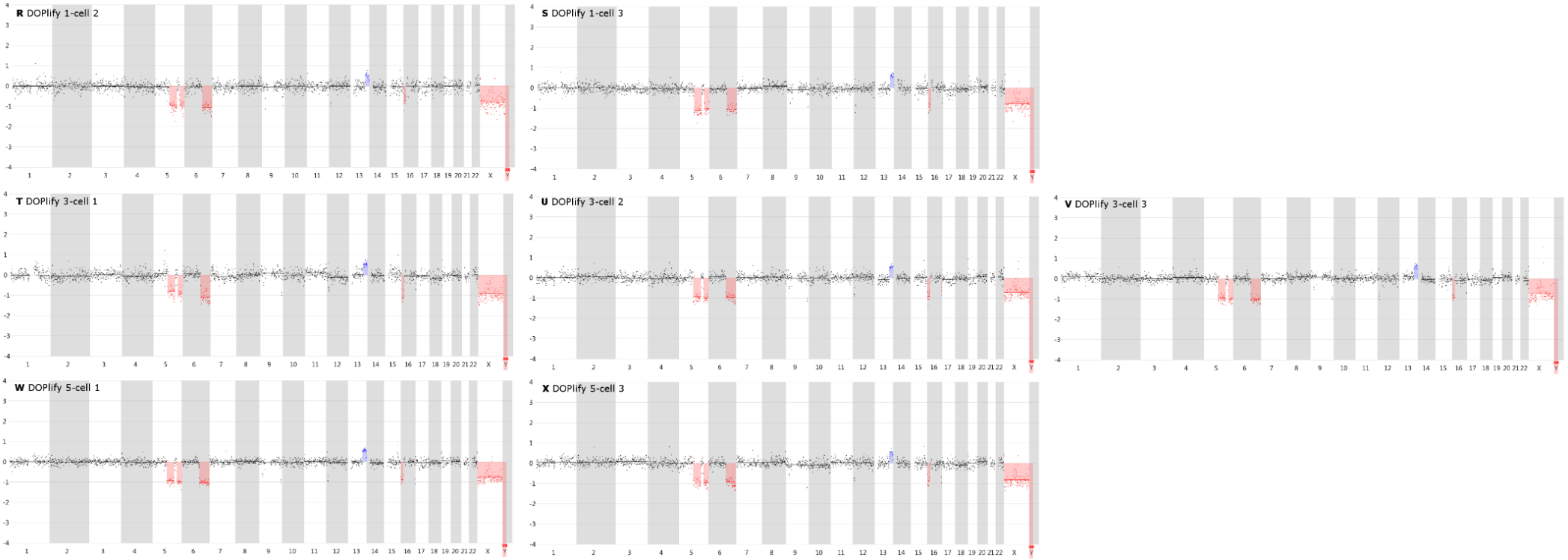

Supplementary Figure S3: CNV line profiles of all samples for a 1Mb window. Picoseq CNV profiles

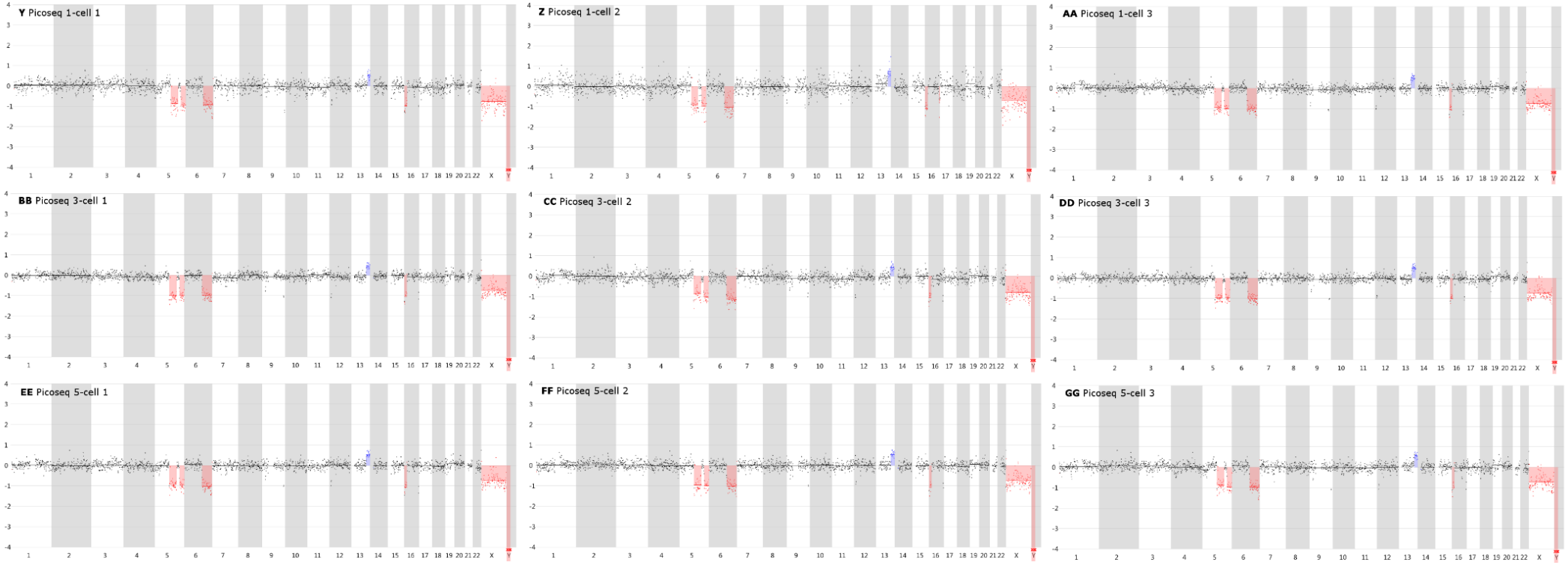

Supplementary Table S2: True and false positives called by ViVar using 1Mb windows. The left side of the table contains all the true positives that are larger than 3Mb. The right side shows the false positives. The column headers indicate the location of the insertion (**in bold**) or the deletion. Two CNVs located on the same chromosomal arm are distinguished by subscript (1) or (2).

		Chr5q$_{(1)}$	Chr5q$_{(2)}$	Chr6q	**Chr13q**	Chr16p	X-Chr	Chr4p	Chr5p	Chr8p	**Chr10q**	Chr10q	**Chr14q**	Chr15q
Bulk		√	√	√	√	√	√							
Ampli-1	1c1	√	√	√		√	√						√	
	1c2	√	√	√		√	√							
	1c3	√	√	√	√	√	√							
	3c1	√	√	√	√	√	√							
	3c2	√	√	√	√	√	√							
	3c3	√	√	√	√	√	√							
	5c1	√	√	√	√	√	√							
	5c2	√	√	√		√	√		√		√			√
REPLI-g	1c1	√	√	√	√	√	√			√				
	1c2	√	√	√	√	√	√							
	1c3	√	√	√	√	√	√	√						
	3c1	√	√	√		√	√		√			√		
	3c2	√	√	√		√	√							
	3c3	√	√	√	√	√	√							
	5c1	√	√	√	√	√	√							
	5c2	√	√	√	√	√	√		√					
	5c3	√	√	√	√	√	√		√					
DOPlify	1c2	√	√	√	√	√	√							
	1c3	√	√	√	√	√	√							
	3c1	√	√	√	√	√	√							
	3c2	√	√	√	√	√	√							
	3c3	√	√	√	√	√	√							
	5c1	√	√	√	√	√	√							
	5c3	√	√	√	√	√	√							
Picoseq	1c1	√	√	√	√	√	√							
	1c2	√	√	√	√	√	√							
	1c3	√	√	√	√	√	√							
	3c1	√	√	√	√	√	√							
	3c2	√	√	√	√	√	√							
	3c3	√	√	√	√	√	√							
	5c1	√	√	√	√	√	√							
	5c2	√	√	√	√	√	√							
	5c3	√	√	√	√	√	√							

Supplementary Figure S4: CNV line profiles of all samples for a 500kb window. REPLI-g CNV profiles

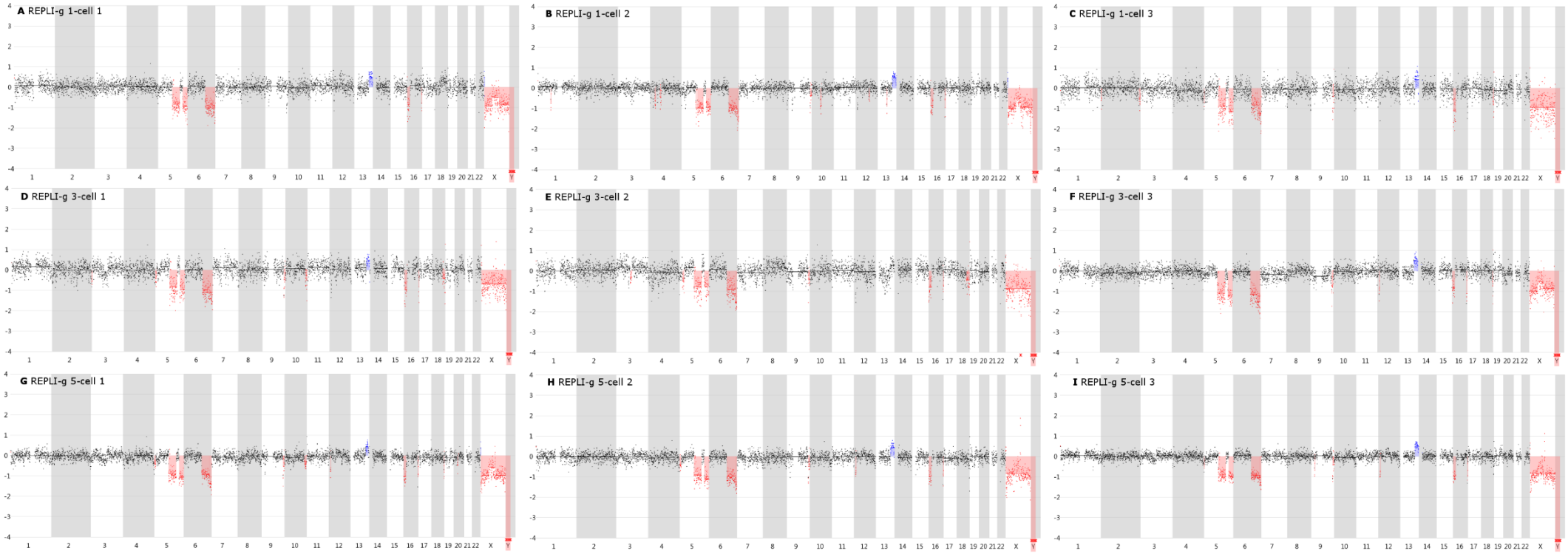

Supplementary Figure S4: CNV line profiles of all samples for a 500kb window. Ampli-1 CNV profiles

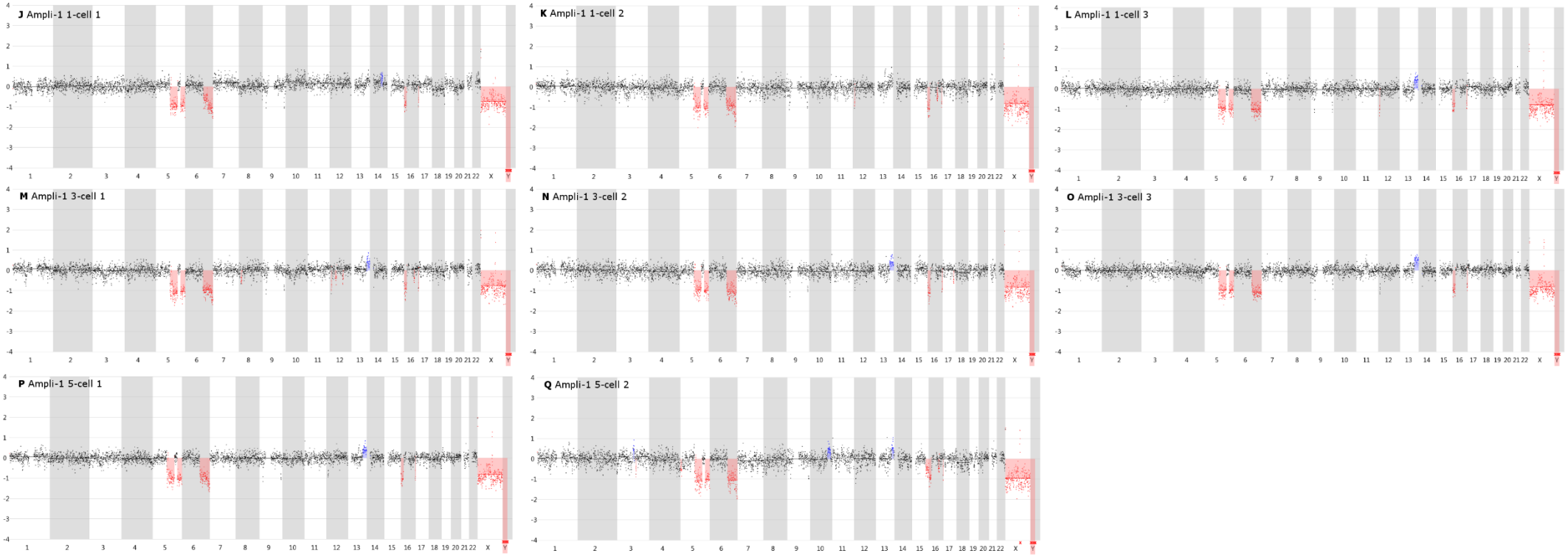

Supplementary Figure S4: CNV line profiles of all samples for a 500kb window. DOPlify CNV profiles

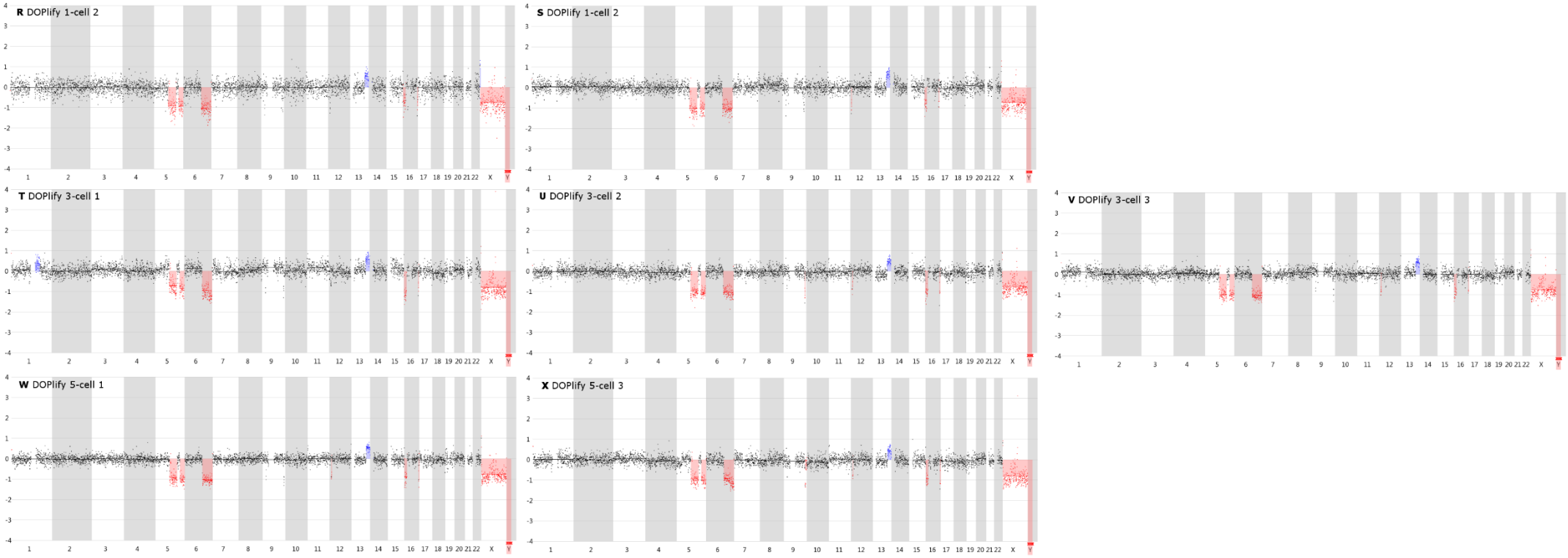

Supplementary figure S4: CNV line profiles of all samples for a 500kb window. Picoseq CNV profiles

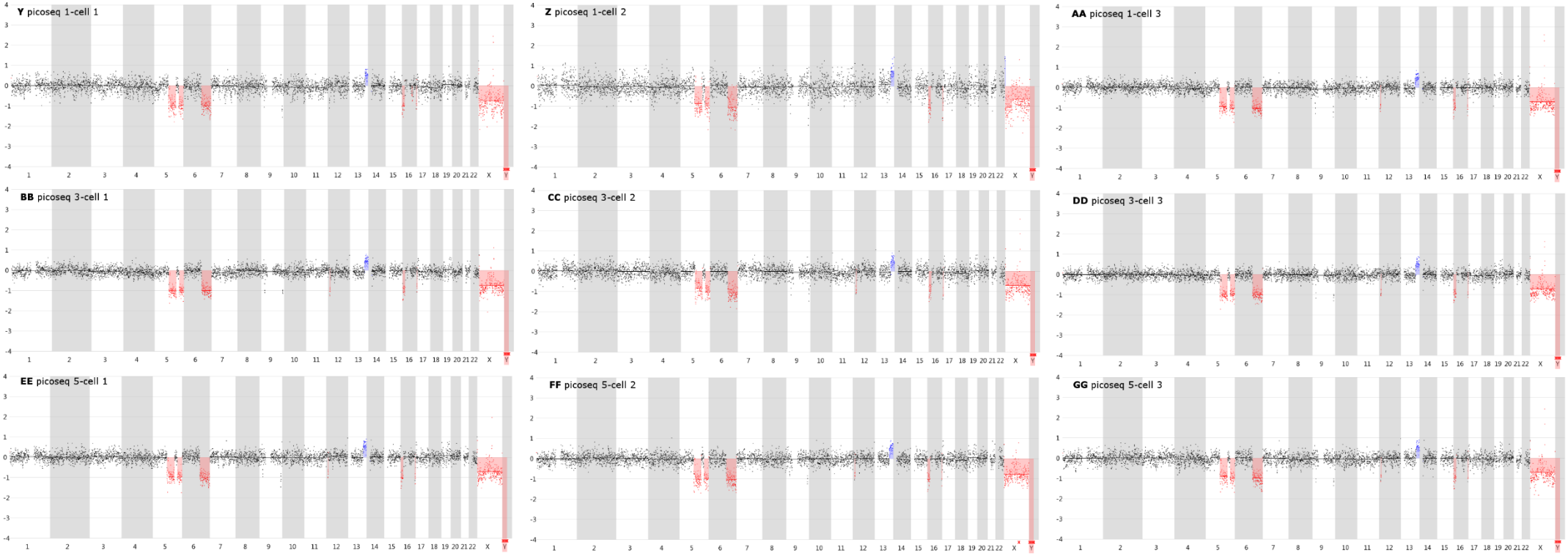

Supplementary Table S3: True and false positives called by ViVar using 500Kb windows. From left to right, separated by a black line: all true positives that are larger than 3Mb; true positives smaller than 3Mb that are called in at least 1 sample; false positives. The column headers indicate the location of the insertion (**in bold**) or the deletion. Two CNVs located on the same chromosomal arm are distinguished by subscript (1) or (2).

		Chr5q$_{(1)}$	Chr5q$_{(2)}$	Chr6q	Chr12p	**Chr13q**	Chr16p	Chr16q	X-Chr	Chr9p	Chr9q	Chr16q$_{(1)}$	Chr1p	**Chr1q**	Chr2p	Chr2q
Bulk		√	√	√		√	√	√	√							
Ampli-1	1c1	√	√	√	√		√	√	√							
	1c2	√	√	√	√		√	√	√			√				
	1c3	√	√	√	√	√	√	√	√			√				
	3c1	√	√	√	√	√	√	√	√			√				
	3c2	√	√	√		√	√	√	√							
	3c3	√	√	√		√	√	√	√							
	5c1	√	√	√		√	√	√	√							
	5c2	√	√	√		√	√	√	√			√				
REPLI-g	1c1	√	√	√		√	√	√	√							
	1c2	√	√	√		√	√	√	√							
	1c3	√	√	√		√	√		√				√			
	3c1	√	√	√		√	√	√	√		√				√	√
	3c2	√	√	√			√	√	√		√					
	3c3	√	√	√	√	√	√	√	√		√					
	5c1	√	√	√	√	√	√	√	√							
	5c2	√	√	√	√	√	√	√	√		√					
	5c3	√	√	√	√	√	√	√	√	√	√					
DOPlify	1c2	√	√	√		√	√	√	√							
	1c3	√	√	√	√	√	√	√	√							
	3c1	√	√	√		√	√	√	√							
	3c2	√	√	√	√	√	√	√	√		√			√		
	3c3	√	√	√	√	√	√	√	√							
	5c1	√	√	√	√	√	√	√	√							
	5c3	√	√	√	√	√	√	√	√		√					
Picoseq	1c1	√	√	√		√	√	√	√			√				
	1c2	√	√	√		√	√	√	√							
	1c3	√	√	√	√	√	√	√	√							
	3c1	√	√	√	√	√	√	√	√							
	3c2	√	√	√	√	√	√	√	√							
	3c3	√	√	√	√	√	√	√	√							
	5c1	√	√	√	√	√	√	√	√							
	5c2	√	√	√	√	√	√	√	√							
	5c3	√	√	√	√	√	√	√	√							

Supplementary Table S3: cont.

		Chr3p	Chr3pq	**Chr3q**	Chr3q	Chr4p	Chr4q(1)	Chr5p(1)	Chr5p(2)	Chr8p	Chr9q(2)	Chr10q(1)	Chr10q(2)	Chr12pq	Chr12q(1)
Ampli-1	1c1														
	1c2														
	1c3														
	3c1									√				√	√
	3c2														
	3c3														
	5c1														
	5c2			√	√			√							
REPLI-g	1c1														
	1c2					√	√				√	√			
	1c3										√				
	3c1							√					√		
	3c2	√							√						
	3c3		√												
	5c1							√					√		
	5c2							√					√		
	5c3							√							
DOPlify	1c2														
	1c3														
	3c1														
	3c2														
	3c3														
	5c1														
	5c3														
Picoseq	1c1														
	1c2														
	1c3														
	3c1														
	3c2														
	3c3														
	5c1														
	5c2														
	5c3														

Supplementary Table S3: Cont.

		Chr12q(2)	Chr13q(1)	Chr13q(2)	Chr17q	Chr18q(1)	Chr18q(2)
Ampli-1	1c1						
	1c2						
	1c3						
	3c1						
	3c2				√		
	3c3						
	5c1						
	5c2						
REPLI-g	1c1						
	1c2	√		√			
	1c3						
	3c1					√	
	3c2					√	
	3c3		√			√	
	5c1						√
	5c2						√
	5c3						
DOPlify	1c2						
	1c3						
	3c1						
	3c2						
	3c3						
	5c1						
	5c3						
Picoseq	1c1						
	1c2						
	1c3						
	3c1						
	3c2						
	3c3						
	5c1						
	5c2						
	5c3						

Chapter VIII: Massively parallel sequencing of micro-manipulated cells targeting a comprehensive panel of disease-causing genes

Lieselot Deleye[1], Yannick Gansemans[1], Dieter De Coninck[1], Filip Van Nieuwerburgh[1,†] & Dieter Deforce[1,†]

[1]Laboratory of Pharmaceutical Biotechnology, Ghent University, Ottergemsesteenweg 460, 9000 Ghent, Belgium.
[†]These authors contributed equally to this work.

PLos One; under review.

1. Abstract

Preimplantation genetic diagnosis (PGD) is used during in-vitro fertilization to select an embryo for implantation, free of chromosomal aberrations or single gene disorders (SGDs) carried by the parents. Shallow whole-genome sequencing has recently become a standard for the genome-wide detection of chromosomal aberrations in PGD. In contrast, SGDs are still routinely diagnosed using PCR-based assays that need to be developed and validated for each individual disease-specific gene fragment. The TruSight One sequencing panel currently covers 12Mb of genomic content, including 4813 genes associated with a clinical phenotype. It has already been successfully applied for prenatal diagnosis of SGDs on DNA obtained from chorionic villi. In that setting, no whole genome amplification (WGA) was required, because enough fetal DNA was available. In PGD however, WGA is required prior to DNA target capture techniques, such as the TruSight One panel. In this study, we compared 4 different WGA methods in combination with the TruSight One sequencing panel to perform single nucleotide polymorphism (SNP) genotyping starting from 3 micro-manipulated cells. Bulk cell samples were processed alongside the WGA samples so serve as a performance reference. Target coverage, coverage uniformity and SNP calling accuracy obtained using any of the WGA methods, is inferior to the results obtained on bulk cell samples. However, results after REPLI-g come close. Compared to the other WGA methods, REPLI-g WGA results in a better coverage of the targeted genomic regions with a more uniform read depth. Consequently, this method also results in a more accurate SNP calling.

2. Introduction

Successful in-vitro fertilization (IVF) may require preimplantation genetic diagnosis (PGD) for the selection of an embryo free of chromosomal aberrations and single gene disorders (SGDs) carried by its parents. Recently, shallow whole genome sequencing has proven to be useful for the genome-wide detection of chromosomal aberrations in PGD (30, 32, 163). SGDs on the other hand, are still routinely diagnosed using PCR-based assays that are developed to target the specific gene fragment(s) involved in a single or a limited number of genetic diseases (39). Development and validated application of these methods is time consuming. Established protocols often require adjustments for couples carrying slightly different mutations (206).

Whole Genome Amplification (WGA) can be used to amplify the DNA of the limited number of cells that can be biopsied from blastocysts for PGD. This pre-amplified DNA can be used to perform multiple PCR reactions, yielding multiple amplicons for the detection of disease-related mutations or insertions/deletions (indels). Massively parallel sequencing (MPS) can be used to sequence a pool of these different amplicons (207). The cost and timescale are reduced by multiplexing different patient samples on a single sequencing run. Still, this approach requires a specific PCR primer design for each disease-associated locus. WGA combined with MPS could also be used to sequence the entire genome of the embryo, allowing simultaneous screening for Single Nucleotide

Polymorphisms (SNPs) and chromosomal aberrations. However, whole genome SNP analysis will need sequencing at high coverage to accurately detect them, which currently is still too expensive for routine clinical applications.

The TruSight One Sequencing Panel (Illumina) targets 4,813 genes associated with known clinical phenotypes and enables simultaneous screening for mutations in these genes on a single sequencing run. Since only the genomic regions of interest are sequenced, a high depth is obtained for a relatively low cost. This panel was already successfully applied to detect SGDs during a prenatal screening using DNA obtained from chorionic villi and amniotic fluid (46). Because only 4-6 trophoblasts can be biopsied in PGD, WGA is required to obtain a sufficient amount of DNA to start the TruSight One DNA capture. Unfortunately, WGA methods might introduce representation bias and nucleotide changes during amplification. Non-uniform amplification of regions across the genome may result in over- or underrepresentation of such genomic regions. Robust detection of mutations, more specifically SNPs, in insufficiently amplified (i.e. underrepresented) regions, can be problematic. Additionally, the introduction of errors in the sequence during amplification could result in mutations being obscured or introduced. The commercially available WGA methods all have their specific strengths and weaknesses and which one to use depends on the downstream application (130). WGA methods based on multiple displacement amplification (MDA) are better suited for SNP detection because they use the high-fidelity phi29 polymerase. Hybrid WGA methods use DNA polymerases lacking proofreading ability which introduces more errors, but yield a more balanced genomic amplification with less over- or underrepresented regions. Both accuracy and amplification uniformity are important for the accurate detection of SNPs and indels with the TruSight panel.

In this study, four different WGA methods were used to amplify DNA isolated from 3 micro-manipulated cells of the well-characterized and extensively sequenced NA12882 cell line of the Illumina Platinum Genome project. The aim of this study is to show whether WGA amplified samples, in combination with the TruSight One Sequencing Panel, can be used to accurately and reproducibly detect SGD, which would encourage the use of this panel for detection of SGDs in PGD, and other applications in which a similar number of cells are obtained. Two semi-random primer mediated hybrid WGA methods (SurePlex and MALBAC) (133, 187, 208), a MDA method (REPLI-g) (33) and a ligation-based WGA method (Ampli1) were assessed.

As WGA methods based on MDA are reportedly better suited for SNP detection (33), because they use the high-fidelity phi29 polymerase and amplify more regions of the genome compared to PCR-based or hybrid methods, it is to be expected that REPLI-g would outperform MALBAC, SurePlex and Ampli1 in this setting. It thus seems logical to choose an MDA based method to achieve a good amplification for downstream target capture and sequencing. If in doubt about which method to choose, a comparison of the different available MDA-based methods would be opportune, but REPLI-g is the MDA WGA method that is currently most widely used.

There are however several reasons why we choose to make the current comparison: The main reason to include the methods MALBAC, SurePlex and Ampli1 on top of REPLI-g is the fact that at the start of this study, no reports were published that show the performance of these WGA methods after target capture. It has been shown that MDA-based WGA methods show a better coverage of the genome when the WGA product is sequenced without previous capture and the resulting reads are mapped. But such results do not indicate that this would hold true when target capture is performed before sequencing. The latter requires a good accuracy on top of a uniform amplification. Our data brings evidence to this speculation. Interestingly, a paper was recently published by Borgström *et al.* (209), comparing the performance of the exact same 4 WGA methods for downstream exome capture sequencing. Their experimental setup is similar to ours, but they use the REPLI-g Mini kit instead of the REPLI-g single cell kit we use. Furthermore, the distinction between MDA-based and hybrid WGA methods is not unambiguous: e.g. MALBAC and SurePLEX use both strand displacement and PCR amplification. The 4 tested WGA methods are currently the most widely used WGA methods.

3. Material & Methods

3.1. Study design

This study was performed on cells from the NA12882 lymphatic male cell line (Coriell Institute, New Jersey, USA). The DNA of this cell line has been sequenced extensively (50X depth on a HiSeq2000) and the sequencing data is available online (http://www.illumina.com/platinumgenomes/). As this data allows for robust SNP detection, the NA12882 genome will be considered the true control reference in this study. We prepared 14 genomic DNA samples, each one starting from 3 NA12882 cells. These were amplified by 4 different WGA methods, resulting in 3 or 5 biological replicates per WGA method (5 for SurePlex, 3 for the others). Additionally, 4 genomic DNA samples were prepared from larger cell numbers and not submitted to WGA (further referred to as bulk DNA samples). The bulk DNA samples were included in the study to evaluate the TruSight kit performance in samples mimicking current clinical application of the kit (46). Subsequent capture of gene regions with the TruSight One Sequencing panel (Illumina, San Diego, CA, USA) was performed on all samples (Figure 1). At the pooling step, four non-amplified bulk DNA samples and the WGA samples were randomly pooled per 3 to ascertain that variations observed after the capture step are caused either by the capture step or the preceding WGA. One MiSeq sequencing run was performed per pool of 3 samples.

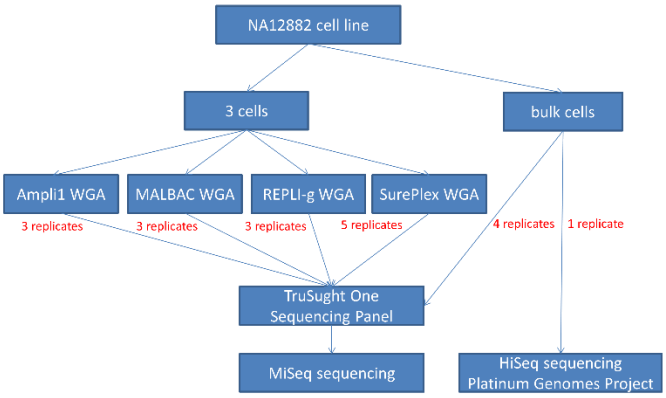

Figure 1: Experimental design.

Three cell samples from the NA12882 cell line were amplified with either Ampli1 (3 replicates), REPLI-g (3 replicates), SurePlex (5 replicates) or MALBAC (3 replicates). Subsequently, samples were randomized for TruSight One capture in pools of 3 and those pools were sequenced on separate MiSeq runs. Four bulk DNA sample from the NA12882 cell line, not amplified before capture, were also randomly included in the pools.

3.2. Growth and isolation of cells

The NA12882 cell line was grown in Roswell Park Memorial Institute (RPMI-1640) medium (Life technologies, Carlsbad, USA), supplemented with 15% fetal bovine serum (Life technologies, Carlsbad, USA) and 2mM L-Glutamine. For optimal growth it was incubated at a temperature of 37°C and a 5% CO_2 level. A known amount of cells was isolated with an ergonomic denuding handle from STRIPPER (Origio, Måløv, Denmark) and MXL3-100 needles with a diameter of 100µm (Origio, Måløv, Denmark). The desired amount of cells was obtained by a serial dilution using spots of sterile phosphate buffered saline (PBS) (Life technologies, Carlsbad, USA) on a Petri dish (5.5cm), performed under an Axiovert 25 light microscope (Zeiss, Jena, Germany). For optimal lysis, all cells were collected in a maximum volume of 1µl. Immediately after collection, all samples were snap frozen in liquid nitrogen.

For each bulk DNA sample, genomic DNA was extracted from $5x10^6$ cells using the DNeasy Blood & Tissue kit (Qiagen Hilden, Germany).

3.3. Whole genome amplification

For MALBAC samples, lysis of the isolated cells and amplification of the genomic DNA was performed using the MALBAC kit (Yikon genomics YK001A/B version 1302.1, Jiangsu, China), following manufacturer's instructions. As a positive control, 1µl of male control DNA (9948; Promega; 10ng/µl) was used at a concentration of 30pg/µl. The blank was 1µl of PBS.

For the SurePlex samples, cell lysis and amplification was performed according to manufacturer's instructions using the SurePlex amplification system (Bluegnome, Cambridge, United Kingdom). As a positive control, 2.5µl of female control DNA (G1521; Promega; 187ng/µl) was used at a concentration of 25pg/µl. The blank consisted of 2.5µl PBS.

For the REPLI-g samples, cell lysis and amplification was performed following manufacturer's instructions using the REPLI-g single cell amplification system (Qiagen, Hilden, Germany). As a positive control, 1µl of female control DNA (Roche; 0.2mg/ml) was used at a concentration of 33.3pg/µl. A 3µl PBS blank was included.

For the Ampli1 samples, cell lysis and amplification was performed following manufacturer's instructions using the Ampli1 WGA system (Silicon Biosystems, Castel Maggiore, Italy). As a positive control, 1µl of female control DNA (Roche; 0.2mg/ml) was used at a concentration of 33.3pg/µl. A blank consisting of 1µl PBS was included.

All samples were purified using the Genomic DNA Clean & Concentrator kit (version 1.0.0, Zymo Research, Irvine, USA) according to the manufacturer's instructions with 5 X binding buffer. Concentration was measured using the Qubit dsDNA High Sensitivity Assay kit (Life technologies, Carlsbad, USA).

3.4. Library preparation and sequencing

Sequencing libraries were prepared starting from 50ng of the WGA-amplified or bulk DNA using the TruSight One Sequencing Panel (Illumina, San Diego, CA, USA). Manufacturer's instructions were followed, except for the enrichment wash step where a thermocycler was used instead of the SciGene TruTemp heating system. The samples were incubated for 30min at 42°C, with a heated lid at 100°C. Samples were fragmented using tagmentation, followed by addition of sequencing indexes during a first PCR amplification. After amplification, 3 samples were pooled equimolar before hybridization of the probes and subsequent capture. Probe hybridization and capture was performed two times. Finally, the captured fragments were enriched during a 2nd PCR.

The amount of sequence-able library fragments was determined by performing a qPCR according to the Sequencing Library qPCR Quantification kit (Illumina, San Diego, USA). Sample pools were diluted to 10nM with elution buffer (EB buffer) (QIAGEN, Hilden, Germany). The control template used for the standard curve was a PhiX control library (10nM). Finally, dual-index, paired-end 150bp sequencing was performed on a MiSeq (Illumina). All sample pools were sequenced on separate MiSeq runs.

3.5. Data analysis

Sequencing read quality was checked using FastQC (v0.11.5) (210). Reads were aligned on the UCSC hg19 reference genome using bwa (v0.7.5) (211). Mapping quality was evaluated using Qualimap (v2.2.1) (212). Duplicate read marking and all bam file manipulations were done using Picardtools (v2.6.0)(213). Reads from the NA12882 Platinum Genome that aligned to the TruSight One Sequencing Panel regions were isolated using bedtools (v2.26) (171). SNP discovery in samples and the NA12882 reference was done using GATK (v3.6)(214) according to best practices instructions. Briefly, base quality scores were recalibrated in a two-pass covariation analysis supplemented with the dbSNP (release 135) (215) and Mills/1000 Genomes (216) data sets as a source of known

variants. SNP calling was then performed at base resolution in discovery mode using an emission confidence threshold of 10 and a call confidence threshold of 30. The final SNP's were obtained by applying the following filter criteria to discard low quality SNPs: QD < 2.0, FS > 60.0, MQ < 40, MQRankSum < -12.5, ReadPosRankSum < -8.0. VCFtools (v0.1.13) (217) and custom Python scripting were used for all SNP comparisons between sample replicates and the NA12882 reference.

3.6. Sensitivity, false discovery rate (FDR) and Genotype concordance

Variants were compared between samples and the reference dataset for positions where both had sequencing data (comparable SNP's). Variants not detected in either the sample or the reference dataset due to lack of sequencing data were counted and labeled as 'no data in sample' and 'no data in reference' respectively. The comparable SNP's were categorized as follows: True positives are defined as variant positions found in both the sample and the reference dataset. False positives are variant positions found in the sample but not in the reference dataset. Positions called as variants in the reference set but not in the sample are labeled false negatives. The sensitivity for SNP calling in a sample was defined as the number of true positives, divided by the sum of true positives and false negatives. The FDR was defined as the number of false positives divided by the sum of true positives and false positives.

4. Results and Discussion

4.1. Coverage and depth

To minimize run bias, samples amplified with the same WGA method were randomized over different MiSeq runs where possible (Table 1). The number of sequenced reads was variable between sample replicates. Two Ampli1 samples had a substantial lower yield than the other samples. This is probably caused by random errors during quantification and equimolar pooling of the sequencing libraries, combined with a variable cluster formation and detection across different sequencing runs. The percentage of reads aligning to the hg19 reference genome was similar for all samples, including the bulk DNA samples (99.81±0.13%), as was the read alignment to the TruSight target regions (59.43±4.06%). This capture efficiency reflects the vendor's performance specifications of the TruSight One kit. Mean depth across the targeted nucleotides correlated with the read yield and varied from 28X to 96X.

The "coverage uniformity" (Table 1) is calculated as the percentage of targeted base positions for which the read depth is greater than 0.2 times the mean depth and thus is a measure for the number of bases that are not underrepresented in the read data. This coverage uniformity was different between the WGA methods, but similar for the repeats within a method. As expected, the coverage for the bulk DNA samples was most uniform (94.80±0.27%). REPLI-g amplified samples displayed a coverage uniformity closest to the bulk DNA samples

(88.41±1.01%). The other WGA methods showed a lower uniformity: Ampli1, MALBAC and SurePlex have a uniformity of respectively 49.26±1.33%, 47.23±0.33% and 49.77±1.42%. Figure 2 visualizes this uneven distribution of reads over the targeted regions by means of different plots. Figure 2a plots the read depth across the targeted regions for one representative sample of each method. Supplementary figure 1 shows the same plots for the other replicate samples. The plot allows to see larger regions with above or below average read depth. In terms of size of these alternating larger regions with high and low depth, there seems to be no pronounced difference between the different WGA methods. The over- and under-represented regions are not the same in the different methods, although there are some similarities: Bulk DNA, Ampli1, REPLI-g and Sureplex have a clear underrepresented region in common. Many of the over- and under-represented regions overlap between MALBAC and Sureplex. Figure 2b and 2c shows Lorenz curves and Gini indexes describing how sequenced bases are distributed over targeted (b) and covered bases (c). The plots clearly show that the distribution of the reads from bulk DNA is closest to the even distribution. Comparing the WGA methods, the read distribution after REPLI-g WGA is closest to the even distribution.

	Sequencing run	Read count	Aligned reads (%)	Aligned reads on target (%)	Mean depth	Coverage uniformity (%)	Target coverage at 1X (%)	Target coverage at 10X (%)	Target coverage at 20X (%)
Bulk DNA-1	1	14810732	99.82	60.91	78.85	95.14	99.60	97.38	92.95
Bulk DNA-2	2	15294678	99.92	63.12	83.20	94.82	99.62	97.22	93.07
Bulk DNA-3	3	19477275	99.86	58.25	95.86	94.75	99.62	97.51	94.43
Bulk DNA-4	3	18900774	99.85	59.48	94.65	94.48	99.60	97.36	94.10
Ampli1-1	1	4959973	99.84	62.27	27.48	47.75	63.29	39.59	29.27
Ampli1-2	2	5341335	99.94	66.62	31.01	50.22	65.96	43.59	33.15
Ampli1-3	4	12784447	99.89	57.82	66.23	49.82	75.63	53.00	43.93
MALBAC-1	5	14138090	99.36	52.02	61.03	47.92	78.59	51.27	39.77
MALBAC-2	6	11352373	99.78	61.06	58.21	46.91	78.90	49.68	38.30
MALBAC-3	5	14045595	99.81	53.72	62.62	46.86	78.76	51.39	40.13
REPLI-g-1	1	12359960	99.86	60.33	64.84	87.25	98.70	90.76	79.02
REPLI-g-2	2	13785283	99.92	59.22	71.01	89.10	98.99	92.84	83.18
REPLI-g-3	4	15937788	99.85	56.65	78.98	88.87	99.08	93.61	85.66
SurePlex-1	5	14277005	99.80	64.30	78.17	49.21	78.81	55.51	45.67
SurePlex-2	6	12662797	99.80	51.99	54.81	48.45	75.48	49.85	39.61
SurePlex-3	3	11649675	99.77	64.07	63.49	49.54	77.87	53.12	42.72
SurePlex-4	6	11670489	99.83	59.53	60.40	52.19	55.35	55.35	44.01
SurePlex-5	4	13676160	99.69	58.32	67.39	49.47	82.80	54.15	43.74

Table 1: Mapping statistics

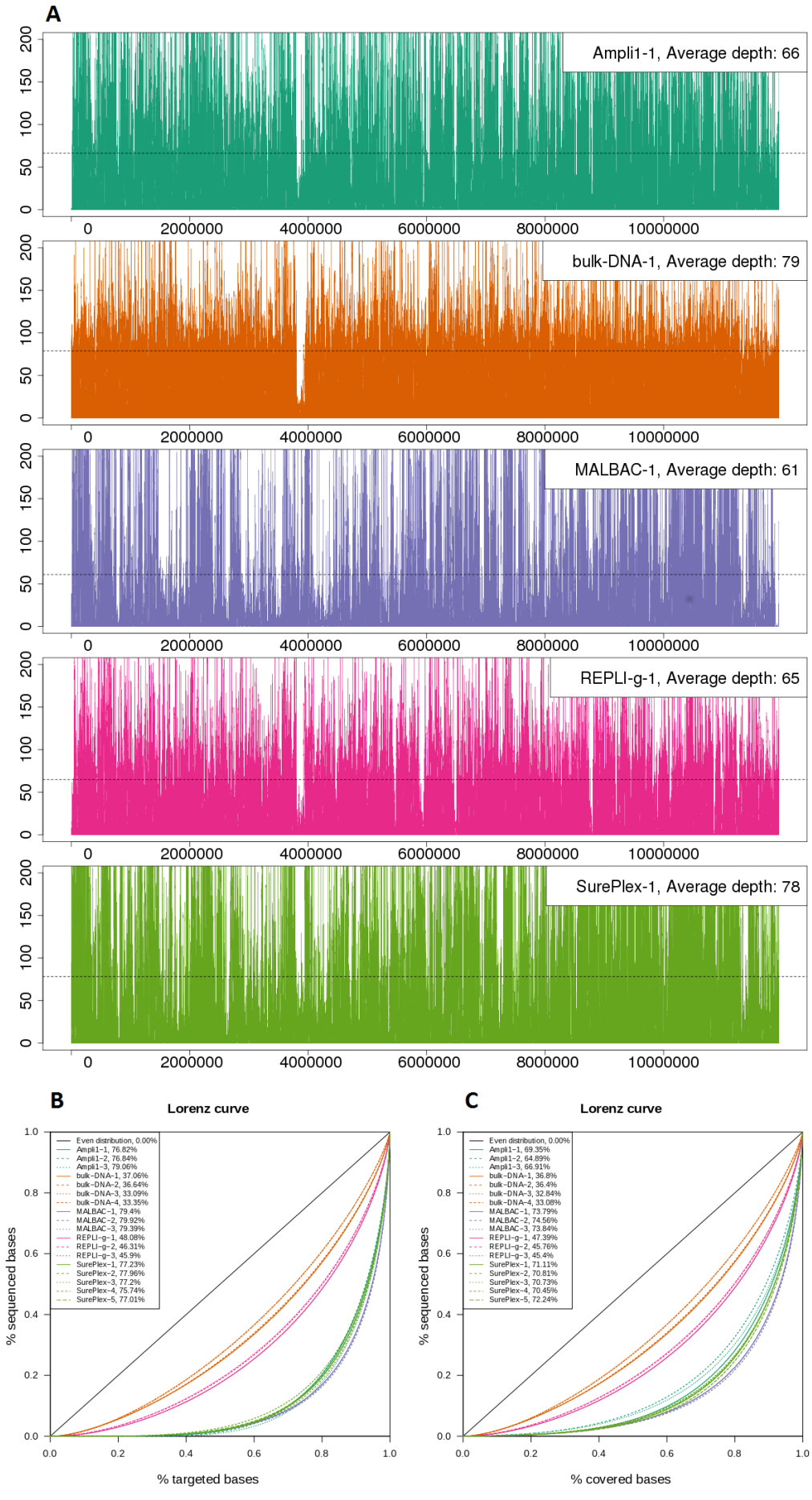
A
Ampli1-1, Average depth: 66
bulk-DNA-1, Average depth: 79
MALBAC-1, Average depth: 61
REPLI-g-1, Average depth: 65
SurePlex-1, Average depth: 78
0
50
100
150
200
0
2000000
4000000
6000000
8000000
10000000
B
Lorenz curve
% sequenced bases
% targeted bases
Even distribution, 0.00%
Ampli1-1, 76.82%
Ampli1-2, 76.84%
Ampli1-3, 79.06%
bulk-DNA-1, 37.06%
bulk-DNA-2, 36.64%
bulk-DNA-3, 33.09%
bulk-DNA-4, 33.35%
MALBAC-1, 79.4%
MALBAC-2, 79.92%
MALBAC-3, 79.39%
REPLI-g-1, 48.08%
REPLI-g-2, 46.31%
REPLI-g-3, 45.9%
SurePlex-1, 77.23%
SurePlex-2, 77.96%
SurePlex-3, 77.2%
SurePlex-4, 75.74%
SurePlex-5, 77.01%
C
Lorenz curve
% sequenced bases
% covered bases
Even distribution, 0.00%
Ampli1-1, 69.35%
Ampli1-2, 64.89%
Ampli1-3, 66.91%
bulk-DNA-1, 36.8%
bulk-DNA-2, 36.4%
bulk-DNA-3, 32.84%
bulk-DNA-4, 33.08%
MALBAC-1, 73.79%
MALBAC-2, 74.56%
MALBAC-3, 73.84%
REPLI-g-1, 47.39%
REPLI-g-2, 45.76%
REPLI-g-3, 45.4%
SurePlex-1, 71.11%
SurePlex-2, 70.81%
SurePlex-3, 70.73%
SurePlex-4, 70.45%
SurePlex-5, 72.24%
0.0
0.2
0.4
0.6
0.8
1.0

Figure 2: Read distribution.
(a) Read depth calculated in 1 kb sliding windows across the concatenated target regions for one sample of each method. (b,c) Lorenz curves and Gini indexes describing how sequenced bases are distributed over targeted (b) and covered (c) regions.

Table 1 also shows the percentages of target regions covered with a minimal depth of 1X, 10X or 20X. For bulk DNA and REPLI-g samples, target region coverage with a minimal depth of 1X was almost complete (99.61±0.01% and; 98.92±0.20% respectively). This percentage was at least 20% lower in Ampli1, MALBAC and SurePlex amplified samples. Considering regions covered with a minimal depth of 10X and 20X, the coverage decreases for all methods. For bulk DNA, the decrease is however smaller compared to the WGA methods. For REPLI-g, the decrease is smaller compared to the other WGA methods. Figure 3 shows what percentage of targeted bases is covered at a minimal read depth range between 1 and 60. The plot shows again that more targeted bases are covered at a higher depth when sequencing bulk DNA. Comparing the WGA methods, REPLI-g results in the highest percentage of targeted bases that are covered at higher depth. The plot also shows the decline in covered targeted bases when considering higher depths. This decline is less steep for bulk DNA and REPLI-g compared to the other WGA methods.

4.2. SNP analysis

The online sequencing data for the Platinum Genome of the NA12882 cell line was mapped against the hg19 reference genome. An in-silico capture was performed on this mapping by isolating the reads aligning inside TruSight target regions. The SNPs called from this data are considered the reference set and were used to calculate the sensitivity and FDR for the samples (Table 2). The bulk DNA samples closely resembled the reference set, with a 96.8 ±0.2% sensitivity and a FDR of only 1.5±0.05%. This reflects a good performance of the capture kit when performed on unamplified DNA as specified in the kit's manual. REPLI-g amplified samples, with a sensitivity of 93.3±1.52% and FDR of 3.0±1.2%, were the only WGA samples that performed nearly as good as the bulk DNA samples. All other WGA methods had a low sensitivity and a high FDR, indicating unreliable results. MALBAC amplified samples had the lowest sensitivity (65.7±14.3%) and the highest FDR (49.6±15.8%). Ampli1 and SurePlex were positioned somewhere in between. SurePlex amplification had a sensitivity of 74.2±2.2% and an FDR of 36.8±8.2%, while Ampli1 had a comparable sensitivity of 73.9±0.5% but a lower FDR of 20.7.±4.2%. SNP analysis reflects the representation bias observed for the Ampli1, MALBAC and SurePlex samples. REPLI-g is the only WGA method producing SNP discovery results close to the bulk DNA samples.

The SNP calls were compared within the replicate samples for each WGA method. The 3 REPLI-g replicates had 6688 true positives and 67 false positives in common, comprising 93.7±1.80% and 32.8±12.05% respectively of the total number of true/false positives for each replicate. Of the common SNP calls, 99.01% are true positives, while 0.99% are false positives. These results were similar to those of the 4 bulk samples, in which 99.2 % of the common SNP calls are true positives and 0.77% are false positives. This indicates that the detected false positives are not

consistent between all replicates, but are introduced more randomly than true positives. True positives on the other hand, are highly consistent between these replicates. These results, as well as those for the other WGA methods are included in Supplementary Table 1.

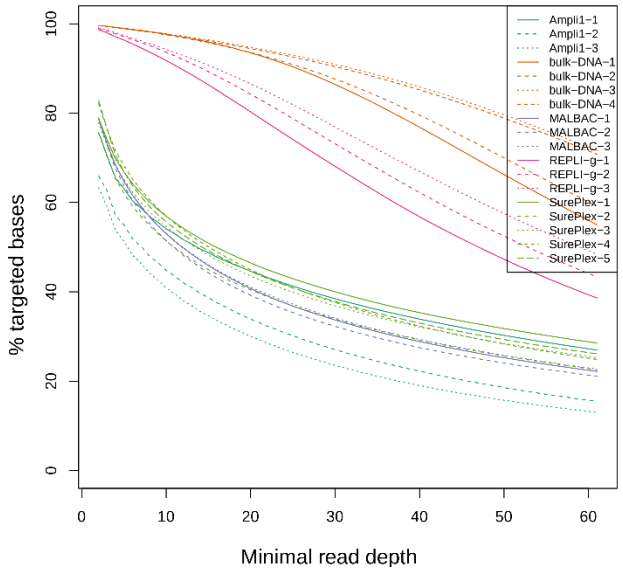

Figure 3: Percent target coverage at various minimum read depths.

Table 2: SNP analysis

	True positives	*False negatives*	*False positives*	*Sensitivity (%)*	*FDR (%)*	*No data in sample*	*No data in reference*
Bulk DNA-1	7480	252	111	96.7	1.5	32	0
Bulk DNA-2	7477	256	108	96.7	1.4	31	0
Bulk DNA-3	7501	226	118	97.1	1.5	37	1
Bulk DNA-4	7479	253	116	96.7	1.5	32	0
Ampli1-1	4415	1517	1501	74.4	25.4	1832	0
Ampli1-2	3762	1327	904	73.9	19.4	2675	0
Ampli1-3	3642	1311	768	73.5	17.4	2811	0
MALBAC-1	3057	3169	6076	49.1	66.5	1538	2
MALBAC-2	4647	1624	2527	74.1	35.2	1493	0
MALBAC-3	4665	1659	4177	73.8	47.2	1440	0
REPLI-g-1	6980	643	325	91.6	4.4	141	4
REPLI-g-2	7199	452	202	94.1	2.7	113	3
REPLI-g-3	7229	438	150	94.3	2.0	97	1
SurePlex-1	4755	1528	3350	75.7	41.3	1481	0
SurePlex-2	4381	1711	3486	71.9	44.3	1672	0
SurePlex-3	4679	1556	2862	75.0	38.0	1529	0
SurePlex-4	4979	1524	1479	76.6	22.9	1261	0
SurePlex-5	4729	1850	2808	71.9	37.3	1185	0

Unamplified samples are already being analyzed using TruSight One in a clinical setting. Our analysis shows similar results when performing TruSight One after REPLI-g WGA on 3 cells. This shows the potential to perform this analysis on biopsied trophoblast cells in a PGD setting. A thorough clinical validation of this technique will be essential to reveal if REPLI-g WGA combined with target capture panels such as TruSight One can be used in PGD for SGD diagnosis.

5. Supplementary information

Supplementary figure 1: Read distribution.

Read depth calculated in 1kb sliding windows across the concatenated target regions for replicate 2 and 3 of each method.

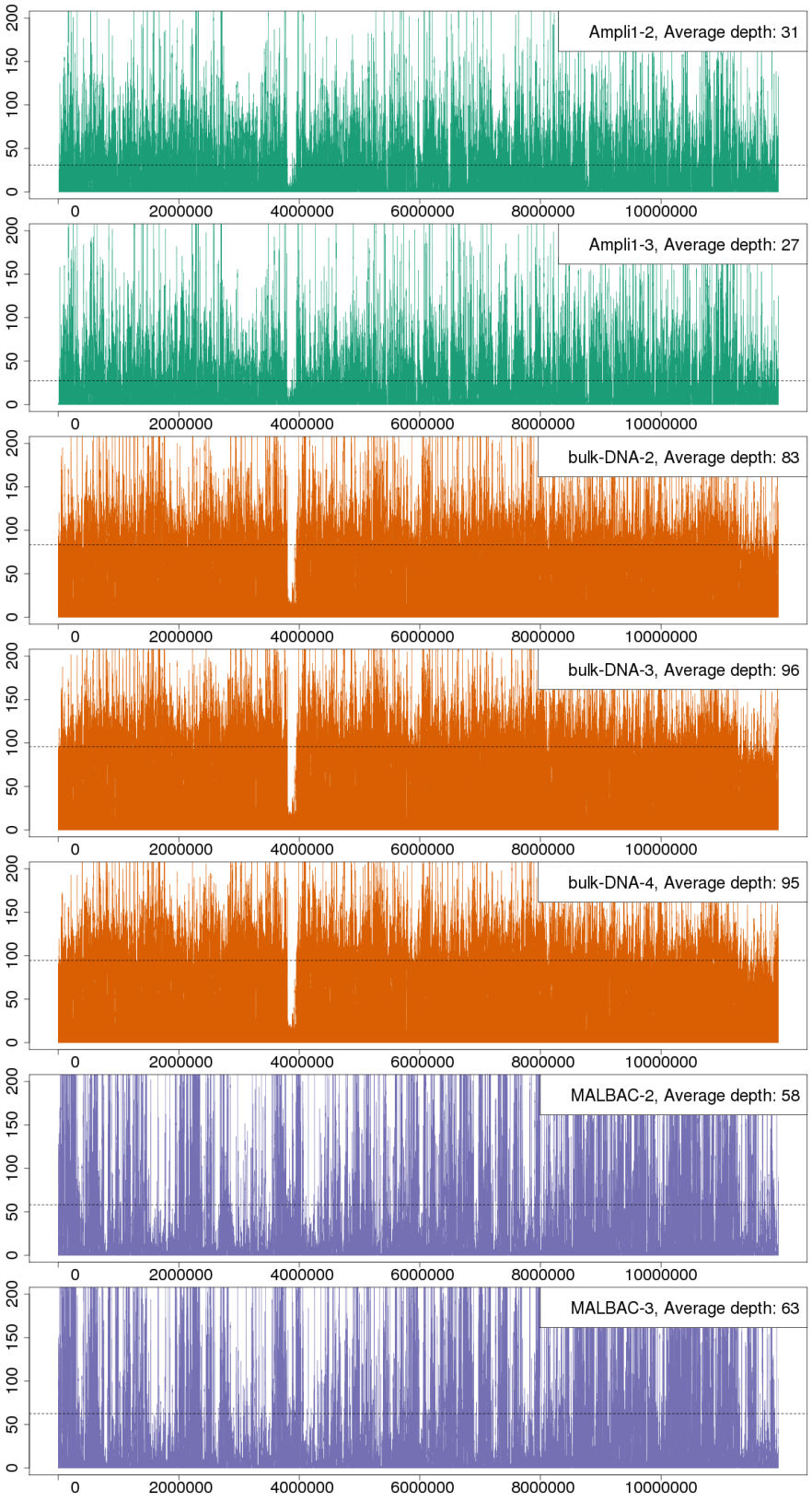
Ampli1-2, Average depth: 31
Ampli1-3, Average depth: 27
bulk-DNA-2, Average depth: 83
bulk-DNA-3, Average depth: 96
bulk-DNA-4, Average depth: 95
MALBAC-2, Average depth: 58
MALBAC-3, Average depth: 63
0
50
100
150
200
0
2000000
4000000
6000000
8000000
10000000

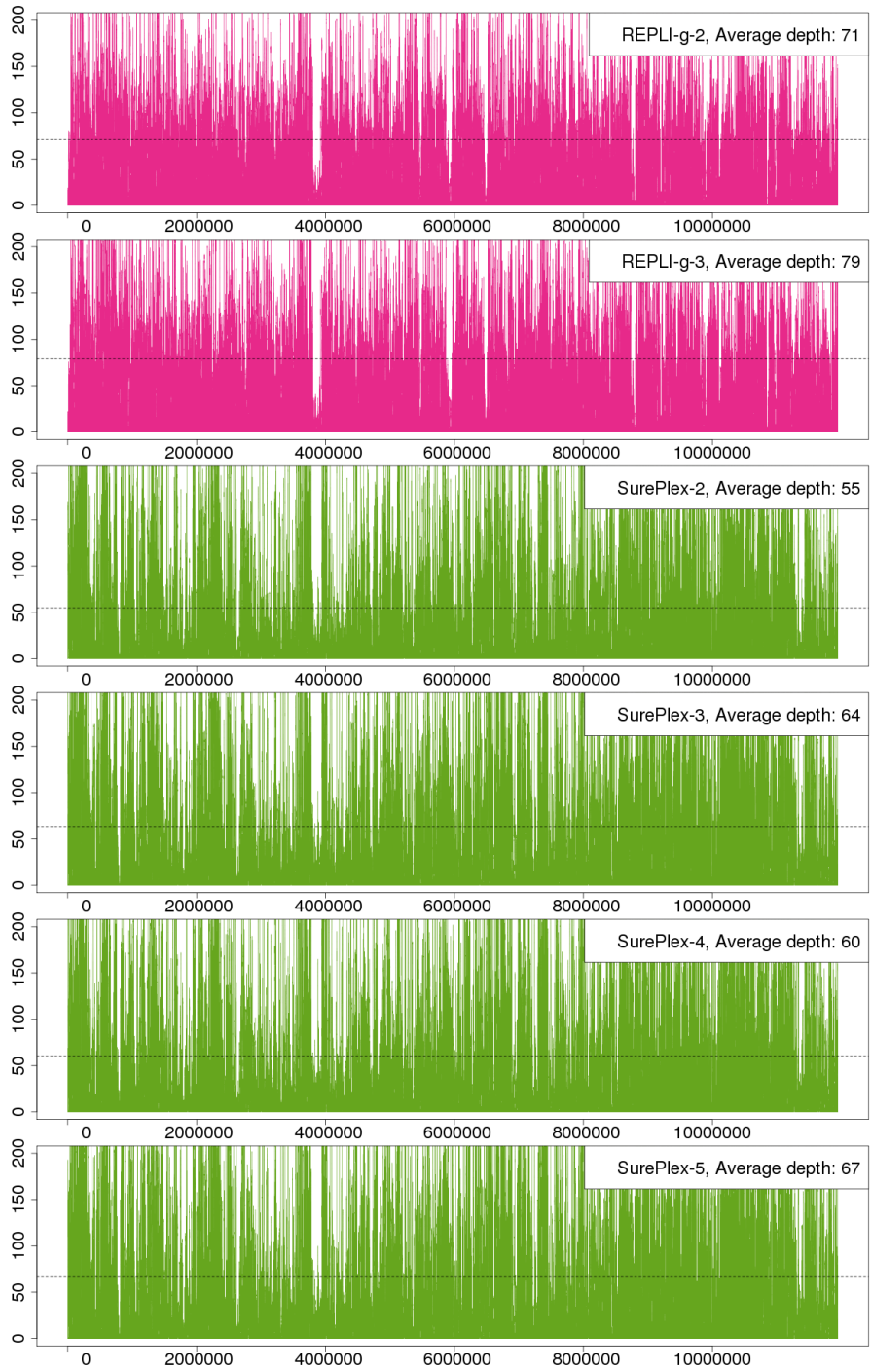
REPLI-g-2, Average depth: 71
REPLI-g-3, Average depth: 79
SurePlex-2, Average depth: 55
SurePlex-3, Average depth: 64
SurePlex-4, Average depth: 60
SurePlex-5, Average depth: 67
0
50
100
150
200
0
2000000
4000000
6000000
8000000
10000000

Supplementary table 1: SNP detection concordance between replicates per WGA method

	Replicate	Number of SNP's	Common SNP's	% of total SNP's	Number of TP	Common TP	% of total TP	Number of FP	Common FP	% of total FP
Bulk DNA-1	1	7591	7383	97.3	7480	7326	97.9	111	57	51.4
Bulk DNA-2	2	7585	7383	97.3	7477	7326	98.0	108	57	52.8
Bulk DNA-3	3	7619	7383	96.9	7501	7326	97.7	118	57	48.3
Bulk DNA-4	4	7595	7383	97.2	7479	7326	98.0	116	57	49.1
Average±SD				97.2±0.19			97.9±0.14			50.4±2.07
Ampli1-1	1	5916	3053	51.6	4415	2979	67.5	1501	74	4.9
Ampli1-2	2	4666	3053	65.4	3762	2979	79.2	904	74	8.2
Ampli1-3	3	4410	3053	69.2	3642	2979	81.8	768	74	9.6
Average±SD				62.1±9.26			76.2±7.61			7.6±2.41
Malbac-1	1	9133	2339	25.6	3057	2316	75.8	6076	23	0.4
Malbac-2	2	7174	2339	32.6	4647	2316	49.8	2527	23	0.9
Malbac-3	3	8842	2339	26.5	4665	2316	49.6	4177	23	0.6
Average±SD				28.2±3.81			58.4±15.07			0.6±0.25
RepliG-1	1	7305	6755	92.5	6980	6688	95.8	325	67	20.6
RepliG-2	2	7401	6755	91.3	7199	6688	92.9	202	67	33.2
RepliG-3	3	7379	6755	91.5	7229	6688	92.5	150	67	44.7
Average±SD				91.8±0.64			93.7±1.80			32.8±12.05
SurePlex-1	1	8105	3393	41.9	4755	3376	71.0	3350	17	0.5
SurePlex-2	2	7867	3393	43.1	4381	3376	77.1	3486	17	0.5
SurePlex-3	3	7541	3393	45.0	4679	3376	72.2	2862	17	0.6
SurePlex-4	4	6458	3393	52.5	4979	3376	67.8	1479	17	1.1
SurePlex-5	5	7537	3393	45.0	4729	3376	71.4	2808	17	0.6
Average±SD				45.5±4.13			71.9±3.35			0.7±0.25

Chapter IX: Short Tandem Repeat analysis after single-cell Whole Genome Amplification

Lieselot Deleye[1,#], Ann-Sophie Vander Plaetsen[1,#], Jana Weymaere[1], Dieter Deforce[1,†], Filip Van Nieuwerburgh[1,†,*]

[1]Laboratory of Pharmaceutical Biotechnology, Ghent University, Ottergemsesteenweg 460, 9000 Ghent, Belgium

[#] These authors contributed equally: L.D. and A.V.P did the set-up, the practical part, data acquisition, data analysis and data interpretation of this project.
[†] These authors jointly supervised.

Scientific Reports; peer reviewed.

1. Abstract

To allow multiple genetic analyses on a single cell, whole genome amplification (WGA) is required. Unfortunately, studies comparing different WGA methods for downstream human identification STR analysis remain absent. Therefore, the aim of this work was to assess the performance of four commercially available WGA kits for downstream human identification STR profiling. The performance was assessed using single or three cells as input. REPLI-g showed a very low dropout rate, as it was the only WGA method in this study that could provide a complete STR profile in some of its samples. Although Ampli1, DOPlify and PicoPLEX do not detect all selected STR markers, they seem suitable for genetic identification in single-cell clinical applications.

2. Introduction

Whole genome amplification (WGA) is unavoidable to allow multiple genetic analyses on single or a low number of cells. WGA increases the amount of input-DNA from pg-level up to ng- or µg-level. However, it is well known that a lot of WGA methods introduce bias during amplification and thereby influence the results of downstream genetic analyses (218, 219). The specific type of bias that is introduced, depends on the WGA method used. Therefore, the WGA method must be chosen according to the downstream application. Some methods will result in a non-uniform coverage, while others will introduce more nucleotide errors (130). A lot of research has already been performed on the influence of WGA on copy number variant (CNV) analysis (187, 197, 199, 209, 220, 221) and targeted genotyping analysis (209). However, studies comparing different WGA methods for human identification short tandem repeat (STR) analysis of a single or a limited number of cells have not been performed so far.

The growing interest in single-cell analysis for clinical applications raises the need to identify single cells. STR analysis for human identification DNA profiling is such a genetic analysis that is often performed on only a limited number of cells. STRs are short DNA-fragments with different lengths (between 100 and 500 base pairs) within the population. A multiplex-PCR is performed to analyze a standard set of STR loci and to create an STR profile. Except for identical twins, each person has a unique STR profile. Single-cell DNA profiling is particularly valuable in the context of cell-based non-invasive prenatal testing. As no specific fetal cell marker has been discovered so far, after the isolation of a single fetal cell from a maternal blood sample, the fetal identity of this cell needs to be confirmed prior to further downstream procedures. This way, maternal cell contamination in the sample can be excluded. Other clinical applications, such as preimplantation genetic diagnosis (PGD), might also apply STR analysis, to assure the nature of the isolated cells (222). After fetal confirmation, genetic analysis such as CNV analysis is performed on this unique cell. Hence, to allow both STR and CNV analysis on a single cell, WGA is required.

Unfortunately, a WGA method that is ideal for STR genotyping might be less suitable for CNV analysis. For example, previous research by Denis *et al.* demonstrates that multiple displacement amplification (MDA) WGA might be

applicable in forensic STR analysis (222). In contrast, MDA is not considered the most preferable WGA method for CNV analysis, as shown in Chapter VII (220). The aim of this work was to assess the performance of four commercially available WGA kits for downstream human identification STR. Ampli1 WGA Kit, DOPlify WGA, REPLI-g Single Cell Kit and PicoPLEX WGA Kit were compared in parallel for their ability to produce WGA product, adequate for human identification STR analysis. REPLI-g single cell kit (Qiagen, Hilden, Germany) is based on this MDA mechanism and has already been shown useful for STR analysis (222). PicoPLEX WGA Kit (Rubicon Genomics Inc., MI 48108, USA) is a hybrid MDA-PCR based WGA method that uses self-inert degenerate primers. During the multiple displacement pre-amplification, an *in vitro* hairpin template library is created, which can then be amplified in a PCR reaction using flanking universal priming sites. PicoPLEX WGA kit has been widely used and the suitability of this kit for CNV analysis on a limited number of cells has been proven by several studies. Ampli1 WGA Kit (Silicon Biosystems, Castel Maggiore, Italy) is a ligation-adapter PCR based WGA method that utilizes a frequent cutter restriction enzyme for the initial fragmentation of the DNA template. One single highly specific primer, complementary to the adapters that are ligated on both sides of each DNA fragment, initiates the following PCR amplification reaction. This ligation based WGA method has already been successfully applied in a cell-based NIPT context. The most recently developed DOPlify WGA kit (Reproductive Health Science, Thebarton, Australia) uses an advanced Degenerate Oligonucleotide Primed PCR (DOP-PCR). In the past, the classical DOP-PCR did not result in reliable CNV or STR analysis (200). Nevertheless, DOPlify Reaction Kit is an advanced version of this classical DOP-PCR and has recently shown promising results for CNV analysis, with minimal bias introduction (Chapter VII). This kit has not yet been tested in the context of STR profiling.

Samples consisting of one or three cells, in triplicate, were collected from a B-lymphoblastoid cell line (B-LCL) using micromanipulation. As many clinical applications are based on single-cell analysis, single-cell samples are used as input in this study. Three-cell samples are included to detect possible differences in the performance of STR analysis after WGA on a few cells compared to a single cell. The lymphoblastoid cell line is representative for most human cells and is ideal as a reference for STR analysis, as it is diploid without any genomic aberrations. The samples were amplified using the four above-mentioned WGA kits and for each sample, a selection of 14 STR loci and the Amelogenin locus were amplified in a multiplex PCR reaction. A bulk DNA sample from the B-LCL was included in the STR-PCR reaction and used as a reference STR-profile against which all sample results were compared.

3. Materials and methods

3.1. Experimental design

In this study, the performance of four WGA kits was examined for STR-genotyping of a limited number of cells from a male B-lymphoblastoid cell line (B-LCL), NA12882. This suspension cell line allowed for isolation of individual cells using micromanipulation. Samples consisting of 1-or 3- cells, in triplicate, were collected for each WGA method.

In parallel, a bulk DNA sample from the cell line was extracted. The 1- and 3-cell samples were amplified using the Ampli1 WGA Kit, DOPlify WGA, REPLI-g Single Cell Kit and PicoPLEX WGA Kit. STR-genotyping was performed on all WGA amplified DNA samples and the bulk sample. The STR-profile from the bulk DNA sample, served as a reference to which all STR-profiles were compared (Figure 1).

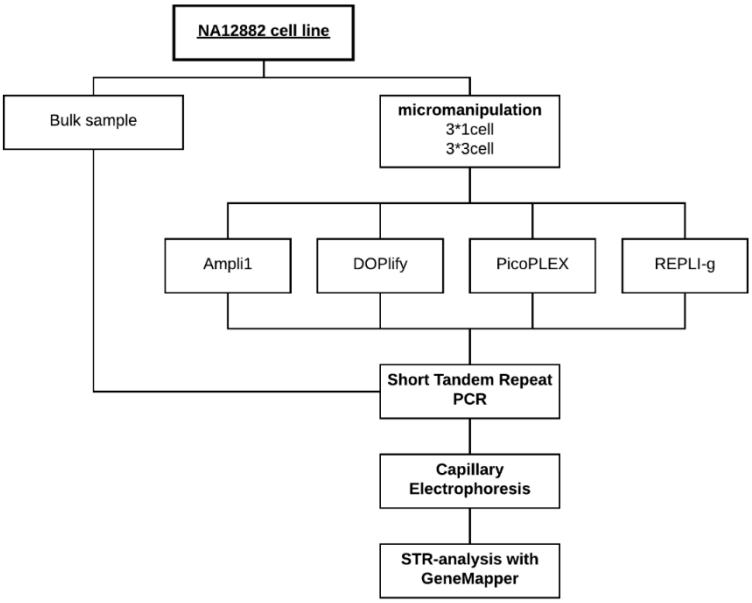

Figure1: Schematic overview of experimental design

A positive control containing saliva was included during STR-PCR to verify the success of the STR-multiplex PCR reaction. A negative control, consisting of H_2O, was included to detect contamination introduced during the STR-PCR.

3.2. Cell culture and isolation

The cells from the B-lymphoblastoid cell line (NA12882), acquired from Coriell Institute for Medical Research (Camden, USA), were grown in Roswell Park Memorial Insititute (RPMI-1640) medium (Life technologies, Carlsbad, USA). This cell medium was supplemented with 15% fetal bovine serum (Life Technologies, Carlsbad, USA), 2mM L-glutamine (Life technologies, Carlsbad, USA) and a mix of penicillin at 100 units/mL and streptomycin at 100 µg/mL (Life technologies, Carlsbad, USA). Cells were cultured at a temperature of 37°C and a 5% CO_2 level. For the micromanipulation of a limited number of cells, an ergonomic denuding handle from STRIPPER (Origio, Måløv, Denmark) and MXL3-100 needles with a diameter of 100µM (Origio, Måløv, Denmark) were used. Starting from a small 10µl spot of cell suspension, a serial dilution was made with sterile phosphate buffered saline (PBS) (Life technologies, Carlsbad, USA) on a Petri dish (5.5cm). Subsequently, the desired amount of cells were picked in a maximum volume of 2.5µL PBS under an Axiovert 25 light microscope (Zeiss, Jena, Germany) and were immediately

transferred to a 0.2mL PCR reaction tube on ice. A bulk DNA sample from the NA12882 cell line was prepared using the DNeasy Blood & Tissue kit (Qiagen, Hilden, Germany) on ± $5*10^6$ cells.

3.3. Whole genome amplification

Cell lysis and amplification for Ampli1 WGA Kit (Silicon Biosystems, Castel Maggiore, Italy), DOPlify WGA (Reproductive Health Science, Thebarton, Australia), REPLI-g Single Cell Kit (Qiagen, Hilden, Germany) and PicoPLEX (Rubicon Genomics Inc., MI 48108, USA) WGA Kit, was performed according to manufacturer's recommendations. A positive control containing ±30pg high quality DNA (Human Genomic DNA, Roche, 100µg (500µl)) was included during each WGA reaction. This control sample was used to check the performance of the WGA kit, without the influences of cell isolation, cell lysis and DNA extraction. A negative control, consisting of 1µl of H_2O, was added to detect contamination introduced during the WGA. The amplified DNA was purified using the Genomic DNA Clean & Concentrator kit (version 1.0.0, Zymo Research, Irvine, USA) using 5x binding buffer, following manufacturer's instructions. DNA concentration was determined using the Qubit dsDNA High Sensitivity Assay kit (Life technologies, Carlsbad, USA).

3.4. STR-genotyping

Purified DNA samples were used as template for the in house multiplex STR-PCR, based on the Promega Powerplex. This multiplex-PCR was used to simultaneously amplify 14 STR loci across the human genome: D3S1358, TH01, D21S11, D18S51, vWA, D8S1179, TPOX, FGA, D5S818, D13S317, SE33, CD4, D7S820, D16S539, and Amelogenin for sex determination. The total volume in each reaction mix was 50µL, containing 2.5U Hotstar Taq polymerase (Qiagen, Hilden, Germany), 0.5 mM $MgCl_2$ (Qiagen, Hilden, Germany), 0.4µg/µL albumin (Sigma-Aldrich, Saint Louis, USA), 1x PCR buffer (Qiagen, Hilden, Germany), 0.15µM-1µM of each primer and 30µL of purified DNA. Supplementary table S1 shows the exact concentrations used for each primer. Respectively 1ng, 1ng, 5ng and 4ng purified DNA from Ampli1, DOPlify, PicoPLEX and REPLI-g amplification product was added to the reaction mixture. The multiplex-PCR was performed in a SimpliAmp Thermal Cycler (Life Technologies, Carlsbad, USA) with an initial denaturation step at 95°C for 15 min, followed by 28 amplification cycles of 94°C for 1 min, 58°C for 1 min and 72°C for 1 min 20 s. A final elongation step at 72°C for 10 min was added. As a positive control, 30µL of a 1:10 dilution of saliva, was used, whereas for the negative control, the sample was replaced by 30µL of H_2O.

3.5. STR-Genotyping analysis

STR profiles for all samples, including the bulk DNA sample, were generated with capillary electrophoresis using the ABI 3500 Genetic Analyzer equipped with GeneMapper ID-x 1.2 software (Applied Biosystems, Carlsbad, USA) following manufacturer's recommendations. A detection threshold of 50 RFU was used to indicate allele peaks. The total dropout rate (DO%) was assessed for all samples and compared between the four WGA methods as well as

between the 1- and 3-cell samples per WGA method. The DO% indicates how many of the expected alleles are missing on the STR profile. The dropout rate was calculated based on the following formula:

$$\left[1 - \left(\frac{total\ number\ of\ observed\ alleles}{total\ number\ of\ expected\ alleles}\right)\right] \times 100\%$$

4. Results & Discussion

4.1. DNA yield

After WGA, the DNA yield was assessed and compared between the four WGA methods (Table 1). The yield was similar for Ampli1, DOPlify and PicoPlex, except for two single cell samples from Ampli1. All samples, except those two, contained ± 1000 ng of DNA. The yield after REPLI-g was considerably higher than the other WGA methods. Yields after either one- or three-cell amplification do not differ significantly for all tested WGA methods.

WGA method	Sample		Concentration (ng/µL)	DNA yield (ng)
Ampli1 WGA kit	1-cell	1	6.14	190.34
		2	37.80	1171.80
		3	18.04	559.24
	3-cell	1	42.00	1302.00
		2	59.40	1841.40
		3	33.00	1023.00
DOPlify reaction kit	1-cell	1	32.60	1010.60
		2	32.60	1010.60
		3	31.60	979.60
	3-cell	1	30.60	948.60
		2	33.40	1035.40
		3	35.40	1097.40
PicoPLEX WGA kit	1-cell	1	60.80	1884.80
		2	52.80	1636.80
		3	54.80	1698.80
	3-cell	1	60.60	1878.60
		2	33.00	1023.00
		3	57.40	1779.40
REPLI-g Single Cell kit	1-cell	1	1200.00	37 200.00
		2	604.00	18 724.00
		3	690.00	21 390.00
	3-cell	1	438.00	13 578.00
		2	384.00	11 904.00
		3	516.00	15 996.00

Table 1: DNA yield after WGA amplification for each used method

The absence of contamination after Ampli1, DOPlify and PicoPLEX WGA was proven by the negligible DNA yield in their respective negative control. However, the negative control from REPLI-g resulted in a concentration of more than 1000 ng/µl. According to the kit's manual, the presence of high DNA yield in negative controls is caused by the

random extension of primer dimers in the absence of a template, generating high-molecular-weight product. The yield for all positive controls was similar to the yield of the cell samples of the corresponding WGA methods.

Overall, the yield after WGA did not indicate any problems during amplification and was certainly high enough to perform both STR analysis and other conceivable downstream genetic analyses.

4.2. Dropouts in STR profiles

The STR profiles of the samples were compared to the reference STR profile of the bulk sample from the NA12882 cell line. The reference profile and the profiles of all samples are shown in Supplementary Figure S1 and S2 respectively. Figure 2 shows for each sample which loci were called in accordance to the reference. Green represents correctly called loci, orange represents an allelic dropout at a heterozygous locus (only one allele of two missing), and red indicates a complete locus dropout (complete locus is missing). The dropout rate was calculated for each sample. The average dropout rate and standard deviation for the different WGA methods is shown in Figure 3.

For REPLI-g WGA, the generated STR profiles were almost identical to the reference profile. Consequently, the dropout rate for single- and three-cell samples amplified with REPLI-g was only 8.33 % ± 11.48 and 2.38 % ± 2.06, respectively. One single-cell sample showed two locus dropouts and three allelic dropouts, while the other REPLI-g samples showed no or maximum one dropout in their STR profile. The dropout rate for samples amplified with Ampli1, DOPlify and PicoPLEX was distinctly higher compared to REPLI-g. In the Ampli1 samples, the dropout seems consistent for certain loci, as a recurrent locus dropout at the same 6 loci was observed in almost all samples. No alleles were detected in all Ampli1 samples for D18S51, AMEL, D8S1179, TPOX, FGA and D7S820 with exception of one single-cell sample showing an allelic dropout for FGA instead of a locus dropout. The dropout rate for single- and three-cell Ampli1 amplification was 60.71 % ± 22.30 and 44.05 % ± 2.06, respectively. The dropout after PicoPLEX and DOPlify WGA seemed more random across the different loci, although some consistency among the samples was noticeable. A dropout for the vWA and D5S818 locus was observed in almost all PicoPLEX samples, whereas for DOPlify almost all samples showed a dropout for TPOX, D7S820 and D16S539. After PicoPLEX WGA, one sample failed to show an STR profile. Therefore, this sample was omitted from the dropout rate calculation for PicoPLEX. Apart from this sample, PicoPLEX samples showed less dropouts compared to both Ampli1 and DOPlify with a dropout rate of 35.71 % ± 3.57 after single-cell amplification and 16.07 % ± 0.00 after three-cell amplification. The dropout rate for DOPlify was 59.52 % ± 12.54 for single-cell samples, whereas for three-cell samples a dropout rate of 34.52 % ± 2.06 was calculated.

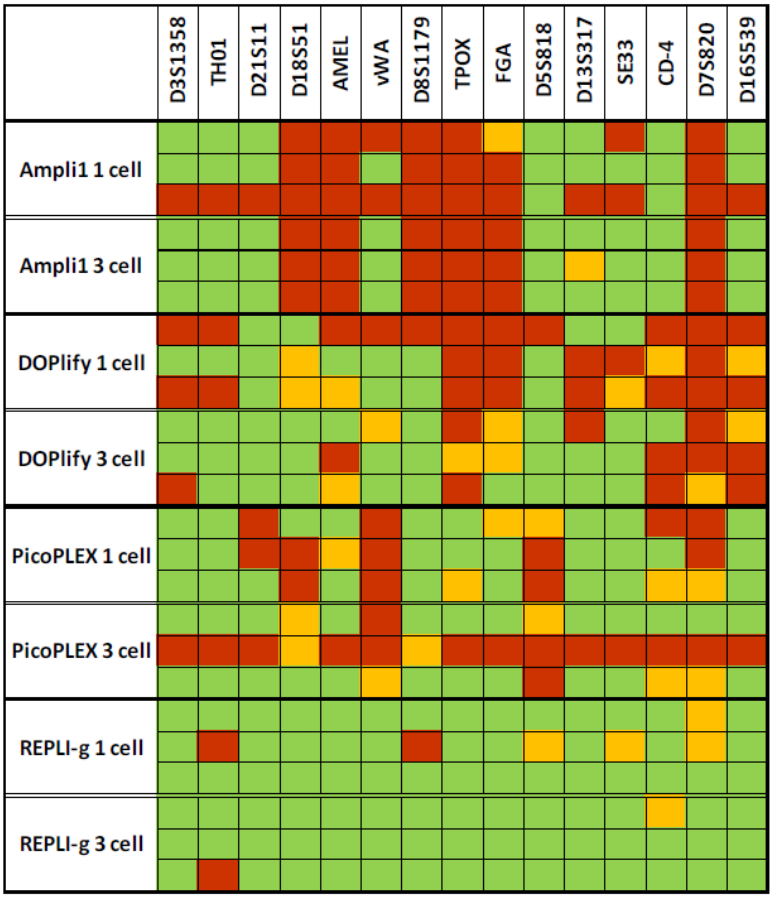

Figure 2: Overview of dropouts in STR profile for each WGA method

This figure illustrates which loci were called in each sample. Green represents correctly called loci; Orange represents an allelic dropout at a heterozygous locus; Red illustrates a complete locus dropout.

Previous studies already indicated that MDA is suitable for STR analysis, but no comparison has been made with other modern WGA techniques. We observed that the MDA method used in this study, REPLI-g, was the only WGA that resulted in complete STR profiles for some of its samples. Because of the branched network formation during WGA, this MDA technology amplifies more regions. Therefore, it is more likely that all STR loci are included during amplification. The recurrent locus dropout of Ampli1 may also be related to its WGA working mechanism. The restriction enzyme might cleave at the STR primer binding sites of these loci, which inhibits their amplification. Therefore, the results for Ampli1 could possibly improve if other loci were selected for STR analysis. PicoPLEX showed slightly better results than both Ampli1 and DOPlify, but the amplification protocol seems less robust, as one of its samples failed to show an STR profile. The pre-amplification during the PicoPLEX amplification protocol uses the MDA technology, which might explain why PicoPLEX is the second best WGA for STR analysis. However, PicoPLEX uses another polymerase than the one used by REPLI-g and no large, branched network is formed during pre-amplification. The four WGA methods showed a slightly better STR profile and less variability between individual samples after three-cell amplification compared to single-cell amplification.

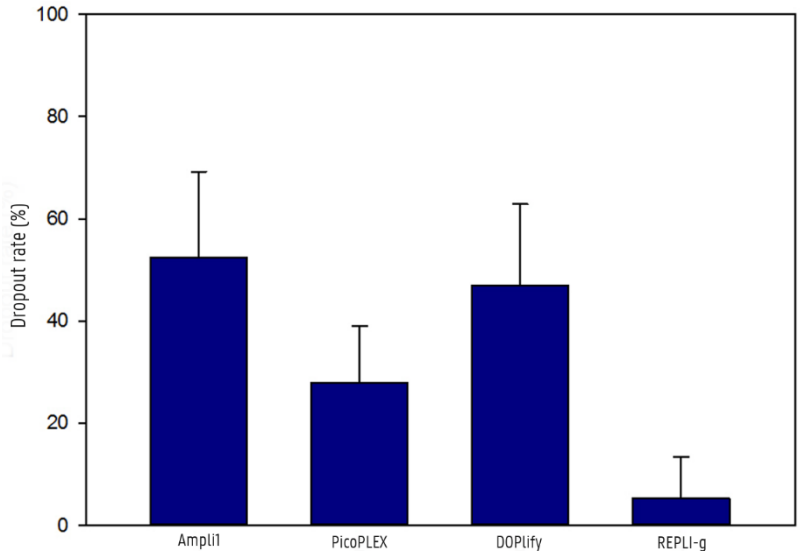

Figure 3: Average Dropout rates per WGA

Nevertheless, in the context of cell-based NIPT, fetal cell identification would also be possible from a partial STR profile. Therefore, Ampli1, PicoPLEX and DOPlify are also suitable for genetic identification in cell-based NIPT or other clinical genetic identification purposes, despite the fact that in most samples only half of the STR markers were detected. In cell-based NIPT or PGD, the WGA products are mainly intended for downstream genetic analysis, such as CNV detection. Therefore, beside STR analysis the WGA product must also be suitable for CNV analysis. REPLI-g showed its suitability for CNV detection on a limited number of cells at a resolution of 3 Mb earlier, but did introduce some representation bias. DOPlify introduced almost no representation bias for CNV calling in that context, but its STR profiling resulted in more dropouts compared to REPLI-g. Both Ampli1 and PicoPLEX showed slightly more representation bias compared to DOPlify for CNV calling, but less compared to REPLI-g.

5. Conclusion

We can conclude that DNA from a limited number of cells is suited for STR profiling after WGA, but the quality of the results will depend on the selected WGA method. REPLI-g has a very low dropout rate, as it is the only method in this study that could provide, in at least some of the samples, a complete STR profile. Although Ampli1, DOPlify and PicoPLEX do not detect all selected STR markers, they seem suited for genetic identification in single-cell clinical applications such as cell-based NIPT.

6. Supplementary information

Supplementary Table S1: Concentration of the STR primers in each PCR reaction mixture

Primer	Concentration	
SE33 F	0,5000	µM
SE33 B	1,0000	µM
D5S818 F	0,5000	µM
D5S818 B	0,5000	µM
FGA F	0,5000	µM
FGA B	0,5000	µM
D13S317 F	0,5000	µM
D13S317 B	0,5000	µM
vWA F	0,5000	µM
vWA B	0,5000	µM
D18S51F	0,5000	µM
D18S51 B	0,5000	µM
Amel F	0,5000	µM
Amel B	0,5000	µM
D21S11 F	0,5000	µM
D21S11 B	0,5000	µM
D3S1358 F	0,5000	µM
D3S1358 B	0,5000	µM
Tho1P16 F	0,5000	µM
Tho1P16 B	0,5000	µM
TPOX F	0,2500	µM
TPOX B	0,2500	µM
D7S820 F	0,6000	µM
D7S820 B	0,6000	µM
D16S539 F	0,8000	µM
D16S539 B	0,8000	µM
D8S1179 F	1,0000	µM
D8S1179 B	1,0000	µM
CD4 F	0,1500	µM
CD4 B	0,6000	µM

Supplementary Figure S1: STR profile from an unamplified bulk sample from the NA12882 cell line.

One peak represents a homozygous locus, whereas two peaks represent a heterozygous locus. The colored box above the peaks indicate the STR markers detected at that locus.

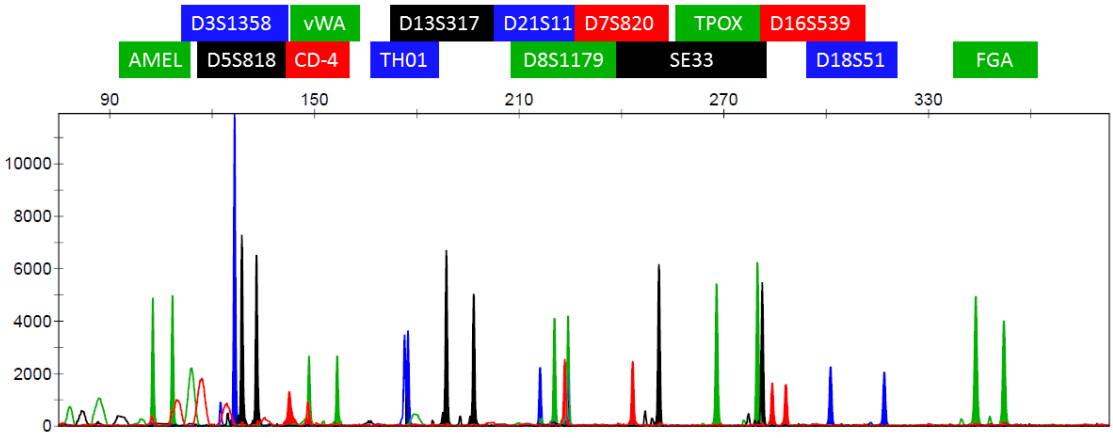

Chapter X: STR profiling and copy number variation analysis on single, preserved cells using current whole genome amplification methods

Lieselot Deleye[1,#], Ann-Sophie Vander Plaetsen[1,#], Senne Cornelis[1,2], Laurentijn Tilleman[1], Filip Van Nieuwerburgh[1,†,*], Dieter Deforce[1,†]

[1]Laboratory of Pharmaceutical Biotechnology, Ghent University, Ottergemsesteenweg 460, 9000 Ghent, Belgium
[2]Department of Life Science Technologies, Imec, 3001 Leuven, Belgium.
[#] These authors contributed equally: L.D. and A.V.P did the set-up, the practical part, data acquisition, data analysis and data interpretation of this project.
[†] These authors jointly supervised.

Scientific Reports; 7: 17189 | DOI: 10.1038/s41598-017-17525-5; Published online 07 December 2017.

1. Abstract

The growing interest in liquid biopsies for cancer research and cell-based non-invasive prenatal testing (NIPT) invigorates the need for improved single cell analysis. In these applications, target cells are extremely rare and fragile in the peripheral circulation, which makes the genetic analysis very challenging. To overcome these challenges, cell stabilization and unbiased whole genome amplification (WGA) are required. This study investigates the performance of four WGA methods on single or a limited number of cells after 24 hour of Streck Cell-Free DNA BCT preservation. The suitability of the DNA, amplified with Ampli1, DOPlify, PicoPLEX and REPLI-g, was assessed for both short tandem repeat (STR) profiling and copy number variant (CNV) analysis after shallow whole genome massively parallel sequencing (MPS). Results demonstrate that Ampli1, DOPlify and PicoPLEX perform well for both applications, with some differences between the methods. Samples amplified with REPLI-g did not result in suitable STR or CNV profiles, indicating that this WGA method is not able to generate high quality DNA after Streck Cell-Free DNA BCT stabilization of the cells.

2. Introduction

In multiple fields of life sciences, single cell analysis is crucial to study the heterogeneity of cell populations or when only a limited number of cells is available (223). This is applicable for liquid biopsies in cancer research, cell-based non-invasive prenatal testing (NIPT) and preimplantation genetic diagnosis (PGD). In the context of liquid cancer biopsies and cell-based NIPT, intact cells in the peripheral circulation are extremely rare and fragile (224, 225).

Considering a single human diploid cell contains only 6-7 pg of genomic DNA, whole genome amplification (WGA) is required to increase the amount of DNA up to ng- or µg-level when multiple genetic analyses or MPS are to be performed on a single cell. According to the manufacturer's instructions, current MPS library preparation kits require a DNA input as low as 1 ng for Nextera XT library preparation and 500 ng for standard Illumina PCR-free library preparation. Recently, several research groups have been studying the performance of different WGA methods for specific applications. As some WGA methods only perform well in certain applications, an overall best performing WGA method does not exist (130, 187, 197, 198, 200, 220, 226). The suitability of a WGA method depends on the intended downstream application. Studies demonstrate that PCR-based methods result in a more balanced genome coverage, which makes them more suitable for CNV analysis, whereas multiple displacement amplification (MDA) based methods are preferred for single nucleotide polymorphism (SNP) detection (130).

This study wants to investigate the performance of several state-of-the-art WGA methods in a setting mimicking cell-based NIPT and liquid cancer biopsy in which single cells are isolated from a patient blood sample. Cell isolation

and downstream application for genetic analysis cannot always be performed on-site and/or immediately upon blood retrieval. Therefore, the potential of transportation and longer storage without the loss of cell quality would be opportune in a clinical setting. The widely-used K_2- or K_3-EDTA blood tubes demand storage at 4°C and blood processing within 6 hours after venipuncture, before nucleated blood cell lysis occurs and cell-free DNA levels increase (227). Several alternative collection devices with cell- and/or DNA-stabilizing properties have emerged such as CellSave tubes, PAXgene tubes and Streck Cell-Free DNA BCT tubes (cfDNA BCTs). Comparative studies of their performance in the context of liquid cancer biopsy testing or cell-free NIPT, agreed that different stabilizing collection devices should be chosen according to the desired application (228-230). The cfDNA BCTs (Streck, Nebraska, USA) appeared best for this study, since the tubes are designed to prevent lysis of nucleated blood cells and circulating epithelial cells by stabilizing these cells and thereby preventing DNA release into the plasma for up to 7 days at temperatures between 15°C to 30°C (229, 230). In contrast to most fixatives, cfDNA BCT reagent claims to be a formalin-free preservative (231, 232). Formalin is known for its damage to DNA through the introduction of chemical modifications such as DNA protein denaturation, protein-DNA cross-linking and methylation of nucleic acids, which influences downstream genetic analyses (233). This formalin-free fixative might stabilize and thereby preserve desired cells without decreasing the DNA quality. As WGA performance depends on the input DNA quality, fixation might also influence the WGA. However, the exact effect on the amplification may possibly differ between the WGA methods.

In this study, the influence of 24 hour Streck Cell-free DNA BCT preservation on four different WGA methods was determined. Samples consisting of 1 or 3 cells, in triplicate, were collected from a lymphoblastoid Loucy cell line after 24 hour preservation. This cell line is valuable for CNV detection performance studies, since it shows some known aneuploidies and CNVs (≥ 3 Mb), as studied and documented in the COSMIC project (203). Four WGA kits, each representing a different WGA method, were selected from earlier performance studies for CNV analysis on single, live cells (187, 220) (Chapters III & VII). The MDA-based WGA method, REPLI-g single cell kit (Qiagen, Hilden, Germany), uses the high-fidelity enzyme, Phi29 polymerase, which holds a proofreading activity and thereby reduces the introduction of nucleotide errors during WGA. The strand displacement activity of the polymerase creates a hyper-branched DNA structure and consequently exponential amplification occurs (234). The PicoPLEX WGA Kit (Rubicon Genomics Inc., MI 48108, USA) combines MDA with standard PCR amplification, utilizing self-inert degenerate primers, which causes semi-linear amplification. PicoPLEX WGA Kit has already proven its utility in clinical settings such as PGD for the detection of CNVs (30, 32). Other PCR-based WGA methods include Ampli1 WGA Kit (Silicon Biosystems, Castel Maggiore, Italy) and DOPlify WGA (Reproductive Health Science, Thebarton, Australia). Ampli1 is a ligation-adapter PCR-based WGA method, which is characterized by an initial restriction enzyme-based fragmentation of the DNA. Therefore, Ampli1 should be more robust for fragmented or degraded DNA templates.

Latest developed DOPlify WGA is based on the straightforward degenerate oligonucleotide primed PCR (DOP-PCR). DOPlify is an advanced DOP-PCR with possibly new primers and new generation polymerases with high fidelity and proofreading activity (201).

As fetal cell isolation from the maternal blood stream is still prone to maternal cell contamination, a short tandem repeat (STR) profiling is often performed on each individual cell to exclude maternal contamination and confirm fetal identity (105). CNV analysis is necessarily for downstream genetic analysis in cell-based NIPT and liquid cancer biopsy. So, after the amplification with REPLI-g single cell kit, Ampli1 WGA Kit, DOPlify WGA and PicoPLEX WGA, both the suitability of the amplified DNA for STR genotyping and CNV detection was assessed.

3. Materials and methods

3.1. Experimental design

In the present study, the performance of four WGA methods on a limited number of cells was examined after 24 hour cell-free DNA BCT preservation (Figure 1). The suitability of the DNA for STR and CNV analysis was studied. A cell suspension from a female lymphoblastoid Loucy cell line (DSMZ, ACC394) was transferred to a cfDNA BCT tube and stored at room temperature for 24 hours (169). For each WGA method, samples consisting of 1 or 3 cells were collected, in triplicate, from this fixed cell suspension, using micromanipulation. In parallel, a bulk DNA sample from the cell line was obtained. This bulk DNA serves as a reference/golden standard to allow impartial conclusions when comparing the WGA methods. The 1- and 3-cell samples were amplified using four different WGA methods. Subsequently, human identification STR analysis, PCR-free Illumina library preparation and massively parallel sequencing (MPS) were performed on all WGA products. STR typing was also performed on the bulk DNA, in parallel, which was used as a reference profile. A reference 180K aCGH profile (Agilent Technologies) from unamplified DNA of a bulk sample of the cell line was available from a previous study (Supplementary Figure S1) (187) (Chapter III). The following reference aneuploidies and CNVs (≥ 3 Mb) were present: a deletion of an entire X-chromosome, two deletions of ±45 Mb (consists of 6 Mb and a 36.5 Mb deletion interspersed by a 2.5 Mb normal ploidy region) and 30 Mb on respectively 5q14.3-q31.1 and 5q33.1-q35.3, a deletion of ±60 Mb on 6q21-q27, a deletion of 3 Mb on 12p13.31-p13.2, a ±26 Mb duplication of 13q31.3-q34, and two deletions of 16 Mb and 3 Mb on respectively 16p13.3-p13.11 and 16q24.2q24.3. CNV calling accuracy after WGA was evaluated in Chapter VII (220) by comparing the CNV calls in all WGA samples with those called in the earlier sequenced bulk DNA sample using 1Mb windows (Supplementary Figure S2).

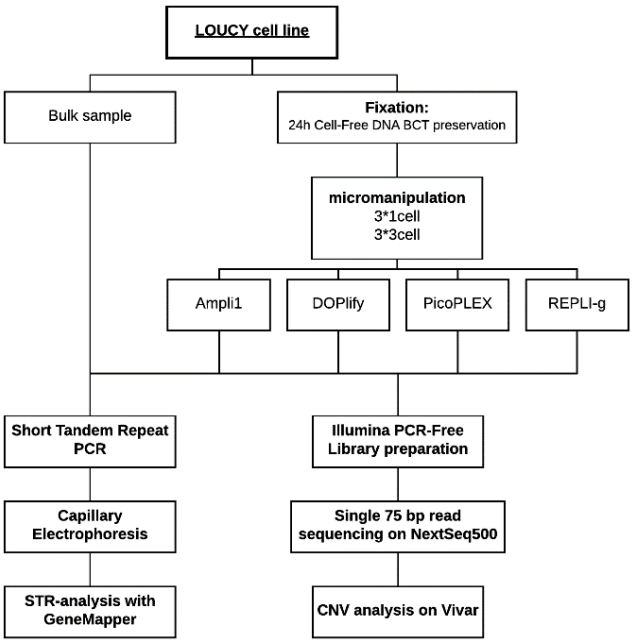

Figure 1: Experimental design.

Cells from the Loucy cell line were preserved for 24 hours in Cell-Free DNA BCT reagent. Samples consisting of 1- or 3-cells were isolated from this fixed cell suspension for each WGA method. Ampli1, DOPlify, PicoPLEX and REPLI-g were used for amplification, followed by Illumina PCR-Free library preparation and next generation sequencing. In parallel, STR-PCR and capillary electrophoresis was performed on all samples, including a bulk sample from the cell line.

A positive control containing 1µL of high quality male control DNA (Human Genomic DNA, Roche, 100 µg (500 µl)) in a concentration of 30 pg/µL was included during each WGA method. This control sample was used to evaluate the performance of the WGA kit, without the influences of cell isolation, cell lysis and DNA extraction. A negative control, consisting of 1µL H_2O, was added to detect contamination introduced during the WGA.

A positive control containing saliva was included during multiplex STR-PCR to verify the success of the PCR reaction. A no-template control (NTC) sample, consisting of H_2O, was included to rule out any non-specific amplification during STR-PCR.

3.2. Cell culture and isolation

The cells from the lymphoblastoid Loucy cell line (DSMZ, ACC394) were grown in Roswell Park Memorial Institute (RPMI-1640) medium (Life technologies, Carlsbad, USA). This cell medium was supplemented with 10 % fetal bovine serum (Life Technologies, Carlsbad, USA) and a mix of penicillin at 100 units/mL and streptomycin at 100 µg/mL (Life technologies, Carlsbad, USA). Cells were cultured at a temperature of 37°C and a 5 % CO_2 level. A Phosphate-buffered saline (PBS) suspension containing 1 * 10^6 cells in 10 mL was transferred to a cfDNA BCT tube and stored at room temperature for 24 hours. A known number of cells was isolated, using micromanipulation, in the same manner as previously described in Chapter VII (220). A bulk DNA sample from the Loucy cell line was prepared using the DNeasy Blood & Tissue kit (Qiagen, Hilden, Germany) on ± 5 * 10^6 cells.

3.3. Whole genome amplification

Cell lysis and amplification with Ampli1 WGA Kit (Silicon Biosystems, Castel Maggiore, Italy), DOPlify WGA (Reproductive Health Science, Thebarton, Australia), REPLI-g Single Cell Kit (Qiagen, Hilden, Germany), and PicoPLEX WGA Kit (Rubicon Genomics Inc., MI 48108, USA) were performed according to manufacturer's recommendations. The amplified DNA was purified using the Genomic DNA Clean & Concentrator kit (version 1.0.0, Zymo Research, Irvine, USA) using 5x binding buffer following manufacturer's instructions. DNA concentration was determined using the Qubit dsDNA High Sensitivity Assay kit (Life technologies, Carlsbad, USA).

3.4. STR-genotyping

The purified DNA samples served as template for the in-house multiplex STR-PCR assay, based on the Promega Powerplex. This multiplex PCR was used to simultaneously amplify the Amelogenin locus and 14 tetrameric STR loci across the human genome: D3S1358, TH01, D21S11, D18S51, vWA, D8S1179, TPOX, FGA, D5S818, D13S317, SE33, CD4, D7S820, and D16S539. The total volume in each reaction mix was 50µL, containing 2.5 U Hotstar Taq polymerase (Qiagen, Hilden, Germany), 0.5 mM $MgCl_2$ (Qiagen, Hilden, Germany), 0.4 µg/µL albumin (Sigma-Aldrich, Saint Louis, USA), 1x PCR buffer (Qiagen, Hilden, Germany), 0.15µM – 1µM of each primer and 30µL of purified DNA. Supplementary Table S1 shows the exact concentrations used for each primer. Respectively 1ng, 1ng, 5ng and 4ng purified DNA from Ampli1, DOPlify, PicoPLEX or REPLI-g amplification product was added to the reaction mixture. The multiplex PCR was performed in a SimpliAmp Thermal Cycler (Life Technologies, Carlsbad, USA) with an initial denaturation step at 95°C for 15 min, followed by 28 amplification cycles of 94°C for 1 min, 58°C for 1 min and 72°C for 1 min 20 s. A final elongation step at 72°C for 10 min was added. As a positive control, 30 µL of a 1:10 dilution of saliva was used, whereas for the non-template control the sample was replaced by 30 µL of H_2O.

3.5. STR-genotyping analysis

STR profiles for all samples, including the bulk DNA sample, were generated with capillary electrophoresis. Separation and analysis of the amplified PCR fragments was performed using the ABI 3500 Genetic Analyzer equipped with GeneMapper ID-x 1.2 software (Applied Biosystems, Carlsbad, USA) following manufacturer's recommendations. A detection threshold of 50 RFU was used to indicate allele peaks. The total dropout rate (DO%) was assessed for all samples and compared between the four WGA methods as well as between the 1- and 3-cell samples per WGA method. The dropout rate was calculated based on the following formula:

$$\left[1 - \left(\frac{total\ number\ of\ observed\ alleles}{total\ number\ of\ expected\ alleles}\right)\right] \times 100\%$$

In this study we analyzed the locus dropout and the allele dropout. The latter means only one allele has dropped out, whereas a locus dropout indicates the complete absence of that locus.

3.6. TruSeq DNA PCR-free HT library preparation

Fragmentation of all WGA products to a mean size distribution of 350 bp was performed using the S2 Focused Ultrasonicator with Adaptive Focused Acoustics (AFA) technology (Covaris, Woburn, USA) according to manufacturer's instructions. Resuspension buffer (provided in the TruSeq DNA PCR-free kit) was used to dilute all samples to a volume of 52.5 µL with a DNA input between 350 ng and 1 µg. Subsequently, library preparation, library quantification and single-end indexed 75 bp sequencing was performed as earlier clarified in Chapter VII (220), respectively using the TruSeq DNA PCR-free HT library preparation kit (Illumina, San Diego, USA), the Sequencing Library qPCR Quantification kit (Illumina, San Diego, USA) and a high-output NextSeq500 flow-cell (Illumina, San Diego, USA).

3.7. CNV data analysis and statistical analysis of the read count variance

CNV data analysis was performed as described in Chapter VII (220) using the ViVar Software (182). The CNV calls were detected based on the QDNAseq algorithm. The results were analyzed using 1Mb windows. The CNV profiles are visualized as line plots in which the windows are represented as dots, ordered based on their genomic position, as indicated by the x-axis. The horizontal lines refer to the segments. The alternating white and gray background identifies the chromosomes while the y-axis shows the median normalized $\log_2$ transformed read counts. Raw sequencing data are deposited in the NCBI Sequence Read Archive under project accession number PRJNA397729. On ViVar they are available under the project: Streck (https://holmes.ugent.be:9090/ViVar/)

The statistical analysis of the average read count variance between the windows across the genome was performed as described in Chapter VII (220). The following formula was used: $\frac{\sum_i^{N-1}\left(\left(\frac{x_i}{a}\right)-\left(\frac{x_{i+1}}{a}\right)\right)^2}{N}$ in which '*N*' is the number of windows, 'x_i' the read count in window *i*, 'x_{i+1}' the read count in the next window *i+1* and *'a'* the median number of reads across all windows. In this formula, the read count in each window was scaled by factor 'a', normalizing the result for the total number of reads that was sequenced for the sample. To test for significant differences of this metric between groups of samples, a Kruskal-Wallis H test was performed. This way, following groups of samples were compared: Ampli1 versus DOPlify versus PicoPLEX for 1 cell samples (N=3), for 3 cells samples (N=3), and for the 1 cell and 3 cells samples taken together (N=6). Comparisons with p-values smaller than 0.05 were considered statistically significant.

3.8. True and false positives

All genomic line profiles were checked for accurate variants. Deletions or duplications in sample CNV profiles that were also called in the reference CNV profile from the bulk DNA sample, were defined as true positives. CNV calls

that are not present in the reference CNV profile were labelled as false positives. The results were compared using 1Mb windows.

4. Results

4.1. Dropouts in STR profiles

STR profiles of the amplified samples were compared with the reference STR profile from the cell line (Supplementary Figure S3). Figure 2 illustrates which loci were called in the 1- and 3-cell samples from all four WGA methods. A locus is called correctly if indicated in green. Orange squares represent allele dropouts in which only one allele of a heterozygous locus is called. A complete locus dropout is illustrated in red.

Ampli1 showed no allele dropouts, but locus dropouts of the Amelogenin locus and the STR loci D18S51 and D7S820 were present in all samples. A locus dropout of the loci D8S1179 and FGA occurred in 5 out of 6 samples whereas a locus dropout of TPOX was present in 4 out of 6 samples. The STR profiles of the 1- and 3-cell samples were very similar. DOPlify showed 0-4 allele dropouts per sample, mainly for the loci D3S1358 and SE33. All DOPlify samples demonstrated a locus dropout of the locus TPOX, whereas the D16S539 locus dropout was present in all samples except one. The CD-4 locus dropout was only seen in the 1-cell samples. No other substantial differences were observed between the 1- and 3-cell samples. The STR profiling of the first 1-cell sample from PicoPLEX was considered as a failure because only 3 out of 15 loci were called correctly. The remaining PicoPLEX 1-cell samples showed some randomly distributed allele dropouts and a few locus dropouts. The dropout of locus D5S818 was present in all but one sample. The 3-cell samples amplified with PicoPLEX resulted in remarkably more complete STR profiles. REPLI-g resulted in unsatisfactory STR profiles with a maximum of 5 correctly called loci per sample.

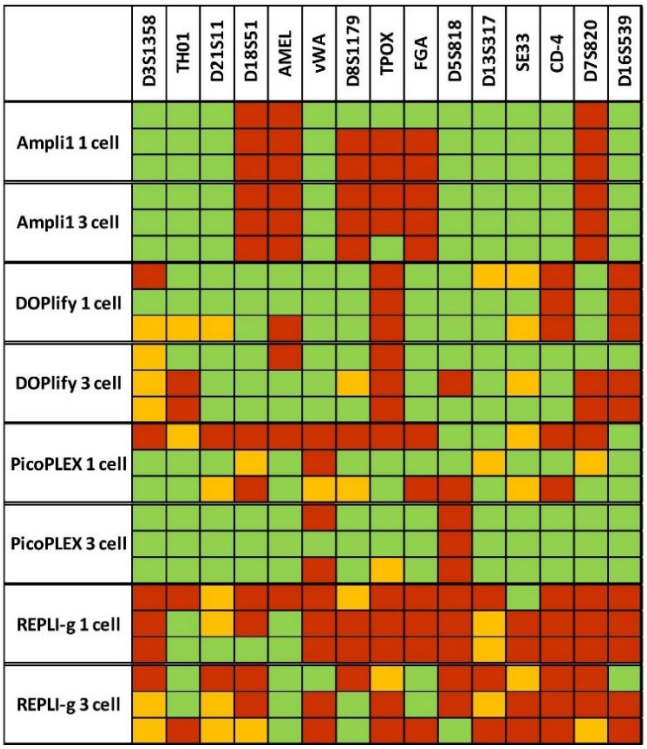

Figure 2: Overview of dropouts in STR profile for each WGA method.

This figure illustrates which loci were called in the 1- and 3-cell samples for each WGA method. Correctly called loci are indicated in green. The orange squares represent allele dropouts, whereas a complete locus dropout is illustrated in red.

Comparing the WGA methods based on the calculated dropout rate, DOPlify and PicoPLEX perform similar on 1-cell samples with a dropout rate of 28 ± 10.6 % and 28 ± 11.3 %. Ampli1 has a dropout rate of 33.3 ± 11.6 %, whereas REPLI-g has the highest dropout rate of 77.3 ± 8.3 %. For 3-cell samples, PicoPLEX excels with a dropout rate of 10.7 ± 6.1 %, followed by DOPlify and Ampli1 with respectively 30.7 ± 14.1 % and 37.3 ± 4.6 %. Again, REPLI-g shows the highest dropout rate of 65.3 ± 2.3 %. PicoPLEX and REPLI-g clearly have a lower dropout rate for 3-cell samples, whereas the number of input cells has a minor impact on Ampli1 and DOPlify, which even show a slightly higher dropout rate for 3-cell samples (Supplementary Figure S4).

4.2. Variance in read counts per window across the genome

The variance in read counts per window across the genome gives an indication for the performance of each WGA method for CNV analysis. Only when the reads are distributed uniformly across the genome, CNVs can be called truthfully. All samples amplified with Ampli1, DOPlify and PicoPLEX showed this desired uniform distribution. Unfortunately, no conventional CNV profiles resulted from the samples amplified with REPLI-g, because the variance in read counts per window was very high, indicating the reads were distributed irregularly across the genome (Supplementary Figure S5). Therefore, no further downstream (statistical) analyses were performed for REPLI-g. Figure 3 illustrates the boxplots of the average variance in read counts per 1 Mb window across the genome for all 1-cell and 3-cell samples of Ampli1, DOPlify and PicoPLEX. Regarding the 3-cell samples, the average variance in read counts was similar within these three WGA methods. For the 1-cell samples, the average variance was also similar, but the boxplots show a bigger difference in variance between the three single cell samples, especially for PicoPLEX. One PicoPLEX single cell sample showed variance that is three times higher, compared to the other PicoPLEX samples. For the 1-cell samples ($p = 0.511$) and the 3-cell samples ($p = 0.829$), the average variance in read counts per window did not differ significantly between the different WGA methods. Moreover, including all samples per WGA method (N=6), no significant difference was observed between the three WGA methods ($P = 0.834$).

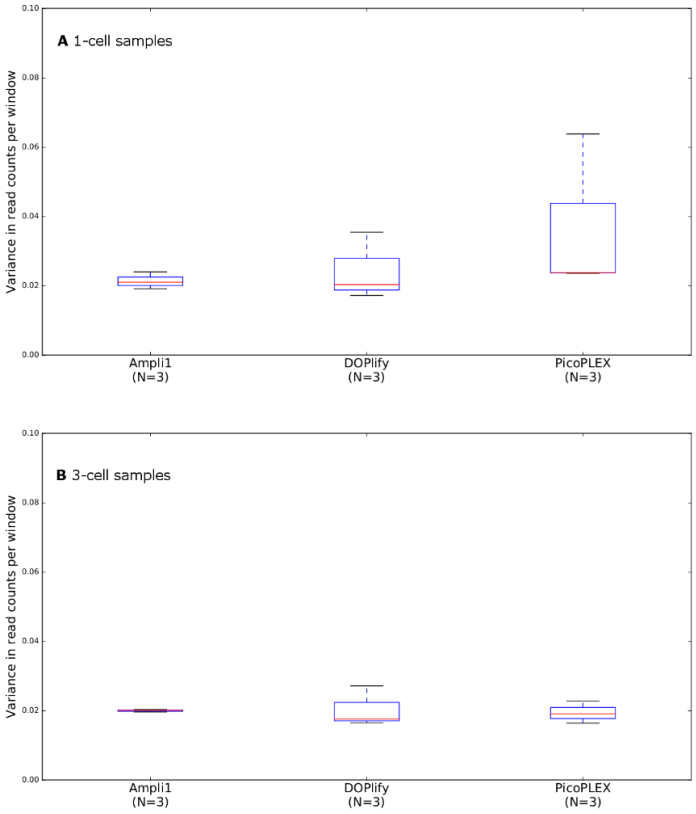

Figure 3: Boxplots of the average variance in read counts per 1 Mb windows across the genome.

(A) Boxplots representing all 1-cell samples for Ampli1, DOPlify and PicoPLEX. (B) Boxplots representing all 3-cell samples for Ampli1, DOPlify and PicoPLEX. REPLI-g was omitted from this figure, because it showed a very high average variance in read counts, indicating that the reads were distributed irregularly across the genome. The red line is the median variance for each WGA. The blue box contains the first and third quartile, whereas the black lines represent the minimum and maximum variance.

4.3. CNV analysis using a 1 Mb window

Supplementary Figure S6 demonstrates the 1Mb window line profiles of all samples, except for REPLI-g. These are also available online (https://holmes.ugent.be:9090/ViVar/). As previously mentioned, REPLI-g was omitted from this CNV analysis. The CNV line profile of one representative 1-cell sample of Ampli1, DOPlify and PicoPLEX is represented in Figure 4. The expected duplications and deletions (≥ 3 Mb), as present in the reference 1Mb CNV line profile sequenced using a bulk sample from the Loucy cell line (as in Chapter VII) (220), were called in all WGA methods, except for one 3-cell sample from PicoPLEX. This sample shows no call for the Chr13q duplication, however, higher read counts per window at this genomic position are clearly notable. One DOPlify 1-cell sample called an extra deletion at the end of chromosome 10, whereas one PicoPLEX 3-cell sample called an extra deletion at the beginning of chromosome 5. Three samples showed an extra deletion at the end of chromosome 16, which is also present in the reference 180K aCGH profile. Supplementary Table S2 indicates the called CNVs per sample. CNV profiles from 1-cell samples showed no notable differences compared with 3-cell samples.

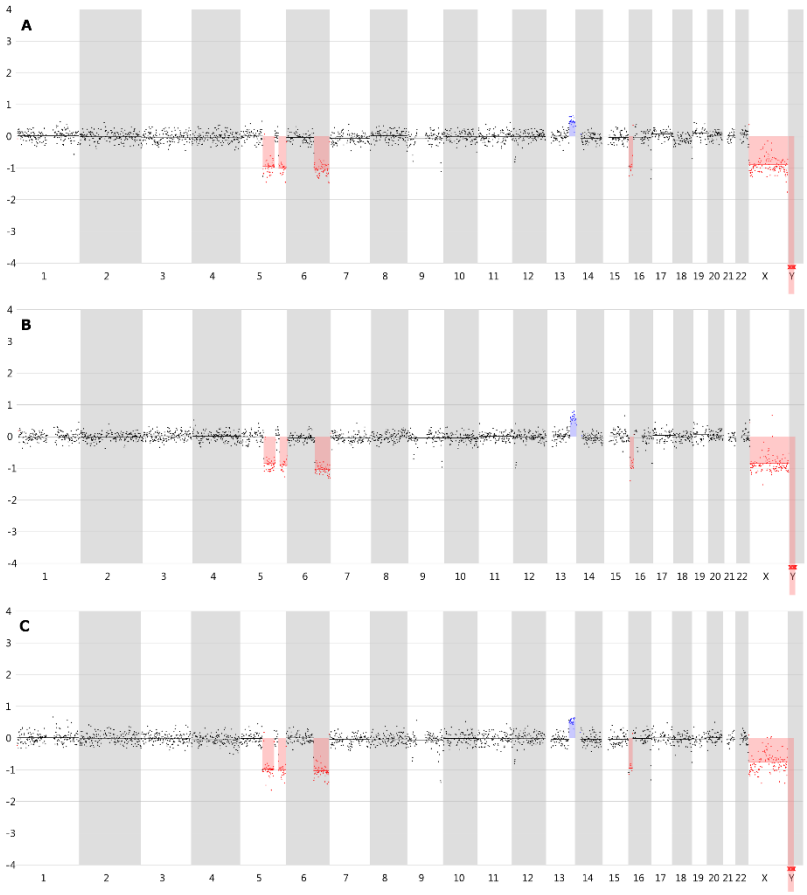

Figure 4: CNV line profiles generated with ViVar using 1Mb windows.

Representative CNV line profile of a (A) 1-cell sample amplified with Ampli1. (B) 1-cell sample amplified with DOPlify. (C) 1-cell sample amplified with PicoPLEX. Segments in red represent deletions, whereas blue segments indicate duplications. As REPLI-g did not result in reliable CNV profiles, it was omitted from this figure.

5. Discussion

The goal of this study was to investigate the performance of four WGA methods on a limited number of cells after 24 hour of Streck cfDNA BCT preservation. Both the suitability of the amplified DNA for STR genotyping and CNV analysis was assessed. It was observed that REPLI-g is not suitable to generate high quality DNA that allows STR genotyping or CNV calling in this specific set-up. The performance of Ampli1, DOPlify and PicoPLEX, on the other hand, was considered as suitable for both applications, with some differences between the three WGA methods.

STR genotyping results in a remarkably high dropout rate for REPLI-g. Moreover, with a maximum of 5 correctly called STR loci per sample, the identity of a single cell is difficult to prove. PicoPLEX showed the lowest dropout rate and therefore performed best for STR genotyping. Still, one PicoPLEX 1-cell sample failed, and the reason for this failure was not clear. Possibly, this WGA protocol is less robust for STR analyses, which should be considered when choosing one over another WGA method. DOPlify and Ampli1 prove to be robust and reproducible WGA methods for STR genotyping of 1-cell and 3-cell samples but show a higher dropout rate than PicoPLEX. A consistent dropout of the same loci in each sample with Ampli1 is notable and can be related to the WGA working mechanism,

as restriction enzymes are used for the initial fragmentation of the DNA. Probably, the enzymes cleave at the STR primer binding sites. This way, PCR amplification of these specific loci is inhibited and consistent locus dropout occurs. If necessary, other STR primers can be selected for the DNA typing after Ampli1 WGA.

The variance in read counts per window across the genome was similar for Ampli1, DOPlify and PicoPLEX. The uniform distribution of reads across the genome allows reliable CNV calling for these WGA methods. One single-cell PicoPLEX sample, which failed to show a descent STR profile as well, now showed a higher variance in read counts per window compared to the others. Nevertheless, the CNV profile of this sample was similar to the others, indicating that the higher variance did not impede correct CNV analysis. As already mentioned above, we attribute these negative results to a lower robustness of the PicoPLEX WGA protocol. This might sporadically lead to a biased amplification, which seems to influence STR genotyping but not CNV analysis. Samples amplified with REPLI-g did not result in CNV profiles, due to the irregular distribution of reads across the genome. The poor performance of REPLI-g might be the result of the exposure of the cells to the cfDNA BCT preservative. Possibly, the preservation hampers the lysis of the cells in the REPLI-g WGA protocol. The assumption that the bad performance of REPLI-g is caused by the cfDNA BCT reagent is supported by the study from Chapter VII (220), which demonstrates a suitable performance of REPLI-g for CNV calling on 1-, 3- and 5-cell samples. This study followed the same experimental set-up, except for the cfDNA BCT preservation step. In both studies, similar boxplots are generated for Ampli1 and DOPlify, indicating that no negative effects on the distribution of reads result from the preservation step.

Ampli1, DOPlify and PicoPLEX resulted in excellent 1Mb window CNV line profiles with only minor differences. Ampli1 shows a 100 % sensitivity and specificity, which means that all expected CNVs are called and that no false positives were present. DOPlify shows almost a 100 % sensitivity, but an extra Chr10q deletion was called in one single cell sample. For this sample, a higher variance in read counts per window across the genome was noted, which might reduce the CNV calling reliability of the ViVar software and probably cause the calling of this incorrect deletion. For PicoPLEX, one sample showed a false-positive Chr5p deletion and a false-negative Chr13q duplication, which reduces the sensitivity and specificity of this method. However, the region corresponding with the Chr13q duplication clearly shows higher read counts. Compared to the other 3-cell samples from PicoPLEX with a 100% sensitivity and specificity, the average variance in read counts per window across the genome was higher, which might again reduce the CNV calling reliability of the ViVar software for this sample. Furthermore, two Ampli1 samples and one PicoPLEX sample showed an extra deletion at Chr16q, which was not considered as a false positive, since this CNV is also present in the 180K aCGH reference profile from the cell line. Comparing this study with the study in Chapter VII (220), DOPlify performs very similar with or without cfDNA BCT preservation, whereas Ampli1 results in a more complete CNV profile with less incorrect calls, when 24 hour cfDNA BCT stabilization of the cells is performed.

After Streck cfDNA BCT preservation, there is no overall best performing WGA method. The most suitable method must be selected based on the intended downstream application. However, REPLI-g can be omitted from the options after cfDNA BCT fixation.

6. Supplementary information

Supplementary Figure S1: 180K array CGH profile from a bulk sample from the Loucy cell line.

All CNVs, as detected in the female Loucy cell line with a resolution of 50kb, are illustrated in this profile. Deletions are indicated as red bars, whereas blue bars indicate insertions.

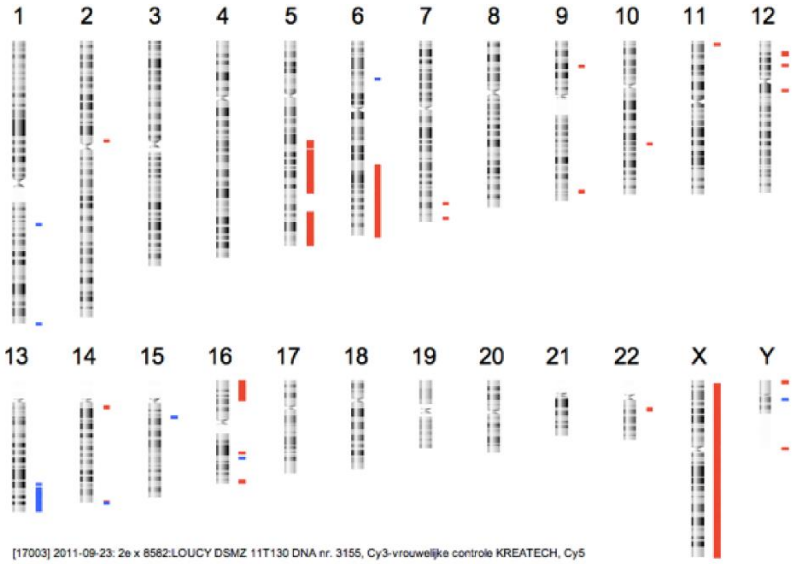

Supplementary Figure S2: 1Mb window CNV line profile from an unamplified bulk sample from the Loucy cell line. Segments in red represent deletions, whereas blue segments indicate duplications.

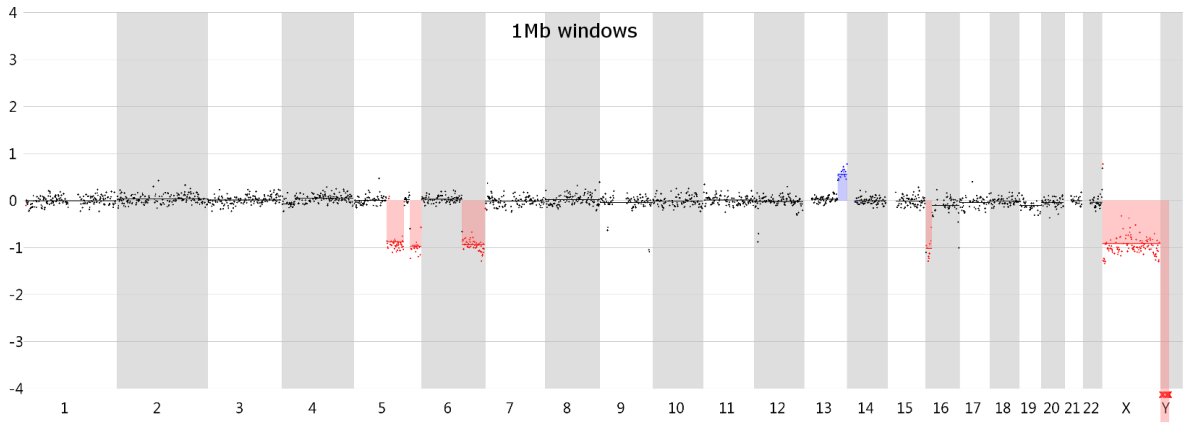

Supplementary Table S1: Concentration of the STR primers in each PCR reaction mixture.

Primer	Concentration	
SE33 F	0,5000	µM
SE33 B	1,0000	µM
D5S818 F	0,5000	µM
D5S818 B	0,5000	µM
FGA F	0,5000	µM
FGA B	0,5000	µM
D13S317 F	0,5000	µM
D13S317 B	0,5000	µM
vWA F	0,5000	µM
vWA B	0,5000	µM
D18S51F	0,5000	µM
D18S51 B	0,5000	µM
Amel F	0,5000	µM
Amel B	0,5000	µM
D21S11 F	0,5000	µM
D21S11 B	0,5000	µM
D3S1358 F	0,5000	µM
D3S1358 B	0,5000	µM
Tho1P16 F	0,5000	µM
Tho1P16 B	0,5000	µM
TPOX F	0,2500	µM
TPOX B	0,2500	µM
D7S820 F	0,6000	µM
D7S820 B	0,6000	µM
D16S539 F	0,8000	µM
D16S539 B	0,8000	µM
D8S1179 F	1,0000	µM
D8S1179 B	1,0000	µM
CD4 F	0,1500	µM
CD4 B	0,6000	µM

Supplementary Figure S3: STR profile from an unamplified bulk sample from the Loucy cell line.

The Amelogenin locus and the 14 tetrameric STR loci are illustrated above the STR profile, indicating the called alleles. One peak represents a homozygous locus, whereas two peaks represent a heterozygous locus.

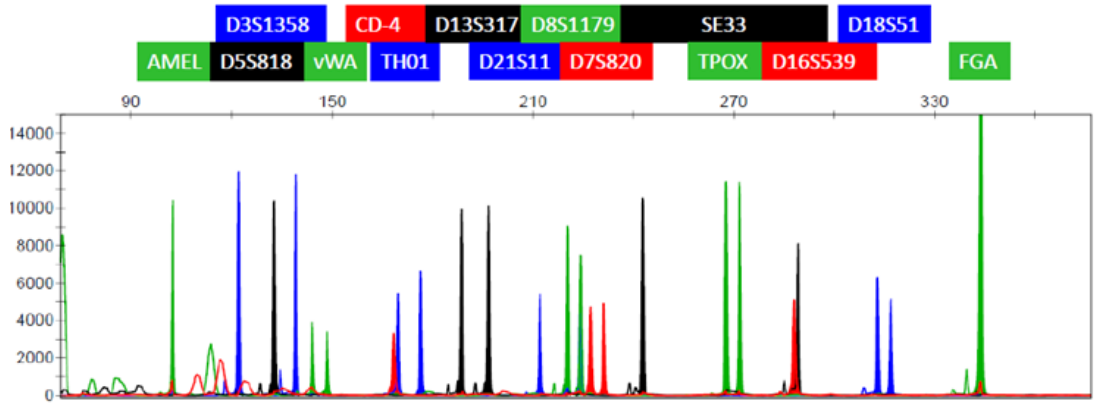

Supplementary Figure S4: Average dropout rate (%) for all 1- and 3-cell samples of the four WGA methods.

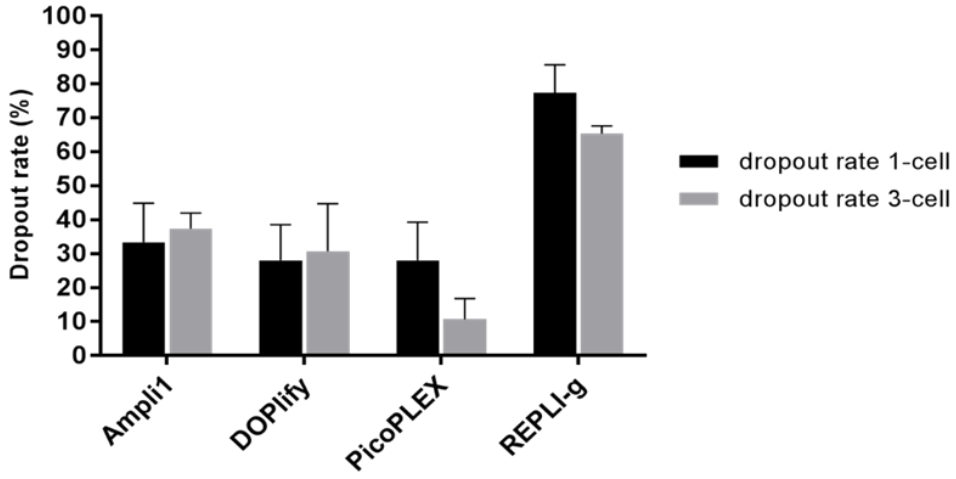

Supplementary Figure S5: 1 Mb window CNV line profiles of REPLI-g samples.

Reads are distributed irregularly across the genome, leading to unusual CNV profiles.

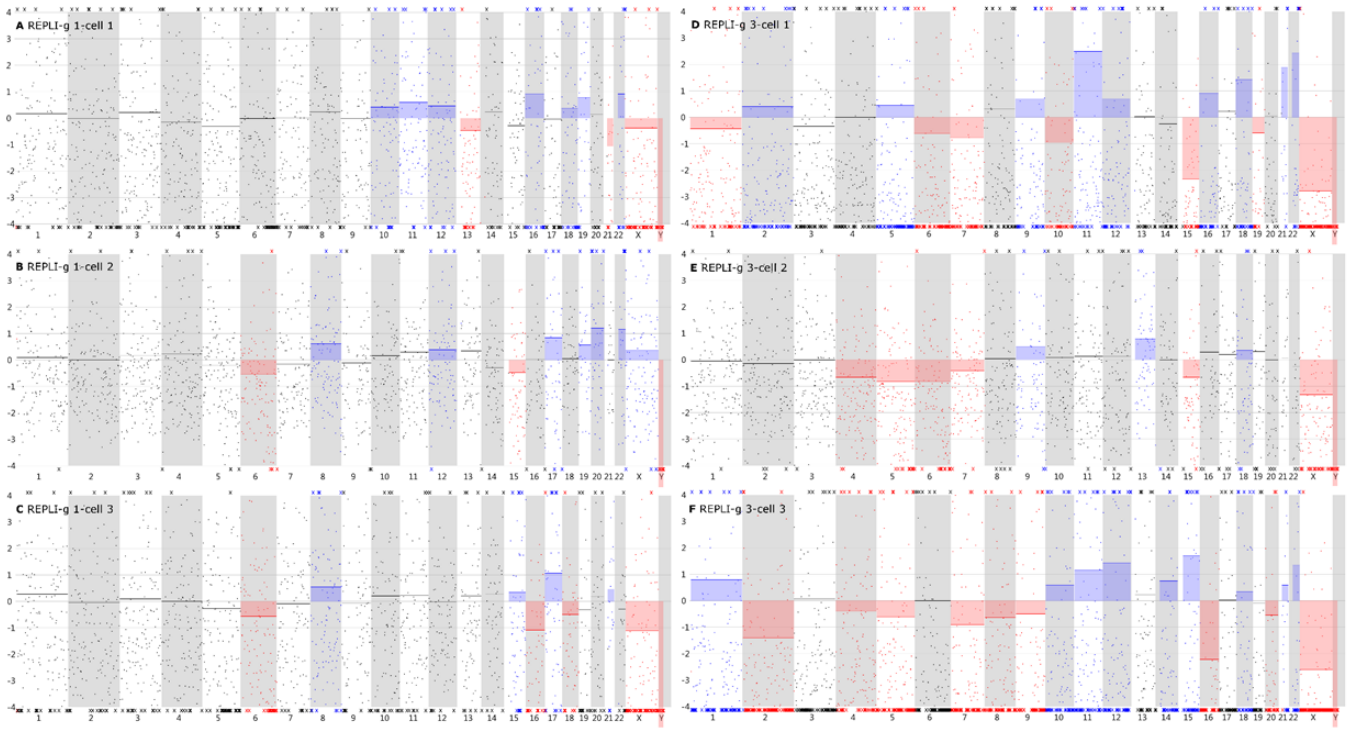

Supplementary Figure S6: 1Mb window CNV line profiles of all Ampli1 samples:

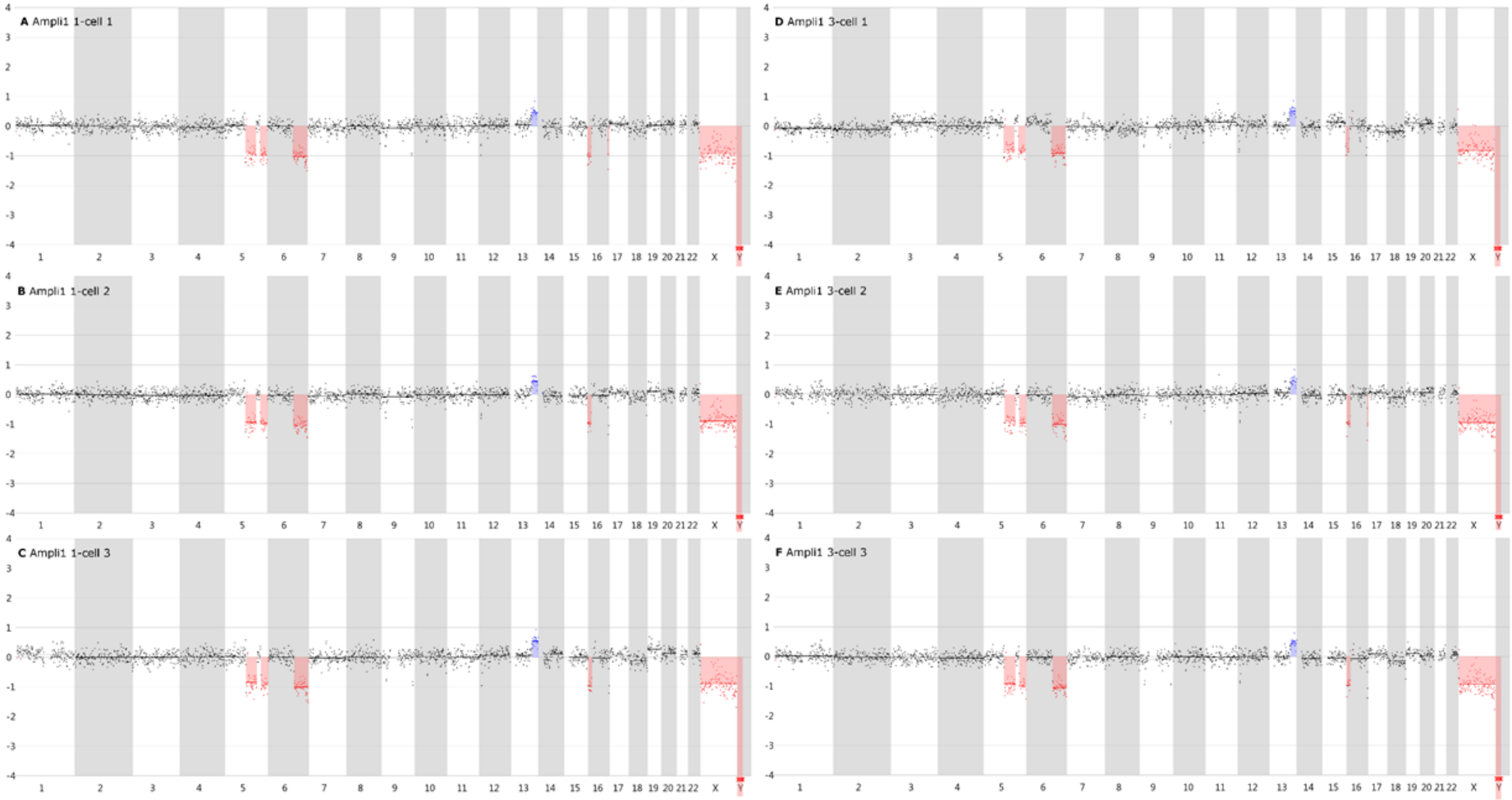

Supplementary Figure S6: 1 Mb window CNV line profiles of all DOPlify samples:

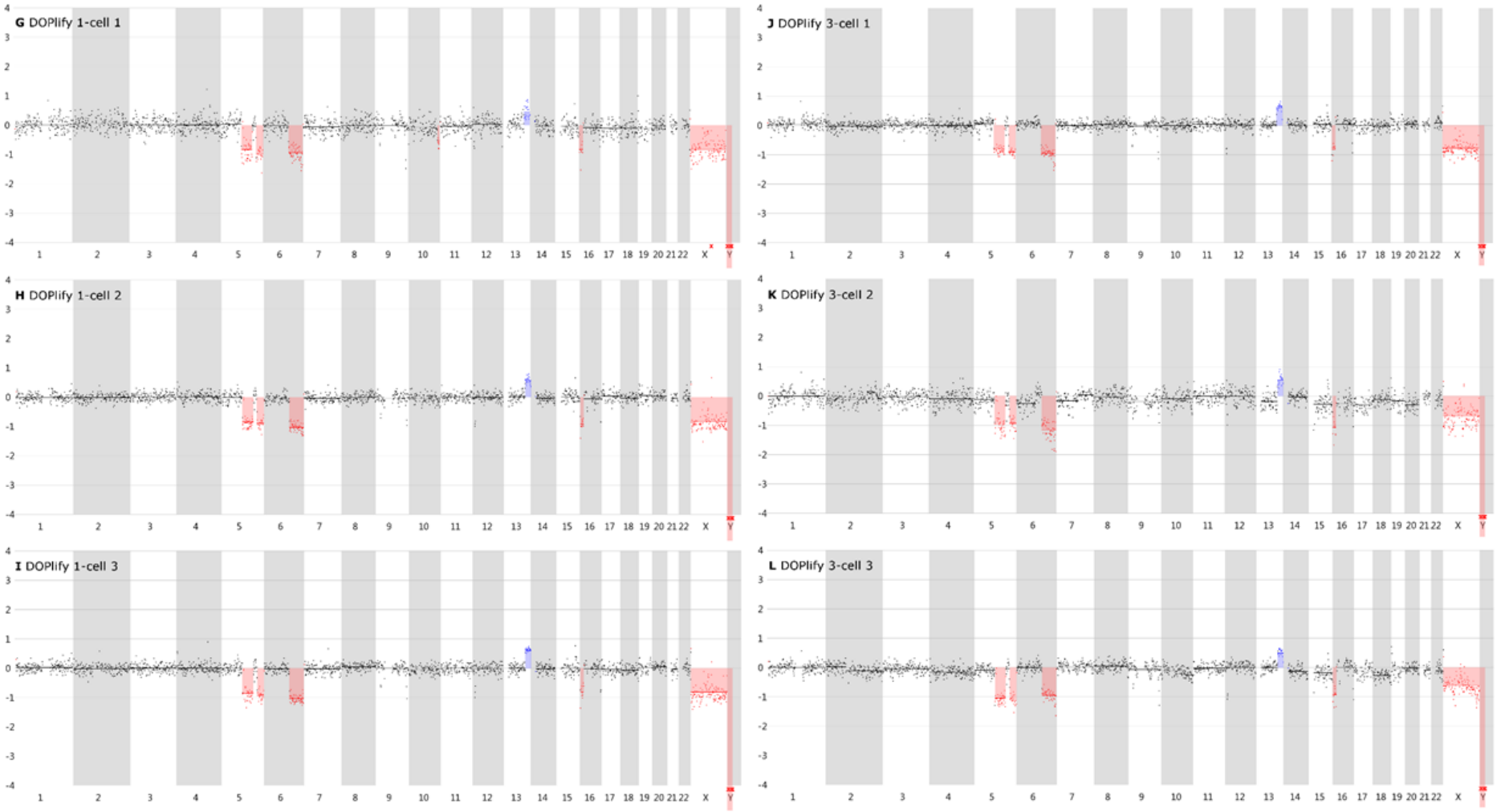

Supplementary Figure S6: 1 Mb window CNV line profiles of all PicoPLEX samples:

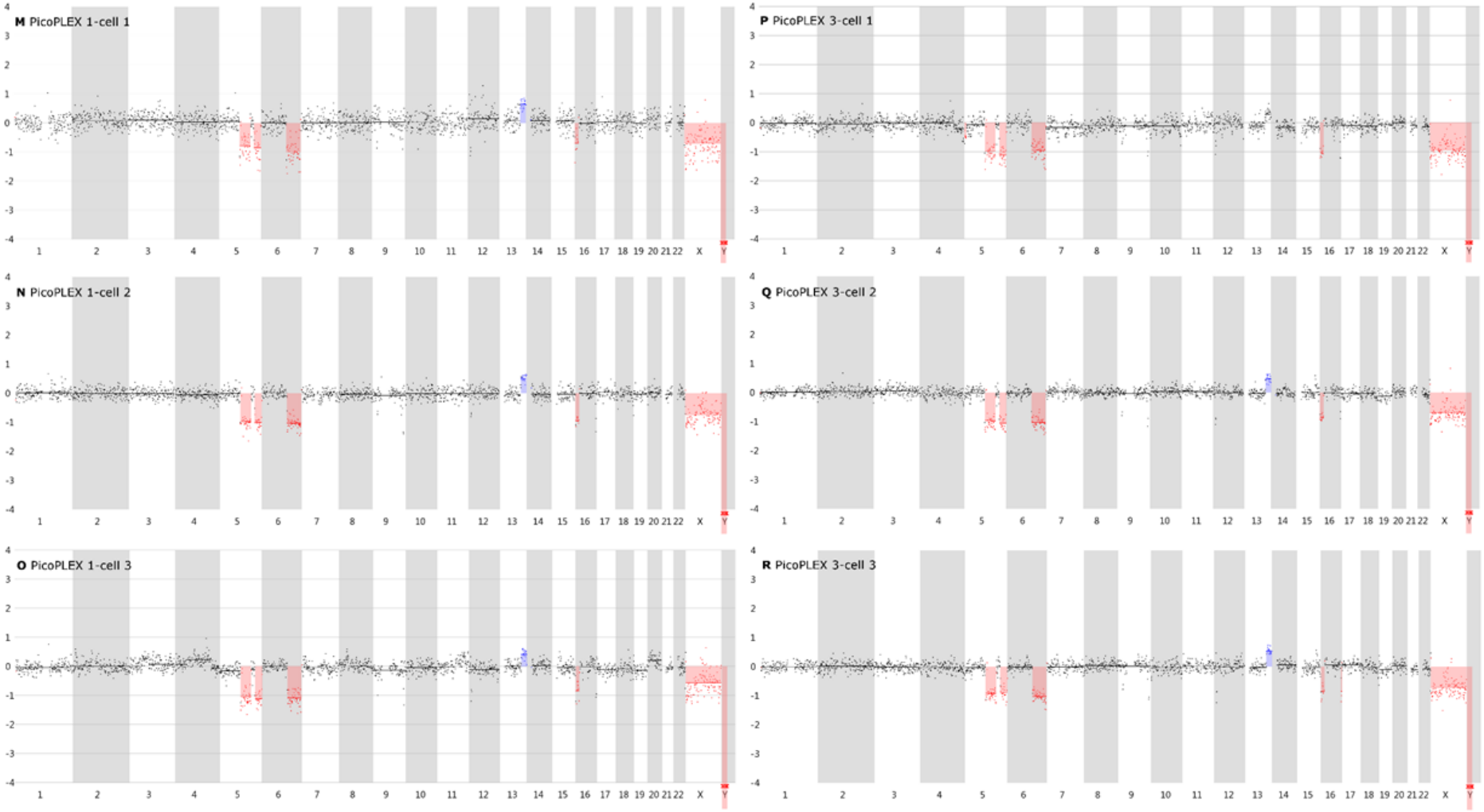

Supplementary Table S2: CNVs called in ViVar using a 1Mb window.

The column headers on the left side of the table show the genomic positions of all deletions or insertions (**in bold**), which are larger than 3 Mb and present in the reference 180 K aCGH profile. Called CNVs are indicated with a 'v'. The column headers on the right side show the location of the incorrectly called CNVs. Subscripts (1) and (2) indicate two different CNVs that are located on the same chromosomal arm.

		Chr5q$_{(1)}$	Chr5q$_{(2)}$	Chr6q	**Chr13q**	Chr16p	Chr16q	X-Chr	Chr5p	Chr10q
Bulk		v	v	v	v	v		v		
Ampli-1	1c1	v	v	v	v	v	v	v		
	1c2	v	v	v	v	v		v		
	1c3	v	v	v	v	v		v		
	3c1	v	v	v	v	v		v		
	3c2	v	v	v	v	v	v	v		
	3c3	v	v	v	v	v		v		
DOPlify	1c1	v	v	v	v	v		v		v
	1c2	v	v	v	v	v		v		
	1c3	v	v	v	v	v		v		
	3c1	v	v	v	v	v		v		
	3c2	v	v	v	v	v		v		
	3c3	v	v	v	v	v		v		
PicoPLEX	1c1	v	v	v	v	v		v		
	1c2	v	v	v	v	v		v		
	1c3	v	v	v	v	v		v		
	3c1	v	v	v		v		v	v	
	3c2	v	v	v	v	v		v		
	3c3	v	v	v	v	v	v	v		

Chapter XI: General discussion & Summary

The results of the individual studies have been discussed thoroughly in the discussion section of each chapter. In this chapter, we will summarize these results and discuss the general outcome of this dissertation.

Our first main goal was the introduction of shallow MPS in PGD for CNV analysis as a possible substitute for aCGH. Before we could accomplish this, we developed a workflow, for CNV analysis after shallow MPS on a limited number of cells and chose a WGA method suitable for such analysis. In **Chapter III** we used such a workflow to demonstrate that SurePlex WGA is better suited for CNV detection after shallow MPS on a limited number of cells compared to MALBAC WGA. A WGA method well suited for CNV analysis should result in a uniform read distribution across the genome. A non-uniform read distribution indicates an over-or under-amplification of certain genomic regions. This would introduce CNVs not present in the original genome or mask real CNVs, and thereby result in a wrong interpretation of the genome. After MALBAC amplification, a non-uniform read distribution resulted in a biased CNV profile. A lot of CNVs were missed and other false positive CNVs were called. In contrast, SurePlex amplification resulted in a more uniform distribution and thereby a more complete CNV profile with less false positives. They are both hybrid PCR methods, using the same amplification mechanism, but with different primers. For MALBAC, these primers might have bound less uniform across the genome or the loop formation might have been suboptimal.
In both methods, the false positive calls were not entirely consistent between the replicates. This indicates that the bias introduced during amplification is rather random and thereby more difficult to predict. The single cell samples showed more bias than the three or five cell samples. It is possible that the random bias is partially smoothed when multiple cells are amplified. The bias improved when using a PCR-free library preparation method, indicating that some bias was also introduced during the enrichment PCR step of library preparation. Nevertheless, some bias was still present after omitting the enrichment PCR, especially for MALBAC, indicating that both WGA and enrichment PCR were responsible for the bias. In general, SurePlex WGA should be suited for PGD on 3 and more cells for CNV detection after shallow MPS.

Subsequently, we applied a similar workflow, using SurePlex WGA, to establish our first goal. In **Chapter IV**, we demonstrated that shallow MPS on trophectoderm biopsies is a preferable alternative for aCGH for the detection of chromosomal and structural abnormalities in PGD embryos. Shallow MPS showed a higher resolution and better signal-to-noise ratio than aCGH. In addition, the cost per sample should drop, as samples could be multiplexed or

combined with samples from other clinical applications (NIPT, exome sequencing) on a single sequencing run. These findings indicate that MPS is more precise and more flexible than aCGH. After MPS the resolution could be increased (by lowering the window size) for certain patients with known cryptic aberrations, yet restricting the analysis to the chromosomal segments of interest to avoid false-positive results genome-wide. ACGH is not that flexible, as the resolution is limited by the distance between the probes. Further, we showed for the first time that Illumina (NextSeq500) and Ion Torrent (Ion Proton) sequencing technologies are both applicable and even interchangeable in this setting. The detailed workflow for CNV detection in PGD has been described in **Chapter V**. In the meantime, shallow MPS has been successfully introduced for the detection of CNVs and aneuploidies in PGD at some genetic centers, such as the medical genetics center of Ghent.

SurePlex WGA proved its value in this clinical setting for the amplification of 4-6 trophoblast cells and a subsequent CNV analysis at ≥3Mb resolution. However, a higher resolution in our study was hampered, probably by the representation bias introduced by our WGA. This representation bias would be even more pronounced if less cells were amplified (Chapter III). In settings, were the analysis of only a single cell is important (cell-based NIPT or heterogeneity detection in a cell population), a better WGA method might be suggested. Therefore, as requested by commercial partners, we tested some other WGA methods for CNV analysis after single cell sequencing, hoping to result in less bias.

The first method tested was TruePrime WGA, which gave rather disappointing results (**Chapter VI**). The read distribution was extremely non-uniform and thereby no descent CNV analysis was possible. This method seemed not suited for CNV analysis after MPS on a limited number of cells. It is, therefore, not surprising that other research articles using this method remain absent. Only one paper, written by the company itself, came out shortly after our paper (192). We suspect that the possible instability of the TthPrimPl primase causes the representation bias during amplification. The stability might be better in house than after shipment to other locations. That would indicate that this version is not yet ready to be launched on the market. We have been contacted shortly after our publication to test their new version and although slightly improved, the results were still disappointing.

In **Chapter VII**, we evaluated DOPlify and PicoPLEX DNA-Seq for their use for CNV detection after MPS on a limited number of cells, compared to Ampli1 and REPLI-g. This time, only using the PCR-free library preparation method. The four WGA methods seemed suitable for CNV detection after MPS on a limited number of cells, but DOPlify and PicoPLEX DNA-Seq excelled. The latter two detected all expected CNVs without false positives, at both a 1Mb and 500kb window. Ampli1 and REPLI-g detected already some false positives at 1Mb and showed, respectively, two times and three times more when analyzed at 500kb. Nevertheless, some smaller CNVs were also more likely to be detected in those samples, suggesting that the local signal-to-noise ratio was lower after Ampli1 and REPLI-G

amplification. Therefore, for those two methods, one should decide between either a higher resolution or less false positives.

DOPlify or PicoPLEX DNA-Seq might be able to replace SurePlex in a clinical PGD setting for chromosomal aberration detection. PicoPLEX DNA-Seq includes the same WGA technology as SurePlex, but without the need for a separate library preparation. In terms of cost, time, contamination risk and error susceptibility, this method might be preferred over conventional SurePlex in a PGD setting with Illumina sequencing. DOPlify is an advanced DOP-PCR, but more details about the advancement are not released. Most likely, Taq polymerase is no longer used, which would be an improvement over the amplification with SurePlex. When it comes to PicoPLEX DNA-Seq versus DOPlify: DOPlify seems to be better for single cell amplification, but two failed samples suggest the method might be less robust. PicoPLEX DNA-Seq is less flexible, as it always results in an Illumina library and is therefore not compatible with Ion Torrent sequencing.

REPLI-g and Ampli1 seem to introduce more bias compared to SurePlex, as no false positives were observed at a 1Mb window for the PCR-free SurePlex samples analyzed in Chapter III. However, this might have been a coincidence, as only three PCR-free SurePlex samples were available to compare. Nevertheless, REPLI-g uses the MDA technology and it is well-known that most hybrid WGA methods are better for CNV detection than the WGA methods based on MDA (130). The mechanism behind Ampli1 is highly depending on the availability of restriction sites. A non-uniform distribution of those sites across the genome, will lead to bias during amplification. REPLI-g amplification introduced more false positives and thereby showed a lower reproducibility than Ampli1. These findings were similar to previous research by Hou *et al.,* where Ampli1 showed a lower amplification bias and a higher accuracy for single-cell CNV detection compared to REPLI-g (198).

In **Chapter VIII,** we focused on an affordable analysis of SNVs across the genome using MPS. This could be another application in PGD, as to improve current detection methods for SGDs methods. Therefore, we applied the TruSight One sequencing panel to analyze multiple SNPs on a limited number of cells. The TruSight One sequencing panel is designed to screen for different SGDs at once in a prenatal setting using CVS. This panel simultaneously captures more than 4800 genomic regions associated with a clinical phenotype and analyzes them on a single sequencing run. As expected, the panel performed different on WGA DNA than on bulk DNA and this difference depended on the applied WGA method. Target coverage, coverage uniformity and SNP calling accuracy obtained using SurePLEX, Ampli1 and MALBAC, was inferior to the results obtained on bulk DNA. However, REPLI-g WGA came close to the results of the bulk DNA. REPLI-g resulted in better coverage of the targeted genomic regions with a more uniform read depth compared to the other WGA methods. Consequently, this method resulted in a more accurate SNP calling than the others. In contrast to CNV detection, MDA WGA methods are preferred over hybrid PCR methods for SNP detection (130), but it was never shown that this also holds true if a capture is performed before SNV detection.

MALBAC and SurePLex both use the Bst polymerase during their pre-amplification step, which has a lower fidelity than the Phi29 polymerase used by REPLI-g. The fidelity of a polymerase is more important for SNP detection than for CNV detection. In Ampli1 WGA it might have been possible that the targeted regions were cut by the restriction enzyme and thereby a lot of regions remained uncaptured. Again, the bias between the replicates in the four methods was not consistent, indicating that the bias was introduced rather random. A very recent study compared four WGA methods for SNP calling after exome sequencing, which is comparable to our setting (209). Their results for MALBAC, Ampli1, REPLI-g mini and SurePlex for variant calling and targeted coverage were comparable to our results.

PicoPLEX DNA-Seq and DOPlify were not included in this study as we initiated this study before they were launched on to the market. Nevertheless, PicoPLEX DNA-Seq applies the SurePlex WGA technology and thereby the results are expected to be similar to SurePlex. Besides, the library formation included in the WGA, is probably not suited as starting material for the panel. It might, however, be interesting to test DOPlify for this application in the future.

In the future, the TruSight One sequencing panel might be a substitute for state-of-the-art technologies for SGD analysis in PGD, if it performs well on amplified material. Although the results after REPLI-g amplification look promising, they do not match the bulk sample entirely. A thorough clinical validation of this panel combined with WGA will be essential before the panel could be applied in the clinic.

For the last part of this dissertation we focused on STR analysis of WGA amplified single cell samples. The genetic identification of a cell might be important in an application, such as cell-based NIPT. In **Chapter IX**, SurePlex, Ampli1, REPLI-g and DOPlify were tested for STR analysis after the amplification of single or three fresh cells. Similar to SNV detection, REPLI-g was the best WGA method for STR detection on fresh cells in this study. REPLI-g was the only WGA in this study that could result in a complete STR profile for at least some of its samples. However, in a cell-based NIPT setting a complete STR profile should not be necessary to determine the genomic identity of a cell. In this setting, the maternal STR profile is compared to the STR profile of the cell. An STR profile, not equal to the maternal profile, but with one of the maternal alleles in each heterogeneous marker, must be fetal. The incomplete profiles of Ampli1, SurePlex and DOPlify could still predict potential fetal identity. After Ampli1 amplification, all samples showed a dropout of the same 6 STR markers, which might be related to the WGA working mechanism. The restriction enzyme probably cleaves at the STR primer binding sites of those regions, thereby PCR amplification at these loci is inhibited. Nevertheless, replacing these STR markers by others might improve STR analysis after Ampli1 WGA. SurePlex and DOPlify show a more random dropout. SurePlex showed a lower dropout rate than DOPlify and Ampli1, but one of its samples failed to show a descent profile. Therefore, DOPlify and Ampli1 seem more robust and reproducible methods.

In cell-based NIPT, STR analysis is only performed to determine if the cell is fetal. The genetic analysis afterwards, such as CNV detection, is more important. Therefore, the applied WGA method should also be able to result in a reliable CNV profile. For instance, MALBAC did not perform well for CNV analysis and was therefore not tested in this study. DOPlify was one of the better methods for CNV detection and might therefore be a suitable candidate in a cell-based NIPT context on fresh cells.

The results for STR analysis were very different when the cells were preserved before amplification, as demonstrated in **Chapter X**. All REPLI-g amplified samples showed a very high dropout rate and lacked thereby the ability to descent the genetic identity of a cell. In contrast, the other WGA methods showed some improvements. It has been described that a long heating step will be necessary to overcome chemical fixation. This might explain why REPLI-g, having the shortest lysis and performed at an overall low temperature, results in such bad results. This time, SurePlex showed the best results, but again one sample failed to show a descent profile. Thereby, it seems again less robust compared to DOPlify and Ampli1, but SurePlex had a lower dropout rate. It was even clearer, after preservation, that Ampli1 samples had a consistent dropout at 6 loci. The STR profiling after Ampli1 could probably be improved by selecting other STR markers. In a cell-based NIPT setting, CNV profiling will again be the most important determinant when deciding on a WGA method. Similar to the STR results after preservation, REPLI-g amplified samples were not able to deduce a descent CNV profile. The other three methods were similar to each other, but Ampli1 was the only one without false positives. For the latter, the CNV detection seems to have improved over the analysis on fresh cells. The CNV profiles after DOPlify and SurePlex were also good, but not improved over fresh cell analysis. Therefore, for cell-based NIPT purposes, Ampli1 might be the preferred candidate. Our results prove that BCT preservation does not hamper DNA analysis, as long as it is combined with an appropriate WGA method.

We can conclude that we laid the foundation to introduce shallow MPS as a substitute for aCGH for CNV and aneuploidy detection in PGD. Subsequently, we characterized the performance of most modern WGA methods in respect to downstream applications such as shallow whole genome sequencing CNV analysis and STR analysis of single fixed and unpreserved cells. Thus, we have the necessary tools ready to perform genetic analysis for cell-based NIPT as soon as fetal cells can be reliably isolated from maternal blood.

Chapter XII: Broader international context, relevance and future perspectives

God blessed them; and God said to them, "Be fruitful and multiply" (Gen 1:28). Apparently, some couples have not been blessed that much, as one in six couples are unable to conceive by natural conception. Fortunately, a lot of these couples might still conceive using ART, and in particular IVF.

The financial and emotional burden of ART, and PGD to lighten the load

Before couples turn to ART, most of them have already been trying for some time to conceive naturally. When they finally turn to IVF/ICSI, most couples need on average 3 cycles before they get pregnant. The financial and emotional burden for those couples should not be underestimated. Every failed implantation can be emotionally very hard on the couple and the average cost per IVF cycle in Europe can vary between € 4000-5000 (ESHRE facts sheet 4; Jan 2017). However, most countries in Europe provide full or partial reimbursement, lowering the financial burden (Figure 1). In the USA, no federal law regulates ART and therefore most treatments are performed within a private market system and can thereby rise up to $ 12400 per cycle (ESHRE facts sheet 4; Jan 2017). Nevertheless, even reimbursement is not unlimited and will stop after a certain amount of cycles. Therefore, it is important that the success rate for IVF/ICSI is high enough to minimize the failures and hence the financial and emotional burden.

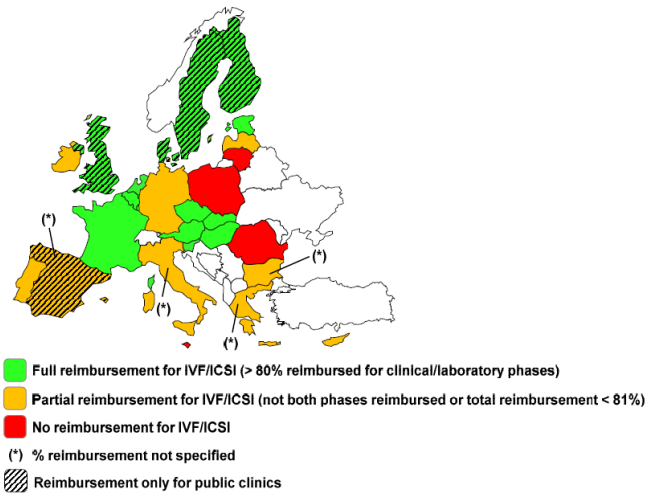

Figure 1: Reimbursement for IVF/ICSI in Europe (SANCO/2008/C6/051)

Unfortunately, some embryos will suffer from genetic abnormalities without obvious abnormal morphological features (12, 19, 20). Without a genetic analysis, such embryos might fail to implant or result in abnormalities in the fetus. Due to PGD/PGS, a genetically normal embryo can be selected for transfer. Before PGD/PGS, the only options for couples producing too much genetically abnormal embryos were: remaining childless, prenatal diagnosis,

adoption or gamete donation. PGD/PGS has shown an added value to the ART outcome when using aCGH for analysis (20, 61). This demonstrates the relevance of PGD/PGS to lower the financial and emotional burden of IVF/ICSI. However, genetic selection of embryos is an ethically charged subject and is therefore not allowed in some countries in Europe (Figure 2). Even if it is prohibited, the costs for genetic analysis are extra on the already very expensive ART treatment. Less fortuned people will therefore still have no access to it. Some countries in Europe have a reimbursement policy for PGD (Figure 2), but not for PGS.

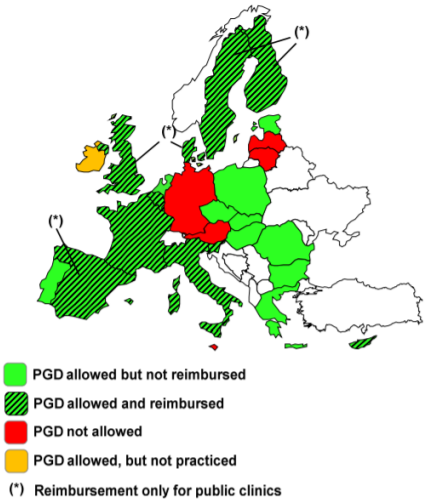

Figure 2: Reimbursement situation for PGD treatment (SANCO/2008/C6/051)

Belgium is one of those countries that is reimbursing PGD. The genetic centers get reimbursed per treatment by the health security system and the patients only have to pay a small personal contribution to the center per treatment. Nevertheless, the patient contribution and reimbursement still not completely cover the costs made by the genetic centers. As PGD will increase the cost and duration of the IVF/ICSI treatment, an efficient detection of the present abnormalities in the embryo is very important. The burden of the treatments on the health security system should also not be underestimated. The money going to failures could have been allocated to better a recourse. Therefore, it is very important that the technologies used for PGD are accurate, provide enough information and have an acceptable price.

Current state-of-the art PGD/PGS technologies for CNV and aneuploidy detection, such as aCGH, proved their value, but the cost is relatively high and the resolution limited. This is where MPS has more room to optimize.

We succeeded in developing a workflow to analyze chromosomal aberrations in PGD after MPS and were able to show a higher accuracy and flexibility of MPS over aCGH (Chapter IV). The quite large amount of research involving MPS in PGD, performed during and since our study, really stresses the relevance of this research worldwide (32, 163, 179, 207). In the meantime, different genetic centers worldwide, among which the one at the UZ Ghent, have implemented MPS for chromosomal aberration detection in PGD. Some live births of healthy babies after MPS PGD

have even been reported already (31, 235, 236). Given the rather recent implementation, randomized controlled trials reporting the added value of MPS over aCGH to the PGD-outcome are still rather scarce (237). General assumptions on the financial benefit of MPS over aCGH also remain difficult, as this will depend on the sample throughput and the overall diagnostic setting. MPS allows not only for multiplexing PGD samples, but also for simultaneous sequencing of PGD samples with samples from other applications (NIPT, exome seq). This will most likely decrease the cost for PGD. However, centers with only a low sample throughput might not experience these financial benefits.

Despite the observation that MPS is more flexible to increase the resolution in PGD compared to conventional techniques, we also observed that the WGA method is a limiting factor to further increase the resolution. A technique used for PGD must be very accurate to decrease financial and emotional burden of the patients. Therefore false positive or missed calls cannot be tolerated. We focused a big part of this dissertation on testing the most modern WGA methods in this context to possibly improve the accuracy of the DNA amplification. REPLI-g, GenomiPhi, GenomePLEX and MALBAC are the most widely applied WGA methods in publications (on average 23/method). The former three are older methods and as fewer WGA methods existed in the past, they were often used. The number of publications using these methods is however declining over time, except for REPLI-g. REPLI-g is still frequently used for SNV calling (Source: Web of Science; PubMed). MALBAC is a WGA method developed by an Asian company and therefore most publications using MALBAC are from that side of the world. Other more recent methods, such as SurePlex and Ampli1, have only been described sporadically. However, we were the first and only group using DOPlify and PicoPLEX DNA-Seq in a study. There is no consensus about the best WGA method, as the performance of a WGA is application dependent (130). Therefore, the choice of the WGA will be very important for the success of the application. Similar to us, others have also been comparing different WGA methods in a specific context (198, 199, 209, 221).

Even if the WGA was not limiting the resolution, the implementation of higher resolution analysis will be a matter of regulation. The regulation of ART and PGD differs around the world, even within Europe differences are observed. In the USA no regulations concerning the use of PGD exists. Therefore, PGD can be used for a variety of controversial purposes, including sex selection, selection for deafness and dwarfism or selection for a sibling who can serve as tissue donor for sick relatives (238). In Europe, all countries have their own specific regulation. For instance, the particular set of conditions for which PGD is permitted in Italy and Switzerland is not regulated as it is in France and the UK, which have a detailed regulatory framework. In the latter, certain authorities regulate when PGD can be offered. In Belgium, no detailed regulations for PGD are set either. Aside from eugenic selection and sex selection for non-medical reasons, the medical genetic centers can decide for themselves when PGD can be applied (239).

In terms of regulation and reimbursement, it is also important to make a distinction between PGD and PGS. PGS is applied in cases with unexplained ART failure, to screen for genetic abnormalities not explained by the parental karyotype. Although the technologies used for chromosomal aberration detection, such as aCGH and MPS, do not differ between PGD and PGS, most reimbursement policies will only apply in case of PGD. Therefore, costs for PGS can rise up to 2000 euros. One of the reasons PGS is still not reimbursed, is the ongoing discussion on the usefulness of PGS. Some European countries, such as Italy, do not even allow PGS (238). Nevertheless, in Chapter IV, we clearly detected aberrations not derived from the parental karyotype in most of the abnormal embryos. Although the evidence on the added value of PGS on ART is growing (30, 240), only very few randomized control trials are available on PGS. The accuracy of PGS is also compromised by the degree of mosaic embryos. Cases have been described where aneuploidy embryos resulted in euploid babies, which could question the accuracy of only one trophectoderm biopsy to predict the ploidy status of the embryo (241). Nevertheless, in most samples, the mosaic status of an embryo can be deduced from the aCGH or MPS CNV profile (242). Therefore, the issue lies not so much with PGS per see, but with the difficult interpretation of mosaic results.

An even more complicated issue is the use of PGS in the case of SGDs. Research showed the value of aneuploidy screening in patients undergoing PGD for SGDs (243). Half of the patients in the study had at least one embryo that was SGD-unaffected but aneuploid. Nowadays, selection based on chromosomal abnormalities and SGDs are two separate tests and thereby two different biopsies.

MPS has the potential to combine PGS for chromosomal aberrations and PGD for SGDs, which would imply only one biopsy to test both. Apart from the ethical discussion on whether to apply MPS for screening in this context, the state-of-the-art methods for SGD detection are time consuming as they are mutation and patient specific. Therefore, MPS might provide an alternative. Efforts have already been made to use MPS for SGDs or a combination of SGDs and aneuploidy detection (137, 207, 236, 244). Those studies use MPS as a targeted approach for one specific SGD. A targeted approach still requires some pre-testing concerning the specific mutation in the parents, which is again time consuming. Whole genome sequencing (WGS) for SNVs is still too expensive and a lot of unknown SNPs and multifactorial treats will be detected, which are difficult to interpret. Especially since some of these detected aberrations might be derived from WGA bias. Given ART is already very time consuming and expensive, another approach might be considered. In this respect, we tested the TruSight One Sequencing panel in this dissertation. By screening for more than 4800 possible disease-causing gene regions at once, we hope to avoid the need for pre-testing. The panel captures only the DNA parts related to these mutations, avoiding WGS and thereby lowering the price and facilitate the interpretation. However, WGA remains necessary to generate enough DNA for the analysis and, more than for CNV detection, the WGA limited the application. Therefore, further research is needed before clinical implementation. This method would also enable the simultaneous analysis of CNVs at a reasonable

resolution as shown before on prenatal samples (46). However, as the combination of the panel with WGA is not yet optimized, we did not yet test CNV analysis with the panel.

If such a panel would ever be applied in a pre-birth diagnostic setting, this would imply serious ethical regulations as it will involve PGS. The importance in combined chromosomal and SGD screening has already been discussed above. However, also de novo gene mutations are common in embryos (245, 246), also indicating the relevance of PGS. In each embryo, 44 to 82 de novo single-nucleotide mutations are expected, with one to two affecting the coding sequence (247-250). Still, concerns are raised about screening the genome for such small aberrations. It might lead to the discovery of variances of unknown significance (VOUS). Nevertheless, this risk is in part avoided by the use of a targeted panel, as the captured regions belong to known disease-causing gene regions. Another issue when using the panel for PGS, is the detection of the carrier status of the fetus. Clear regulations should be set to deal with such information, before implementing this type of screening in a diagnostic setting.

The worldwide implementation of cell-free NIPT

Lately, cell-free NIPT has been in the news a lot, as from the first of July, Belgium is the first country in Europe that reimburses cell-free NIPT. This test analyzes cell-free DNA in the blood of a pregnant woman after venipuncture. The way the media introduced the test to the people, wrongly assumes that this test can replace invasive prenatal testing. The technique is indeed safer than invasive techniques, but it has no diagnostic value. It will only test for Down syndrome (trisomy 21), Edwards syndrome (Trisomy 18) and Patau syndrome (trisomy 13). The test has only a 99% accuracy and is therefore only recommended as a screening test. Invasive testing is still strongly recommended after receiving a positive NIPT result. Nevertheless, cell-free NIPT screening is more accurate than current serum marker screening and ultrasound imaging (251, 252).

Today, cell-free NIPT is a worldwide application. It was first introduced in Hong Kong in 2011 (NIFTY) and was soon after introduced commercially in the US (253-255). The global NIPT market is estimated to reach a value of $3.62 billion by 2019 (256). MaterniT21Plus by Sequenom (San Diego, CA, USA) was the first commercially available cell-free test in the US, followed by Verify (Verinata Health, Redwood City, CA, USA), Harmony (Ariosa Diagnostics, San Jose, CA, USA), Panorama (Natera, San Carlos, CA, USA), and ext. Those companies offer their tests worldwide in over 60 countries, but North America accounts for more than half of their market (256). Other companies, such as LifeCodexx, are also located in Europe and have a mainly European market. The disadvantage of the commercialization, is the uncontrolled cost and the lack of counseling. CVS and amniocentesis are nearly always reimbursed in some way, but NIPT costs can rise up to $3000 in the US and €850 in Europe (254). However some private insurance companies start to include NIPT in their assortment. If such a test is performed independent of any clinician, the lack of counseling offered to the patient complicates the interpretation of the results. However,

nowadays NIPT is no longer solely offered by commercial companies, but also genetic centers often offer in-house optimized and validated tests (such as those in Belgium). Such centers can provide more information concerning the results. The increased accuracy over the current screening systems should lower the number of unnecessary invasive procedures. On the other hand, also a lot of couples will wrongly assume that the diagnostic value of this test is similar to invasive techniques. As a consequence, practitioners will have to perform less invasive procedures. As this is a rather delicate procedure, less practice might lower the quality of the tests. However, the decrease in reimbursement allocated to CVS and amniocentesis will probably not yet outweigh the extra burden introduced to our health security system by this test. There is need for a single, safe, accurate test, performed early in pregnancy that might replace both tests.

A good non-invasive prenatal diagnosis (NIPD) test should be able to replace the invasive prenatal tests by a safe one, with the same diagnostic value. As the cell-free fetal DNA can never be physically separated from the abundance of maternal DNA, the genetic analysis will probably never parallel the invasive diagnosis (133). There is growing evidence that intact fetal cells can be isolated from the maternal blood circulation. Prenatal diagnosis on such cells, could probably replace invasive prenatal techniques. A cell-based NIPT workflow should be able to isolate rare, pure and intact fetal cells with well-preserved genomic DNA from a blood tube, to perform single cell genetic testing for fetal identity and abnormalities up to small CNVs. In this respect, we developed already a workflow during this dissertation to perform genetic testing for both fetal identity and chromosomal aberrations on single fresh or fixed cells.

Cell-based NIPT: The holy grail in prenatal diagnosis?

Since the discovery that fetal cells are present in the maternal blood circulation during pregnancy in 1959, people have been trying for years to isolate them. The research came to a slow start, as they had difficulties to prove the fetal nature and mainly focused on lymphocytes. After some initial promising studies with fetal nucleated red blood cells, the interest regarding these cells began to grow extensively, resulting in the ‘golden era’ of circulating fetal cell research between 1993 and 2003 (103, 257) (Figure 3). Nevertheless, failure to detect fetal cells in every pregnancy and an inability to obtain a correct diagnosis, dampened the initial enthusiasm for circulating fetal cells (103).

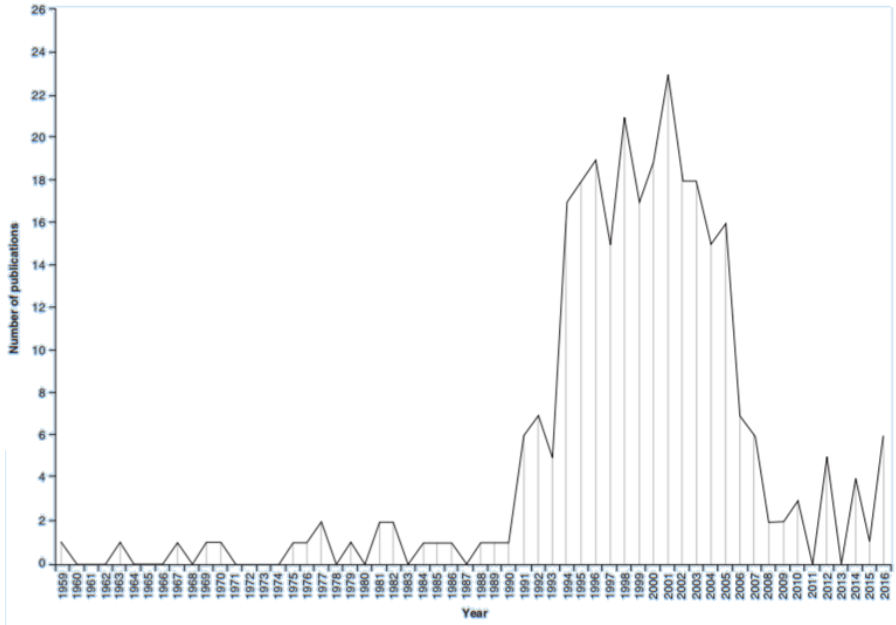

Figure 3: Number of publications targeting fetal cells in maternal blood (257)

The last couple of years, the interest for cell-based NIPT has raised again after some successful research with fetal trophoblasts (258-260). Technical evolutions over the recent years have further enhanced the development of isolation techniques around the world. The group from P. Paterlini-Brechot (Rarecells, Université Paris Descartes) was among the first to publish a successful prenatal diagnosis from fetal trophoblast cells isolated from maternal blood samples during pregnancy (105, 109, 261, 262). They used an in-house developed ISET system combined with laser microdissection to isolate trophoblasts based on size. Thereby, they were able to perform prenatal targeted diagnosis for cystic fibrosis and spinal muscular dystrophy (105, 109). Originally, their research focused on the size-based isolation of CTCs from the blood of cancer patients (109, 263-265), but they soon discovered that the ISET could also be applied for trophoblast isolation. Tumor cells and trophoblast cells both show a distinct cell size compared to the surrounding blood cells.

So far, only a few groups around the world were able to perform a genome-wide prenatal diagnosis from isolated fetal trophoblasts. This low number is probably caused by the challenges that this research faces. First of all, no specific fetal marker has been discovered yet. Therefore, antibody labeling will only enrich your sample for fetal cells, not result in a pure fetal cell sample. Second, due to the rarity of these cells, the initial enrichment step must be able to lose a large part of the unwanted cells, without losing too much of the targeted cells. The detection techniques after labeling/enrichment should be able to spot those target cells between large amounts of non-target cells. Third, the cells should be isolated as single cells to first prove their fetal nature before genetic analysis. Fourth, a DNA amplification step will be obligatory due to the rarity of the cells. Finally, the DNA of the fetal cells must remain intact during all of these manipulations to provide a reliable diagnosis.

Researchers from Baylor College of Medicine (Houston, Texas, US) were the first ones to report a successful genome-wide diagnosis for small CNVs from fetal trophoblasts isolated from maternal blood samples (110). They did not rely on the trophoblast size for cell enrichment, but used antibody labeling combined with automatic single cell scanning and picking using the CyteFinder (RareCyte Inc.). Shortly thereafter, ARCEDI (Veijle, Denmark) published similar results, detecting large chromosomal aberrations, using a patented antibody mix for magnetic enrichment and automatic scanning using a MetaSystems scanner with an in-house developed cell classifier (259). Although, the group from Rarecells in Paris was among the first to report fetal cell isolation in the maternal blood circulation, they only reported results after a targeted diagnosis. Some time ago our research group started collaborating with them to perform genome-wide analysis on their single trophoblasts isolated from an ISET filter. As we already developed a workflow for CNV analysis in PGD, we believe this approach could also be applied to cells isolated from the maternal blood.

Those three groups are among the most promising for cell-based NIPT so far. However, they are not ready to replace the invasive techniques in routine diagnostics. Baylor and ARCEDI still seem to lose a lot of cells during trophoblast enrichment, as their yield is only ±0.4 cells/ml of blood. According to previous reports one to six cells per milliliter of maternal blood should be present (107). Although Rarecells was able to enrich a bit more cells, they are not ready to perform a genome-wide analysis on the trophoblasts. The quality of the samples after laser microdissection limits the analysis possibilities. Our collaboration with Rarecells is still ongoing and we hope to be able to perform a genome-wide analysis in the near future.

To implement cell-based NIPT in the routine genetic diagnostics, more than one cell per patient will be essential. Breman *et al.* suggests to have at least five cells per patient and in cases with possible confined placental mosaicism (CPM) a second blood sample with 10-20 cells might be necessary (110). Single cell analysis is always a bit tricky as WGA might have caused some bias in the DNA. When enough cells are analyzed, we could probably identify the bias. However, we could also consider to combine the DNA from the different WGA products and conduct a single analysis for the combined cells. As the amplification bias is rather random, the bias should be partially eliminated after combining different WGA samples. However, CPM will then be more difficult to detect. More research will be needed to define the frequency of CPM in cell-based NIPT from trophoblasts. Although, it will probably be similar to the 1-2% observed in CVS.

Rarecells has already shown that their technique is applicable to both CTC and fetal cell isolation. The field of CTC research is a lot bigger than the small niche of researchers looking for fetal cells. Nevertheless, fetal cell research might profit from the fast technological developments for CTC enrichment. Our research group recently initiated the development of a workflow for cell-based NIPT based on a workflow for CTC enrichment. As our group already

has a lot of experience with DNA analyses on a limited number of cells, we hope to be able to safeguard the DNA quality for a proper STR and CNV analysis after fixation, staining, enrichment, isolation and amplification. The influence of two of these factors, fixation and amplification, has already been studied in this dissertation.

The implementation of a cell-based NIPT for prenatal diagnosis will lower the occurrence of miscarriages due to invasive technologies and might therefore lower the threshold for some couples to perform a genetic analysis on their fetus. In this respect, cell-based NIPT can lower the number of unprepared parents or decrease the burden on the health security system for the lifetime costs of an affected child (266). It might also decrease the number of unnecessary abortions performed due to false positive cell-free NIPT, as a lot of couples do not choose to perform a follow up invasive test after cell-free NIPT.

Future technological evolutions might further complicate the interpretation of genetic data.

Recent introduction of third generation sequencing might improve the analysis of single cells. Technologies, such as PacBio and NanoPore, do no longer need a clonal amplification step, which might partly reduce amplification bias. They are also able to create much longer reads than current technologies, which will improve the allocation of reads to their genomic location. However, they do not yet have the throughput and accuracy to sequence the complete human genome. Besides that, bias introduced during clonal amplification alone cannot explain the presence of all false CNVs we detected in our samples and omission will therefore not solve all bias. The possibility for long read sequencing will not even apply for whole genome amplified DNA, as the fragment length after WGA will still limit the read length.

Nevertheless, newer sequencing technologies might further evolve towards immediate sequencing of unamplified single cells and therefore enable further drop in the resolution possible for genetic diagnosis. However, the interpretation of such results will be more complicated and needs to be accompanied by a strong regulation and genetic counseling possibilities. This even posed already problems for invasive microarray testing (267-269) and pediatric whole genome/exome sequencing (270). There is currently no consensus on how to clinically manage VOUS (271) and when to return these incidental findings to patients (267, 268). A worldwide consensus will never be possible as too many difference exist between countries and even within some countries (ex. different states in the US). It is obvious that technical evolutions in genetic diagnostics will have to be accompanied with evolutions in counseling systems and genetic regulation. However, I believe that within the near future cell-based NIPT will be ready to either replace or coexist with the current invasive technologies.

Algemene discussie & Samenvatting

In de discussie sectie van ieder hoofdstuk werden de resultaten van de individuele studies reeds grondig besproken. In dit hoofdstuk zullen we deze resultaten samenvatten en de algemene bevindingen bespreken.

Onze eerste doelstelling was om shallow MPS te introduceren in PGD als mogelijke vervanger voor array comparatieve genome hybridisatie (aCGH) voor de analyse van chromosomale aberraties. Vooraleer we dit konden bereiken, ontwikkelden we eerst een algemene workflow, om op een gelimiteerde hoeveelheid cellen kopie nummer variatie (CNV) analyse uit te voeren na shallow MPS en dit met behulp van de gepaste whole genome amplificatie (WGA) methode. In **Hoofdstuk III** gebruikten we deze workflow om aan te tonen dat SurePlex WGA, vergeleken met MALBAC, beter geschikt was voor CNV-analyse na 'shallow MPS' van een gelimiteerde hoeveelheid cellen. Een geschikte WGA-methode voor CNV-analyse moet resulteren in een uniforme read distributie over het volledige genoom. Een niet-uniforme distributie van de reads zou kunnen wijzen op een over- of onder-amplificatie van bepaalde genomische regio's. Dit zou CNV's introduceren die oorspronkelijk niet aanwezig waren in het genoom of bestaande CNV's maskeren, wat zou leiden tot een verkeerde interpretatie van de genoomsequentie. Na amplificatie met MALBAC was de read distributie niet-uniform, resulterend in een biased CNV-profiel. Er werden een groot aantal CNVs gemist, terwijl er andere vals positieve CNV's wel werden gecalled. SurePlex amplificatie resulteerde daarentegen in een meer uniforme read distributie, met als gevolge een min of meer compleet CNV-profiel met minder vals positieven. Beide methoden zijn hybride PCR-methoden die, op de primers na, ongeveer hetzelfde amplificatie mechanisme gebruiken. Het is mogelijk dat de primers, gebruikt tijdens MALBAC-amplificatie, niet uniform binden aan het genoom of dat de loop vorming suboptimaal is doorgegaan.
Na beide methoden waren de vals positieve calls niet volledig consistent tussen de verschillende replicaten. Dit wijst er mogelijks op dat de amplificatie bias random werd geïntroduceerd en daarbij dus moeilijk te voorspellen valt. De één-cel samples vertoonden meer bias dan de drie- en vijf-cel samples. We zagen de bias verminderen wanneer we gebruik maakten van de PCR-vrije library preparatie methode. Dit toont aan dat een deel van de bias waarschijnlijk veroorzaakt werd door de enrichment PCR-stap tijdens de library preparatie. Desalniettemin, een deel van de bias bleef toch aanwezig na het weglaten van de enrichment PCR, zeker voor MALBAC-samples. De bias was dus afkomstig van zowel de WGA, als de enrichment PCR. Deze studie toonde ons dat SurePlex WGA mogelijks kan gebruikt worden voor CNV-detectie in PGD na shallow MPS van drie of meer cellen.

Daaropvolgend hebben we een gelijkaardige workflow, gebruik makende van SurePlex WGA, aangewend om ons eerste doel te bereiken. In **Hoofdstuk IV** toonden we aan dat shallow MPS op trophectoderm biopsieën een voorkeur geniet op aCGH voor het detecteren van chromosomale en structurele abnormaliteiten in PGD-embryo's. Met shallow MPS kon een hogere resolutie en een betere signal-to-noise ratio behaald worden in vergelijking met aCGH. Daarnaast kunnen veel stalen met elkaar en met stalen van andere applicaties (NIPT, exome sequencing) samen gesequeneerd worden op één run, waardoor de kost per sample zou moeten dalen. Deze bevindingen tonen aan dat MPS preciezer en flexibeler is dan aCGH. Voor bepaalde patiënten met een gekende kleinere afwijking kan de resolutie na MPS nog verlaagd worden (door de window size te verkleinen), specifiek voor dat chromosomale segment, zonder daarbij meer vals positieven te detecteren in de rest van het genoom. ACGH is hierin niet zo flexibel, want de resolutie is gelimiteerd tot de afstand tussen de probes. Vervolgens toonden we ook als één van de eersten aan dat de Illumina (NextSeq500) en Ion Torrent (Ion Proton) sequenerings-technologieën beiden toepasbaar waren in deze context en gelijkaardige resultaten vertoonden. De bovenstaande workflow werd in detail beschreven in **Hoofdstuk V**. Ondertussen wordt shallow MPS al succesvol toegepast voor CNV en aneuploidy detectie in PGD in verschillende genetische centra, waaronder het medisch genetisch centrum van Gent.

In deze klinische setting was SurePlex WGA zeker geschikt voor de amplificatie van 4-6 trophoblast cellen en een CNV-analyse aan een ≥ 3Mb resolutie. Een hogere resolutie in deze studie werd echter wel verhinderd door de representatie bias geïntroduceerd door de WGA. Naarmate minder cellen geamplificeerd worden zal deze bias nog toenemen (Hoofdstuk III). Dit geeft aan dat in een setting waar single-cel analyse heel belangrijk is (cel-gebaseerde NIPT of de detectie van heterogeniteit in een cel-populatie), een betere WGA-methode zal moeten worden aangewend. Daarom hebben wij, op verzoek van een aantal commerciële partners, een aantal andere WGA-methodes uitgetest voor CNV-analyse na single-cel sequenering, hopelijk resulterend in minder bias.

De eerste methode die getest werd, TruePrime WGA, gaf teleurstellende resultaten (**Hoofdstuk VI**). De read distributie was absoluut niet uniform en maakte het onmogelijk om een deftig CNV-profiel te bepalen. Onze resultaten suggereren dat TruePrime WGA niet geschikt is voor CNV-detectie na MPS van een gelimiteerd aantal cellen. Het kan dan ook geen verrassing zijn dat tot nog toe geen artikels werden gepubliceerd waarin deze methode werd toegepast. Het enige artikel dat te vinden is, is er één van het bedrijf dat de kit produceert (192). Wij vermoeden dat de instabiliteit van het TthPrimPl primase aan de basis ligt van de representatie bias. Het is mogelijk dat de stabiliteit van het primase erop achteruit gaat tijdens het verschepen naar andere locaties. Dit zou aantonen dat deze versie van de kit nog niet klaar is voor distributie. Kort na het publiceren van onze resultaten werden wij gecontacteerd om de nieuwe versie van hun kit te testen. Jammer genoeg waren deze resultaten niet veel beter dan hun eerste versie.

In **Hoofdstuk VII** werden DOPlify en PicoPLEX DNA-Seq vergeleken met Ampli1 en REPLI-g voor CNV-detectie na MPS van een gelimiteerd aantal cellen. Deze keer werd enkel de PCR-vrije library preparatie techniek toegepast. Alle vier de WGA-methoden lijken toepasbaar voor CNV-detectie na MPS van een gelimiteerd aantal cellen, maar DOPlify en PicoPlex DNA-Seq blonken uit. Na deze laatste twee werden alle verwachte CNV's gedetecteerd, zonder vals positieven en dit zowel bij een 1Mb als een 500kb window. Na Ampli1 en REPLI-g werden reeds vals positieven gedetecteerd bij een 1Mb window en steeg het aantal tot respectievelijk twee- en driemaal zoveel bij een 500kb window. Niettegenstaande werden sommige kleinere CNV's wel beter gedetecteerd in deze samples, wat kan wijzen op een lagere lokale signal-to-noise ratio na Ampli1 en REPLI-g amplificatie. Om deze reden zal men, voor deze twee methoden, de afweging moeten maken tussen enerzijds een hogere resolutie en anderzijds minder vals positieven.

DOPlify en PicoPLEX DNA-Seq zouden mogelijks SurePlex kunnen vervangen voor het detecteren van chromosomale aberraties in een klinische PGD-setting. PicoPLEX DNA-Seq gebruikt dezelfde WGA-technologie als SurePlex, maar de library preparatie is geïntegreerd tijdens de amplificatie. Dit maakt een aparte library preparatie onnodig. Qua kosten, tijd, contaminatierisico en gevoeligheid voor fouten, is deze methode te verkiezen boven SurePlex in een PGD-setting met Illumina sequenering. DOPlify is een geavanceerde DOP-PCR, maar meer details over de technologie werden niet vrijgegeven. Hoogstwaarschijnlijk werd het Taq polymerase vervangen, wat een verbetering zou zijn t.o.v. SurePlex. Als we DOPlify met PicoPLEX DNA-Seq vergelijken dan stellen we vast dat DOPlify beter is voor single-cel amplificatie, maar de twee gefaalde samples suggereren wel dat de methode minder robuust is dan PicoPLEX DNA-Seq. Aan de andere kant is PicoPLEX DNA-Seq minder flexibel, want deze resulteert altijd in een Illumina library en is dus niet compatibel met Ion Torrent sequencing.

In vergelijking met SurePlex lijken REPLI-g en Ampli1 meer bias te introduceren. Er werden namelijk geen vals positieven gedetecteerd in de drie PCR-vrije SurePlex samples uit Hoofdstuk III. Echter, dit zou ook kunnen berusten op toeval, aangezien slechts drie PCR-vrije SurePlex samples beschikbaar zijn ter vergelijking. Toch, REPLI-g maakt gebruik van de MDA-technologie en het is gekend dat hybride WGA-methoden beter zijn voor CNV-'detectie dan WGA-methoden met de MDA-technologie (130). Het mechanisme achter Ampli1 hangt dan weer af van de beschikbaarheid van restrictie sites. Een niet-uniforme distributie van deze sites langs het genoom zal leiden tot bias tijdens de amplificatie. Ampli1 vertoonde wel een iets hogere reproduceerbaarheid dan REPLI-g, daar die laatste meer vals positieven introduceerde. Deze bevindingen waren vergelijkbaar met een voorgaande studie door Hou *et al.*, waarbij Ampli1 een lagere amplificatie bias en een accuratere single-cel CNV detectie vertoonde dan REPLI-g (198).

In **Hoofdstuk VIII** hebben we ons gefocusseerd op het vinden van een betaalbare genoom-wijde analyse voor single nucleotide variaties (SNV's) gebruikmakende van MPS, die mogelijks een applicatie zou kunnen worden in PGD. Hiervoor hebben we het TruSight One sequencing panel getest om, vertrekkende van een gelimiteerd aantal cellen, meerdere SNV's simultaan te analyseren. Het TruSight One sequencing panel werd oorspronkelijk ontwikkeld om te screenen voor verschillende monogenetische aandoeningen in een prenatale setting na de vlokkentest. Dit panel voert een simultane capture uit van 4800 genomische regio's die geassocieerd zijn met bepaalde monogenetische aandoeningen en analyseert deze in één sequencing run. In een PGD-setting zal WGA nodig zijn om de kleine hoeveelheid startmateriaal te amplificeren. Zoals verwacht waren de resultaten verschillend voor WGA-DNA en bulk-DNA en we zagen dat dit verschil afhankelijk was van de gebruikte WGA-methode. De combinatie van SurePlex, Ampli1 en MALBAC WGA met het panel leek het niet goed te doen, want een groot aantal SNV's werd gemist of verkeerd gecalled. De combinatie van REPLI-g WGA met het panel was beter en meer vergelijkbaar met de resultaten van een bulk sample. De targeted coverage en variant calling kwam dicht in de buurt van de resultaten van de bulk samples. REPLI-g maakt gebruik van de MDA WGA-technologie en zou dus beter geschikt zijn voor SNV calling vergeleken met hybride WGA methoden (130). Echter, werd nog niet aangetoond dat dit ook geldt wanneer een capture is uitgevoerd vóór de SNV-analyse. MALBAC en SurePlex gebruiken beide het Bst polymerase voor hun pre-amplificatie stap en dit heeft een lagere betrouwbaarheid dan Phi29 polymerase gebruikt door REPLI-g. De betrouwbaarheid van de polymerase is veel belangrijker in deze context dan bij CNV-detectie. Ampli1 kan mogelijk gefaald hebben door een samenloop van de target sites van het panel en de zones geknipt door het restrictie-enzym, met als gevolg dat een aantal regio's niet kunnen gecaptured worden. Opnieuw was de bias tussen de verschillende replicaten in de vier methoden niet consistent en zal de introductie van bias tijdens amplificatie dus hoogstwaarschijnlijk random verlopen.

PicoPLEX DNA-Seq en DOPlify werden niet getest in deze studie want bij aanvang waren deze nog niet gelanceerd op de markt. Desalniettemin, PicoPLEX DNA-Seq gebruikt dezelfde WGA-technologie als SurePlex, waardoor we dus gelijkaardige resultaten kunnen verwachten. Bovendien resulteert deze WGA in een library die hoogstwaarschijnlijk niet kan gebruikt worden als startmateriaal voor het panel. In de toekomst kan het interessant zijn om eventueel nog DOPlify te testen in deze setting. Indien het panel goed zou werken op WGA-materiaal, zou het eventueel de state-of-the-art technologieën voor SGD-analyse in PGD kunnen vervangen. Hoewel de resultaten na REPLI-g amplificatie er veel belovend uitzien, zijn er toch nog grote verschillen met de bulk samples. Er zal dus nog een grondige klinische validatie nodig zijn van dit panel in combinatie met WGA vooraleer het kan toegepast worden in de kliniek.

Het laatste deel van deze thesis focust op STR-analyse in WGA geamplificeerde single cel samples. De genetische identificatie van een cel kan belangrijk zijn in applicaties zoals cel-gebaseerde NIPT. In **Hoofdstuk IX** werd nagegaan

of STR-analyse mogelijk was na amplificatie van één of drie cellen met SurePlex, Ampli1, REPLI-g of DOPlify. Gelijkaardig met de resultaten voor SNV-analyse, was REPLI-g wederom de beste WGA-methode. REPLI-g was de enige WGA-methode in deze studie die een volledig STR-profiel kon bepalen van tenminste sommige van zijn stalen. Echter, een compleet STR-profiel is niet noodzakelijk om de genetische identiteit van een cel te bepalen in een cel-gebaseerde NIPT-context. Een foetaal profiel zal bij heterogene merkers één allel van de moeder hebben en één allel van de vader. Het profiel van de moeder zal dus vergeleken worden met het nieuwe profiel en daaruit wordt dan afgeleid of het een zuiver maternale cel is of niet. Ampli1, SurePlex en DOPlify resulteerden meestal in een half STR-profiel, wat voldoende is om het foetale karakter van de cellen af te leiden. Na Ampli1 was de drop-out van een zestal regio's consistent tussen de verschillende samples, wat zou kunnen gerelateerd zijn aan het werkingsmechanisme van Ampli1. Het restrictie-enzym zal waarschijnlijk knippen aan de STR-primerbindingsite in deze regio's, waardoor hun amplificatie wordt geblokkeerd. Deze loci zouden kunnen vervangen worden door loci buiten de restricitezones, waardoor Ampli1 in een beter STR-profiel zou kunnen resulteren. De drop-out na SurePlex en DOPlify is meer random. SurePlex lijkt meer geschikt voor STR-analyse dan DOPlify en Ampli1, maar één van zijn samples vertoonde wel geen bruikbaar STR-profiel. Daardoor lijken DOPlify en Ampli1 robuuster en bijgevolg ook reproduceerbaarder.

In een cel-gebaseerde NIPT-setting is STR-analyse enkel nodig om zeker te zijn dat de geanalyseerde cel foetaal is. De genetische analyse, zoals CNV-detectie, is veel belangrijker in deze diagnostische setting. Daardoor is het belangrijk dat de gebruikte WGA-methode ook leidt tot een betrouwbare CNV-analyse. Bijvoorbeeld, MALBAC resulteerde in een mindere CNV-analyse en werd daarom niet getest in deze studie. DOPlify was één van de betere voor CNV-detectie en zou dus weleens de meest geschikte kandidaat kunnen zijn in een cel-gebaseerde NIPT-setting op verse cellen.

De STR-resultaten zijn echter verschillend wanneer de cellen gepreserveerd zijn vóór amplificatie **(Hoofdstuk X).** Na REPLI-g amplificatie was er enorm veel drop-out en kon er dus geen genomisch profiel worden bepaald. Het werd al eerder aangetoond dat een voldoende lange heating-stap bij cel lyse belangrijk zal zijn bij het voorkomen van chemische fixatie. Dit kan verklaren waarom REPLI-g, met de kortste lyse stap en de lage temperatuur, zorgt voor de slechtste resultaten. In tegenstelling tot REPLI-g toonden de andere WGA-methoden een lichte verbetering na fixatie. SurePlex had de laagste drop-out rate, maar opnieuw viel één van de stalen uit. Daardoor lijkt deze opnieuw minder robuust dan DOPlify en Ampli1. Echter, in een cel-gebaseerde NIPT-setting zal CNV-analyse alweer een belangrijke determinant zijn bij het kiezen van een WGA-methode. Voor REPLI-g waren de CNV-resultaten even onbruikbaar als zijn STR-resultaten. De andere drie WGA-methoden toonden vergelijkbare CNV-profielen met elkaar, al was Ampli1 de enige zonder vals positieven. Voor deze laatste was zelf een kleine verbetering zichtbaar t.o.v. CNV-analyse op verse cellen. Het werd na fixatie nog duidelijker dat de drop-outs na Ampli1 niet random zijn en

dus mogelijks te verbeteren met een betere plaatsing van de gekozen loci. Onze resultaten suggereren dat Ampli1 de meest geschikte kandidaat zou zijn voor cel-gebaseerde NIPT op gefixeerde cellen. We toonden in deze studie ook aan dat BCT-preservatie de DNA-analyse niet in de weg staat, zolang het gecombineerd worden met een geschikte WGA-methode.

Uit deze thesis concluderen we dat we mee de fundering gelegd hebben voor de introductie van shallow MPS in PGD voor CNV en aneuploidy detectie, als een vervanger van aCGH. Verder hebben we ook de prestatie van de meest moderne WGA-methodes bestudeerd voor onder andere shallow MPS CNV-analyse en STR-analyse op single gefixeerde en niet-gepreserveerde cellen. Bijgevolg hebben we de nodige tools klaar voor een genetische analyse in cel-gebaseerde NIPT, van zodra het mogelijk is om foetale cellen betrouwbaar uit het maternaal bloed te isoleren.

References

1. European IVFMCftESoHR, Embryology, Calhaz-Jorge C, de Geyter C, Kupka MS, de Mouzon J, et al. Assisted reproductive technology in Europe, 2012: results generated from European registers by ESHRE. Hum Reprod. 2016;31(8):1638-52.
2. Kanehl ELSaJ. Utilization of art services in developed countries and impact on cross-border reproductive care. In: Hershberger ELSPE, editor. Fertility and Assisted Reproductive Technology (ART): Springer; 2016.
3. Scott L, Alvero R, Leondires M, Miller B. The morphology of human pronuclear embryos is positively related to blastocyst development and implantation. Hum Reprod. 2000;15(11):2394-403.
4. Dennis SJ, Thomas MA, Williams DB, Robins JC. Embryo morphology score on day 3 is predictive of implantation and live birth rates. J Assist Reprod Genet. 2006;23(4):171-5.
5. Balaban B, Urman B, Isiklar A, Alatas C, Aksoy S, Mercan R, et al. The effect of pronuclear morphology on embryo quality parameters and blastocyst transfer outcome. Hum Reprod. 2001;16(11):2357-61.
6. De Placido G, Wilding M, Strina I, Alviggi E, Alviggi C, Mollo A, et al. High outcome predictability after IVF using a combined score for zygote and embryo morphology and growth rate. Hum Reprod. 2002;17(9):2402-9.
7. Fisch JD, Rodriguez H, Ross R, Overby G, Sher G. The Graduated Embryo Score (GES) predicts blastocyst formation and pregnancy rate from cleavage-stage embryos. Hum Reprod. 2001;16(9):1970-5.
8. Giorgetti C, Terriou P, Auquier P, Hans E, Spach JL, Salzmann J, et al. Embryo score to predict implantation after in-vitro fertilization: based on 957 single embryo transfers. Hum Reprod. 1995;10(9):2427-31.
9. Van Royen E, Mangelschots K, De Neubourg D, Valkenburg M, Van de Meerssche M, Ryckaert G, et al. Characterization of a top quality embryo, a step towards single-embryo transfer. Hum Reprod. 1999;14(9):2345-9.
10. Edwards RG, Fishel SB, Cohen J, Fehilly CB, Purdy JM, Slater JM, et al. Factors influencing the success of in vitro fertilization for alleviating human infertility. J In Vitro Fert Embryo Transf. 1984;1(1):3-23.
11. Leese HJ. Quiet please, do not disturb: a hypothesis of embryo metabolism and viability. Bioessays. 2002;24(9):845-9.
12. Magli MC, Gianaroli L, Ferraretti AP, Lappi M, Ruberti A, Farfalli V. Embryo morphology and development are dependent on the chromosomal complement. Fertil Steril. 2007;87(3):534-41.
13. Munne S. Chromosome abnormalities and their relationship to morphology and development of human embryos. Reprod Biomed Online. 2006;12(2):234-53.
14. Ziebe S, Petersen K, Lindenberg S, Andersen AG, Gabrielsen A, Andersen AN. Embryo morphology or cleavage stage: how to select the best embryos for transfer after in-vitro fertilization. Hum Reprod. 1997;12(7):1545-9.
15. O'Leary T, Heindryckx B, Lierman S, Van der Jeught M, Duggal G, De Sutter P, et al. Derivation of human embryonic stem cells using a post-inner cell mass intermediate. Nat Protoc. 2013;8(2):254-64.
16. Balaban B, Yakin K, Urman B. Randomized comparison of two different blastocyst grading systems. Fertil Steril. 2006;85(3):559-63.
17. Kovacic VVB. Importance of blastocyst morphology in selection for tranfer. In: Wu B, editor. Advances in embryo tranfer: InTech; 2012.
18. Magli MC, Jones GM, Gras L, Gianaroli L, Korman I, Trounson AO. Chromosome mosaicism in day 3 aneuploid embryos that develop to morphologically normal blastocysts in vitro. Hum Reprod. 2000;15(8):1781-6.
19. Staessen C, Platteau P, Van Assche E, Michiels A, Tournaye H, Camus M, et al. Comparison of blastocyst transfer with or without preimplantation genetic diagnosis for aneuploidy screening in couples with advanced maternal age: a prospective randomized controlled trial. Hum Reprod. 2004;19(12):2849-58.
20. Yang Z, Liu J, Collins GS, Salem SA, Liu X, Lyle SS, et al. Selection of single blastocysts for fresh transfer via standard morphology assessment alone and with array CGH for good prognosis IVF patients: results from a randomized pilot study. Mol Cytogenet. 2012;5(1):24.
21. Munne S, Cohen J. Chromosome abnormalities in human embryos. Hum Reprod Update. 1998;4(6):842-55.
22. Voullaire L, Wilton L, McBain J, Callaghan T, Williamson R. Chromosome abnormalities identified by comparative genomic hybridization in embryos from women with repeated implantation failure. Mol Hum Reprod. 2002;8(11):1035-41.
23. Narchi H. Reducing birth defects- The cost- Effective and global way forward. In: Engels JV, editor. Birth defects: New research: Nova Science; 2006. p. 201-38.
24. Simopoulou M, Harper JC, Fragouli E, Mantzouratou A, Speyer BE, Serhal P, et al. Preimplantation genetic diagnosis of chromosome abnormalities: implications from the outcome for couples with chromosomal rearrangements. Prenat Diagn. 2003;23(8):652-62.
25. Fragouli E, Alfarawati S, Daphnis DD, Goodall NN, Mania A, Griffiths T, et al. Cytogenetic analysis of human blastocysts with the use of FISH, CGH and aCGH: scientific data and technical evaluation. Hum Reprod. 2011;26(2):480-90.
26. McArthur SJ, Leigh D, Marshall JT, Gee AJ, De Boer KA, Jansen RP. Blastocyst trophectoderm biopsy and preimplantation genetic diagnosis for familial monogenic disorders and chromosomal translocations. Prenat Diagn. 2008;28(5):434-42.
27. Scriven PN, Kirby TL, Ogilvie CM. FISH for pre-implantation genetic diagnosis. J Vis Exp. 2011(48).
28. Bejjani BA, Shaffer LG. Application of array-based comparative genomic hybridization to clinical diagnostics. J Mol Diagn. 2006;8(5):528-33.
29. Lucito R, Healy J, Alexander J, Reiner A, Esposito D, Chi M, et al. Representational oligonucleotide microarray analysis: a high-resolution method to detect genome copy number variation. Genome Res. 2003;13(10):2291-305.

30. Deleye L, Dheedene A, De Coninck D, Sante T, Christodoulou C, Heindryckx B, et al. Shallow whole genome sequencing is well suited for the detection of chromosomal aberrations in human blastocysts. Fertil Steril. 2015;104(5):1276-85 e1.
31. Tan Y, Yin X, Zhang S, Jiang H, Tan K, Li J, et al. Clinical outcome of preimplantation genetic diagnosis and screening using next generation sequencing. Gigascience. 2014;3(1):30.
32. Wells D, Kaur K, Grifo J, Glassner M, Taylor JC, Fragouli E, et al. Clinical utilisation of a rapid low-pass whole genome sequencing technique for the diagnosis of aneuploidy in human embryos prior to implantation. J Med Genet. 2014;51(8):553-62.
33. Treff NR, Su J, Tao X, Northrop LE, Scott RT, Jr. Single-cell whole-genome amplification technique impacts the accuracy of SNP microarray-based genotyping and copy number analyses. Mol Hum Reprod. 2011;17(6):335-43.
34. Treff NR, Scott RT, Jr. Four-hour quantitative real-time polymerase chain reaction-based comprehensive chromosome screening and accumulating evidence of accuracy, safety, predictive value, and clinical efficacy. Fertil Steril. 2013;99(4):1049-53.
35. Sermon KD, Michiels A, Harton G, Moutou C, Repping S, Scriven PN, et al. ESHRE PGD Consortium data collection VI: cycles from January to December 2003 with pregnancy follow-up to October 2004. Hum Reprod. 2007;22(2):323-36.
36. Harton GL, De Rycke M, Fiorentino F, Moutou C, SenGupta S, Traeger-Synodinos J, et al. ESHRE PGD consortium best practice guidelines for amplification-based PGD. Hum Reprod. 2011;26(1):33-40.
37. Sermon K. Current concepts in preimplantation genetic diagnosis (PGD): a molecular biologist's view. Hum Reprod Update. 2002;8(1):11-20.
38. Thornhill AR, Snow K. Molecular diagnostics in preimplantation genetic diagnosis. J Mol Diagn. 2002;4(1):11-29.
39. Dreesen J, Destouni A, Kourlaba G, Degn B, Mette WC, Carvalho F, et al. Evaluation of PCR-based preimplantation genetic diagnosis applied to monogenic diseases: a collaborative ESHRE PGD consortium study. Eur J Hum Genet. 2014;22(8):1012-8.
40. Brezina PR, Benner A, Rechitsky S, Kuliev A, Pomerantseva E, Pauling D, et al. Single-gene testing combined with single nucleotide polymorphism microarray preimplantation genetic diagnosis for aneuploidy: a novel approach in optimizing pregnancy outcome. Fertil Steril. 2011;95(5):1786 e5-8.
41. Handyside AH, Harton GL, Mariani B, Thornhill AR, Affara N, Shaw MA, et al. Karyomapping: a universal method for genome wide analysis of genetic disease based on mapping crossovers between parental haplotypes. J Med Genet. 2010;47(10):651-8.
42. Obradors A, Fernandez E, Oliver-Bonet M, Rius M, de la Fuente A, Wells D, et al. Birth of a healthy boy after a double factor PGD in a couple carrying a genetic disease and at risk for aneuploidy: case report. Hum Reprod. 2008;23(8):1949-56.
43. Obradors A, Fernandez E, Rius M, Oliver-Bonet M, Martinez-Fresno M, Benet J, et al. Outcome of twin babies free of Von Hippel-Lindau disease after a double-factor preimplantation genetic diagnosis: monogenetic mutation analysis and comprehensive aneuploidy screening. Fertil Steril. 2009;91(3):933 e1-7.
44. Rechitsky S, Verlinsky O, Kuliev A. PGD for cystic fibrosis patients and couples at risk of an additional genetic disorder combined with 24-chromosome aneuploidy testing. Reprod Biomed Online. 2013;26(5):420-30.
45. Treff NR, Tao X, Schillings WJ, Bergh PA, Scott RT, Jr., Levy B. Use of single nucleotide polymorphism microarrays to distinguish between balanced and normal chromosomes in embryos from a translocation carrier. Fertil Steril. 2011;96(1):e58-65.
46. Russo CD, Di Giacomo G, Cignini P, Padula F, Mangiafico L, Mesoraca A, et al. Comparative study of aCGH and Next Generation Sequencing (NGS) for chromosomal microdeletion and microduplication screening. J Prenat Med. 2014;8(3-4):57-69.
47. Harper JC, Boelaert K, Geraedts J, Harton G, Kearns WG, Moutou C, et al. ESHRE PGD Consortium data collection V: cycles from January to December 2002 with pregnancy follow-up to October 2003. Hum Reprod. 2006;21(1):3-21.
48. De Vos A, Staessen C, De Rycke M, Verpoest W, Haentjens P, Devroey P, et al. Impact of cleavage-stage embryo biopsy in view of PGD on human blastocyst implantation: a prospective cohort of single embryo transfers. Hum Reprod. 2009;24(12):2988-96.
49. Kokkali G, Traeger-Synodinos J, Vrettou C, Stavrou D, Jones GM, Cram DS, et al. Blastocyst biopsy versus cleavage stage biopsy and blastocyst transfer for preimplantation genetic diagnosis of beta-thalassaemia: a pilot study. Hum Reprod. 2007;22(5):1443-9.
50. Johnson DS, Cinnioglu C, Ross R, Filby A, Gemelos G, Hill M, et al. Comprehensive analysis of karyotypic mosaicism between trophectoderm and inner cell mass. Mol Hum Reprod. 2010;16(12):944-9.
51. Cimadomo D, Capalbo A, Ubaldi FM, Scarica C, Palagiano A, Canipari R, et al. The Impact of Biopsy on Human Embryo Developmental Potential during Preimplantation Genetic Diagnosis. Biomed Res Int. 2016;2016:7193075.
52. Scott RT, Jr., Upham KM, Forman EJ, Zhao T, Treff NR. Cleavage-stage biopsy significantly impairs human embryonic implantation potential while blastocyst biopsy does not: a randomized and paired clinical trial. Fertil Steril. 2013;100(3):624-30.
53. Veiga A, Sandalinas M, Benkhalifa M, Boada M, Carrera M, Santalo J, et al. Laser blastocyst biopsy for preimplantation diagnosis in the human. Zygote. 1997;5(4):351-4.
54. Dimitriadou E, Van der Aa N, Cheng J, Voet T, Vermeesch JR. Single cell segmental aneuploidy detection is compromised by S phase. Mol Cytogenet. 2014;7:46.
55. Los FJ, Van Opstal D, van den Berg C. The development of cytogenetically normal, abnormal and mosaic embryos: a theoretical model. Hum Reprod Update. 2004;10(1):79-94.
56. van Echten-Arends J, Mastenbroek S, Sikkema-Raddatz B, Korevaar JC, Heineman MJ, van der Veen F, et al. Chromosomal mosaicism in human preimplantation embryos: a systematic review. Hum Reprod Update. 2011;17(5):620-7.
57. Evsikov S, Verlinsky Y. Mosaicism in the inner cell mass of human blastocysts. Hum Reprod. 1998;13(11):3151-5.
58. Vanneste E, Voet T, Le Caignec C, Ampe M, Konings P, Melotte C, et al. Chromosome instability is common in human cleavage-stage embryos. Nat Med. 2009;15(5):577-83.
59. Voet T, Vanneste E, Van der Aa N, Melotte C, Jackmaert S, Vandendael T, et al. Breakage-fusion-bridge cycles leading to inv dup del occur in human cleavage stage embryos. Hum Mutat. 2011;32(7):783-93.
60. Voet T, Vanneste E, Vermeesch JR. The human cleavage stage embryo is a cradle of chromosomal rearrangements. Cytogenet Genome Res. 2011;133(2-4):160-8.
61. Scott RT, Jr., Upham KM, Forman EJ, Hong KH, Scott KL, Taylor D, et al. Blastocyst biopsy with comprehensive chromosome screening and fresh embryo transfer significantly increases in vitro fertilization implantation and delivery rates: a randomized controlled trial. Fertil Steril. 2013;100(3):697-703.

62. Seki S, Mazur P. The dominance of warming rate over cooling rate in the survival of mouse oocytes subjected to a vitrification procedure. Cryobiology. 2009;59(1):75-82.
63. Van Landuyt L, Stoop D, Verheyen G, Verpoest W, Camus M, Van de Velde H, et al. Outcome of closed blastocyst vitrification in relation to blastocyst quality: evaluation of 759 warming cycles in a single-embryo transfer policy. Hum Reprod. 2011;26(3):527-34.
64. Roque M, Valle M, Guimaraes F, Sampaio M, Geber S. Freeze-all policy: fresh vs. frozen-thawed embryo transfer. Fertil Steril. 2015;103(5):1190-3.
65. Debost-Legrand A, Laurichesse-Delmas H, Francannet C, Perthus I, Lemery D, Gallot D, et al. False positive morphologic diagnoses at the anomaly scan: marginal or real problem, a population-based cohort study. BMC Pregnancy Childbirth. 2014;14:112.
66. Gekas J, Langlois S, Ravitsky V, Audibert F, van den Berg DG, Haidar H, et al. Non-invasive prenatal testing for fetal chromosome abnormalities: review of clinical and ethical issues. Appl Clin Genet. 2016;9:15-26.
67. Jacobson CB, Barter RH. Intrauterine diagnosis and management of genetic defects. Am J Obstet Gynecol. 1967;99(6):796-807.
68. I. EM. Reproductive risks and prenatal diagnosis: Appleton & Lange; 1992.
69. Wapner RJ, Martin CL, Levy B, Ballif BC, Eng CM, Zachary JM, et al. Chromosomal microarray versus karyotyping for prenatal diagnosis. N Engl J Med. 2012;367(23):2175-84.
70. Manning M, Hudgins L, Professional P, Guidelines C. Array-based technology and recommendations for utilization in medical genetics practice for detection of chromosomal abnormalities. Genet Med. 2010;12(11):742-5.
71. Miller DT, Adam MP, Aradhya S, Biesecker LG, Brothman AR, Carter NP, et al. Consensus statement: chromosomal microarray is a first-tier clinical diagnostic test for individuals with developmental disabilities or congenital anomalies. Am J Hum Genet. 2010;86(5):749-64.
72. Akolekar R, Beta J, Picciarelli G, Ogilvie C, D'Antonio F. Procedure-related risk of miscarriage following amniocentesis and chorionic villus sampling: a systematic review and meta-analysis. Ultrasound Obstet Gynecol. 2015;45(1):16-26.
73. Ogilvie C, Akolekar R. Pregnancy Loss Following Amniocentesis or CVS Sampling-Time for a Reassessment of Risk. J Clin Med. 2014;3(3):741-6.
74. Lo YM, Corbetta N, Chamberlain PF, Rai V, Sargent IL, Redman CW, et al. Presence of fetal DNA in maternal plasma and serum. Lancet. 1997;350(9076):485-7.
75. Hochstenbach R, Nikkels PG, Elferink MG, Oudijk MA, van Oppen C, van Zon P, et al. Cell-free fetal DNA in the maternal circulation originates from the cytotrophoblast: proof from an unique case. Clin Case Rep. 2015;3(6):489-91.
76. Lo YM, Tein MS, Lau TK, Haines CJ, Leung TN, Poon PM, et al. Quantitative analysis of fetal DNA in maternal plasma and serum: implications for noninvasive prenatal diagnosis. Am J Hum Genet. 1998;62(4):768-75.
77. Society for Maternal-Fetal Medicine Publications Committee. Electronic address pso. #36: Prenatal aneuploidy screening using cell-free DNA. Am J Obstet Gynecol. 2015;212(6):711-6.
78. Larion S, Warsof SL, Romary L, Mlynarczyk M, Peleg D, Abuhamad AZ. Uptake of noninvasive prenatal testing at a large academic referral center. Am J Obstet Gynecol. 2014;211(6):651 e1-7.
79. Wax JR, Cartin A, Chard R, Lucas FL, Pinette MG. Noninvasive prenatal testing: impact on genetic counseling, invasive prenatal diagnosis, and trisomy 21 detection. J Clin Ultrasound. 2015;43(1):1-6.
80. Williams J, 3rd, Rad S, Beauchamp S, Ratousi D, Subramaniam V, Farivar S, et al. Utilization of noninvasive prenatal testing: impact on referrals for diagnostic testing. Am J Obstet Gynecol. 2015;213(1):102 e1-6.
81. Beaudet AL. Using fetal cells for prenatal diagnosis: History and recent progress. Am J Med Genet C Semin Med Genet. 2016;172(2):123-7.
82. Cheung SW, Patel A, Leung TY. Accurate description of DNA-based noninvasive prenatal screening. N Engl J Med. 2015;372(17):1675-7.
83. Walsh JM, Goldberg JD. Fetal aneuploidy detection by maternal plasma DNA sequencing: a technology assessment. Prenat Diagn. 2013;33(6):514-20.
84. Boon EM, Faas BH. Benefits and limitations of whole genome versus targeted approaches for noninvasive prenatal testing for fetal aneuploidies. Prenat Diagn. 2013;33(6):563-8.
85. Herzenberg LA, Bianchi DW, Schroder J, Cann HM, Iverson GM. Fetal cells in the blood of pregnant women: detection and enrichment by fluorescence-activated cell sorting. Proc Natl Acad Sci U S A. 1979;76(3):1453-5.
86. Schindler AM, Martin-du-Pan R. Prenatal diagnosis of fetal lymphocytes in the maternal blood. Obstet Gynecol. 1972;40(3):340-6.
87. Walknowska J, Conte FA, Grumbach MM. Practical and theoretical implications of fetal-maternal lymphocyte transfer. Lancet. 1969;1(7606):1119-22.
88. Schroder J, Tiilikainen A, De la Chapelle A. Fetal leukocytes in the maternal circulation after delivery. I. Cytological aspects. Transplantation. 1974;17(4):346-54.
89. Ciaranfi A, Curchod A, Odartchenko N. [Post-partum survival of fetal lymphocytes in the maternal blood]. Schweiz Med Wochenschr. 1977;107(5):134-8.
90. Grosset L, Barrelet V, Odartchenko N. Antenatal fetal sex determination from maternal blood during early pregnancy. Am J Obstet Gynecol. 1974;120(1):60-3.
91. Sargent IL, Choo YS, Redman CW. Isolating and analyzing fetal leukocytes in maternal blood. Ann N Y Acad Sci. 1994;731:147-53.
92. Kleihauer E, Braun H, Betke K. [Demonstration of fetal hemoglobin in erythrocytes of a blood smear]. Klin Wochenschr. 1957;35(12):637-8.
93. Holzgreve W, Garritsen HS, Ganshirt-Ahlert D. Fetal cells in the maternal circulation. J Reprod Med. 1992;37(5):410-8.
94. Bianchi DW, Flint AF, Pizzimenti MF, Knoll JH, Latt SA. Isolation of fetal DNA from nucleated erythrocytes in maternal blood. Proc Natl Acad Sci U S A. 1990;87(9):3279-83.
95. Bianchi DW, Mahr A, Zickwolf GK, Houseal TW, Flint AF, Klinger KW. Detection of fetal cells with 47,XY,+21 karyotype in maternal peripheral blood. Hum Genet. 1992;90(4):368-70.
96. Ganshirt-Ahlert D, Burschyk M, Garritsen HS, Helmer L, Miny P, Horst J, et al. Magnetic cell sorting and the transferrin receptor as potential means of prenatal diagnosis from maternal blood. Am J Obstet Gynecol. 1992;166(5):1350-5.
97. Miltenyi S, Muller W, Weichel W, Radbruch A. High gradient magnetic cell separation with MACS. Cytometry. 1990;11(2):231-8.
98. Ganshirt D, Garritsen H, Miny P, Holzgreve W. Fetal cells in maternal circulation throughout gestation. Lancet. 1994;343(8904):1038-9.

99. Hamada H, Arinami T, Sohda S, Hamaguchi H, Kubo T. Mid-trimester fetal sex determination from maternal peripheral blood by fluorescence in situ hybridization without enrichment of fetal cells. Prenat Diagn. 1995;15(1):78-81.
100. Holzgreve W, Ghezzi F, Di Naro E, Ganshirt D, Maymon E, Hahn S. Disturbed feto-maternal cell traffic in preeclampsia. Obstet Gynecol. 1998;91(5 Pt 1):669-72.
101. Slunga-Tallberg A, el-Rifai W, Keinanen M, Ylinen K, Kurki T, Klinger K, et al. Maternal origin of nucleated erythrocytes in peripheral venous blood of pregnant women. Hum Genet. 1995;96(1):53-7.
102. Slunga-Tallberg A, el-Rifai W, Keinanen M, Ylinen K, Kurki T, Klinger K, et al. Maternal origin of transferrin receptor positive cells in venous blood of pregnant women. Clin Genet. 1996;49(4):196-9.
103. Bianchi DW, Simpson JL, Jackson LG, Elias S, Holzgreve W, Evans MI, et al. Fetal gender and aneuploidy detection using fetal cells in maternal blood: analysis of NIFTY I data. National Institute of Child Health and Development Fetal Cell Isolation Study. Prenat Diagn. 2002;22(7):609-15.
104. Oudejans CB, Tjoa ML, Westerman BA, Mulders MA, Van Wijk IJ, Van Vugt JM. Circulating trophoblast in maternal blood. Prenat Diagn. 2003;23(2):111-6.
105. Mouawia H, Saker A, Jais JP, Benachi A, Bussieres L, Lacour B, et al. Circulating trophoblastic cells provide genetic diagnosis in 63 fetuses at risk for cystic fibrosis or spinal muscular atrophy. Reprod Biomed Online. 2012;25(5):508-20.
106. Bulmer JN, Johnson PM. Antigen expression by trophoblast populations in the human placenta and their possible immunobiological relevance. Placenta. 1985;6(2):127-40.
107. Hatt L, Brinch M, Singh R, Moller K, Lauridsen RH, Schlutter JM, et al. A new marker set that identifies fetal cells in maternal circulation with high specificity. Prenat Diagn. 2014;34(11):1066-72.
108. Emad A, Bouchard EF, Lamoureux J, Ouellet A, Dutta A, Klingbeil U, et al. Validation of automatic scanning of microscope slides in recovering rare cellular events: application for detection of fetal cells in maternal blood. Prenat Diagn. 2014;34(6):538-46.
109. Beroud C, Karliova M, Bonnefont JP, Benachi A, Munnich A, Dumez Y, et al. Prenatal diagnosis of spinal muscular atrophy by genetic analysis of circulating fetal cells. Lancet. 2003;361(9362):1013-4.
110. Breman AM, Chow JC, U'Ren L, Normand EA, Qdaisat S, Zhao L, et al. Evidence for feasibility of fetal trophoblastic cell-based noninvasive prenatal testing. Prenat Diagn. 2016;36(11):1009-19.
111. Head IM, Saunders JR, Pickup RW. Microbial Evolution, Diversity, and Ecology: A Decade of Ribosomal RNA Analysis of Uncultivated Microorganisms. Microb Ecol. 1998;35(1):1-21.
112. Kanagawa T. Bias and artifacts in multitemplate polymerase chain reactions (PCR). J Biosci Bioeng. 2003;96(4):317-23.
113. Kurata S, Kanagawa T, Magariyama Y, Takatsu K, Yamada K, Yokomaku T, et al. Reevaluation and reduction of a PCR bias caused by reannealing of templates. Appl Environ Microbiol. 2004;70(12):7545-9.
114. von Wintzingerode F, Gobel UB, Stackebrandt E. Determination of microbial diversity in environmental samples: pitfalls of PCR-based rRNA analysis. FEMS Microbiol Rev. 1997;21(3):213-29.
115. Lichter P, Ledbetter SA, Ledbetter DH, Ward DC. Fluorescence in situ hybridization with Alu and L1 polymerase chain reaction probes for rapid characterization of human chromosomes in hybrid cell lines. Proc Natl Acad Sci U S A. 1990;87(17):6634-8.
116. Telenius H, Carter NP, Bebb CE, Nordenskjold M, Ponder BA, Tunnacliffe A. Degenerate oligonucleotide-primed PCR: general amplification of target DNA by a single degenerate primer. Genomics. 1992;13(3):718-25.
117. Troutt AB, McHeyzer-Williams MG, Pulendran B, Nossal GJ. Ligation-anchored PCR: a simple amplification technique with single-sided specificity. Proc Natl Acad Sci U S A. 1992;89(20):9823-5.
118. Sabina J, Leamon JH. Bias in Whole Genome Amplification: Causes and Considerations. Methods Mol Biol. 2015;1347:15-41.
119. Zhang L, Cui X, Schmitt K, Hubert R, Navidi W, Arnheim N. Whole genome amplification from a single cell: implications for genetic analysis. Proc Natl Acad Sci U S A. 1992;89(13):5847-51.
120. Alsmadi O, Alkayal F, Monies D, Meyer BF. Specific and complete human genome amplification with improved yield achieved by phi29 DNA polymerase and a novel primer at elevated temperature. BMC Res Notes. 2009;2:48.
121. Cassandra L. SaCC. Genomics: The science and technology behind the human genome project. Journal of chemical education1999.
122. Iserte JA, Stephan BI, Goni SE, Borio CS, Ghiringhelli PD, Lozano ME. Family-specific degenerate primer design: a tool to design consensus degenerated oligonucleotides. Biotechnol Res Int. 2013;2013:383646.
123. Pinard R, de Winter A, Sarkis GJ, Gerstein MB, Tartaro KR, Plant RN, et al. Assessment of whole genome amplification-induced bias through high-throughput, massively parallel whole genome sequencing. BMC Genomics. 2006;7:216.
124. Cheung VG, Nelson SF. Whole genome amplification using a degenerate oligonucleotide primer allows hundreds of genotypes to be performed on less than one nanogram of genomic DNA. Proc Natl Acad Sci U S A. 1996;93(25):14676-9.
125. Spits C, Sermon K. PGD for monogenic disorders: aspects of molecular biology. Prenat Diagn. 2009;29(1):50-6.
126. Dean FB, Hosono S, Fang L, Wu X, Faruqi AF, Bray-Ward P, et al. Comprehensive human genome amplification using multiple displacement amplification. Proc Natl Acad Sci U S A. 2002;99(8):5261-6.
127. Lage JM, Leamon JH, Pejovic T, Hamann S, Lacey M, Dillon D, et al. Whole genome analysis of genetic alterations in small DNA samples using hyperbranched strand displacement amplification and array-CGH. Genome Res. 2003;13(2):294-307.
128. Dean FB, Nelson JR, Giesler TL, Lasken RS. Rapid amplification of plasmid and phage DNA using Phi 29 DNA polymerase and multiply-primed rolling circle amplification. Genome Res. 2001;11(6):1095-9.
129. Zhang DY, Brandwein M, Hsuih T, Li HB. Ramification amplification: a novel isothermal DNA amplification method. Mol Diagn. 2001;6(2):141-50.
130. de Bourcy CF, De Vlaminck I, Kanbar JN, Wang J, Gawad C, Quake SR. A quantitative comparison of single-cell whole genome amplification methods. PLoS One. 2014;9(8):e105585.
131. Lizardi PM, Huang X, Zhu Z, Bray-Ward P, Thomas DC, Ward DC. Mutation detection and single-molecule counting using isothermal rolling-circle amplification. Nat Genet. 1998;19(3):225-32.
132. Langmore JP. Rubicon Genomics, Inc. Pharmacogenomics. 2002;3(4):557-60.

133. Zong C, Lu S, Chapman AR, Xie XS. Genome-wide detection of single-nucleotide and copy-number variations of a single human cell. Science. 2012;338(6114):1622-6.
134. Czyz ZT, Klein CA. Deterministic Whole-Genome Amplification of Single Cells. Methods Mol Biol. 2015;1347:69-86.
135. Pirker C, Raidl M, Steiner E, Elbling L, Holzmann K, Spiegl-Kreinecker S, et al. Whole genome amplification for CGH analysis: Linker-adapter PCR as the method of choice for difficult and limited samples. Cytometry A. 2004;61(1):26-34.
136. Shapiro E, Biezuner T, Linnarsson S. Single-cell sequencing-based technologies will revolutionize whole-organism science. Nat Rev Genet. 2013;14(9):618-30.
137. Cline J, Braman JC, Hogrefe HH. PCR fidelity of pfu DNA polymerase and other thermostable DNA polymerases. Nucleic Acids Res. 1996;24(18):3546-51.
138. Hogrefe HH, Cline J, Lovejoy AE, Nielson KB. DNA polymerases from hyperthermophiles. Methods Enzymol. 2001;334:91-116.
139. Aviel-Ronen S, Qi Zhu C, Coe BP, Liu N, Watson SK, Lam WL, et al. Large fragment Bst DNA polymerase for whole genome amplification of DNA from formalin-fixed paraffin-embedded tissues. BMC Genomics. 2006;7:312.
140. Coombs NJ, Gough AC, Primrose JN. Optimisation of DNA and RNA extraction from archival formalin-fixed tissue. Nucleic Acids Res. 1999;27(16):e12.
141. Srinivasan M, Sedmak D, Jewell S. Effect of fixatives and tissue processing on the content and integrity of nucleic acids. Am J Pathol. 2002;161(6):1961-71.
142. Tokuda Y, Nakamura T, Satonaka K, Maeda S, Doi K, Baba S, et al. Fundamental study on the mechanism of DNA degradation in tissues fixed in formaldehyde. J Clin Pathol. 1990;43(9):748-51.
143. Williams C, Ponten F, Moberg C, Soderkvist P, Uhlen M, Ponten J, et al. A high frequency of sequence alterations is due to formalin fixation of archival specimens. Am J Pathol. 1999;155(5):1467-71.
144. Douglas MP, Rogers SO. DNA damage caused by common cytological fixatives. Mutat Res. 1998;401(1-2):77-88.
145. Lander ES, Linton LM, Birren B, Nusbaum C, Zody MC, Baldwin J, et al. Initial sequencing and analysis of the human genome. Nature. 2001;409(6822):860-921.
146. Sanger F, Nicklen S, Coulson AR. DNA sequencing with chain-terminating inhibitors. Proc Natl Acad Sci U S A. 1977;74(12):5463-7.
147. Hutchison CA, 3rd. DNA sequencing: bench to bedside and beyond. Nucleic Acids Res. 2007;35(18):6227-37.
148. Morozova O, Marra MA. Applications of next-generation sequencing technologies in functional genomics. Genomics. 2008;92(5):255-64.
149. Shendure J, Ji H. Next-generation DNA sequencing. Nat Biotechnol. 2008;26(10):1135-45.
150. Mardis ER. A decade's perspective on DNA sequencing technology. Nature. 2011;470(7333):198-203.
151. Metzker ML. Sequencing technologies - the next generation. Nat Rev Genet. 2010;11(1):31-46.
152. Knierim E, Lucke B, Schwarz JM, Schuelke M, Seelow D. Systematic comparison of three methods for fragmentation of long-range PCR products for next generation sequencing. PLoS One. 2011;6(11):e28240.
153. Illumina. Sequencing power for every scale 2015 [Available from: https://www.illumina.com/content/dam/illumina-marketing/documents/products/brochures/brochure_sequencing_systems_portfolio.pdf.
154. Jain M, Fiddes IT, Miga KH, Olsen HE, Paten B, Akeson M. Improved data analysis for the MinION nanopore sequencer. Nat Methods. 2015;12(4):351-6.
155. Derrington IM, Butler TZ, Collins MD, Manrao E, Pavlenok M, Niederweis M, et al. Nanopore DNA sequencing with MspA. Proc Natl Acad Sci U S A. 2010;107(37):16060-5.
156. Manrao EA, Derrington IM, Pavlenok M, Niederweis M, Gundlach JH. Nucleotide discrimination with DNA immobilized in the MspA nanopore. PLoS One. 2011;6(10):e25723.
157. Wallace EV, Stoddart D, Heron AJ, Mikhailova E, Maglia G, Donohoe TJ, et al. Identification of epigenetic DNA modifications with a protein nanopore. Chem Commun (Camb). 2010;46(43):8195-7.
158. Teo SM, Pawitan Y, Ku CS, Chia KS, Salim A. Statistical challenges associated with detecting copy number variations with next-generation sequencing. Bioinformatics. 2012;28(21):2711-8.
159. Miller CA, Hampton O, Coarfa C, Milosavljevic A. ReadDepth: a parallel R package for detecting copy number alterations from short sequencing reads. PLoS One. 2011;6(1):e16327.
160. Scheinin I, Sie D, Bengtsson H, van de Wiel MA, Olshen AB, van Thuijl HF, et al. DNA copy number analysis of fresh and formalin-fixed specimens by shallow whole-genome sequencing with identification and exclusion of problematic regions in the genome assembly. Genome Res. 2014;24(12):2022-32.
161. Olshen AB, Venkatraman ES, Lucito R, Wigler M. Circular binary segmentation for the analysis of array-based DNA copy number data. Biostatistics. 2004;5(4):557-72.
162. Fedick A, Su J, Jalas C, Treff NR. High-throughput real-time PCR-based genotyping without DNA purification. BMC Res Notes. 2012;5:573.
163. Fiorentino F, Biricik A, Bono S, Spizzichino L, Cotroneo E, Cottone G, et al. Development and validation of a next-generation sequencing-based protocol for 24-chromosome aneuploidy screening of embryos. Fertil Steril. 2014;101(5):1375-82.
164. Treff NR, Su J, Tao X, Levy B, Scott RT, Jr. Accurate single cell 24 chromosome aneuploidy screening using whole genome amplification and single nucleotide polymorphism microarrays. Fertil Steril. 2010;94(6):2017-21.
165. Van Loo P, Voet T. Single cell analysis of cancer genomes. Current opinion in genetics & development. 2014;24:82-91.
166. Fiegler H, Carr P, Douglas EJ, Burford DC, Hunt S, Scott CE, et al. DNA microarrays for comparative genomic hybridization based on DOP-PCR amplification of BAC and PAC clones. Genes, chromosomes & cancer. 2003;36(4):361-74.
167. Sermon K, Lissens W, Joris H, Van Steirteghem A, Liebaers I. Adaptation of the primer extension preamplification (PEP) reaction for preimplantation diagnosis: single blastomere analysis using short PEP protocols. Mol Hum Reprod. 1996;2(3):209-12.
168. Ning L. Quantitative comparison of single-cell sequencing methods using hippocampal neurons biorxiv. 2014.
169. Ben-Bassat H, Shlomai Z, Kohn G, Prokocimer M. Establishment of a human T-acute lymphoblastic leukemia cell line with a (16;20) chromosome translocation. Cancer genetics and cytogenetics. 1990;49(2):241-8.

170. Li H, Handsaker B, Wysoker A, Fennell T, Ruan J, Homer N, et al. The Sequence Alignment/Map format and SAMtools. Bioinformatics. 2009;25(16):2078-9.
171. Quinlan AR, Hall IM. BEDTools: a flexible suite of utilities for comparing genomic features. Bioinformatics. 2010;26(6):841-2.
172. Duan J, Zhang JG, Deng HW, Wang YP. Comparative studies of copy number variation detection methods for next-generation sequencing technologies. PLoS One. 2013;8(3):e59128.
173. Talseth-Palmer BA, Bowden NA, Hill A, Meldrum C, Scott RJ. Whole genome amplification and its impact on CGH array profiles. BMC Res Notes. 2008;1:56.
174. Leo A, Walker AM, Lebo MS, Hendrickson B, Scholl T, Akmaev VR. A GC-wave correction algorithm that improves the analytical performance of aCGH. J Mol Diagn. 2012;14(6):550-9.
175. Baslan T, Kendall J, Rodgers L, Cox H, Riggs M, Stepansky A, et al. Genome-wide copy number analysis of single cells. Nat Protoc. 2012;7(6):1024-41.
176. Harper JC, Sengupta SB. Preimplantation genetic diagnosis: state of the art 2011. Hum Genet. 2012;131(2):175-86.
177. Forman EJ, Hong KH, Ferry KM, Tao X, Taylor D, Levy B, et al. In vitro fertilization with single euploid blastocyst transfer: a randomized controlled trial. Fertil Steril. 2013;100(1):100-7 e1.
178. Schoolcraft WB, Katz-Jaffe MG. Comprehensive chromosome screening of trophectoderm with vitrification facilitates elective single-embryo transfer for infertile women with advanced maternal age. Fertil Steril. 2013;100(3):615-9.
179. Yin X, Tan K, Vajta G, Jiang H, Tan Y, Zhang C, et al. Massively parallel sequencing for chromosomal abnormality testing in trophectoderm cells of human blastocysts. Biology of reproduction. 2013;88(3):69.
180. Vandekerckhove F, Gerris J, Vansteelandt S, De Baerdemaeker A, Tilleman K, De Sutter P. Delaying the oocyte maturation trigger by one day leads to a higher metaphase II oocyte yield in IVF/ICSI: a randomised controlled trial. Reprod Biol Endocrinol. 2014;12:31.
181. Gardner DK SW. In-vitro culture of human blastocysts. Towards reproductive certainty: fertility and genetics beyond 1999. New York: The Parthenon Publishing Group; 1999. p. 378-88.
182. Sante T, Vergult S, Volders PJ, Kloosterman WP, Trooskens G, De Preter K, et al. ViVar: A Comprehensive Platform for the Analysis and Visualization of Structural Genomic Variation. PLoS One. 2014;9(12):e113800.
183. Li H. Aligning sequence reads, clone sequences and assembly contigs with BWA-MEM. Oxford University Press. 2013;00 no. 00 201.
184. Team RC. R: A Language and Environment for Statistical Computing. In: Computing RFfS, editor. 2013.
185. Consortium EP. An integrated encyclopedia of DNA elements in the human genome. Nature. 2012;489(7414):57-74.
186. Pugh TJ, Delaney AD, Farnoud N, Flibotte S, Griffith M, Li HI, et al. Impact of whole genome amplification on analysis of copy number variants. Nucleic Acids Res. 2008;36(13):e80.
187. Deleye L, De Coninck D, Christodoulou C, Sante T, Dheedene A, Heindryckx B, et al. Whole genome amplification with SurePlex results in better copy number alteration detection using sequencing data compared to the MALBAC method. Sci Rep. 2015;5:11711.
188. Roque M, Valle M, Guimaraes F, Sampaio M, Geber S. Freeze-all policy: fresh vs. frozen-thawed embryo transfer. Fertility and sterility. 2015.
189. Zhao M, Wang Q, Wang Q, Jia P, Zhao Z. Computational tools for copy number variation (CNV) detection using next-generation sequencing data: features and perspectives. BMC Bioinformatics. 2013;14 Suppl 11:S1.
190. Langmead B, Trapnell C, Pop M, Salzberg SL. Ultrafast and memory-efficient alignment of short DNA sequences to the human genome. Genome Biol. 2009;10(3):R25.
191. Macaulay IC, Voet T. Single cell genomics: advances and future perspectives. PLoS Genet. 2014;10(1):e1004126.
192. Picher AJ, Budeus B, Wafzig O, Kruger C, Garcia-Gomez S, Martinez-Jimenez MI, et al. TruePrime is a novel method for whole-genome amplification from single cells based on TthPrimPol. Nat Commun. 2016;7:13296.
193. Von Neumann J. KRH, Bellinson H.R., and Hart B.I. The Mean Square Successive Difference. The annals of Mathematical Statistics. 1941;12(2):153-62.
194. Lohr JG, Adalsteinsson VA, Cibulskis K, Choudhury AD, Rosenberg M, Cruz-Gordillo P, et al. Whole-exome sequencing of circulating tumor cells provides a window into metastatic prostate cancer. Nat Biotechnol. 2014;32(5):479-84.
195. Polzer B, Medoro G, Pasch S, Fontana F, Zorzino L, Pestka A, et al. Molecular profiling of single circulating tumor cells with diagnostic intention. EMBO Mol Med. 2014;6(11):1371-86.
196. Zhang C, Guan Y, Sun Y, Ai D, Guo Q. Tumor heterogeneity and circulating tumor cells. Cancer Lett. 2016;374(2):216-23.
197. Deleye L, De Coninck D, Dheedene A, De Sutter P, Menten B, Deforce D, et al. Performance of a TthPrimPol-based whole genome amplification kit for copy number alteration detection using massively parallel sequencing. Sci Rep. 2016;6:31825.
198. Hou Y, Wu K, Shi X, Li F, Song L, Wu H, et al. Comparison of variations detection between whole-genome amplification methods used in single-cell resequencing. Gigascience. 2015;4:37.
199. Li N, Wang L, Wang H, Ma M, Wang X, Li Y, et al. The Performance of Whole Genome Amplification Methods and Next-Generation Sequencing for Pre-Implantation Genetic Diagnosis of Chromosomal Abnormalities. J Genet Genomics. 2015;42(4):151-9.
200. Huang L, Ma F, Chapman A, Lu S, Xie XS. Single-Cell Whole-Genome Amplification and Sequencing: Methodology and Applications. Annu Rev Genomics Hum Genet. 2015;16:79-102.
201. Arneson N, Hughes S, Houlston R, Done S. Whole-Genome Amplification by Degenerate Oligonucleotide Primed PCR (DOP-PCR). CSH Protoc. 2008;2008:pdb prot4919.
202. Forbes SA, Bindal N, Bamford S, Cole C, Kok CY, Beare D, et al. COSMIC: mining complete cancer genomes in the Catalogue of Somatic Mutations in Cancer. Nucleic Acids Res. 2011;39(Database issue):D945-50.
203. Forbes SA, Tang G, Bindal N, Bamford S, Dawson E, Cole C, et al. COSMIC (the Catalogue of Somatic Mutations in Cancer): a resource to investigate acquired mutations in human cancer. Nucleic Acids Res. 2010;38(Database issue):D652-7.
204. McConnell MJ, Lindberg MR, Brennand KJ, Piper JC, Voet T, Cowing-Zitron C, et al. Mosaic copy number variation in human neurons. Science. 2013;342(6158):632-7.
205. Zilina O, Koltsina M, Raid R, Kurg A, Tonisson N, Salumets A. Somatic mosaicism for copy-neutral loss of heterozygosity and DNA copy number variations in the human genome. BMC Genomics. 2015;16:703.

206. Koehler U. SU, Mayer V., Holinski-Feder E. Preimplantation genetic diagnosisfor Monogenic Disorders and Chromosomal Rearrangements – The German Perspective. J Reproduktionsmed Endokrinol. 2013;10(1):38–44.
207. Treff NR, Fedick A, Tao X, Devkota B, Taylor D, Scott RT, Jr. Evaluation of targeted next-generation sequencing-based preimplantation genetic diagnosis of monogenic disease. Fertil Steril. 2013;99(5):1377-84 e6.
208. Liang L, Wang CT, Sun X, Liu L, Li M, Witz C, et al. Identification of chromosomal errors in human preimplantation embryos with oligonucleotide DNA microarray. PLoS One. 2013;8(4):e61838.
209. Borgstrom E, Paterlini M, Mold JE, Frisen J, Lundeberg J. Comparison of whole genome amplification techniques for human single cell exome sequencing. PLoS One. 2017;12(2):e0171566.
210. S. A. FastQC: a quality control tool for high throughput sequence data 2010 [Available from: http://www.bioinformatics.babraham.ac.uk/projects/fastqc/.
211. Li H, Durbin R. Fast and accurate short read alignment with Burrows-Wheeler transform. Bioinformatics. 2009;25(14):1754-60.
212. Garcia-Alcalde F, Okonechnikov K, Carbonell J, Cruz LM, Gotz S, Tarazona S, et al. Qualimap: evaluating next-generation sequencing alignment data. Bioinformatics. 2012;28(20):2678-9.
213. Institute B. Picardtools [Available from: https://broadinstitute.github.io/picard/.
214. McKenna A, Hanna M, Banks E, Sivachenko A, Cibulskis K, Kernytsky A, et al. The Genome Analysis Toolkit: a MapReduce framework for analyzing next-generation DNA sequencing data. Genome Res. 2010;20(9):1297-303.
215. Sherry ST, Ward MH, Kholodov M, Baker J, Phan L, Smigielski EM, et al. dbSNP: the NCBI database of genetic variation. Nucleic Acids Res. 2001;29(1):308-11.
216. Mills RE, Pittard WS, Mullaney JM, Farooq U, Creasy TH, Mahurkar AA, et al. Natural genetic variation caused by small insertions and deletions in the human genome. Genome Res. 2011;21(6):830-9.
217. Danecek P, Auton A, Abecasis G, Albers CA, Banks E, DePristo MA, et al. The variant call format and VCFtools. Bioinformatics. 2011;27(15):2156-8.
218. Barber AL, Foran DR. The utility of whole genome amplification for typing compromised forensic samples. J Forensic Sci. 2006;51(6):1344-9.
219. Findlay I, Ray P, Quirke P, Rutherford A, Lilford R. Allelic drop-out and preferential amplification in single cells and human blastomeres: implications for preimplantation diagnosis of sex and cystic fibrosis. Hum Reprod. 1995;10(6):1609-18.
220. Deleye L, Tilleman L, Vander Plaetsen AS, Cornelis S, Deforce D, Van Nieuwerburgh F. Performance of four modern whole genome amplification methods for copy number variant detection in single cells. Sci Rep. 2017;7(1):3422.
221. Ning L, Li Z, Wang G, Hu W, Hou Q, Tong Y, et al. Quantitative assessment of single-cell whole genome amplification methods for detecting copy number variation using hippocampal neurons. Sci Rep. 2015;5:11415.
222. Denis D KD, De Matos D.G., Miller K, R Scott, Palmer S. Whole Genome Amplification (WGA) and Short Tandem Repeat Analysis (STR) of Single Blastomeres for Embryo Fingerprinting and Embryo Genomics. Fertility sterility. 2005;84.
223. Babayan A, Alawi M, Gormley M, Muller V, Wikman H, McMullin RP, et al. Comparative study of whole genome amplification and next generation sequencing performance of single cancer cells. Oncotarget. 2016.
224. Alix-Panabieres C, Pantel K. Challenges in circulating tumour cell research. Nat Rev Cancer. 2014;14(9):623-31.
225. Fiddler M. Fetal Cell Based Prenatal Diagnosis: Perspectives on the Present and Future. J Clin Med. 2014;3(3):972-85.
226. Normand E, Qdaisat S, Bi W, Shaw C, Van den Veyver I, Beaudet A, et al. Comparison of three whole genome amplification methods for detection of genomic aberrations in single cells. Prenat Diagn. 2016;36(9):823-30.
227. Zhang Y, Li Q, Hui N, Fei M, Hu Z, Sun S. Effect of formaldehyde treatment on the recovery of cell-free fetal DNA from maternal plasma at different processing times. Clin Chim Acta. 2008;397(1-2):60-4.
228. Medina Diaz I, Nocon A, Mehnert DH, Fredebohm J, Diehl F, Holtrup F. Performance of Streck cfDNA Blood Collection Tubes for Liquid Biopsy Testing. PLoS One. 2016;11(11):e0166354.
229. Qin J, Alt JR, Hunsley BA, Williams TL, Fernando MR. Stabilization of circulating tumor cells in blood using a collection device with a preservative reagent. Cancer Cell Int. 2014;14(1):23.
230. Toro PV, Erlanger B, Beaver JA, Cochran RL, VanDenBerg DA, Yakim E, et al. Comparison of cell stabilizing blood collection tubes for circulating plasma tumor DNA. Clin Biochem. 2015;48(15):993-8.
231. Das K, Dumais J, Basiaga S, Krzyzanowski GD. Carbon-13 nuclear magnetic resonance analysis of formaldehyde free preservatives. Acta Histochem. 2013;115(5):481-6.
232. Qin J, Sanmann JN, Kittrell JS, Althof PA, Kaspar EE, Hunsley BA. A formalin-free method for stabilizing cells for nucleic acid amplification, hybridization and next-generation sequencing. BMC Res Notes. 2015;8:755.
233. Miething F, Hering S, Hanschke B, Dressler J. Effect of fixation to the degradation of nuclear and mitochondrial DNA in different tissues. J Histochem Cytochem. 2006;54(3):371-4.
234. Zheng YM, Wang N, Li L, Jin F. Whole genome amplification in preimplantation genetic diagnosis. J Zhejiang Univ Sci B. 2011;12(1):1-11.
235. Fiorentino F, Bono S, Biricik A, Nuccitelli A, Cotroneo E, Cottone G, et al. Application of next-generation sequencing technology for comprehensive aneuploidy screening of blastocysts in clinical preimplantation genetic screening cycles. Hum Reprod. 2014;29(12):2802-13.
236. Yan L, Huang L, Xu L, Huang J, Ma F, Zhu X, et al. Live births after simultaneous avoidance of monogenic diseases and chromosome abnormality by next-generation sequencing with linkage analyses. Proc Natl Acad Sci U S A. 2015;112(52):15964-9.
237. Yang Z, Lin J, Zhang J, Fong WI, Li P, Zhao R, et al. Randomized comparison of next-generation sequencing and array comparative genomic hybridization for preimplantation genetic screening: a pilot study. BMC Med Genomics. 2015;8:30.
238. M.J. B. Comparative preimplantation genetic diagnosis policy in Europe and the USA and its implications for reproductive tourism. Reprod Biomed Online. 2017:7.
239. Pennings G. Belgian law on medically assisted reproduction and the disposition of supernumerary embryos and gametes. Eur J Health Law. 2007;14(3):251-60.
240. Christodoulou C, Dheedene A, Heindryckx B, van Nieuwerburgh F, Deforce D, De Sutter P, et al. Preimplantation genetic diagnosis for chromosomal rearrangements with the use of array comparative genomic hybridization at the blastocyst stage. Fertil Steril. 2017;107(1):212-9 e3.

241. Gleicher N, Vidali A, Braverman J, Kushnir VA, Barad DH, Hudson C, et al. Accuracy of preimplantation genetic screening (PGS) is compromised by degree of mosaicism of human embryos. Reprod Biol Endocrinol. 2016;14(1):54.
242. Munne S, Wells D. Detection of mosaicism at blastocyst stage with the use of high-resolution next-generation sequencing. Fertil Steril. 2017;107(5):1085-91.
243. Goldman KN, Nazem T, Berkeley A, Palter S, Grifo JA. Preimplantation Genetic Diagnosis (PGD) for Monogenic Disorders: the Value of Concurrent Aneuploidy Screening. J Genet Couns. 2016;25(6):1327-37.
244. Rechitsky S, Pakhalchuk T, San Ramos G, Goodman A, Zlatopolsky Z, Kuliev A. First systematic experience of preimplantation genetic diagnosis for single-gene disorders, and/or preimplantation human leukocyte antigen typing, combined with 24-chromosome aneuploidy testing. Fertil Steril. 2015;103(2):503-12.
245. Lynch M. Rate, molecular spectrum, and consequences of human mutation. Proc Natl Acad Sci U S A. 2010;107(3):961-8.
246. Roach JC, Glusman G, Smit AF, Huff CD, Hubley R, Shannon PT, et al. Analysis of genetic inheritance in a family quartet by whole-genome sequencing. Science. 2010;328(5978):636-9.
247. Francioli LC, Polak PP, Koren A, Menelaou A, Chun S, Renkens I, et al. Genome-wide patterns and properties of de novo mutations in humans. Nat Genet. 2015;47(7):822-6.
248. Gilissen C, Hehir-Kwa JY, Thung DT, van de Vorst M, van Bon BW, Willemsen MH, et al. Genome sequencing identifies major causes of severe intellectual disability. Nature. 2014;511(7509):344-7.
249. Goldmann JM, Wong WS, Pinelli M, Farrah T, Bodian D, Stittrich AB, et al. Parent-of-origin-specific signatures of de novo mutations. Nat Genet. 2016;48(8):935-9.
250. Michaelson JJ, Shi Y, Gujral M, Zheng H, Malhotra D, Jin X, et al. Whole-genome sequencing in autism identifies hot spots for de novo germline mutation. Cell. 2012;151(7):1431-42.
251. Russo ML, Blakemore KJ. A historical and practical review of first trimester aneuploidy screening. Semin Fetal Neonatal Med. 2014;19(3):183-7.
252. Shamshirsaz AA, Benn P, Egan JF. The role of second-trimester serum screening in the post-first-trimester screening era. Clin Lab Med. 2010;30(3):667-76.
253. Agarwal A, Sayres LC, Cho MK, Cook-Deegan R, Chandrasekharan S. Commercial landscape of noninvasive prenatal testing in the United States. Prenat Diagn. 2013;33(6):521-31.
254. Chandrasekharan S, Minear MA, Hung A, Allyse M. Noninvasive prenatal testing goes global. Sci Transl Med. 2014;6(231):231fs15.
255. Lau TK, Chan MK, Lo PS, Chan HY, Chan WS, Koo TY, et al. Clinical utility of noninvasive fetal trisomy (NIFTY) test--early experience. J Matern Fetal Neonatal Med. 2012;25(10):1856-9.
256. Non-invasive Prenatal Testing (NIPT) Market (BambniTest, Harmony, informaSeq, MaterniT21 PLUS, NIFTY, Panorama, PrenaTest, verifi, VisibiliT and Others) - Global Industry Analysis, Size, Volume, Share, Growth, Trends and Forecast 2014 - 20222015:[112 p.].
257. Singh R, Hatt L, Ravn K, Vogel I, Petersen OB, Uldbjerg N, et al. Fetal cells in maternal blood for prenatal diagnosis: a love story rekindled. Biomark Med. 2017.
258. Guetta E, Gutstein-Abo L, Barkai G. Trophoblasts isolated from the maternal circulation: in vitro expansion and potential application in non-invasive prenatal diagnosis. J Histochem Cytochem. 2005;53(3):337-9.
259. Kolvraa S, Singh R, Normand EA, Qdaisat S, van den Veyver IB, Jackson L, et al. Genome-wide copy number analysis on DNA from fetal cells isolated from the blood of pregnant women. Prenat Diagn. 2016;36(12):1127-34.
260. van Wijk IJ, Griffioen S, Tjoa ML, Mulders MA, van Vugt JM, Loke YW, et al. HLA-G expression in trophoblast cells circulating in maternal peripheral blood during early pregnancy. Am J Obstet Gynecol. 2001;184(5):991-7.
261. Saker A, Benachi A, Bonnefont JP, Munnich A, Dumez Y, Lacour B, et al. Genetic characterisation of circulating fetal cells allows non-invasive prenatal diagnosis of cystic fibrosis. Prenat Diagn. 2006;26(10):906-16.
262. Vona G, Beroud C, Benachi A, Quenette A, Bonnefont JP, Romana S, et al. Enrichment, immunomorphological, and genetic characterization of fetal cells circulating in maternal blood. Am J Pathol. 2002;160(1):51-8.
263. Ilie M, Long E, Butori C, Hofman V, Coelle C, Mauro V, et al. ALK-gene rearrangement: a comparative analysis on circulating tumour cells and tumour tissue from patients with lung adenocarcinoma. Ann Oncol. 2012;23(11):2907-13.
264. Paterlini-Brechot P. Organ-specific markers in circulating tumor cell screening: an early indicator of metastasis-capable malignancy. Future Oncol. 2011;7(7):849-71.
265. Vona G, Sabile A, Louha M, Sitruk V, Romana S, Schutze K, et al. Isolation by size of epithelial tumor cells : a new method for the immunomorphological and molecular characterization of circulatingtumor cells. Am J Pathol. 2000;156(1):57-63.
266. Benn P, Curnow KJ, Chapman S, Michalopoulos SN, Hornberger J, Rabinowitz M. An Economic Analysis of Cell-Free DNA Non-Invasive Prenatal Testing in the US General Pregnancy Population. PLoS One. 2015;10(7):e0132313.
267. Bernhardt BA, Kellom K, Barbarese A, Faucett WA, Wapner RJ. An exploration of genetic counselors' needs and experiences with prenatal chromosomal microarray testing. J Genet Couns. 2014;23(6):938-47.
268. Bernhardt BA, Soucier D, Hanson K, Savage MS, Jackson L, Wapner RJ. Women's experiences receiving abnormal prenatal chromosomal microarray testing results. Genet Med. 2013;15(2):139-45.
269. de Jong A, Dondorp WJ, Macville MV, de Die-Smulders CE, van Lith JM, de Wert GM. Microarrays as a diagnostic tool in prenatal screening strategies: ethical reflection. Hum Genet. 2014;133(2):163-72.
270. Tabor HK, Murray JC, Gammill HS, Kitzman JO, Snyder MW, Ventura M, et al. Non-invasive fetal genome sequencing: opportunities and challenges. Am J Med Genet A. 2012;158A(10):2382-4.
271. Green RC, Berg JS, Grody WW, Kalia SS, Korf BR, Martin CL, et al. ACMG recommendations for reporting of incidental findings in clinical exome and genome sequencing. Genet Med. 2013;15(7):565-74.

Curriculum vitae

Lieselot Deleye

Personalia

Surname:	Deleye
Name:	Lieselot
Nationality:	Belgian
Place & date of birth:	Kortrijk, 24th of January 1990
Address:	José Vermeerschplein 5, 8501 Heule
Phone:	+32 476 59 46 78
Email:	Lieselot.Deleye@telenet.be or Lieselot.Deleye@ugent.be

Education

2013-2017:	PhD in Pharmaceutical Sciences, Ghent University Laboratory of Pharmaceutical biotechnology
2008-2013:	Biomedical Sciences at KULAK/KULeuven Major in research (English master) Thesis: The role of vitamin D in skeletal muscle weakness in COPD Graduated with: Magna cum laude
2001-2008:	High school general secondary education at Lyceum O.L.V. Vlaanderen Kortrijk: First and second grade: Latin Third grade: Science/Mathematics

Professional experience

2014-present	Supervisor master theses (4 students)
2013-present	Practicum educator: Practicum pharmaceutical biotechnology (±8 students); Practicum phytochemistry (±40 students)

Additional education

2017	Cell isolation at University of Twente (The Nederlands)
2017	Lab on a chip and sensor technology at IMEC (Leuven)
2016	Project management (UGent)
2016	Introduction to 'R' (certificate) (UGent)
2015	English writing skills (certificate) (UGent)
2015	Multidisciplinary seminar series on Bioinformatics (UGent)
2013	Instrumental technical skills certificate (nursing internship)
2012	Internship at St.Thomas University Miami (USA; July): 'Interaction of sugars on prostate cancer cells leading to its progression' with Professor Severine Vanslambrouck; achieved an A.
2012	Forensic science class at St.Thomas University Miami (USA; July) by Prof. Dr. Apr. Dieter Deforce; achieved an A
2012	Certificate for Laboratory Animal Sciences (cat B)
2012	Internship at the Experimental Gynecology lab KULeuven (Oncology) (4 weeks)

A1 Publications

PUBLISHED

Deleye L, De Coninck D, Christodoulou C, Sante T, Dheedene A, Heindryckx B, et al. **Whole genome amplification with SurePlex results in better copy number alteration detection using sequencing data compared to the MALBAC method.** Sci Rep. 2015;5:11711.

Deleye L, Dheedene A, De Coninck D, Sante T, Christodoulou C, Heindryckx B, et al. **Shallow whole genome sequencing is well suited for the detection of chromosomal aberrations in human blastocysts**. Fertil Steril. 2015;104(5):1276-85 e1.

Deleye L, De Coninck D, Dheedene A, De Sutter P, Menten B, Deforce D, et al. **Performance of a TthPrimPol-based whole genome amplification kit for copy number alteration detection using massively parallel sequencing.** Sci Rep. 2016;6:31825.

Cornelis S, Gansemans Y, Deleye L, Deforce D, Van Nieuwerburgh F. **Forensic SNP Genotyping using Nanopore MinION sequencing.** Sci. Rep. 2017 ; 7 : 41759.

Deleye L, Tilleman L, Vander Plaetsen AS, Cornelis S, Deforce D, Van Nieuwerburgh F. **Performance of four modern whole genome amplification methods for copy number variant detection in single cells.** Sci Rep. 2017;7(1):3422.

Deleye L, Vander Plaetsen AS, Cornelis S, Tilleman L, Van Nieuwerburgh F, Deforce D. **STR profiling and Copy Number Variation analysis on single, preserved cells using current Whole Genome Amplification methods.** Sci Rep. 2017; 7: 17189.

SUBMITTED

Deleye L, Gansemans Y, De Coninck D, Van Nieuwerburgh F, Deforce D. **Massively parallel sequencing of micro-manipulated cells targeting a comprehensive panel of disease-causing genes.** PLos ONE.

Deleye L, Vander Plaetsen AS, Cornelis S, Deforce D, Van Nieuwerburgh F. **Human identification STR analysis after single-cell whole genome amplification.** Sci Rep. peer review October 2017

Book chapter

Deleye L, De Coninck D, Deforce D, Van Nieuwerburgh F. **Genome-wide Copy Number Alteration Detection in Preimplantation Genetic Diagnosis** (Chapter 3) In: Head S.R., Ordoukhanaian P and Salomon D.R., editors. Next generation sequencing: Methods and Protocols. New York: Springer 2018. 10.1007/978-1-4939-7514-3.

Presentations at (inter)national conferences

Jan 2015	Revolutionizing Next-Generation Sequencing : Tools and Technologies; Leuven, Belgium	Poster presentation
May 2015	Single cell “omics” in reproduction; Leuven, Belgium	Oral presentation
Nov 2015	Advances in prenatal molecular diagnostics, Boston, USA	Poster presentation
May 2016	Knowledge for growth, Ghent, Belgium	Poster presentation
Nov 2016	Advances in prenatal molecular diagnostics, Boston, USA	Poster presentation
Apr 2017	Advances in prenatal molecular diagnostics Europe, Lisbon, Portugal	Oral presentation